UNIVERSITY OF LEEDS

Air quality in China: Trends, drivers and mitigation

Ben Silver

Submitted in accordance with the requirements for the degree of Doctor of Philosophy

The University of Leeds

School of Earth and Environment

June 2021

Intellectual Property

The candidate confirms that the work submitted is his own, except where work which has formed part of jointly authored publications has been included. The contribution of the candidate and the other authors to this work has been explicitly indicated below. The candidate confirms that appropriate credit has been given within the thesis where reference has been made to the work of others.

Chapter 2 consists of the following publication:
B. Silver, C. L. Reddington, S. R. Arnold, and D. V. Spracklen (2018). "Substantial changes in air pollution across China during 2015-2017". In: *Environmental Research Letters* 13.11. DOI: 10.1088/1748-9326/aae718

Conceptualization of the work was done by the candidate, with support from CLR, SRA and DVS. The candidate collected and analysed the data, produced the figures and prepared the manuscript. A final draft was produced with assistance from all authors.

Chapter 3 consists of the following publication:
B. Silver, L. Conibear, C. L. Reddington, C. Knote, S. R. Arnold, and D. V. Spracklen (2020a). "Pollutant emission reductions deliver decreased PM2.5-caused mortality across China during 2015-2017". In: *Atmospheric Chemistry and Physics* 20.20, pp. 11683–11695. DOI: 10.5194/acp-20-11683-2020

Conceptualization of the work was done by the candidate, DVS, SRA and CLR. Model simulations were carried out by the candidate, with assistance from CLR and LC, and model automation scripts provided by CK. The candidate performed the comparison with observation data and trend analyses. LC performed the health impact analyses. The candidate prepared the figures and manuscript. A final draft was produced with assistance from all authors.

Chapter 4 consists of the following publication:

B. Silver, X. He, S. R. Arnold, and D. V. Spracklen (2020b). "The impact of COVID-19 control measures on air quality in China". In: *Environmental Research Letters* 15.8, p. 084021. DOI: 10.1088/1748-9326/aba3a2

Conceptualization of the work was done by the candidate, with assistance from DVS and SRA. The most recent observational data was provided by XH. The candidate analysed the data, prepared the figures and manuscript. A final draft was produced with assistance from all authors.

Acknowledgements

Firstly I would like to thank my supervisors Dom, Steve and Carly. Your support, kindness and flexibility has been invaluable and I could not imagine a better team of supervisors. Thank you for gently pushing me to achieve things I never expected to be capable of.

Thank you to the AIA Group Limited for providing funding for my project.

My research would not have been possible without the generosity of two people who I have never met. The first is Merrick Lex Berman at the Center for Geographic Analysis at Harvard, who is an expert in online repositories of China's air quality data, and pointed me to `https://beijingair.sinaapp.com/` (now `https://quotsoft.net/`), which became the main source of measurement data for my research. These websites are operated by Xiaolei Wang, who scrapes and distributes this valuable data which is almost impossible to obtain officially. Thanks to you both. Also thanks to the people who helped me download the data from the Baidu drive: Wendy, Eugene, Xinyue, Xiaoyang and Fan.

Big shout-out to everyone in my office, 10.127, especially to Richard (Pope) who helped maintain the quiet and respectful environment that was essential for long days of solemn academic toil. Seriously though, thank you for making the experience of starting my PhD a lot less scary. Thanks to bosom buddies Amy and Ananth, for providing secretarial and mathematical support inside office hours, as well as domestic support (to varying degrees) outside. Thank you to Jess and Ailish for radiating productive vibes in my direction and lots of technical help, and Xuemei for Chinese language translations.

Also at Leeds, I am grateful to Richard (Rigby) for his IT wizardry that got me out of many tight spots, Luke for all his work making using and understanding the WRF-Chem model much less painful, and to Tom, Laura and Ailish for sharing that pain and being great company on international excursions. Thanks to all my housemates and friends in Leeds, especially to my current cohabitants: Iain, Callum, Jamie, Hamish and Will who

have kept my spirits up during lockdown thesis writing. Shoutout fellow PhD hopefuls Adan, Fanta, Viv, Nads and Olly we really out here.

During my PhD I was lucky enough to be required to take regular trips to Hong Kong, including research visits at the Hong Kong University of Science and Technology, and the Chinese University of Hong Kong. Thank you to Jimmy Fung and Lin Su at HKUST, and Steve Yim and Amos Tai at CUHK for hosting me. Particularly strong and heartfelt thanks go to the students and researchers who I met on these visits who made me feel welcome and accompanied me for hundreds of meals: Ali, Paula, Utkarsh, Thanh, Mac, Alan, Felix, Shirley - I hope to see you again someday. Also big shout-out to my other HK friends who looked after me during turbulent times: Rebekah, Grace, Louis, Bonnie, Helios, JiaJia and Boba, it is now your turn to visit me in the UK. One final HK-based person who cannot go unmentioned, as he was my main motivation for returning again and again, is Sam Gor (譚仔三哥). Thank you for your vegetarian mixian with hot and numbing soup, with dong lai cha siu bing.

Thanks to those who inspired me to take this path, and who have been role models throughout my life: Daniel, Dominique, John and Sonia.

Finally, and most importantly, thank you to my mum, Philippa, for all the support you have given me throughout this process. I am sorry that it got in the way of more important projects such as the allotment. I dedicate this thesis to you, as well as Peter, David, Dan, Dave, Matt, Esther, Bertie, Lily and Alf.

Abstract

The size of the People's Republic of China's (henceforth 'China') economy has increased by 75-fold since economic reforms began in the late 1970s. Environmental policies were initially lax, especially during the 1980s and 1990s, which led to a substantial deterioration in China's air quality. Megacity regions frequently experience episodes of smog, particularly during stagnant weather conditions. During these episodes, high concentrations of aerosols have been recorded. High concentrations of ambient fine aerosol (with an aerodynamic diameter of $<2.5\ \mu g\,m^{-3}$), known as $PM_{2.5}$, has been identified as one of the most significant environmental risk factors that causes premature deaths by epidemiological research. Over 1 million deaths each year have been attributed to high ambient $PM_{2.5}$ exposure in China.

Since the 2000s, air pollution control measures in China have become increasingly stringent. This has resulted in improvements in air quality, which have been observed by satellites, estimated in emission inventories, and since 2011 have been observed by a new national monitoring network consisting of over 1600 ground-based stations. The network records hourly concentrations of $PM_{2.5}$, as well as nitrogen dioxide (NO_2), ozone (O_3) and sulphur dioxide (SO_2). My analysis of the trends in this network found that during 2015-2017, the national median $PM_{2.5}$ trend was $-3.4\ \mu g\,m^{-3}\,yr^{-1}$, SO_2 $-1.9\ \mu g\,m^{-3}\,yr^{-1}$, NO_2 had no overall trend, and the trend in 'maximum daily 8-hour mean' O_3 was 4.7 $\mu g\,m^{-3}\,yr^{-1}$. Negative $PM_{2.5}$ and SO_2 trends were significant at 53% and 59% of stations respectively. Positive O_3 trends were significant at 50% of stations. There were negative trends in NO_2 at 22% of stations, and positive at 26%.

Atmospheric air pollutant concentrations are determined not only by emissions, but by meteorological conditions, which influence their dispersion, chemical reaction rates and sinks. Therefore, inter-annual variability in meteorological conditions can be a confounding factor when evaluating the impact of China's recent air quality control policies us-

ing observed trends. To untangle the competing drivers of meteorology and emissions, I used a regional atmospheric chemistry model, the 'Weather Research and Forecasting model coupled with Chemistry (WRF-Chem), to simulate air quality over China during 2015-2017. I simulated a scenario where emission changes were investigated, and compared this to a counterfactual where emissions were fixed. The model was able to reproduce the magnitude of observed $PM_{2.5}$ trends in the variable emissions scenario ($-3.5\ \mu g\, m^{-3}\, yr^{-1}$), but not in the fixed emissions scenario $-0.6\ \mu g\, m^{-3}\, yr^{-1}$, demonstrating that changes were primarily driven by the emissions changes. Using an exposure-response function from recent a disease burden study, we estimated that during this period $PM_{2.5}$-associated deaths reduced by 150 000 yr^{-1}. The observed positive trend in ozone was not reproduced by either scenario, suggesting that emissions change estimates were inaccurate or important processes are missing from WRF-Chem.

The COVID-19 outbreak and associated control measures gave a unique opportunity to analyse the effects of a sudden and irregular sectoral activity reduction, where emissions rates dropped in the industry and transport sectors, but were largely unchanged in electricity generation and residential sectors. I used measurement data from China's monitoring network to estimate the impact on air quality of the 'lockdown' measures. I constructed an estimate from 2020 air quality based on 2015-2019 trends and seasonal cycles, along with the air quality impact of the Lunar New Year holiday. By comparing this with observed concentrations, I found that during the first ~2 months following the lockdown in Wuhan, NO_2 concentrations were 27.0% lower on average across China. $PM_{2.5}$ and PM_{10} concentrations were 10.5 and 21.4% lower respectively. O_3 concentrations were increased during the first ~2 weeks of lockdown, but overall remained around expected concentrations during the entire period. After lockdown measures were relaxed in April, pollutant concentrations returned to expected levels.

Contents

1 Introduction **1**

1.1 Background 1

1.1.1 Constituents of air pollution 3

1.1.2 Major sources of air pollution in China 7

1.1.3 Health effects 9

1.2 Physicochemical processing of pollutants in the atmosphere 12

1.2.1 Dispersion and transport 13

1.2.2 Aerosol growth and formation 14

1.2.3 Sinks 15

1.2.4 Feedbacks 16

1.2.5 Seasonal variability 17

1.3 Numerical air quality modelling 17

1.3.1 The WRF-Chem model 18

1.4 Air Quality Monitoring 19

1.4.1 In-situ measurements 19

1.4.2 Remote sensing of surface pollutants 22

1.5 Air quality Trends in China 23

1.5.1 Evolution of air quality control policy in China 23

1.5.2 Emissions trends 25

1.5.3 Measured air quality trends 26

1.6 Aims and Objectives 31

2 Substantial changes in air pollution across China during 2015–2017 **62**

3 Pollutant emission reductions deliver decreased $PM_{2.5}$-caused mortality across China during 2015–2017 **82**

4 The impact of COVID-19 control measures on air quality in China **107**

5 Conclusions **129**

5.1 Synthesis of results 129

5.1.1 Key findings 130

5.2 Discussion of uncertainties 133

5.2.1 Uncertainties in trend estimates 133

5.2.2 Model uncertainties and limitations 133

5.3 Future research directions 134

A Supplementary material for Chapter 2 **141**

B Supplementary material for Chapter 3 **149**

C Supplementary material for Chapter 4 **155**

List of Figures

1.1 NASA VIIRS City Lights map showing megacities 2
1.2 Schematic of O_3 formation reactions 4
1.3 O_3 regimes plot 5
1.4 Satellite image of China 8
1.5 $PM_{2.5}$ exposure-response curves 11
1.6 Atmospheric chemistry and transport processes schematic 13
1.7 Provinces of China map 26

2.1 Map of air quality monitoring stations in China 66
2.2 2015-2017 trends of $PM_{2.5}$, O_3 MDA8, NO_2 and SO_2 69
2.3 Boxplots of air quality trends by province 71

3.1 Histograms comparing observed and modelled trends 90
3.2 Maps comparing observed and modelled trends 92
3.3 Violin plot of measured and simulated concentration trends during 2015 to 2017. 94
3.4 Change in $PM_{2.5}$-attributed premature mortality map 96

4.1 NO_2 time series decomposition analysis. 111
4.2 Air quality trends during 2015-2019 113
4.3 Detrended seasonal cycles of NO_2, $PM_{2.5}$, PM_{10}, O_3, SO_2 and CO 114
4.4 Air quality peturbation during Lunar New Year holiday of NO_2, $PM_{2.5}$, PM_{10}, O_3, SO_2 and CO 115
4.5 Air quality anomaly time series during COVID-19 lockdown 117
4.7 Z-score time series during COVID-19 lockdown. 120
4.6 Map of air quality anomalies during COVID-19 lockdown 121

List of Tables

1.1 Sectoral emissions proportions from the Multi-resolution Emission Inventory for China for 2010 7

2.1 Number of concentration time series for each pollutant and number of stations removed during each stage of data checking 67

3.1 Total emissions from Multi-resolution Emission Inventory for China for 2015-2017 86

3.2 WRF-Chem model evaluation statistics 89

4.1 The proportion of stations that record their minimum and maximum 7 day mean residual during the lockdown period. 116

4.2 Median 7 day mean residual (7DMR) concentrations during the lockdown period 118

5.1 Comparison of the three-year trends estimated in Chapter 2 and five-year trends estimated in Chapter 4 133

Chapter 1

Introduction

1.1 Background

Air pollution is defined as 'the presence of substances in the atmosphere that can cause adverse effects to man and the environment' (Abhishek Tiwary, 2010). The term 'air pollutants' can refer to a range of species in the atmosphere, which can include greenhouse gases, particulate matter, toxic gases, dust, metals, ash, soot, microbes and organic compounds, which have a range of effects, e.g. reducing visibility, causing acute and chronic disease, infection, positive or negative radiative forcing and acid rain. In this text, 'air pollutants' will chiefly refer to the 'criteria pollutants,' particulate matter (PM), nitrogen oxides (NO_x), sulphur dioxide (SO_2), ozone (O_3) and Volatile Organic Compounds (VOCs), which are those most commonly emitted from anthropogenic activities and associated with negative health impacts.

The People's Republic of China (henceforth 'China') has developed its economy rapidly since economic reforms starting in the late 1970s, but this has come with the cost of major environmental degradation, including serious water, soil, and air pollution (The World Bank and State Enviromental Protection Administration, 2007). The increase in fossil fuel consumption, as well as industrial production, vehicle use and fertiliser application has driven an increase in air pollutant emissions, of which China now emits 18-35% of the world's total (Hoesly et al., 2018; Zheng et al., 2018a). This has resulted in a deterioration of air quality in China, with visibility decreasing as particulate haze envelops industrialised regions of the country, particularly in winter (Ding and Liu, 2014; Fu et al., 2014).

Over the past few decades, evidence of the severity of the negative impacts of China's poor

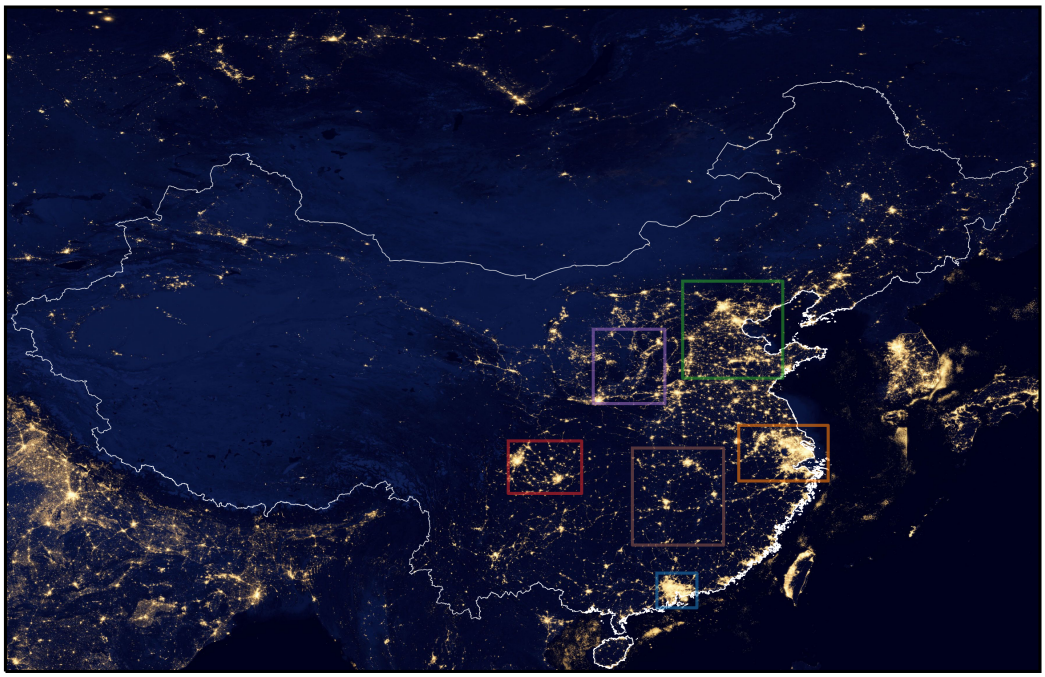

Figure 1.1: Megacity regions plotted over NASA VIIRS City Lights in 2012. Megacities, which are defined as cities with populations greater than 10 million, emerged in China during the 1990s (Chan and Yao, 2008). Regions such as Beijing-Tianjin-Hebei, the Pearl River Delta and the Yangtze River Delta can be described as megalopolises, where several megacities have merged into continuous urban regions. Night light locations are indicative of the population distribution of China, which is denser in eastern areas.

air quality has mounted. Mean winter particulate matter with a diameter of < 2.5 μm ($PM_{2.5}$) concentrations in the most heavily polluted cities in the northeast of China have remained over 10 times higher than the World Health Organisation's (WHO) guideline annual mean concentration of 10 $\mu g\, m^{-3}$ (Ma et al., 2014; Zhang and Cao, 2015). Outdoor exposure to $PM_{2.5}$ and O_3 pollution is estimated to cause in excess of 1 million premature deaths every year in China (Apte et al., 2015; Lelieveld et al., 2015; Gu and Yim, 2016; Cohen et al., 2017; Silver et al., 2020), with its health impacts costing around 1% of national Gross Domestic Product (GDP) (Xia et al., 2016).

The Global Burden of Disease study uses a combination of measured and modelled values of $PM_{2.5}$ concentrations to calculate the health effects of air pollution for each country. As part of this they estimate the mean annual exposure to $PM_{2.5}$, which weights concentrations by population distribution. In 2013, China had the 2nd highest population-weighted mean $PM_{2.5}$ concentrations, behind Mauritania (Brauer et al., 2016).

1.1.1 Constituents of air pollution

Gaseous Pollutants

NO_x refers to the sum of NO and NO_2. They are often measured together since they are involved in rapid photochemical cycling between each-other. NO_x is emitted from the combustion of fossil fuels primarily as NO, which is then rapidly oxidised by O_3 or radicals to form NO_2 (Kampa and Castanas, 2008). NO also has natural sources in the troposphere, such as lightning and soil microbes, although these sources are relatively small compared to anthropogenic emissions (Guenther et al., 2000).

Shortly after emission in the daytime, NO is oxidised to NO_2 by O_3, which is then photolysed back to NO, producing an oxygen atom ($O(^3P)$), which reforms O_3 (Figure 1.2a). No net O_3 formation results.

$$NO + O_3 \longrightarrow NO_2 + O_2 \quad \text{(R 1.1)}$$

$$NO_2 + h\nu \longrightarrow O(^3P) + NO \quad \text{(R 1.2)}$$

$$O(^3P) + O_2 \longrightarrow O_3 \quad \text{(R 1.3)}$$

However, hydroxyl (HO_2) and peroxy (RO_2) radicals, from the degradation of VOCs, NO

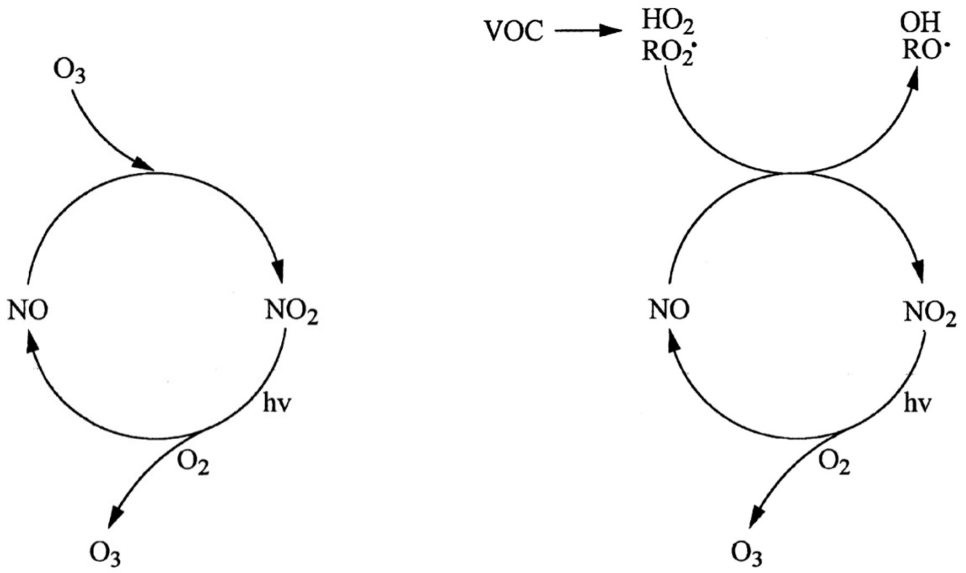

(a) Without VOCs present (b) With VOCs present

Figure 1.2: Schematic of O_3 formation reactions reproduced from Sillman (1999)

can be oxidised to NO_2 without the consumption of O_3. Upon photolysis of the NO_2, net formation of O_3 occurs (Figure 1.2b). For example, with methane:

$$CH_4 + OH \longrightarrow CH_3 + H_2O \quad \text{(R 1.4)}$$

$$CH_3 + O_2 \longrightarrow CH_3O_2 \quad \text{(R 1.5)}$$

$$CH_3O_2 + NO \longrightarrow CH_3O + NO_2 \quad \text{(R 1.6)}$$

HO_2 can also regenerate NO_2 by oxidising NO. HO_2 can be produced by the reaction of CO with OH, or as a by-product the degradation of VOCs.

$$CO + OH \longrightarrow CO_2 + H \quad \text{(R 1.7)}$$

$$H + O_2 \longrightarrow HO_2 \quad \text{(R 1.8)}$$

$$CH_3O + O_2 \longrightarrow CH_2O + HO_2 \quad \text{(R 1.9)}$$

$$HO_2 + NO \longrightarrow OH + NO_2 \quad \text{(R 1.10)}$$

Otherwise, if concentrations of NO are low, O_3 will be lost when it is photolysed, and the excited oxygen formed reacts with water vapour to form OH instead of reforming O_3.

Furthermore, O_3 loss results from the reaction with OH (as well as HO_2).

Daytime O_3 concentrations are therefore controlled by the concentration of NO_x (NO_x-limited regime), unless there is insufficient VOC concentration for net O_3 formation (VOC-limited regime). The rate of O_3 formation can be estimated if concentrations of NO_x and VOCs are known (Figure 1.3), however, formation rate is also effected by meteorological factors such as sunlight and humidity (Sillman, 1999). This has implications for pollution control, as the rate of O_3 formation is highly non-linear in response to its precursors. For example, reducing VOC emissions in a NO_x- limited regime will not initially result in reduced O_3 formation (Cohan et al., 2005). VOC-limited regimes are generally found in heavily polluted urban areas that are saturated with NO_x, whereas NO_x-limited regimes are found in suburban or rural areas (Finlayson-Pitts and Pitts, 1993). In NO_x-limited regimes, reducing VOC concentration will have no effect on the rate of O_3 formation (arrow A in Figure 1.3). In VOC-limited regimes, reducing NO_x increases O_3 formation (arrow B in Figure 1.3), due reductions in to 'NO_x titration' and loss of HO_x. NO_x titration occurs because NO_x emissions are primarily NO, which reacts with O_3 as shown in 1.2a. In the presence of high NO_x emissions, or at night, the rate of O_3 reformation by NO_2 photolysis is less than O_3 loss by reacting with NO (Sillman, 1999).

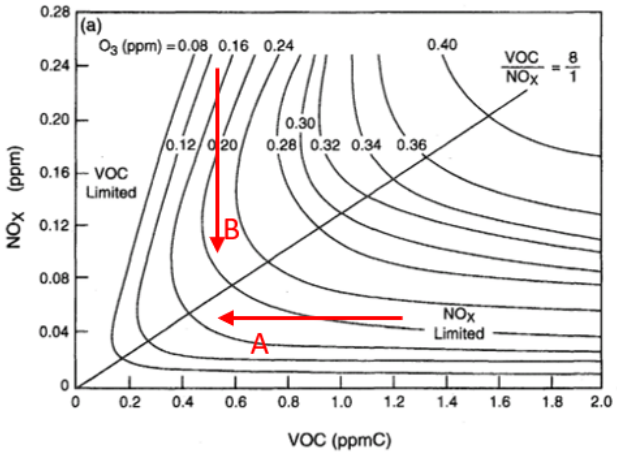

Figure 1.3: Peak O_3 isopleths generated from box model from initial mixtures of NO_x and VOCs in air. Adapted from Finlayson-Pitts and Pitts (1993)

At night, the chemistry of O_3 and nitrogen oxides differs, due to the absence of sunlight and consequent absence of OH radicals. NO is still oxidised by O_3 to NO_2, but cannot be photolysed back to NO. NO_2 can also be oxidised by O_3 to form the nitrate radical, NO_3. In the daytime, this is rapidly photolysed back to NO_2 or NO depending on light wavelength. At night, NO_2 can react with NO_3 to form N_2O_5, which can react heterogenously on aerosol surfaces with H_2O to form HNO_3. This is an important loss process at nighttime, when OH levels are low, and during winter, when nights are longer (Stavrakou et al., 2013). NO_3 and N_2O_5 act as reservoirs for NO_2 at night (Wayne et al., 1991; Brown et al., 2006). NO_x can also react with the peroxylacetyl radical, a product of VOC oxidation,

to form peroxyacetyl nitrate (PAN) (Singh and Hanst, 1981). PAN is relatively stable at low temperatures, so it can be transported over long distances at night, during winter or in the free troposphere, so acts as a reservoir for photochemically polluted air as it can decompose to reform NO_2 (Nielsen et al., 1981).

As well as its human health impact, O_3 is known to damage plants, causing an additional economic impact through decreased crop yields. Van Dingenen et al. (2009) estimated that in 2000, O_3 crop damage caused $14-26 billion of losses globally, around 20% of which occurred in China. Since 2000, East Asia has been the region with the strongest increases in measured tropospheric O_3 concentration (Fleming et al., 2018).

SO_2 is a toxic gas with natural and anthropogenic sources and is an air pollutant due to its toxicity and being the primary contributor to acid rain, while also being a major constituent of secondary aerosol, the sulphate fraction of which has a negative radiative forcing (Smith et al., 2001). The largest natural sources of SO_2 are volcanic and biogenic (Bates et al., 1992), whereas most of the anthropogenic SO_2 is released by coal burning, followed by oil burning, industrial processes and biomass burning (Smith et al., 2001). SO_2 acts as an irritant in the respiratory system, causing restriction of the airways which effects the lungs and heart rate (Tunnicliffe et al., 2001). Separating the health effect of SO_2 is difficult as concentrations usually co-vary with other pollutants such as PM and NO_2. Furthermore, there is no evidence that a threshold exists below which health effects are negligible (WHO, 2006).

Organic semivolatile compounds are emitted as gases, a volatile organic compound (VOC), and are aged by oxidisation by OH, O_3 and NO_2, forming less volatile compounds that condense onto aerosol particles (Seinfeld and Pandis, 2006). These compounds can contribute to the rapid growth of haze as they condense into aerosol particles (Peng et al., 2021).

Aerosols

Particulate matter, or aerosol, refers to a mixture of solid particles and/or liquid droplets that are suspended in air, and is constituted of a variety of natural and anthropogenic compounds. Aerosol can be primary, when it is emitted into the atmosphere directly as particles, or secondary, when particles condense from precursor gases (nucleation) or when gaseous compounds condense onto existing aerosol particles (condensation) (Boucher,

Table 1.1: Emission estimates by sectors in China, 2010 (derived from MEIC v1.2, www.meicmodel.org). Sector emission proportion expressed as percent, total column in Tg Adapted from Li et al. (2017b)

Species	Power	Industry	Residential	Transportation	Solvent use	Agriculture
SO_2	27	57	15	1	0	0
NO_x	34	34	6	26	0	0
CO	2	44	42	12	0	0
NMVOCs	0	35	22	10	32	0
NH_3	0	3	4	0	0	93
PM_{10}	6	39	52	3	0	0
$PM_{2.5}$	7	50	38	4	0	0
BC	0	34	50	16	0	0
OC	0	18	79	3	0	0

2015).

Aerosol particle diameters range from a few nanometres (nm), to around 100 micrometres (μm). The smallest particles are referred to as the nucleation and aitken modes (<100 nm), which represent particles that have condensed from the gas-phase and begin to grow by condensation. Particles with diameters of 0.1-2.5 μm are referred to as accumulation mode, which continue to grow by condensation as well as coagulation. Larger particles are referred to as coarse mode, and are emitted by mechanical processes such as dust suspension (Seinfeld and Pandis, 2006).

Zhang et al. (2012b) present the results of two years of speciated aerosol measurements from 16 sites across China, of the coarse fraction PM_{10}[1]. They find on average that 35% of PM_{10} is of mineral origin, which includes desert dust, fugitive dust and coal ash, which increases to 60% in Northwestern China, which contains large area of desert (Figure 1.4). Sulphate (SO_4^{2-}) and organic carbon (OC) each account for around 15% of total PM_{10}, nitrate (NO_3^-) 7% and ammonium (NH_4^+) 5%. In the finer aerosol fraction, $PM_{2.5}$[2], typically contains a higher proportion of the secondary species SO_4^{2-}, NO_3^- and NH_4^+, which can constitute 22-54% of $PM_{2.5}$ mass in megacity regions, while carbonaceous matter accounts for 27-42% (Chan and Yao, 2008).

1.1.2 Major sources of air pollution in China

China has the largest industrial output of any country in the world, having almost double that of the EU and triple of the US (CIA, 2016). As such, most industrial sectors are well

[1] this includes particles up to a diameter of 10 μm, which includes the fine fraction
[2] this includes particles up to a diameter of 2.5 μm

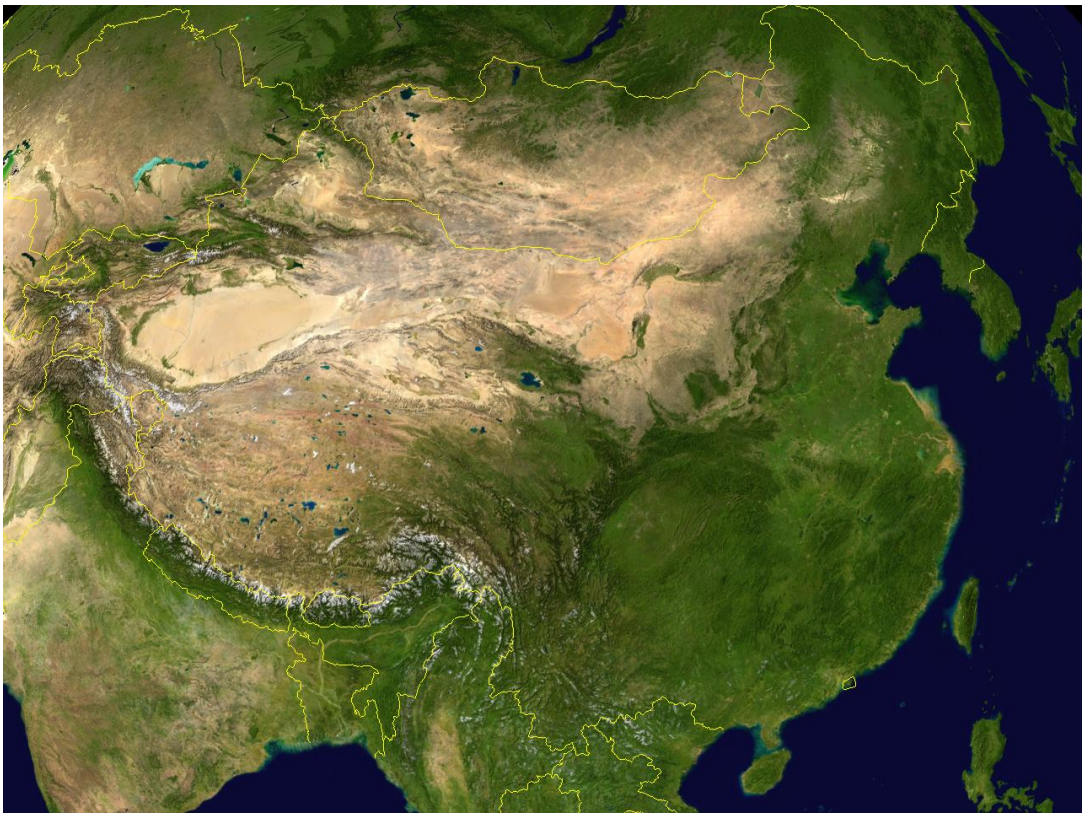

Figure 1.4: NASA satellite image of China. Shows location mountainous regions (the Tibetan Plateau), deserts and plains. Image is public domain and reproduced from Wikimedia Commons `https://commons.wikimedia.org/wiki/File:China_100.78713E_35.63718N.jpg`

represented, including cement, iron and steel manufacturing, which are heavily polluting. Industrial emissions are partly generated by fossil fuel burning in industrial boilers, which produces similar emissions to power generation (NO_x and SO_2), as well as by the industrial processes themselves, which can emit PM, CO, heavy metals and incomplete combustion products (Wang et al., 2016). Additionally, the petroleum industry is a significant emitter of VOCs, which occurs during their production, storage, transport and use as raw materials (Li et al., 2017b). The industrial sector is estimated to be the largest single contributor of emissions of SO_2 (57%), NO_x (34%), CO (44%), non-methane VOCs (NMVOCs) (35%) and $PM_{2.5}$ (50%) in 2010 (Table 1.1). Processes in the cement industry are particularly large emitters of primary PM, with Lei et al. (2011) estimating that it is responsible for 27% and 29% of $PM_{2.5}$ and PM_{10} all sector emissions respectively (Liu et al., 2021).

China is also the world's largest consumer of electricity, although in per capita terms it ranks 64th (Wikipedia Contributors, 2021). China's electricity demand is growing, but at an increasingly slower rate (1.1% in 2019) (BP, 2019). The majority of China's electricity is

generated by burning coal, the proportion of which has remained around 60% since 1990 (IEA, 2020). Coal typically contains 0.5-5% sulphur by weight, resulting in SO_2 emissions (Chou, 2012). NO_2 is also produced due to high combustion temperatures, as well as some PM (Liu et al., 2015) (Table 1.1).

The residential sector, i.e. domestic fuel burning for cooking and heating, produces CO, VOC, PM and black carbon (BC) emissions on a similar scale to the industrial sector, and is the major emitter of organic carbon (OC) (Table 1.1). Residential emissions comprise a high proportion of total emissions, despite a relatively low total energy consumption (<10%), as relatively low grades of fuel such as raw coal and crop residues are burned in a relatively inefficient manner (Li et al., 2017b). The health effects caused by emissions from the residential sector are greater, as they contribute to both indoor and ambient deterioration in air quality.

The transport sector is responsible for a high proportion of NO_x emissions, BC, CO and NMVOCs (Table 1.1). Its emissions are relatively low compared with the power, industry and residential sectors, but it contributes significantly to exposure due to emissions occurring in densely populated urban areas.

The agricultural sector emits the majority of ammonia, due to fertiliser use. The estimate shown in Table 1.1 does not include emissions from crop burning or agricultural vehicles and machinery (Li et al., 2017b).

1.1.3 Health effects

The harmful health impacts of air pollution was made clear by now notorious 20^{th} Century air pollution events in the US and Europe, such as the Donora Pennsylvania Smog in 1948 and the Great Smog of London in 1956, during which the healthy and vulnerable alike collapsed and died in the streets (Stanek et al., 2011). These events led to the first national air pollution control laws being passed (Jacobs et al., 2018), and also precipitated a host of toxicological and epidemiological studies aiming to understand and quantify the effects of air pollution on human health.

The World Health Organisation's Air quality guidelines

The WHO reviews the available literature on the health effects of air pollution to produce 'Air Quality Guidelines' (AQGs) for use by policy-makers worldwide. The pollutants

included are NO_2, SO_2, O_3, PM and CO. The AQGs are pollutant concentration thresholds above which evidence shows mortality increases. However for PM and O_3, there is no known threshold below which there is no safe concentration (Krzyzanowski and Cohen, 2008). For each pollutant species (except O_3), there are two different averaging times, which reflects the potential for acute and chronic health effects. The WHO also gives three interim targets that are less ambitious than the AQGs, i.e. they are higher concentration thresholds, 'to promote steady progress towards meeting [the AQGs]' (WHO, 2006).

Epidemiological evidence

Epidemiological studies estimate the health impacts of air pollution analysing longitudinal cohort datasets to isolate statistical relationships between air pollutant exposure levels and disease (Pope et al., 1995). Cohort studies track large groups (usually tens of thousands of people) over long stretches of time (decades), recording their incidences of morbidity and mortality. Across the cohort, pollutant exposure for each individual is estimated. Then, a statistical analysis is performed to adjust for confounding factors, such as age, sex, smoking and socioeconomic status, which isolates the change in risk resulting from air pollutant exposure (Dominici et al., 2003).

In epidemiology, exposure refers to 'a factor that may be associated with an outcome of interest' (Lee and Pickard, 2013). Epidemiological studies have often used air pollutant concentration time series from point monitoring networks to estimate exposure (Özkaynak et al., 2013). However, due to the high spatial and temporal heterogeneity of pollutant concentrations (see Figure 1.2), point measurements can only capture a limited portion of their variability, causing inaccuracies in exposure estimates. Using data from chemical transport models can give improved estimates of exposure (Conti et al., 2017), as they can estimate pollutant levels more generally over an area (i.e. a grid box of a Eulerian model), or more accurately over complex topographies (i.e. dispersion models). In reality, exposure levels may vary greatly according to the path individuals take through space and time among high levels of heterogeneity in pollutant concentrations. More accurate pollutant exposure estimates can be obtained using real-time exposure assessment methods, by tracking individuals with technologies such as mobile positioning data (e.g. GPS on mobile phones), and measuring their local ambient pollution levels using wearable pollution sensors (Fang and Lu, 2012).

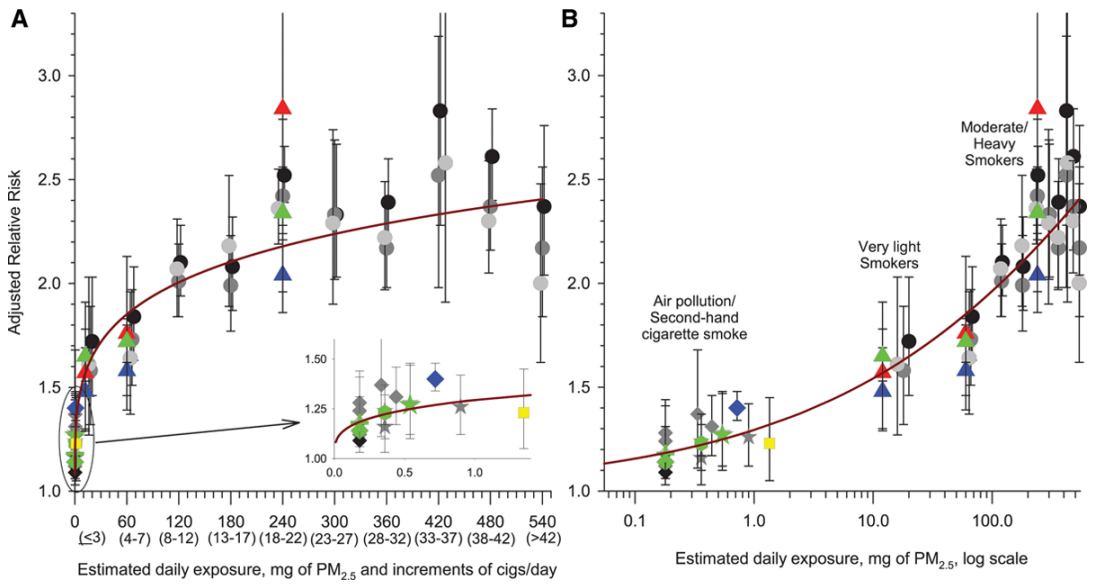

Figure 1.5: An illustration of an integrated exposure response curve for risk of cardiovascular disease and exposure to $PM_{2.5}$. Reproduced from Pope et al. (2018)

By combining multiple cohort studies of ambient pollutant exposure with first and second-hand smoking studies, relative risk for several diseases resulting from long-term $PM_{2.5}$ exposure can be estimated over the entire commonly-found range of annual mean concentrations (Burnett et al., 2014). This is referred to as an integrated exposure response (IER) curve (Figure 1.5), which was developed as part of the WHO as part of its Global Burden of Disease study. More recently, Burnett et al. (2018) have combined data from 41 cohorts to model the risk attributable to outdoor $PM_{2.5}$. Their model, the 'Global Exposure Mortality Model (GEMM),' can estimate risk over 97% of the global $PM_{2.5}$ exposure range, without the need for smoking studies. They could extend the estimate up to 84 $\mu g\,m^{-3}$ due to the inclusion of Yin et al. (2017), a study of a cohort of men in China.

There is sufficient epidemiological evidence to link ambient air pollution exposure to an increased risk of ischaemic heart disease, stroke, lung cancer, chronic obstructive pulmonary disease (COPD), and acute lower respiratory tract infections (Lim et al., 2012). The GEMM can be used to predict the individual burden of each disease type, as well as for non-communicable diseases along with lower respiratory infections. Burnett et al. (2018) estimates that in 2015, globally there were 8.9 million avoidable deaths attributable to ambient $PM_{2.5}$, with 2.47 million of these in China. From the minimum exposure of 2.4 $\mu g\,m^{-3}$, they find a supralinear association with risk up to ~15 $\mu g\,m^{-3}$, then a near linear exposure up to 84 $\mu g\,m^{-3}$.

Though the statistical epidemiology approaches described above represent the current

best available method of estimating air pollution-caused health effects from empirical evidence, there are several assumptions implicit in current studies. As the majority of ambient $PM_{2.5}$ measurements are total mass concentration, most epidemiological studies are unable to isolate the risk of individual components of aerosol (Kushta et al., 2018). This is referred to as the assumption of equal toxicity. Some studies that are able to estimate risk from separate components of aerosol, find significant differences in toxicity, e.g. Thurston et al. (2016) who find that $PM_{2.5}$ emitted by coal combustion has a ~5 times greater risk than $PM_{2.5}$ in general.

There is also epidemiological evidence to support a relationship between long-term ambient O_3 exposure and elevated mortality, with the GBD 2015 study attributing it 254 000 deaths (Cohen et al., 2017). Jerrett et al. (2009) used data from a US cohort study to model the effects of $PM_{2.5}$ and O_3 on mortality, finding that O_3 was associated with an increased risk of COPD independent of $PM_{2.5}$ exposure. However, they note the results from other studies were inconclusive. Subsequently, a larger cohort study, Turner et al. (2016), has also found significant associations with circulatory mortality.

As well as the epidemiological evidence, toxicological studies can elucidate the mechanisms by which air pollutants cause disease. Fine particulate matter is deposited in the lungs and can enter the circulatory system, triggering inflammatory responses that injure lung and heart tissues (Simkhovich et al., 2008). While O_3 in the stratosphere protects life from harmful UV radiation, in the inhalation of tropospheric O_3 damages the lungs as it is a strong oxidant (Mehlman and Borek, 1987).

1.2 Physicochemical processing of pollutants in the atmosphere

The determining factor influencing surface air quality is most often meteorological conditions rather that emissions alone (Jacob and Winner, 2009). This is demonstrated by the high explanatory power of statistical models that use meteorological variables to forecast air quality (Sousa et al., 2007; Tai et al., 2010; Grange et al., 2018).

The concentration of air pollutants is determined by the emission flux combined with atmospheric processes including transport, loss and/or production via chemical reactions and loss by deposition (Figure 1.6). While pollutant emissions directly impact surface air quality, they also peturb atmospheric chemistry, and have radiative forcing effects, either directly, or through the formation of secondary aerosols and O_3. Perturbations can further

affect emissions, atmospheric concentrations and sinks via feedback effects.

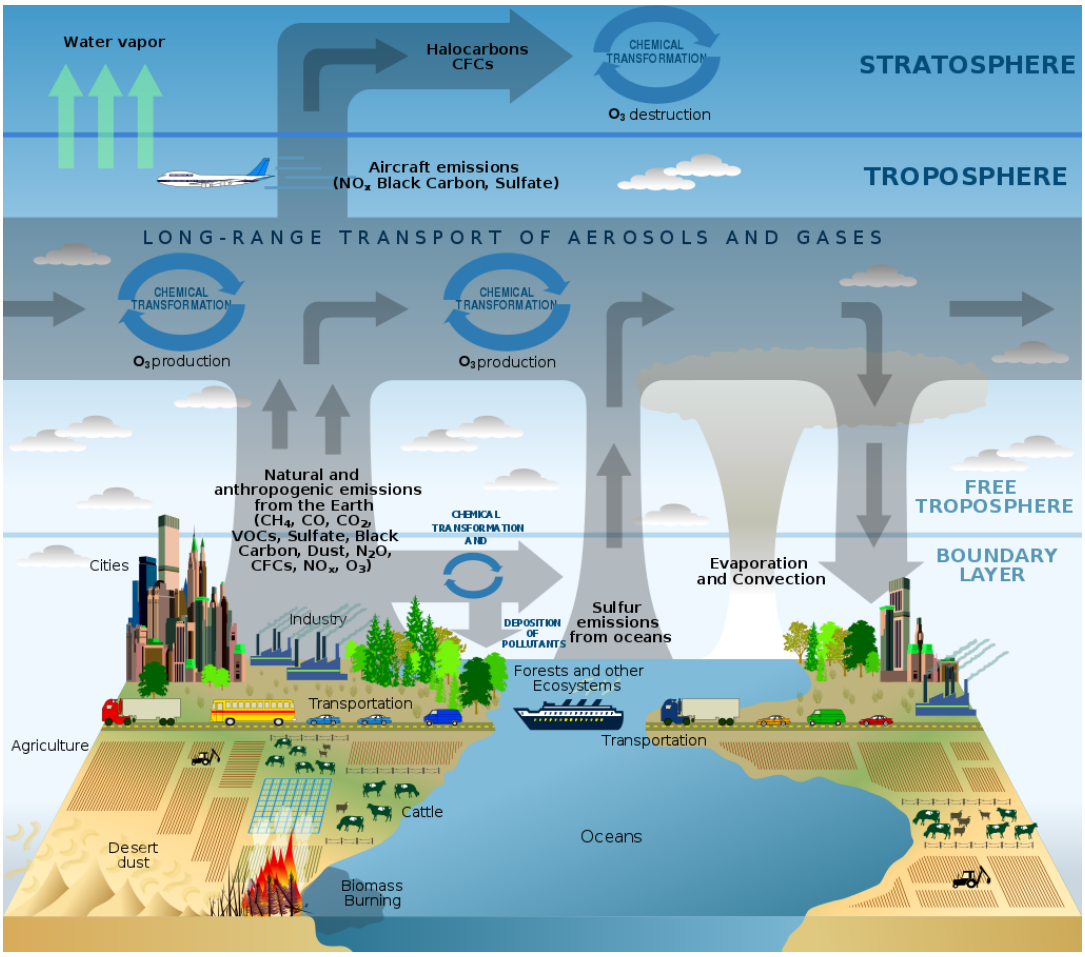

Figure 1.6: Schematic showing pollutant emissions sectors, transport, chemical transformation and loss processes in the atmosphere. Public domain image reproduced from `https://commons.wikimedia.org/wiki/File:Atmosphere_composition_diagram-en.svg`

1.2.1 Dispersion and transport

Pollutants are mainly emitted at or close to the Earth's surface. Atmospheric stability dictates whether polluted air is well mixed through the troposphere or trapped closer to ground level. In the daytime, convection driven by solar heating causes the lower portion of the atmosphere to be unstable, mixing pollutants away from the surface (the 'mixed' layer). Solar heating is reduced under cloudy conditions, and not present at night, and radiative cooling of the surface leads to more stable conditions that trap pollutants in a shallower mixed layer, under a temperature inversion. The pollutant species of NO_x, SO_2, tropospheric O_3 and aerosols can have atmospheric lifetimes in the order of hours to weeks, meaning that they can be advected through the atmosphere at local and regional scales (Seinfeld and Pandis, 2006), which can enhance pollutant levels downwind

of sources (Nevers, 1999).

The degree of dispersion of air pollutants varies regionally within China. Areas of greater solar radiation, such as the northwestern desert regions (see Figure 1.4), have deeper boundary layer heights than eastern regions in the summer, but experience subsidence in the winter (Su et al., 2018; Guo et al., 2019). Shallow boundary layers, capped by strong temperature inversions and stagnant conditions are implicated in causing winter haze episodes in eastern China, which are also amplified by terrains that limit dispersion (Zhao et al., 2013; Guo et al., 2014; Zhang et al., 2015).

Certain synoptic meteorological situations have been associated with both reducing local dispersion of pollutants and increasing long-range transport. During December to February, the winter monsoon causes widespread cold fronts to move south. The winter monsoon is often implicated in advecting heavier air pollution from northern regions to central and southern regions, where it can transport pollutants such as $PM_{2.5}$ over 2000 km in 2 days (Wang et al., 2017; Qin et al., 2016). Radiosonde measurements and model simulations show that pollutants from northern regions can be advected into the free troposphere, transported southwards, then subside back to the surface, where they contribute significantly to local pollution (Shi et al., 2020; Kang et al., 2019). The passage of a cold front also creates a strong capping inversion and reduces the mixed layer height, which increases humidity, creating ideal conditions for secondary aerosol formation (Peng et al., 2021).

Another synoptic driver of air pollutant dispersion in China are large-scale circulation features such as the summer monsoon and typhoons. The northwards procession of the summer monsoon through east China brings heavy rainfall and clean oceanic air masses, enhancing ventilation, which reduces $PM_{2.5}$, CO and O_3 during June to August, with high concentrations returning in its wake (Zhang et al., 2010; Zhao et al., 2010). The distant passage of a typhoon near Taiwan or Japan can induce subsiding air masses over southern China, causing heatwaves, low wind speeds and rainfall, which leads to poor air quality events during late summer to early autumn (Jiang et al., 2015; Chow et al., 2018).

1.2.2 Aerosol growth and formation

The formation and loss rates of aerosols in the atmosphere are dependent on the physical and chemical state of the atmosphere, i.e. temperature, humidity and the vapour pres-

sure of gases (Boucher, 2015). The formation of secondary aerosols accounts for a large proportion of $PM_{2.5}$, estimated as 30-77% in Chinese megacities (Huang et al., 2015; Wang et al., 2019).

Nucleation is the process by which new aerosol particles are formed in the atmosphere from precursor gas-phase species. Under the right conditions, nucleation can produce sudden bursts of tiny (1-3 nanometre) new particle formation (NPF), that grow further by condensation and coagulation (Lee et al., 2019). The nucleation of sulphuric acid is central to NPF (Kulmala and Kerminen, 2008), where H_2SO_4 forms from the reaction of SO_2 and OH, with nucleation rate depending on temperature, humidity, and the concentration of other species such as NH_3 and O_3 (Li et al., 2017a). There is also evidence that nucleation of semi-volatile organic species can produce NPF (Metzger et al., 2010; Tröstl et al., 2016). NPF tends to occur in relatively clean conditions, as the resulting aerosol particles subsequently grow by scavenging NPF precursors (Yao et al., 2018). However, measurement campaigns in Chinese megacity regions also observe frequent NPF events (Xiao et al., 2015; Wu et al., 2007; Guo et al., 2014).

The dominant process for transfer of mass from gas-phase species into aerosol particles is by condensation of semivolatile compounds such as H_2SO_4 and organic compounds onto existing aerosol particles (Boucher, 2015). Although sulphate is key to forming new particles, large fractions of $PM_{2.5}$ in China are found to be organic (Huang et al., 2015). The rate of condensation of semivolatile organics into aerosol particles is influenced by temperature, which controls their volatility and the rate at which they are oxidised (Stolzenburg et al., 2018). Hygroscopic growth of aerosols, which is partly dependent on atmospheric relative humidity, can influence the rates of chemical reactions within particles, condensation rates and physical properties (Duplissy et al., 2011; Wang et al., 2019). The contribution of secondary aerosol formation from organic compounds, nitrates, sulphate and ammonia is greater than the contribution from primary emissions during stagnation-induced haze events (Sun et al., 2019; Peng et al., 2021).

1.2.3 Sinks

Trace gases and particles in the atmosphere are removed ultimately by either dry or wet deposition. Dry deposition is the 'transport of gaseous and particulate species from the atmosphere onto surfaces in the absence of precipitation' (Seinfeld and Pandis, 2006). Rates of dry deposition onto different surfaces (e.g. urban, cropland, forests) are determined

experimentally and quantified as roughness lengths.

Another important meteorological process for air quality is precipitation (or lack thereof). Particles with diameters >0.1 μg can be captured by drops in clouds or by falling drops (Nevers, 1999). Wet deposition is the main atmospheric sink for PM (Jacob and Winner, 2009). Over 80% of BC particles are lost by wet deposition (Koch et al., 2009).

1.2.4 Feedbacks

Aerosol emissions and formation result in a direct radiative forcing effect, which can be positive, as some aerosols (e.g. black carbon) absorb solar radiation, or negative when the aerosol scatters light (e.g. sulphate, nitrate, organic carbon). Estimates tend to agree that the net direct radiative forcing from primary anthropogenic aerosols is negative (Myhre, 2009). As well as the direct effect due to forcing from aerosol emissions generated, aerosols also effect climate by changing cloud reflectivity and patterns of cloud formation, which are termed aerosol-radiation and aerosol-cloud interactions (Boucher et al., 2013). These occur due to radiative forcing from aerosols which effects atmospheric stability, and their ability to change the properties of clouds (Johnson et al., 2004; Lohmann and Feichter, 2004).

High aerosol loadings in the boundary layer can scatter and reflect incoming radiation, reducing heat flux into the boundary layer, which makes it more stable, and consequently can amplify pollutant build-up and formation (Li et al., 2017d). Black carbon is an absorbing aerosol, and when concentrations are enhanced in the upper boundary layer, heating can favour formation of a temperature inversion, which depresses the boundary layer and traps pollution (Ding et al., 2016).

Increased aerosol loading over China and East Asia may also be weakening the summer monsoon, which results in lower rainfalls in the more polluted northern China regions, and lower ventilation during monsoon season throughout the east coast (Zhao et al., 2010; Zhu et al., 2012). There has been a shift in precipitation across China with the south becoming wetter and the north drying, which has been partly attributed to positive forcing effect of black carbon aerosols (Ramanathan and Carmichael, 2008). A 35 year record of surface wind speed measurements in China shows there is a declining trend (Guo et al., 2011).

1.2.5 Seasonal variability

With the exception of O_3, air quality is worse in the winter in China, mainly due to the combination of increased fuel (particularly coal) consumption for heating, together with more stagnant meteorological conditions, and reduced precipitation (Lou et al., 2019). Emissions also vary seasonally, with emissions resulting from heating and residential sectors being elevated in the winter (Zhang and Smith, 2007). There is also seasonal variability in biomass burning, which peaks at various times of year during spring to summer in different regions of China (Streets et al., 2003). Agricultural fertiliser application peaks in the summer, which induces seasonal variability in ammonia emissions (Huang et al., 2012). Biogenic emissions of VOCs such as isoprene tend to peak in the summer, when temperatures are highest (Palmer et al., 2006).

Seasonal variability in pollutant concentrations is also driven by seasonal meteorological variability. For example, the rate of O_3 formation increases under warmer temperatures and greater UV radiation, partly explaining its summer peak (Steiner et al., 2010; Xu et al., 2011). In the case of NO_x, its summer minimum is partly explained by a shorter chemical lifetime due to higher OH concentrations (Uno et al., 2007).

1.3 Numerical air quality modelling

As explained in the previous section, atmospheric pollutant concentrations depend on the complex interactions of physical and chemical processes. Numerical models of atmospheric chemistry are an attempt to represent these processes mathematically. They allow us to test theories of atmospheric physics and chemistry, simulate past and future scenarios, and provide estimates of air pollutant concentrations with high spatial and temporal coverage. However, as the saying goes: 'all models are wrong, but some are useful (Box, 1979)', so it is essential to validate models by comparing their predictions with observations.

Numerical models draw upon a wide scope of scientific knowledge to construct a set of equations that serve to approximate concentrations of gases and aerosols in the atmosphere. These range from the fundamental, physical laws, such as conservation of mass, the ideal gas law, and Newton's laws of motion; to the empirically derived such as chemical reaction rates, parametrisations of turbulent processes and interactions with the land surface. Additional input data required are estimates of pollutant emission volumes, land

surface maps and and an estimate of initial and boundary conditions for the model to evolve from (Brasseur and Jacob, 2017).

1.3.1 The WRF-Chem model

The Weather Research and Forecasting Model with Chemistry (WRF-Chem) is a regional numerical air pollution model. Simulating a region allows for a higher model resolution and more complex chemistry to be used than in a global model, due to computing restraints. 'Fully-coupled' refers to the simultaneous simulation of the model physics (i.e. meteorology) and chemistry (i.e. emissions, transport, deposition, chemical transformation, aerosol interactions, photolysis and radiation), which allows physiochemical interactions and feedbacks to be captured (Grell et al., 2005).

Separate modules within WRF-Chem are used to provide emissions within the domain for anthropogenic, biogenic, dust and fire sources.

A gridded inventory file is used to provide the anthropogenic emissions input within the domain, of species including primary aerosols (including inorganic and organic species), NO_x, SO_2, CO, NH_3 and VOCs. These emissions are estimated using a bottom-up emission inventory technique, that involves mapping sources, estimating their activity and accounting for the effect of any control equipment. For China, the Multi-resolution Emission Inventory for China (MEIC) inventory provides recent estimates of anthropogenic emissions using a database of point sources such as power and cement plants, county-level vehicle emission estimates, estimates of residential emissions using national survey data, and shipping emissions using dynamic shipping data (Li et al., 2017b).

Biogenic emissions are calculated online (i.e. they depend on modelled meteorology) using the Model of Emissions of Gases and Aerosols from Nature (MEGAN) (Guenther et al., 2006). MEGAN combines a mapping of plant functional types and their emission activities of species such as isoprene, with the meteorological input variables of temperature, sunlight [3], humidity, wind speed and soil moisture.

Dust emissions are also calculated online by combining a map of vegetation cover and soil types, with empirically based parametrisations that estimate dust emissions based on meteorological and land-surface parameters such as friction velocity, roughness length and soil moisture (Kang et al., 2011; LeGrand et al., 2019).

[3] specifically photosynthetic photon flux density

Biomass burning emissions are estimated from satellite observations of fires. The locations of fire hotspots are referenced with a map of land-use classifications, and empirically derived emission factors to estimate the emissions of air pollutants (Wiedinmyer et al., 2011).

At each timestep, the model must solve equations that calculate the production and loss of chemical species in each grid box that result from chemical reactions and advection (Brasseur and Jacob, 2017). Due to computational limits, chemical solvers must represent only a subset of all the known atmospheric chemical reactions and their rates. As computers grow more powerful, a greater number of species can be represented. For example, in the first version of the Model of Ozone and Related chemical Tracers (MOZART), 46 gas-phase species, 28 photolysis reactions, and 112 kinetic reactions were represented, but in the newest version this has increased to 151, 65, 287 (Emmons et al., 2020). Processes that occur at scales smaller than a model grid cell are parametrised rather than explicitly simulated. Such processes include deep convection, wet scavenging and lightning (Brasseur and Jacob, 2017).

1.4 Air Quality Monitoring

1.4.1 In-situ measurements

Direct measurements of air pollutant properties using an instrument samples the air in its vicinity are known as 'in-situ measurements.' The majority of in-situ measurements are taken from ground level monitoring stations, but measurements can also be taken above the surface, using balloons, sondes and aircraft. The non-profit organisation 'OpenAQ' (`openaq.org`) collects, visualises and disseminates air quality data from monitoring stations across the world. Measurement of air quality has become increasingly widespread, and OpenAQ now have data from over 130 countries, which now includes over 12 000 locations where reference grade measurements are taken at surface monitoring stations.

In China, a network of over 1600 urban air quality monitoring stations has been established by the China National Environmental Monitoring Centre ('the CNEMC network'). The CNEMC's monitoring stations measure ambient concentrations of $PM_{2.5}$, PM_{10}, NO_2, SO_2, O_3 and CO. In this section air quality monitoring techniques will be introduced, with reference to the equipment used in the CNEMC network. The history of air quality monitoring in China will be discussed in Section 1.5.3.

Aerosol measurements

Early mass measurements of atmospheric aerosols were performed by the gravimetric technique, which remains in use today. Aerosol collected on the filter of known mass, is left to equilibrate for a standard length of time (e.g. 24 hours), in a temperature and humidity-controlled environment, and then the filter is weighed (Watson et al., 2017). Gravitational measurement methods cannot measure aerosol in real-time, often taking weeks-months to process filters, and may need longer (several hours-days) measurement periods to collect enough aerosol for an accurate measurement (Chung et al., 2001).

More recently, newer methods allow measurement of aerosol mass continuously in real-time. In the CNEMC network $PM_{2.5}$ and PM_{10} are measured using 'beta attenuation' (BA) or 'tapered element oscillating microbalance' (TEOM) monitors (Guo et al., 2017). In BA monitors, aerosol is collected on filter tape, and the amount of β radiation that is attenuated as it passes through the aerosol is measured, and the aerosol mass is derived by calibration of the BA rate with gravimetrically measured aerosol (Macias and Husar, 1976). The TEOM measures the mass of aerosol by detecting the frequency of an oscillating tapered tube, with a filter on which aerosol is collected at its end. The TEOM is calibrated by placing a known mass on the filter (Patashnick and Rupprecht, 1991).

Comparison of the three measurement techniques shows some discrepancies that depend on the aerosol composition and meteorological conditions, particularly the humidity (Triantafyllou et al., 2016). In BA and TEOM monitors, aerosol samples are heated to evaporate liquid water, but this process may also evaporate the semi-volatile organics content of the aerosol (Hauck et al., 2004).

As well as measuring the mass concentration of a size fraction of aerosol, aerosol mass spectrometry (AMS) can be used to identify the concentrations of individual aerosol species. Such speciated concentration measurements are less frequent, due to the relatively high cost of the equipment used (Nash et al., 2006). AMS measurements differentiate the major non-refractory fractions of aerosol, e.g. organic (OA), sulphate, nitrate and ammonium. The organic fraction can be further characterised by elemental analysis, which yields the ratios of C, O, N and H atoms in the OA (Aiken et al., 2007). By analysing elemental ratios, inferences can be made about organic aerosol sources and ageing Huang et al. (2011). Further analysis of AMS results using the Positive Matrix Factorisation (PMF) technique (Reff et al., 2007; Ulbrich et al., 2009), can group the spec-

tra into factors that are associated with particular sources. For example, Song et al. (2006) use PMF analysis of filter measurements to apportion $PM_{2.5}$ into eight sources: biomass burning, secondary sulfates, secondary nitrates, coal combustion, industry, motor vehicles, road dust and desert dust. See Li et al. (2017c) for a review of speciated aerosol measurements in China.

Gaseous pollutants

Various monitors are used to measure the concentrations of NO_2, SO_2, O_3 and CO throughout the CNEMC network. The ambient air quality standard detailing air quality measurement protocols (GB3095-2012), issued by the Ministry for Environment Protection in 2012 (now Ministry for Ecology and Environment) is only available in Chinese. Zhao et al. (2016b) report that SO_2 is measured using the ultraviolet fluorescence method, NO_2 using the chemiluminescence method, O_3 using ultraviolet spectrophotometry, and CO is measured using infrared absorption.

Measurement error in the CNEMC network

Several sources of measurement error exist in pollutant concentration time series. Wu et al. (2018) analysed data from the CNEMC network and found several types of measurement error. These are:

- Periods of low variance caused by instrument malfunction, such as when the instrument pump is stuck or filter tape depleted.
- Periodic outliers that occur every 24 hours and are caused by erroneous measurements taken during calibration.
- Occasions when $PM_{2.5}$ values are greater than PM_{10}, which is caused by the lower accuracy of PM_{10} monitors, which are often 10 years older than the $PM_{2.5}$ monitors.

They develop an automatic outlier detection method, and during 2014-2016, they estimate 0.92% of $PM_{2.5}$, 5.68% of PM_{10}, 0.73% of SO_2, 0.65% of NO_2, 1.03% of CO, and 0.86% of O_3 hourly measurements are outliers caused by measurement error.

1.4.2 Remote sensing of surface pollutants

Aerosol pollutants

Remote sensing of aerosols relies on their ability to absorb and scatter light, which can be measured from the ground or space. The light extinction can be 'inverted' using physical equations to provide an estimate of aerosol concentrations (Boucher, 2015). The amount of light blocked by aerosols (light extinction) is known as the aerosol optical depth (AOD), and ground-based measures of AOD give some of the earliest estimates of trends in aerosol concentrations in China (and the world). The AErosol RObotic NETwork (AERONET) provides global coverage of ground-based AOD measurements, which can be used to validate the satellite retrievals of AOD, together providing high spatial coverage (Sinyuk et al., 2020).

The validated satellite AOD products can be used to estimate surface PM concentrations, using statistical modelling. Statistical models are built to relate AOD, and other predictors such as land use data and meteorology, to surface measured and simulated PM values. Van Donkelaar et al. (2016) used this technique to generate a global gridded estimate of $PM_{2.5}$ concentrations. Ma et al. (2016) applied a similar technique in China, to generate a record of $PM_{2.5}$ concentrations, extending back to 2004, before widespread air quality measurements were available.

Gaseous pollutants

Spectrometers such as the Ozone Monitoring Instrument (OMI), aboard NASA's Aura Satellite can provide high global coverage of trace gases including NO_2, SO_2 and O_3 (Levelt et al., 2006). Aura is in a sun-synchronous orbit, meaning that it passes over the same location on the Earth's surface at the same time each day. OMI operates at nadir, meaning it peers downwards through the atmosphere, so generating spectra that represent the combined tropospheric and stratospheric absorptions.

The vertical column density (VCD) of tropospheric NO_2 is separated by an algorithm which combines data from a global chemical transport model (TM4), surface elevation and albedo data, and meteorological analysis data (Boersma et al., 2011; Geffen, 2016). Satellite derived VCDs of NO_2 have been used to validate emission estimates from power stations (Wang et al., 2012) and validate emission inventory trends (Zhang et al., 2012a; De Foy et al., 2016). VCDs can be used as an independent variable in a statistical modelling

of NO_2 surface concentrations, which can be validated using surface measurements (Zhan et al., 2018).

SO_2 columns can be retrieved from OMI measurements by a similar process (Krotkov et al., 2006). They have been used to observe regions of heavy pollution in China (Krotkov et al., 2008), estimate emissions via inverse modelling (Qu et al., 2019) and estimate trends in ground level SO_2 concentrations (Zhang et al., 2021).

1.5 Air quality Trends in China

1.5.1 Evolution of air quality control policy in China

China's rapid economic development began in earnest after the death of Mao Zedong in 1976, which ended the Cultural Revolution period. During Mao's rule, attempts to increase agricultural and industrial productivity through radical, utopian reforms led to widespread environmental destruction, while the chaos and famine caused by the Cultural revolution restricted economic growth (Field, 1986; Shapiro, 2001). Though environmental damage by deforestation and soil degradation during this period was immense, it is likely that ambient air quality was better relative to the subsequent decades, as electricity generation, industrial production and vehicle ownership were a small fraction of current levels (Levine et al., 1992). Of China's cumulative CO_2 emissions, 92% have occurred since 1976 (Ritchie and Roser, 2017). However, individual exposure to harmful air pollution would have been high during the industrial efforts of the 'Great Leap Forward' (1958-1962) where as many as 90 million people took part in 'backyard steel smelting' (Shapiro, 2001), and conditions in factories were poor (Orleans and Suttmeier, 1970).

Mao's successor, Deng Xiaoping ushered in a period of economic reforms and relative stability. During the next 40 years, China's gross domestic product increased by over 75 times (The World Bank, 2021). As with most countries (Churchill et al., 2018), China's environmental degradation has subsequently followed a typical 'Environmental Kuznets Curve' inverted U-shaped trajectory (Wu et al., 2014; Li et al., 2016). China's economic growth has been tightly coupled with a rise in energy consumption (Azomahou et al., 2001; Shiu and Lam, 2004; Næss and Høyer, 2009), the demand for which has been met mostly by fossil fuel combustion, driving an increase in CO_2 emissions, of which it is now the world leader (Gregg et al., 2008).

China began its modern environmental protection efforts after sending a delegation to the 1972 United Nations Stockholm Conference on the Human Environment (Feng and Liao, 2016). In 1979, China introduced the Environmental Protection Law, which gave the Environmental Protection Bureau powers to supervise industrial air pollutant emissions and levy fines for non-compliance with limits (Feng and Liao, 2016), but during reforms in 1982-1983 it was made subservient to the Ministry of Construction, which set back any enforcement of environmental policies well into the 1990s (Muldavin, 2000). In 1982, China first established its National Ambient Air Quality Standards (NAAQS), which have been continuously tightened since (Zhao et al., 2016a). In 1987, the 'Air Pollution Prevention and Control Law' was adopted, which fines for exceedance of emission limits, but enforcement of its 'broad but vague' articles was generally lax (Alford and Liebman, 2001).

During this period of transition to a market-based economy, China prioritised economic growth, with environmental controls lagging behind, pursuing 'pollute now, control later,' policies (Pang et al., 2019), with government campaigns running with slogans such as 'Development is the fundamental principle' and 'Gold mines override clean water and green mountains' (Zhang et al., 2016).

Despite having developed a comprehensive environmental legal framework to control pollution during the 1980s and 1990s, most control methods were not widely enforced until the 2000s (Florig et al., 2002; Beyer, 2006). In 1998, sweeping reforms promoted the environmental protection administration to ministerial level (Jahiel, 1998). Early efforts focussed on reducing SO_2 emissions that were causing severe acid rain, by establishing the 'Two Control Zones,' in which measures such as installing flue gas desuphurisation (FGD) control equipment and limiting the production of high-sulphur coal were stipulated (Hao et al., 2001). However, enforcement was weak, and there was a surge in coal production during 2002-2006, during which acid rain worsened (Schreifels et al., 2012). The 11^{th} Five Year Plan (FYP) in 2006 finally made emissions reduction targets mandatory for local governments, and emissions began to decline (Lu et al., 2020a). By 2010, there were FGD facilities installed at 86% of coal-fired power plants.

Other enforcement measures were gradually strengthened, included the banning of vehicle imports and use that did not meet emissions standards, and the increase of fines and punishment for non-compliant industrial polluters (Feng and Liao, 2016).

Economic growth, measured by GDP, remained the most important factor in the perfor-

mance appraisals that control promotion of local government officials within the Communist Party (Li and Zhou, 2005). But since the 11th FYP (2006-2010), quantitative environmental targets, including meeting the NAAQS, have become a mandatory 'veto factor' for promotion (Jin et al., 2016), though they remain unimportant compared with economic targets (Feng et al., 2018).

During the winter of 2012-13, particularly widespread and severe air pollution events caused public outcry (The Guardian, 2013), with the government responding by issuing an air quality action plan to further strengthen air quality improvement legislation. Controlling air pollution and wider environmental reform is one method by which the Chinese Communist Party maintains legitimacy (Flatø, 2021). Key measures during the 2010s have been implementing more stringent emissions standards for power and industrial plants, phasing out of smaller inefficient industrial plants, replacing residential coal burning with electricity and natural gas, and further strengthening of vehicle emission standards (Zheng et al., 2018a).

Another driver of environmental damage in China is the export of dirty industrial processes downstream to less developed countries. As highly developed countries improved their own environmental standards, they increased their imports from China, thus relocating their emissions (Guan et al., 2014; Zhang et al., 2017b). Some of this is transported back to the receiving country via transnational or transcontinental transport (Wild and Akimoto, 2001; Lin et al., 2014). In turn, investment by China abroad, as its environmental and labour regulations improve, could result in the transfer of polluting industries to less developed countries.

Since around 1990, China's energy efficiency has been improving (Guan et al., 2008), and it now looks set to deliver early on its Paris Agreement commitment to peak CO_2 emissions by 2030 (Green and Stern, 2017). In 2020, China committed to be carbon neutral by 2060 (McGrath, 2020). China's carbon emission mitigation efforts are predicted to have substantial co-benefits to its air pollutant emissions (Dong et al., 2015; Li et al., 2019; Peng et al., 2017)

1.5.2 Emissions trends

Attempts to estimate air pollution emissions in China began in the early 1990s, prompted mainly by concerns of acidifying pollutants and CO_2 emissions. The first emission inven-

tory of Asian SO_x and NO_x emissions was carried out in 1991 (Kato, 1996), and contains provincial level estimates of China's SO_x and NO_x emissions during 1975-1987. They estimated that in 1975, China was already the largest emitter of SO_x (10.1 Tg yr^{-1}) and NO_x (3.7 Tg yr^{-1}) in Asia. By 1987, they estimate that China's emissions of both species had doubled. This inventory was made available in 1x1 degree gridded format (Akimoto and Narita, 1994). Despite early regulation attempts in China, SO_2 emissions continued to grow, with Streets et al. (2000) estimating that emissions reached 27.0 Tg yr^{-1} by 1997, while NO_x had reached 12.0 Tg yr^{-1} in 1995 (Streets and Waldhoff, 2000). NO_x emissions continued to grow, with the MEIC inventory estimating that in 2010 they had reached 34 Tg yr^{-1} (1.1), before peaking around 2012 and decreasing to 22 Tg yr^{-1} by 2017 (Zheng et al., 2018a). Zheng et al. (2018b) also report a decline in SO_2 emissions by over half in under a decade, decreasing from 27.8 in 2010, to 10.5 Tg yr^{-1} in 2017.

1.5.3 Measured air quality trends

Figure 1.7: Provinces and provincial capital cities of China.

Official government reports of China's air quality date back to at least 1981, and give annual mean estimates of air quality up to the present day. However, during these four

decades, China's air quality monitoring network has gone through substantial changes. Spatial coverage and frequency of monitoring stations has increased (Zhang et al., 2020), as well as the temporal frequency. Monitoring protocols and equipment has been updated several times.

Until 2012, air quality monitoring equipment was under the control of provincial and municipal environmental protection bureaus (EPB). EPBs were under the control of local party officials, who relied on good environmental performance for promotion in the Cadre Evaluation System. This created an incentive for EPBs to misreport air quality data to achieve targets, such as the 85% blue sky days target, the effects of which are detectable in data from this period (Andrews, 2008; Ghanem and Zhang, 2014)

Reliability of post-2012 measurements has improved (Liang et al., 2016; Stoerk, 2016), as the monitoring network was 'federalised' i.e. taken out of the control of local EPBs, with the data being directly relayed to the Ministry of Ecology and Environment (MEE). Anomalies detected in the data (as a result of monitoring error) have decreased during 2014-2016 (Wu et al., 2018). Data availability has improved, as air quality measurements went from being only available in statistical yearbooks, to being displayed in real-time on an official website. However, access to historical data is still restricted, as reported by OpenAQ as of July 2020, key criterea for the CNEMC data to be considered 'open' are not met (OpenAQ, 2020).

Despite the improvements, an incentive remains for local officials to tamper with monitoring stations, and fraud attempts are regularly detected and punished with fines and imprisonment. The central government is attempting to crack down on fraud, and began to conduct surprise inspections in 2017, resulting in the disciplining of 12 000 local officials and more than $130 million in fines (Turiel and Kaufmann, 2021). Turiel and Kaufmann (2021) analysed CNEMC data between 2015-2017 and found statistical evidence of under-reporting of $PM_{2.5}$ concentrations during air pollution events by comparing CNEMC monitors to those operated by US consulates.

Aerosol trends

In the 1980s and 1990s, most of the aerosol measurements taken in China were of total suspended PM, (TSP), followed by PM_{10} measurements being introduced during 2000-2005, and $PM_{2.5}$ during 2008-2012 (Zhang et al., 2020). He et al. (2002) report a 3% yr^{-1}

decline in TSP during 1990-1999. Zhang et al. (2020) report a summary of official reports, indicating that annual mean TSP concentrations fell from 702 $\mu g\,m^{-3}$ in 1981 to 258 $\mu g\,m^{-3}$ in 2000, after which monitoring was switched to PM_{10}, which fell from 113 $\mu g\,m^{-3}$ in 2000 to 71 $\mu g\,m^{-3}$ in 2017.

Prior to the establishment of the CNEMC network in 2012, there were few measurements of $PM_{2.5}$ trends, but satellite and modelling studies suggest its concentrations generally increased until around 2011. Using satellite data Van Donkelaar et al. (2016) estimate the trend in $PM_{2.5}$ in Beijing was 2.4 $\mu g\,m^{-3}\,yr^{-1}$ during 1998-2012, and a trend of 1.63 $\mu g\,m^{-3}\,yr^{-1}$ in the East Asia region [4]. Peng et al. (2016) used satellite data and found trends of 2.21 $\mu g\,m^{-3}\,yr^{-1}$ in the polluted megacity regions (see Figure 1.1) of China during 1999 to 2011. 1998-2012 trends were estimated by Han et al. (2015) as 1.83 $\mu g\,m^{-3}\,yr^{-1}$ in urban areas and 1.71 $\mu g\,m^{-3}\,yr^{-1}$ in cropland.

Then, satellite studies observe the peaking of $PM_{2.5}$ concentrations, with Ma et al. (2016) finding a trend of 1.97 $\mu g\,m^{-3}\,yr^{-1}$ during 2004-2007, follow by -0.46 $\mu g\,m^{-3}\,yr^{-1}$ during 2008-2013. Lin et al. (2018) estimated $PM_{2.5}$ mean concentrations of 0.04 $\mu g\,m^{-3}\,yr^{-1}$ during 2001-2005, -0.65 $\mu g\,m^{-3}\,yr^{-1}$ during 2006-2010, and -2.33 $\mu g\,m^{-3}\,yr^{-1}$ during 2011-2015. Xue et al. (2019) estimated the national peak to have occurred during 2008-2013, with 2000-2007 having a trend of 2.01 $\mu g\,m^{-3}\,yr^{-1}$ and 2013-2016 of -4.5 $\mu g\,m^{-3}\,yr^{-1}$.

The steep negative trend in $PM_{2.5}$ across China continued to be observed by the CNEMC network during 2013-2018, with Kong et al. (2021) estimating a nationwide trend of -5.8 $\mu g\,m^{-3}\,yr^{-1}$.

Ozone

The earliest estimates of an ozone trend in China originate from long term monitoring conducted at background sites. This includes the positive trend of 0.58% yr^{-1} during 1994-2007 at a coastal background site in Hong Kong (Wang et al., 2009), and the positive trend of 0.24-0.28 ppbv yr^{-1} recorded at Mount Waliguan, which is located at 3.8 km above sea level on the Tibetan plateau.

The Tropospheric Ozone Assessment Report (TOAR) used data from 557 monitoring stations in East Asia to calculate the summer trend in daily mean O_3 as 0.22 and 0.52 ppbv yr^{-1} in rural and urban areas, respectively (Chang et al., 2017). Though the vast majority

[4] Their East Asia region also includes parts of North and South Korea, part of Japan and Taiwan, but is dominated by eastern China.

of stations used in the TOAR analysis were outside China, in Taiwan, South Korea and Japan, due to their downwind location, modelling studies demonstrate that China's emissions account for a large component of their local trends (Yamaji et al., 2012; Nagashima et al., 2017).

Satellite data is valuable in filling the temporal gap in China's surface O_3 trends due to the relative lack of available monitoring station data in China prior to 2012. However, satellite sensors are limited to detecting the O_3 present in the entire atmospheric column, which can introduce large uncertainties in tropospheric O_3 trend estimates. Aircraft and sonde measurements of O_3 vertical profiles can be used to estimate boundary layer O_3 concentrations. Shen et al. (2019) compare Ozone Monitoring Instrument (OMI) data from 2005-2009 with 2013-2017, finding an increase in the mean afternoon O_3 concentrations across much of southern China. Verstraeten et al. (2015) find a positive trend of 1.08% yr^{-1} over eastern China during 2005-2010 using retrievals for NASA's Aura satellite.

Since 2012, data from the CNEMC network has been available, which can be used to calculate the average urban O_3 trend. Lu et al. (2020b) found that median O_3 levels measured at 243 sites across 69 cities increased by 1.7 ppbv yr^{-1} or 2.2 ppbv yr^{-1} for maximum daily 8-hour mean ozone.

VOCs

Jin and Holloway (2015) used OMI data, finding that in most of China, trends in HCHO are weak and insignificant during 2005-2013. They found a positive trend in the North China Plain region, and negative in the Yangtze River Delta and Pearl River Delta (see 1.1 for locations). They suggest that the positive trend in anthropogenic VOC emissions is being offset or negated by decreases in biogenic emissions due to land use and climate change. A recent modelling study estimates the HCHO trend using GEOS-Chem, finding a positive trend of 1.43% yr^{-1} during 2015-2019 (Sun et al., 2020).

Rainwater pH

Rainwater pH measurements are a useful proxy for atmospheric SO_2 and NO_2 concentrations before direct measurements were widespread. In the early 1980s, rainwater pH in the southern Chinese cities of Chongqing and Guiyang was recorded to be 4.14 and 4.02 respectively (Zhao and Sun, 1986), low enough to cause forest damage (Zhao et al., 1988). During 1982 to 1990, Wang and Wang (1995) report that the pH of rain water from

five Chinese cities became more acidic. Acid rain (defined as pH < 5.6) became more widespread and severe in China during 1990 up until 2006, since when it has trended towards reduced acidity (Qu and Han, 2021). However, the trend in rainwater is not only determined by the NO_3^- and SO_4^{2-}, as they can be neutralised by Ca^{2+} and NH_4^+, which are found in higher concentrations in northern China due to its alkaline soils (Zhao and Sun, 1986). Therefore, proposed reductions in NH_3 emissions to alleviate $PM_{2.5}$ pollution could cause rainwater pH to drop again, which could outweigh the benefits of the air quality improvement (Liu et al., 2019).

NO_2

Official government air quality reports switched from reporting NO_x to NO_2 concentrations in 2000. During both the 1982-2000 and 2001-2018, government data shows annual mean NO_x/NO_2 concentrations remaining relatively constant, at 45 $\mu g\,m^{-3}$ and 30 $\mu g\,m^{-3}$ respectively (Zhang et al., 2020).

Satellite monitoring of NO_2 columns across China during 1996-2005 found positive trends over highly populated megacity regions (see Figure 1.1), with the strongest found in the North China Plain, Yangtze River Delta, and Pear River Delta (A et al., 2006). Satellite monitoring of NO_2 column values in the North China Plain region found a slight increase of 4.79% during 2006-2015 (Si et al., 2019). It appears that NO_2 concentrations began to decrease in the Pearl River Delta during 2006-2011, at 1.2 ppbv as recorded by monitoring stations in the regions network (Li et al., 2014). An increase of 55% in column NO_2 was observed by satellite in Henan province during 2005-2011, followed by a decrease of 28% during 2011-2014 after the installation of selective catalytic reduction systems to remove NO_x from flue gas of plants (Zhang et al., 2017a).

Multiple satellite and modelling studies find that NO_2 concentrations peak in 2011-2012 (A et al., 2017; Krotkov et al., 2016; Irie et al., 2016). Shah et al. (2020) use satellite data combined with model analysis and find that NO_2 decreased over central eastern China during 2012-2018, by around 25%. Kong et al. (2021) use CNEMC data to estimate a negative trend of $-2.6\ \mu g\,m^{-3}\,yr^{-1}$ across China during 2013-2018, with negative trends also found in each region.

SO_2

Studies estimating SO_2 trends in mainland China begin in the late 1990s. Some earlier measurements exist that indicate SO_2 levels were high in the 1980s. In 1982, annual mean concentrations of SO_2 were as high as 393 $\mu g\,m^{-3}$ in Guiyang, 260 $\mu g\,m^{-3}$ in Chongqing, 158 $\mu g\,m^{-3}$ in Beijing and 132 $\mu g\,m^{-3}$ in Shenyang (Zhao et al., 1988). By 1995, this had reduced to 230, 160, 100 and 110 in the same cities respectively (Hao et al., 2000). He et al. (2002) report that during 1990-1999, annual mean SO_2 concentrations across China decreased from around 80-110 $\mu g\,m^{-3}$ to 50-60 $\mu g\,m^{-3}$. The declining SO_2 concentrations before the emissions had decreased (see section 1.5.2) is likely due the start of implementation of control technologies such as flue-gas desulphurisation (FGD) and coal washing (Hao et al., 2000), which were not accounted for in emissions estimates such as Streets and Waldhoff (2000).

Ambient SO_2 concentrations continued a general decline in the 2000s. At a regional background site in North China, Shangdianzi, an SO_2 trend of -0.3 ppb yr^{-1} was recorded during 2004-2009 (Lin et al., 2012b). During 2005-2009, steep declines in SO_2 were recorded in Beijing ($-6.5\,\mu g\,m^{-3}\,yr^{-1}$), Shanghai ($-8.7\,\mu g\,m^{-3}\,yr^{-1}$), Guangzhou ($-3.5\,\mu g\,m^{-3}\,yr^{-1}$) and Chengdu ($-6.9\,\mu g\,m^{-3}\,yr^{-1}$) (see Figure 1.7 for locations of cities; Lin et al., 2012).

SO_2 total column densities were observed to decrease above new coal fired power plants built between 2005-2007 as FGD was subsequently installed during 2007-2008 (Li et al., 2010). Satellite measurements show a negative trend in Henan province, which consumes 8% of coal in China, during 2008-2014 (Zhang et al., 2017a), with another analysis showing a negative trend in the whole of East China during the same period (Fu et al., 2017). In the Inner Mongolia province, a trend of -1.6% yr^{-1} was observed during 2007-2016 (Zheng et al., 2018b).

Recent estimates using data from the CNEMC network indicate that SO_2 has decreased on average by $-6.2\,\mu g\,m^{-3}\,yr^{-1}$ during 2013-2018 (Kong et al., 2021).

1.6 Aims and Objectives

At the start of this PhD project (in 2017), there were very few published studies that used the CNEMC air quality monitoring network due to the lack of data availability. Assessments of air quality trends had relied mostly upon bottom-up emission estimates, satellite

measurements and the summaries included in official government reports. Due to the lack of temporal and spatial coverage of in-situ measurement data, many numerical modelling or satellite estimates of air pollutant concentrations were relatively uncertain. This uncertainty reduced the confidence in health impact assessments and air quality control policy assessments.

The aims of this thesis will be to collect and use the CNEMC data to produce the most comprehensive analysis of recent air quality trends in China. Then, establish whether a numerical model driven by recent emissions estimates can reproduce the observed trends, and impact of emission perturbations.

Quantify recent air quality trends in China

- Collect a dataset of the latest Chinese air quality monitoring data including Hong Kong and Taiwanese data.
- Establish the statistical significance of trends in $PM_{2.5}$, NO_2, SO_2, and O_3 across China
- Examine spatial differences in the trends between Chinese megacity regions and provinces.
- Conduct a literature review so that current trends can be compared with those estimated with remote sensing and emission inventory estimates.

Use the WRF-Chem model to establish the drivers of observed trends

- Assess the capability of the WRF-Chem model to capture recent trends in air quality.
- Establish to what extent variation of meteorology or emissions have driven changes in air quality.
- Estimate the change in the magnitude air quality health impacts driven by recent trends.

Examine impacts of short-term emission perturbation during the COVID-19 lockdown on air quality in China

- Quantify the effects of short-term emission changes on air quality that occurred during early 2020 using the CNEMC network
- Use time series decomposition analysis to account for trends and seasonality when

assessing the COVID-19 impact

Chapters 2, 3 and 4 consist of three published papers, with their supporting information found in Appendices A, B and C respectively. A summary of the key findings synthesised from the published papers is presented in Chapter 5, along with discussion of uncertainties and proposals for future research topics that follow from the results in this thesis.

References

A, R. J. van der, Peters, D. H., Eskes, H., Boersma, K. F., Van Roozendael, M., De Smedt, I., and Kelder, H. M. (2006). "Detection of the trend and seasonal variation in tropospheric NO2 over China". In: *Journal of Geophysical Research Atmospheres* 111.12. DOI: 10.1029/2005JD006594.

A, R. J. van der, Mijling, B., Ding, J., Elissavet Koukouli, M., Liu, F., Li, Q., Mao, H., and Theys, N. (2017). "Cleaning up the air: Effectiveness of air quality policy for SO2 and NOx emissions in China". In: *Atmospheric Chemistry and Physics* 17.3, pp. 1775–1789. DOI: 10.5194/acp-17-1775-2017.

Abhishek Tiwary, I. W. (2010). *Air Pollution : Measurement, Modelling and Mitigation, Fourth Edition*. 2018, pp. 102–162.

Aiken, A. C., DeCarlo, P. F., and Jimenez, J. L. (2007). "Elemental analysis of organic species with electron ionization high-resolution mass spectrometry". In: *Analytical Chemistry* 79.21, pp. 8350–8358. DOI: 10.1021/ac071150w.

Akimoto, H. and Narita, H. (1994). "Distribution of SO2, NOx and CO2 emissions from fuel combustion and industrial activities in Asia with 1° × 1° resolution". In: *Atmospheric Environment*. DOI: 10.1016/1352-2310(94)90096-5.

Alford, W. P. and Liebman, B. L. (2001). "Clean Air, Clear Processes? The Struggle over Air Pollution Law in the People's Republic of China". In: *Hastings Law Journal* 52.3, p. 703.

Andrews, S. Q. (2008). "Inconsistencies in air quality metrics: 'Blue Sky' days and PM10 concentrations in Beijing". In: *Environmental Research Letters* 3.3, p. 034009. DOI: 10.1088/1748-9326/3/3/034009.

Apte, J. S., Marshall, J. D., Cohen, A. J., and Brauer, M. (2015). "Addressing Global Mortality from Ambient PM2.5". In: *Environmental Science and Technology* 49.13, pp. 8057–8066. DOI: 10.1021/acs.est.5b01236.

Azomahou, T., Phu, N. V., and Laisney, F. (2001). "Economic growth and CO2 emissions: a nonparametric approach". In: pp. 1–28. URL: http://www.beta-umr7522.fr/productions/publications/2001/2001-01.pdf.

Bates, T. S., Lamb, B. K., Guenther, A., Dignon, J., and Stoiber, R. E. (1992). "Sulfur Emissions to the Atmosphere from Natural Sources". In: *Journal of Atmospheric Chemistry* 14, pp. 315–337.

Beyer, S. (2006). "Environmental Law and Policy in the People's Republic of China". In: *Chinese Journal of International Law* 5.1, pp. 185–211. DOI: 10.1093/chinesejil/jmk002.

Boersma, K. F., Eskes, H. J., Dirksen, R. J., Van Der A, R. J., Veefkind, J. P., Stammes, P., Huijnen, V., Kleipool, Q. L., et al. (2011). "An improved tropospheric NO2 column retrieval algorithm for the Ozone Monitoring Instrument". In: *Atmospheric Measurement Techniques* 4.9, pp. 1905–1928. DOI: 10.5194/amt-4-1905-2011.

Boucher, O., Randall, D., Artaxo, P., Bretherton, C., Feingold, G., Forster, P., Kerminen, V., Kondo, Y., et al. (2013). *: Clouds and Aerosols. In: Climate Change 2013: The Physical Science Basis. Contribution of Working Group I to the Fifth Assessment Report of the Intergovernmental Panel on Climate Change*. Tech. rep.

Boucher, O. (2015). "Atmospheric Aerosols". In: *Atmospheric Aerosols*. Dordrecht: Springer Netherlands. Chap. Atmospheri, pp. 9–24. DOI: 10.1007/978-94-017-9649-1_1.

Box, G. (1979). "Robustness in the Strategy of Scientific Model Building". In: *Robustness in Statistics*, pp. 201–236. DOI: 10.1016/b978-0-12-438150-6.50018-2.

BP (2019). *Insights from the Evolving transition scenario – China*. URL: https://www.bp.com/content/dam/bp/business-sites/en/global/corporate/pdfs/energy-economics/energy-outlook/bp-energy-outlook-2019-country-insight-china.pdf (visited on 04/27/2021).

Brasseur, G. P. and Jacob, D. J. (2017). *Modeling of atmospheric chemistry*. Cambridge University Press, pp. 1–606. DOI: 10.1017/9781316544754.

Brauer, M., Freedman, G., Frostad, J., Van Donkelaar, A., Martin, R. V., Dentener, F., Dingenen, R. V., Estep, K., et al. (2016). "Ambient Air Pollution Exposure Estimation for the Global Burden of Disease 2013". In: *Environmental Science and Technology* 50.1, pp. 79–88. DOI: 10.1021/acs.est.5b03709.

Brown, S. S., Neuman, J. A., Ryerson, T. B., Trainer, M., Dubé, W. P., Holloway, J. S., Warneke, C., Gouw, J. A. de, et al. (2006). "Nocturnal odd-oxygen budget and its implications for ozone loss in the lower troposphere". In: *Geophysical Research Letters* 33.8, p. L08801. DOI: 10.1029/2006GL025900.

Burnett, R., Chen, H., Szyszkowicz, M., Fann, N., Hubbell, B., Pope, C. A., Apte, J. S., Brauer, M., et al. (2018). "Global estimates of mortality associated with longterm exposure to outdoor fine particulate matter". In: *Proceedings of the National Academy of Sciences of the United States of America* 115.38, pp. 9592–9597. DOI: 10.1073/pnas.1803222115.

Burnett, R. T., Arden Pope, C., Ezzati, M., Olives, C., Lim, S. S., Mehta, S., Shin, H. H., Singh, G., et al. (2014). "An integrated risk function for estimating the global burden of disease attributable to ambient fine particulate matter exposure". In: *Environmental Health Perspectives* 122.4, pp. 397–403. DOI: 10.1289/ehp.1307049.

Chan, C. K. and Yao, X. (2008). "Air pollution in mega cities in China". In: *Atmospheric Environment* 42.1, pp. 1–42. DOI: 10.1016/j.atmosenv.2007.09.003.

Chang, K.-L., Petropavlovskikh, I., Copper, O. R., Schultz, M. G., and Wang, T. (2017). "Regional trend analysis of surface ozone observations from monitoring networks in eastern North America, Europe and East Asia". In: *Elem Sci Anth* 5.0, p. 50. DOI: 10.1525/elementa.243.

Chou, C. L. (2012). "Sulfur in coals: A review of geochemistry and origins". In: *International Journal of Coal Geology* 100, pp. 1–13. DOI: 10.1016/j.coal.2012.05.009.

Chow, E. C., Li, R. C., and Zhou, W. (2018). "Influence of Tropical Cyclones on Hong Kong Air Quality". In: *Advances in Atmospheric Sciences* 35.9, pp. 1177–1188. DOI: 10.1007/s00376-018-7225-4.

Chung, A., Chang, D. P., Kleeman, M. J., Perry, K. D., Cahill, T. A., Dutcher, D., McDougall, E. M., and Stroud, K. (2001). "Comparison of real-time instruments used to monitor

airborne particulate matter". In: *Journal of the Air and Waste Management Association* 51.1, pp. 109–120. DOI: 10.1080/10473289.2001.10464254.

Churchill, S. A., Inekwe, J., Ivanovski, K., and Smyth, R. (2018). "The Environmental Kuznets Curve in the OECD: 1870–2014". In: *Energy Economics* 75, pp. 389–399. DOI: 10.1016/j.eneco.2018.09.004.

CIA (2016). *Gdp - Composition, By Sector of Origin*. URL: https://www.cia.gov/library/publications/the-world-factbook/fields/2012.html (visited on 04/27/2021).

Cohan, D. S., Hakami, A., Hu, Y., and Russell, A. G. (2005). "Nonlinear response of ozone to emissions: Source apportionment and sensitivity analysis". In: *Environmental Science and Technology* 39.17, pp. 6739–6748. DOI: 10.1021/es048664m.

Cohen, A. J., Brauer, M., Burnett, R., Anderson, H. R., Frostad, J., Estep, K., Balakrishnan, K., Brunekreef, B., et al. (2017). "Estimates and 25-year trends of the global burden of disease attributable to ambient air pollution: an analysis of data from the Global Burden of Diseases Study 2015". In: *The Lancet* 389.10082, pp. 1907–1918. DOI: 10.1016/S0140-6736(17)30505-6.

Conti, G., Heibati, B., Kloog, I., Fiore, M., and Ferrante, M. (2017). "A review of AirQ Models and their applications for forecasting the air pollution health outcomes". In: *Environmental Science and Pollution Research* 24.7, pp. 6426–6445. DOI: 10.1007/s11356-016-8180-1.

De Foy, B., Lu, Z., and Streets, D. G. (2016). "Satellite NO2 retrievals suggest China has exceeded its NOx reduction goals from the twelfth Five-Year Plan". In: *Scientific Reports* 6. DOI: 10.1038/srep35912.

Ding, A. J., Huang, X., Nie, W., Sun, J. N., Kerminen, V. M., Petäjä, T., Su, H., Cheng, Y. F., et al. (2016). "Enhanced haze pollution by black carbon in megacities in China". In: *Geophysical Research Letters* 43.6, pp. 2873–2879. DOI: 10.1002/2016GL067745.

Ding, Y. H. and Liu, Y. J. (2014). "Analysis of long-term variations of fog and haze in China in recent 50 years and their relations with atmospheric humidity". In: *Science China Earth Sciences* 57.1, pp. 36–46. DOI: 10.1007/s11430-013-4792-1.

Dominici, F., Sheppard, L., and Clyde, M. (2003). "Health effects of air pollution: A statistical review". In: *International Statistical Review* 71.2, pp. 243–276. DOI: 10.1111/j.1751-5823.2003.tb00195.x.

Dong, H., Dai, H., Dong, L., Fujita, T., Geng, Y., Klimont, Z., Inoue, T., Bunya, S., et al. (2015). "Pursuing air pollutant co-benefits of CO2 mitigation in China: A provincial leveled analysis". In: *Applied Energy* 144, pp. 165–174. DOI: 10.1016/j.apenergy.2015.02.020.

Duplissy, J., De Carlo, P. F., Dommen, J., Alfarra, M. R., Metzger, A., Barmpadimos, I., Prevot, A. S., Weingartner, E., et al. (2011). "Relating hygroscopicity and composition of organic aerosol particulate matter". In: *Atmospheric Chemistry and Physics* 11.3, pp. 1155–1165. DOI: 10.5194/acp-11-1155-2011.

Emmons, L. K., Schwantes, R. H., Orlando, J. J., Tyndall, G., Kinnison, D., Lamarque, J. F., Marsh, D., Mills, M. J., et al. (2020). "The Chemistry Mechanism in the Community Earth System Model Version 2 (CESM2)". In: *Journal of Advances in Modeling Earth Systems* 12.4, e2019MS001882. DOI: 10.1029/2019MS001882.

Fang, T. B. and Lu, Y. (2012). "Personal real-time air pollution exposure assessment methods promoted by information technological advances". In: *Annals of GIS* 18.4, pp. 279–288. DOI: 10.1080/19475683.2012.727866.

Feng, G. F., Dong, M., Wen, J., and Chang, C. P. (2018). "The impacts of environmental governance on political turnover of municipal party secretary in China". In: *Environmental Science and Pollution Research*. DOI: 10.1007/s11356-018-2499-8.

Feng, L. and Liao, W. (2016). "Legislation, plans, and policies for prevention and control of air pollution in China: Achievements, challenges, and improvements". In: *Journal of Cleaner Production* 112, pp. 1549–1558. DOI: 10.1016/j.jclepro.2015.08.013.

Field, R. M. (1986). "The Performance of Industry During the Cultural Revolution: Second Thoughts". In: *The China Quarterly* 108, pp. 625–642. DOI: 10.1017/S0305741000037103.

Finlayson-Pitts, B. J. and Pitts, J. N. (1993). "Atmospheric chemistry of tropospheric ozone formation: Scientific and regulatory implications". In: *Air and Waste* 43.8, pp. 1091–1100. DOI: 10.1080/1073161X.1993.10467187.

Flatø, H. (2021). "Trust is in the air: pollution and Chinese citizens' attitudes towards local, regional and central levels of government". In: *Journal of Chinese Governance*. DOI: 10.1080/23812346.2021.1875675.

Fleming, Z. L., Doherty, R. M., Von Schneidemesser, E., Malley, C. S., Cooper, O. R., Pinto, J. P., Colette, A., Xu, X., et al. (2018). "Tropospheric ozone assessment report: Present-day ozone distribution and trends relevant to human health". In: *Elem Sci Anth* 6.1, p. 12. DOI: 10.1525/elementa.273.

Florig, H. K., Sun, G., and Song, G. (2002). "Evolution of particulate regulation in China - Prospects and challenges of exposure-based control". In: *Chemosphere* 49.9, pp. 1163–1174. DOI: 10.1016/S0045-6535(02)00246-1.

Fu, G. Q., Xu, W. Y., Yang, R. F., Li, J. B., and Zhao, C. S. (2014). "The distribution and trends of fog and haze in the North China Plain over the past 30 years". In: *Atmospheric Chemistry and Physics* 14.21, pp. 11949–11958. DOI: 10.5194/acp-14-11949-2014.

Fu, X., Wang, S., Xing, J., Zhang, X., Wang, T., and Hao, J. (2017). "Increasing Ammonia Concentrations Reduce the Effectiveness of Particle Pollution Control Achieved via SO2 and NOX Emissions Reduction in East China". In: *Environmental Science and Technology Letters* 4.6, pp. 221–227. DOI: 10.1021/acs.estlett.7b00143.

Geffen, J. V. (2016). *TROPOMI ATBD of the total and tropospheric NO 2 data products Jos van Geffen*. Tech. rep. 2. URL: https://sentinel.esa.int/documents/247904/2476257/Sentinel-5P-TROPOMI-ATBD-NO2-data-products.

Ghanem, D. and Zhang, J. (2014). "'Effortless Perfection:' Do Chinese cities manipulate air pollution data?" In: *Journal of Environmental Economics and Management* 68.2, pp. 203–225. DOI: 10.1016/j.jeem.2014.05.003.

Grange, S. K., Carslaw, D. C., Lewis, A. C., Boleti, E., and Hueglin, C. (2018). "Random forest meteorological normalisation models for Swiss PM10 trend analysis". In: *Atmospheric Chemistry and Physics* 18.9, pp. 6223–6239. DOI: 10.5194/acp-18-6223-2018.

Green, F. and Stern, N. (2017). "China's changing economy: implications for its carbon dioxide emissions". In: *Climate Policy* 17.4, pp. 423–442. DOI: 10.1080/14693062.2016.1156515.

Gregg, J. S., Andres, R. J., and Marland, G. (2008). "China: Emissions pattern of the world leader in CO2 emissions from fossil fuel consumption and cement production". In: *Geophysical Research Letters* 35.8, p. L08806. DOI: 10.1029/2007GL032887.

Grell, G. A., Peckham, S. E., Schmitz, R., McKeen, S. A., Frost, G., Skamarock, W. C., and Eder, B. (2005). "Fully coupled "online" chemistry within the WRF model". In: *Atmospheric Environment*. DOI: 10.1016/j.atmosenv.2005.04.027.

Gu, Y. and Yim, S. H. (2016). "The air quality and health impacts of domestic trans-boundary pollution in various regions of China". In: *Environment International* 97, pp. 117–124. DOI: 10.1016/j.envint.2016.08.004.

Guan, D., Hubacek, K., Weber, C. L., Peters, G. P., and Reiner, D. M. (2008). "The drivers of Chinese CO2emissions from 1980 to 2030". In: *Global Environmental Change* 18.4, pp. 626–634. DOI: 10.1016/j.gloenvcha.2008.08.001.

Guan, D., Su, X., Zhang, Q., Peters, G. P., Liu, Z., Lei, Y., and He, K. (2014). "The socioeconomic drivers of China's primary PM2.5 emissions". In: *Environmental Research Letters* 9.2, p. 024010. DOI: 10.1088/1748-9326/9/2/024010.

Guenther, A., Karl, T., Harley, P., Wiedinmyer, C., Palmer, P. I., and Geron, C. (2006). "Estimates of global terrestrial isoprene emissions using MEGAN (Model of Emissions of Gases and Aerosols from Nature)". In: *Atmospheric Chemistry and Physics* 6.11, pp. 3181–3210. DOI: 10.5194/acp-6-3181-2006.

Guenther, A., Geron, C., Pierce, T., Lamb, B., Harley, P., and Fall, R. (2000). "Natural emissions of non-methane volatile organic compounds, carbon monoxide, and oxides of nitrogen from North America". In: *Atmospheric Environment* 34.12, pp. 2205–2230. DOI: 10.1016/S1352-2310(99)00465-3.

Guo, H., Cheng, T., Gu, X., Wang, Y., Chen, H., Bao, F., Shi, S., Xu, B., et al. (2017). "Assessment of PM2.5 concentrations and exposure throughout China using ground observations". In: *Science of the Total Environment* 601-602, pp. 1024–1030. DOI: 10.1016/j.scitotenv.2017.05.263.

Guo, H., Xu, M., and Hu, Q. (2011). "Changes in near-surface wind speed in China: 1969-2005". In: *International Journal of Climatology* 31.3, pp. 349–358. DOI: 10.1002/joc.2091.

Guo, J., Li, Y., Cohen, J. B., Li, J., Chen, D., Xu, H., Liu, L., Yin, J., et al. (2019). "Shift in the Temporal Trend of Boundary Layer Height in China Using Long-Term (1979–2016) Radiosonde Data". In: *Geophysical Research Letters* 46.11, pp. 6080–6089. DOI: 10.1029/2019GL082666.

Guo, S., Hu, M., Zamora, M. L., Peng, J., Shang, D., Zheng, J., Du, Z., Wu, Z., et al. (2014). "Elucidating severe urban haze formation in China". In: *Proceedings of the National Academy of Sciences of the United States of America* 111.49, pp. 17373–17378. DOI: 10.1073/pnas.1419604111.

Han, L., Zhou, W., and Li, W. (2015). "City as a major source area of fine particulate (PM2.5) in China". In: *Environmental Pollution* 206, pp. 183–187. DOI: 10.1016/j.envpol.2015.06.038.

Hao, J., Wang, S., Liu, B., and He, K. (2001). "Plotting of acid rain and sulfur dioxide pollution control zones and integrated control planning in China". In: *Water, Air, and Soil Pollution* 130.1-4 II, pp. 259–264. DOI: 10.1023/A:1013823505195.

Hao, J., Wang, S., Liu, B., and He, K. (2000). "Designation of acid rain and SO2 Control Zones and control policies in China". In: *Journal of Environmental Science and Health - Part A Toxic/Hazardous Substances and Environmental Engineering* 35.10, pp. 1901–1914. DOI: 10.1080/10934520009377085.

Hauck, H., Berner, A., Gomiscek, B., Stopper, S., Puxbaum, H., Kundi, M., and Preining, O. (2004). "On the equivalence of gravimetric PM data with TEOM and beta-attenuation measurements". In: *Journal of Aerosol Science* 35.9, pp. 1135–1149. DOI: 10.1016/j.jaerosci.2004.04.004.

He, K., Huo, H., and Zhang, Q. (2002). "Urban air pollution in China: Current status, characteristics, and progress". In: *Annual Review of Energy and the Environment* 27, pp. 397–431. DOI: 10.1146/annurev.energy.27.122001.083421.

Hoesly, R. M., Smith, S. J., Feng, L., Klimont, Z., Janssens-Maenhout, G., Pitkanen, T., Seibert, J. J., Vu, L., et al. (2018). "Historical (1750-2014) anthropogenic emissions of reactive gases and aerosols from the Community Emissions Data System (CEDS)". In: *Geoscientific Model Development* 11.1, pp. 369–408. DOI: 10.5194/gmd-11-369-2018.

Huang, R. J., Zhang, Y., Bozzetti, C., Ho, K. F., Cao, J. J., Han, Y., Daellenbach, K. R., Slowik, J. G., et al. (2015). "High secondary aerosol contribution to particulate pollution during haze events in China". In: *Nature* 514.7521, pp. 218–222. DOI: 10.1038/nature13774.

Huang, X. F., He, L. Y., Hu, M., Canagaratna, M. R., Kroll, J. H., Ng, N. L., Zhang, Y. H., Lin, Y., et al. (2011). "Characterization of submicron aerosols at a rural site in Pearl River Delta of China using an Aerodyne High-Resolution Aerosol Mass Spectrometer". In: *Atmospheric Chemistry and Physics* 11.5, pp. 1865–1877. DOI: 10.5194/acp-11-1865-2011.

Huang, X., Song, Y., Li, M., Li, J., Huo, Q., Cai, X., Zhu, T., Hu, M., and Zhang, H. (2012). "A high-resolution ammonia emission inventory in China". In: *Global Biogeochemical Cycles* 26.1, n/a–n/a. DOI: 10.1029/2011GB004161.

IEA (2020). *China Country Profile*. URL: https://www.iea.org/countries/china (visited on 04/27/2021).

Irie, H., Muto, T., Itahashi, S., Kurokawa, J.-i., and Uno, I. (2016). "Turnaround of Tropospheric Nitrogen Dioxide Pollution Trends in China, Japan, and South Korea". In: *Sola* 12.0, pp. 170–174. DOI: 10.2151/sola.2016-035.

Jacob, D. J. and Winner, D. A. (2009). "Effect of climate change on air quality". In: *Atmospheric Environment* 43.1, pp. 51–63. DOI: 10.1016/j.atmosenv.2008.09.051.

Jacobs, E. T., Burgess, J. L., and Abbott, M. B. (2018). "The Donora Smog Revisited: 70 Years After the Event That Inspired the Clean Air Act". In: *American journal of public health*. DOI: 10.2105/AJPH.2017.304219.

Jahiel, A. R. (1998). "The organization of environmental protection in China". In: *China Quarterly* 156, pp. 757–787. DOI: 10.1017/s030574100005133x.

Jerrett, M., Burnett, R. T., Pope, C. A., Ito, K., Thurston, G., Krewski, D., Shi, Y., Calle, E., and Thun, M. (2009). "Long-Term Ozone Exposure and Mortality". In: *New England Journal of Medicine* 360.11, pp. 1085–1095. DOI: 10.1056/nejmoa0803894.

Jiang, Y. C., Zhao, T. L., Liu, J., Xu, X. D., Tan, C. H., Cheng, X. H., Bi, X. Y., Gan, J. B., et al. (2015). "Why does surface ozone peak before a typhoon landing in southeast China?"

In: *Atmospheric Chemistry and Physics* 15.23, pp. 13331–13338. DOI: 10.5194/acp-15-13331-2015.

Jin, X. and Holloway, T. (2015). "Spatial and temporal variability of ozone sensitivity over China observed from the Ozone Monitoring Instrument". In: *Journal of Geophysical Research* 120.14, pp. 7229–7246. DOI: 10.1002/2015JD023250.

Jin, Y., Andersson, H., and Zhang, S. (2016). "Air pollution control policies in China: A retrospective and prospects". In: *International Journal of Environmental Research and Public Health* 13.12. DOI: 10.3390/ijerph13121219.

Johnson, B. T., Shine, K. P., and Forster, P. M. (2004). "The semi-direct aerosol effect: Impact of absorbing aerosols on marine stratocumulus". In: *Quarterly Journal of the Royal Meteorological Society* 130.599 PART B, pp. 1407–1422. DOI: 10.1256/qj.03.61.

Kambara, S., Takarada, T., Toyoshima, M., and Kato, K. (1995). "Relation between functional forms of coal nitrogen and NOx emissions from pulverized coal combustion". In: *Fuel* 74.9, pp. 1247–1253. DOI: 10.1016/0016-2361(95)00090-R.

Kampa, M. and Castanas, E. (2008). "Human health effects of air pollution". In: *Environmental Pollution* 151.2, pp. 362–367. DOI: 10.1016/j.envpol.2007.06.012.

Kang, H., Zhu, B., Gao, J., He, Y., Wang, H., Su, J., Pan, C., Zhu, T., and Yu, B. (2019). "Potential impacts of cold frontal passage on air quality over the Yangtze River Delta, China". In: *Atmospheric Chemistry and Physics* 19.6, pp. 3673–3685. DOI: 10.5194/acp-19-3673-2019.

Kang, J. Y., Yoon, S. C., Shao, Y., and Kim, S. W. (2011). "Comparison of vertical dust flux by implementing three dust emission schemes in WRF/Chem". In: *Journal of Geophysical Research Atmospheres* 116.9, p. 9202. DOI: 10.1029/2010JD014649.

Kato, N. (1996). "Analysis of structure of energy consumption and dynamics of emission of atmospheric species related to the global environmental change (SOx, NOx, and CO2) in Asia". In: *Atmospheric Environment*. DOI: 10.1016/1352-2310(95)00110-7.

Koch, D., Schulz, M., Kinne, S., McNaughton, C., Spackman, J. R., Balkanski, Y., Bauer, S., Berntsen, T., et al. (2009). "Evaluation of black carbon estimations in global aerosol

models". In: *Atmospheric Chemistry and Physics* 9.22, pp. 9001–9026. DOI: 10.5194/acp-9-9001-2009.

Kong, L., Tang, X., Zhu, J., Wang, Z., Li, J., Wu, H., Wu, Q., Chen, H., et al. (2021). "A 6-year-long (2013-2018) high-resolution air quality reanalysis dataset in China based on the assimilation of surface observations from CNEMC". In: *Earth System Science Data* 13.2, pp. 529–570. DOI: 10.5194/essd-13-529-2021.

Krotkov, N. A., Cam, S. A., Krueger, A. J., Bhartia, P. K., and Yang, K. (2006). "Band residual difference algorithm for retrieval of SO2 from the aura Ozone Monitoring Instrument (OMI)". In: *IEEE Transactions on Geoscience and Remote Sensing* 44.5, pp. 1259–1266. DOI: 10.1109/TGRS.2005.861932.

Krotkov, N. A., McClure, B., Dickerson, R. R., Carn, S. A., Li, C., Bhartia, P. K., Yang, K., Krueger, A. J., et al. (2008). "Validation of SO2 retrievals from the Ozone Monitoring Instrument over NE China". In: *Journal of Geophysical Research Atmospheres* 113.16, D16S40. DOI: 10.1029/2007JD008818.

Krotkov, N. A., McLinden, C. A., Li, C., Lamsal, L. N., Celarier, E. A., Marchenko, S. V., Swartz, W. H., Bucsela, E. J., et al. (2016). "Aura OMI observations of regional SO2 and NO2 pollution changes from 2005 to 2015". In: *Atmospheric Chemistry and Physics* 16.7, pp. 4605–4629. DOI: 10.5194/acp-16-4605-2016.

Krzyzanowski, M. and Cohen, A. (2008). "Update of WHO air quality guidelines". In: *Air Quality, Atmosphere & Health* 1.1, pp. 7–13. DOI: 10.1007/s11869-008-0008-9.

Kulmala, M. and Kerminen, V. M. (2008). "On the formation and growth of atmospheric nanoparticles". In: *Atmospheric Research* 90.2-4, pp. 132–150. DOI: 10.1016/j.atmosres.2008.01.005.

Kushta, J., Pozzer, A., and Lelieveld, J. (2018). "Uncertainties in estimates of mortality attributable to ambient PM2.5 in Europe". In: *Environmental Research Letters* 13.6, p. 064029. DOI: 10.1088/1748-9326/aabf29.

Lee, S. H., Gordon, H., Yu, H., Lehtipalo, K., Haley, R., Li, Y., and Zhang, R. (2019). "New Particle Formation in the Atmosphere: From Molecular Clusters to Global Climate".

In: *Journal of Geophysical Research: Atmospheres* 124.13, pp. 7098–7146. DOI: 10.1029/2018JD029356.

Lee, T. A. and Pickard, A. S. (2013). *Exposure Definition and Measurement*. Agency for Healthcare Research and Quality (US), pp. 45–58. URL: https://www.ncbi.nlm.nih.gov/books/NBK126191/.

LeGrand, S. L., Polashenski, C., Letcher, T. W., Creighton, G. A., Peckham, S. E., and Cetola, J. D. (2019). "The AFWA dust emission scheme for the GOCART aerosol model in WRF-Chem v3.8.1". In: *Geoscientific Model Development* 12.1, pp. 131–166. DOI: 10.5194/gmd-12-131-2019.

Lei, Y., Zhang, Q., Nielsen, C., and He, K. (2011). "An inventory of primary air pollutants and CO2emissions from cement production in China, 1990-2020". In: *Atmospheric Environment* 45.1, pp. 147–154. DOI: 10.1016/j.atmosenv.2010.09.034.

Lelieveld, J., Evans, J. S., Fnais, M., Giannadaki, D., and Pozzer, A. (2015). "The contribution of outdoor air pollution sources to premature mortality on a global scale". In: *Nature* 525.7569, pp. 367–371. DOI: 10.1038/nature15371.

Levelt, P. F., Van Den Oord, G. H., Dobber, M. R., Mälkki, A., Visser, H., De Vries, J., Stammes, P., Lundell, J. O., and Saari, H. (2006). "The ozone monitoring instrument". In: *IEEE Transactions on Geoscience and Remote Sensing* 44.5, pp. 1093–1100. DOI: 10.1109/TGRS.2006.872333.

Levine, M. D., Feng Liu, and Sinton, J. E. (1992). "China's energy system: historical evolution, current issues, and prospects". In: *Annual review of energy and the environment. Vol. 17*. DOI: 10.1146/annurev.eg.17.110192.002201.

Li, C., Zhang, Q., Krotkov, N. A., Streets, D. G., He, K., Tsay, S.-C., and Gleason, J. F. (2010). "Recent large reduction in sulfur dioxide emissions from Chinese power plants observed by the Ozone Monitoring Instrument". In: *Geophysical Research Letters* 37.8. DOI: 10.1029/2010GL042594.

Li, G., Bei, N., Cao, J., Huang, R., Wu, J., Feng, T., Wang, Y., Liu, S., et al. (2017a). "A possible pathway for rapid growth of sulfate during haze days in China". In: *Atmospheric Chemistry and Physics* 17.5, pp. 3301–3316. DOI: 10.5194/acp-17-3301-2017.

Li, H. and Zhou, L. A. (2005). "Political turnover and economic performance: The incentive role of personnel control in China". In: *Journal of Public Economics*. DOI: 10.1016/j.jpubeco.2004.06.009.

Li, J., Lu, K., Lv, W., Li, J., Zhong, L., Ou, Y., Chen, D., Huang, X., and Zhang, Y. (2014). "Fast increasing of surface ozone concentrations in Pearl River Delta characterized by a regional air quality monitoring network during 2006-2011". In: *Journal of Environmental Sciences (China)* 26.1, pp. 23–36. DOI: 10.1016/S1001-0742(13)60377-0.

Li, M., Liu, H., Geng, G., Hong, C., Liu, F., Song, Y., Tong, D., Zheng, B., et al. (2017b). "Anthropogenic emission inventories in China: A review". In: *National Science Review* 4.6, pp. 834–866. DOI: 10.1093/nsr/nwx150.

Li, N., Chen, W., Rafaj, P., Kiesewetter, G., Schöpp, W., Wang, H., Zhang, H., Krey, V., and Riahi, K. (2019). "Air Quality Improvement Co-benefits of Low-Carbon Pathways toward Well below the 2 °c Climate Target in China". In: *Environmental Science and Technology* 53.10, pp. 5576–5584. DOI: 10.1021/acs.est.8b06948.

Li, S., Williams, G., and Guo, Y. (2016). "Health benefits from improved outdoor air quality and intervention in China". In: *Environmental Pollution* 214, pp. 17–25. DOI: 10.1016/j.envpol.2016.03.066.

Li, Y. J., Sun, Y., Zhang, Q., Li, X., Li, M., Zhou, Z., and Chan, C. K. (2017c). "Real-time chemical characterization of atmospheric particulate matter in China: A review". In: *Atmospheric Environment* 158, pp. 270–304. DOI: 10.1016/j.atmosenv.2017.02.027.

Li, Z., Guo, J., Ding, A., Liao, H., Liu, J., Sun, Y., Wang, T., Xue, H., et al. (2017d). "Aerosol and boundary-layer interactions and impact on air quality". In: *National Science Review* 4.6, pp. 810–833. DOI: 10.1093/nsr/nwx117.

Liang, X., Li, S., Zhang, S., Huang, H., and Chen, S. X. (2016). "PM2.5 data reliability, consistency, and air quality assessment in five Chinese cities". In: *Journal of Geophysical Research* 121.17, pp. 10, 220–10, 236. DOI: 10.1002/2016JD024877.

Lim, S. S., Vos, T., Flaxman, A. D., Danaei, G., Shibuya, K., Adair-Rohani, H., Amann, M., Anderson, H. R., et al. (2012). "A comparative risk assessment of burden of disease and injury attributable to 67 risk factors and risk factor clusters in 21 regions, 1990-

2010: A systematic analysis for the Global Burden of Disease Study 2010". In: *The Lancet* 380.9859, pp. 2224–2260. DOI: 10.1016/S0140-6736(12)61766-8.

Lin, C. Q., Liu, G., Lau, A. K., Li, Y., Li, C. C., Fung, J. C., and Lao, X. Q. (2018). "High-resolution satellite remote sensing of provincial PM2.5trends in China from 2001 to 2015". In: *Atmospheric Environment* 180, pp. 110–116. DOI: 10.1016/j.atmosenv.2018.02.045.

Lin, J., Pan, D., Davis, S. J., Zhang, Q., He, K., Wang, C., Streets, D. G., Wuebbles, D. J., and Guan, D. (2014). "China's international trade and air pollution in the United States". In: *Proceedings of the National Academy of Sciences* 111.5, pp. 1736–1741. DOI: 10.1073/pnas.1312860111.

Lin, M., Tao, J., Chan, C. Y., Cao, J. J., Zhang, Z. S., Zhu, L. H., and Zhang, R. J. (2012a). "Regression analyses between recent air quality and visibility changes in megacities at four haze regions in china". In: *Aerosol and Air Quality Research* 12.6, pp. 1049–1061. DOI: 10.4209/aaqr.2011.11.0220.

Lin, W., Xu, X., Ma, Z., Zhao, H., Liu, X., and Wang, Y. (2012b). "Characteristics and recent trends of sulfur dioxide at urban, rural, and background sites in North China: Effectiveness of control measures". In: *Journal of Environmental Sciences* 24.1, pp. 34–49. DOI: 10.1016/S1001-0742(11)60727-4.

Liu, F., Zhang, Q., Tong, D., Zheng, B., Li, M., Huo, H., and He, K. B. (2015). "High-resolution inventory of technologies, activities, and emissions of coal-fired power plants in China from 1990 to 2010". In: *Atmospheric Chemistry and Physics* 15.23, pp. 13299–13317. DOI: 10.5194/acp-15-13299-2015.

Liu, J., Tong, D., Zheng, Y., Cheng, J., Qin, X., Shi, Q., Yan, L., Lei, Y., and Zhang, Q. (2021). "Carbon and air pollutant emissions from China's cement industry 1990-2015: Trends, evolution of technologies, and drivers". In: *Atmospheric Chemistry and Physics* 21.3, pp. 1627–1647. DOI: 10.5194/acp-21-1627-2021.

Liu, M., Huang, X., Song, Y., Tang, J., Cao, J., Zhang, X., Zhang, Q., Wang, S., et al. (2019). "Ammonia emission control in China would mitigate haze pollution and nitrogen deposition, but worsen acid rain". In: *Proceedings of the National Academy of Sciences of the United States of America* 116.16, pp. 7760–7765. DOI: 10.1073/pnas.1814880116.

Lohmann, U. and Feichter, J. (2004). "Global indirect aerosol effects: a review". In: *Atmospheric Chemistry and Physics Discussions* 4.6, pp. 7561–7614. DOI: 10.5194/acpd-4-7561-2004.

Lou, S., Yang, Y., Wang, H., Smith, S. J., Qian, Y., and Rasch, P. J. (2019). "Black Carbon Amplifies Haze Over the North China Plain by Weakening the East Asian Winter Monsoon". In: *Geophysical Research Letters* 46.1, pp. 452–460. DOI: 10.1029/2018GL080941.

Lu, X., Zhang, S., Xing, J., Wang, Y., Chen, W., Ding, D., Wu, Y., Wang, S., et al. (2020a). "Progress of Air Pollution Control in China and Its Challenges and Opportunities in the Ecological Civilization Era". In: *Engineering* 6.12, pp. 1423–1431. DOI: 10.1016/j.eng.2020.03.014.

Lu, X., Zhang, L., Wang, X., Gao, M., Li, K., Zhang, Y., Yue, X., and Zhang, Y. (2020b). "Rapid Increases in Warm-Season Surface Ozone and Resulting Health Impact in China since 2013". In: *Environmental Science and Technology Letters*. DOI: 10.1021/acs.estlett.0c00171.

Ma, Z., Hu, X., Huang, L., Bi, J., and Liu, Y. (2014). "Estimating ground-level PM2.5 in china using satellite remote sensing". In: *Environmental Science and Technology* 48.13, pp. 7436–7444. DOI: 10.1021/es5009399.

Ma, Z., Hu, X., Sayer, A. M., Levy, R., Zhang, Q., Xue, Y., Tong, S., Bi, J., et al. (2016). "Satellite-based spatiotemporal trends in PM2.5concentrations: China, 2004-2013". In: *Environmental Health Perspectives* 124.2, pp. 184–192. DOI: 10.1289/ehp.1409481.

Macias, E. S. and Husar, R. B. (1976). "Atmospheric Particulate Mass Measurement with Beta Attenuation Mass Monitor". In: *Environmental Science and Technology* 10.9, pp. 904–907. DOI: 10.1021/es60120a015.

McGrath, M. (2020). *Climate change: China aims for 'carbon neutrality by 2060'*. URL: https://www.bbc.com/news/science-environment-54256826 (visited on 04/09/2021).

Mehlman, M. A. and Borek, C. (1987). "Toxicity and biochemical mechanisms of ozone". In: *Environmental Research* 42.1, pp. 36–53. DOI: 10.1016/S0013-9351(87)80005-1.

Metzger, A., Verheggen, B., Dommen, J., Duplissy, J., Prevot, A. S., Weingartner, E., Riipinen, I., Kulmala, M., et al. (2010). "Evidence for the role of organics in aerosol par-

ticle formation under atmospheric conditions". In: *Proceedings of the National Academy of Sciences of the United States of America* 107.15, pp. 6646–6651. DOI: 10.1073/pnas.0911330107.

Muldavin, J. (2000). "The paradoxes of environmental policy and resource management in reform-era China". In: *Economic Geography* 76.3, pp. 244–271. DOI: 10.1111/j.1944-8287.2000.tb00143.x.

Myhre, G. (2009). "Consistency between satellite-derived and modeled estimates of the direct aerosol effect". In: *Science* 325.5937, pp. 187–190. DOI: 10.1126/science.1174461.

Næss, P. and Høyer, K. G. (2009). "The emperor's green clothes: Growth, decoupling, and capitalism". In: *Capitalism, Nature, Socialism* 20.3, pp. 74–95. DOI: 10.1080/10455750903215753.

Nagashima, T., Sudo, K., Akimoto, H., Kurokawa, J., and Ohara, T. (2017). "Long-term change in the source contribution to surface ozone over Japan". In: *Atmospheric Chemistry and Physics*. DOI: 10.5194/acp-17-8231-2017.

Nash, D. G., Baer, T., and Johnston, M. V. (2006). "Aerosol mass spectrometry: An introductory review". In: *International Journal of Mass Spectrometry* 258.1-3, pp. 2–12. DOI: 10.1016/j.ijms.2006.09.017.

Nevers, N. de (1999). "Air Pollution Control Engineering". In: 2nd. Singapore: McGraw-Hill, pp. 95–106, 111–114, 239–241.

Nielsen, T., Samuelsson, U., Grennfelt, P., and Thomsen, E. L. (1981). *Peroxyacetyl nitrate in long-range transported polluted air*. Tech. rep. 5833, pp. 553–555. DOI: 10.1038/293553a0.

OpenAQ (2020). *Open Air Quality Data: The Global State of Play*. Tech. rep. URL: https://openaq.org/assets/files/2020%7B%5C_%7DOpenData%7B%5C_%7DStateofPlay.pdf.

Orleans, L. A. and Suttmeier, R. P. (1970). "The Mao ethic and environmental quality". In: *Science* 170.3963, pp. 1173–1176. DOI: 10.1126/science.170.3963.1173.

Özkaynak, H., Baxter, L. K., Dionisio, K. L., and Burke, J. (2013). "Air pollution exposure prediction approaches used in air pollution epidemiology studies". In: *Journal of Exposure Science and Environmental Epidemiology* 23.6, pp. 566–572. DOI: 10.1038/jes.2013.15.

Palmer, P. I., Abbot, D. S., Fu, T. M., Jacob, D. J., Chance, K., Kurosu, T. P., Guenther, A., Wiedinmyer, C., et al. (2006). "Quantifying the seasonal and interannual variability of North American isoprene emissions using satellite observations of the formaldehyde column". In: *Journal of Geophysical Research Atmospheres* 111.12, p. D12315. DOI: 10.1029/2005JD006689.

Pang, R., Zheng, D., Shi, M., and Zhang, X. (2019). "Pollute first, control later? Exploring the economic threshold of effective environmental regulation in China's context". In: *Journal of Environmental Management* 248, p. 109275. DOI: 10.1016/j.jenvman.2019.109275.

Patashnick, H. and Rupprecht, E. G. (1991). "Continuous pm-10 measurements using the tapered element oscillating microbalance". In: *Journal of the Air and Waste Management Association* 41.8, pp. 1079–1083. DOI: 10.1080/10473289.1991.10466903.

Peng, J., Chen, S., Lü, H., Liu, Y., and Wu, J. (2016). "Spatiotemporal patterns of remotely sensed PM2.5concentration in China from 1999 to 2011". In: *Remote Sensing of Environment* 174, pp. 109–121. DOI: 10.1016/j.rse.2015.12.008.

Peng, J., Hu, M., Shang, D., Wu, Z., Du, Z., Tan, T., Wang, Y., Zhang, F., and Zhang, R. (2021). "Explosive secondary aerosol formation during severe haze in the north china plain". In: *Environmental Science and Technology* 55.4, pp. 2189–2207. DOI: 10.1021/acs.est.0c07204.

Peng, W., Yang, J., Wagner, F., and Mauzerall, D. L. (2017). "Substantial air quality and climate co-benefits achievable now with sectoral mitigation strategies in China". In: *Science of the Total Environment* 598, pp. 1076–1084. DOI: 10.1016/j.scitotenv.2017.03.287.

Pope, C. A., Bates, D. V., and Raizenne, M. E. (1995). "Health effects of particulate air pollution: Time for reassessment?" In: *Environmental Health Perspectives* 103.5, pp. 472–480. DOI: 10.1289/ehp.95103472.

Pope, C. A., Cohen, A. J., and Burnett, R. T. (2018). "Cardiovascular disease and fine particulate matter lessons and limitations of an integrated exposure-response approach". In: *Circulation Research* 122.12, pp. 1645–1647. DOI: 10.1161/CIRCRESAHA.118.312956.

Qin, K., Wu, L., Wong, M. S., Letu, H., Hu, M., Lang, H., Sheng, S., Teng, J., et al. (2016). "Trans-boundary aerosol transport during a winter haze episode in China revealed by ground-based Lidar and CALIPSO satellite". In: *Atmospheric Environment* 141, pp. 20–29. DOI: 10.1016/j.atmosenv.2016.06.042.

Qu, R. and Han, G. (2021). "A critical review of the variation in rainwater acidity in 24 Chinese cities during 1982–2018". In: *Elementa: Science of the Anthropocene* 9.1. DOI: 10.1525/elementa.2021.00142.

Qu, Z., Henze, D. K., Li, C., Theys, N., Wang, Y., Wang, J., Wang, W., Han, J., et al. (2019). "SO2 Emission Estimates Using OMI SO2 Retrievals for 2005–2017". In: *Journal of Geophysical Research: Atmospheres* 124.14, pp. 8336–8359. DOI: 10.1029/2019JD030243.

Ramanathan, V. and Carmichael, G. (2008). "Global and regional climate changes due to black carbon". In: *Nature Geoscience* 1.4, pp. 221–227. DOI: 10.1038/ngeo156.

Reff, A., Eberly, S. I., and Bhave, P. V. (2007). "Receptor modeling of ambient particulate matter data using positive matrix factorization: Review of existing methods". In: *Journal of the Air and Waste Management Association* 57.2, pp. 146–154. DOI: 10.1080/10473289.2007.10465319.

Ritchie, H. and Roser, M. (2017). "CO2 and Greenhouse Gas Emissions". In: *Our World in Data*. URL: https://ourworldindata.org/co2-and-other-greenhouse-gas-emissions%20https://ourworldindata.org/co2/country/china.

Schreifels, J. J., Fu, Y., and Wilson, E. J. (2012). "Sulfur dioxide control in China: Policy evolution during the 10th and 11th Five-year Plans and lessons for the future". In: *Energy Policy* 48, pp. 779–789. DOI: 10.1016/j.enpol.2012.06.015.

Seinfeld, J. H. and Pandis, S. N. (2006). "The Atmosphere". In: *Atmospheric Chemistry and Physics: From Air Pollution to Climate Change*. John Wiley & Sons, Ltd. Chap. 1.

Shah, V., J. Jacob, D., Li, K., Silvern, R., Zhai, S., Liu, M., Lin, J., and Zhang, Q. (2020). "Effect of changing NOx lifetime on the seasonality and long-term trends of satellite-observed tropospheric NO2 columns over China". In: *Atmospheric Chemistry and Physics* 20.3, pp. 1483–1495. DOI: 10.5194/acp-20-1483-2020.

Shapiro, J. (2001). *Mao's war against nature: Politics and the environment in revolutionary China*. Cambridge University Press.

Shen, L., Jacob, D. J., Liu, X., Huang, G., Li, K., Liao, H., and Wang, T. (2019). "An evaluation of the ability of the Ozone Monitoring Instrument (OMI) to observe boundary layer ozone pollution across China: Application to 2005-2017 ozone trends". In: *Atmospheric Chemistry and Physics*. DOI: 10.5194/acp-19-6551-2019.

Shi, C., Nduka, I. C., Yang, Y., Huang, Y., Yao, R., Zhang, H., He, B., Xie, C., et al. (2020). "Characteristics and meteorological mechanisms of transboundary air pollution in a persistent heavy PM2.5 pollution episode in Central-East China". In: *Atmospheric Environment* 223, p. 117239. DOI: 10.1016/j.atmosenv.2019.117239.

Shiu, A. and Lam, P. L. (2004). "Electricity consumption and economic growth in China". In: *Energy Policy* 32.1, pp. 47–54. DOI: 10.1016/S0301-4215(02)00250-1.

Si, Y., Wang, H., Cai, K., Chen, L., Zhou, Z., and Li, S. (2019). "Long-term (2006–2015) variations and relations of multiple atmospheric pollutants based on multi-remote sensing data over the North China Plain". In: *Environmental Pollution* 255, p. 113323. DOI: 10.1016/j.envpol.2019.113323.

Sillman, S. (1999). "The relation between ozone, NO(x) and hydrocarbons in urban and polluted rural environments". In: *Atmospheric Environment* 33.12, pp. 1821–1845. DOI: 10.1016/S1352-2310(98)00345-8.

Silver, B., Conibear, L., Reddington, C. L., Knote, C., Arnold, S. R., and Spracklen, D. V. (2020). "Pollutant emission reductions deliver decreased PM2.5-caused mortality across China during 2015-2017". In: *Atmospheric Chemistry and Physics* 20.20, pp. 11683–11695. DOI: 10.5194/acp-20-11683-2020.

Simkhovich, B. Z., Kleinman, M. T., and Kloner, R. A. (2008). "Air Pollution and Cardiovascular Injury. Epidemiology, Toxicology, and Mechanisms". In: *Journal of the American College of Cardiology* 52.9, pp. 719–726. DOI: 10.1016/j.jacc.2008.05.029.

Singh, H. B. and Hanst, P. L. (1981). "Peroxyacetyl nitrate (PAN) in the unpolluted atmosphere: An important reservoir for nitrogen oxides". In: *Geophysical Research Letters* 8.8, pp. 941–944. DOI: 10.1029/GL008i008p00941.

Sinyuk, A., Sinyuk, A., Holben, B. N., Eck, T. F., Eck, T. F., M. Giles, D., M. Giles, D., Slutsker, I., et al. (2020). "The AERONET Version 3 aerosol retrieval algorithm, associated uncertainties and comparisons to Version 2". In: *Atmospheric Measurement Techniques* 13.6, pp. 3375–3411. DOI: 10.5194/amt-13-3375-2020.

Smith, S. J., Pitcher, H., and Wigley, T. (2001). "Global and regional anthropogenic sulfur dioxide emissions". In: *Global and Planetary Change* 29.1, pp. 99–119. DOI: 10.1016/S0921-8181(00)00057-6.

Song, Y., Zhang, Y., Xie, S., Zeng, L., Zheng, M., Salmon, L. G., Shao, M., and Slanina, S. (2006). "Source apportionment of PM2.5 in Beijing by positive matrix factorization". In: *Atmospheric Environment* 40.8, pp. 1526–1537. DOI: 10.1016/j.atmosenv.2005.10.039.

Sousa, S. I., Martins, F. G., Alvim-Ferraz, M. C., and Pereira, M. C. (2007). "Multiple linear regression and artificial neural networks based on principal components to predict ozone concentrations". In: *Environmental Modelling and Software* 22.1, pp. 97–103. DOI: 10.1016/j.envsoft.2005.12.002.

Stanek, L. W., Brown, J. S., Stanek, J., Gift, J., and Costa, D. L. (2011). "Air pollution toxicology-a brief review of the role of the science in shaping the current understanding of air pollution health risks". In: *Toxicological Sciences*. DOI: 10.1093/toxsci/kfq367.

Stavrakou, T., Müller, J. F., Boersma, K. F., Van Der A., R. J., Kurokawa, J., Ohara, T., and Zhang, Q. (2013). "Key chemical NOx sink uncertainties and how they influence top-down emissions of nitrogen oxides". In: *Atmospheric Chemistry and Physics* 13.17, pp. 9057–9082. DOI: 10.5194/acp-13-9057-2013.

Steiner, A. L., Davis, A. J., Sillman, S., Owen, R. C., Michalak, A. M., and Fiore, A. M. (2010). "Observed suppression of ozone formation at extremely high temperatures due to chemical and biophysical feedbacks". In: *Proceedings of the National Academy of Sciences of the United States of America* 107.46, pp. 19685–19690. DOI: 10.1073/pnas.1008336107.

Stoerk, T. (2016). "Statistical corruption in Beijing's air quality data has likely ended in 2012". In: *Atmospheric Environment* 127, pp. 365–371. DOI: 10.1016/j.atmosenv.2015.12.055.

Stolzenburg, D., Fischer, L., Vogel, A. L., Heinritzi, M., Schervish, M., Simon, M., Wagner, A. C., Dada, L., et al. (2018). "Rapid growth of organic aerosol nanoparticles over a wide tropospheric temperature range". In: *Proceedings of the National Academy of Sciences of the United States of America* 115.37, pp. 9122–9127. DOI: 10.1073/pnas.1807604115.

Streets, D. G. and Waldhoff, S. T. (2000). "Present and future emissions of air pollutants in China: SO2, NO(x), and CO". In: *Atmospheric Environment*. DOI: 10.1016/S1352-2310(99)00167-3.

Streets, D. G., Yarber, K. F., Woo, J. H., and Carmichael, G. R. (2003). "Biomass burning in Asia: Annual and seasonal estimates and atmospheric emissions". In: *Global Biogeochemical Cycles* 17.4, n/a–n/a. DOI: 10.1029/2003gb002040.

Streets, D. G., Tsai, N. Y., Akimoto, H., and Oka, K. (2000). "Sulfur dioxide emissions in Asia in the period 1985-1997". In: *Atmospheric Environment*. DOI: 10.1016/S1352-2310(00)00187-4.

Su, T., Li, Z., and Kahn, R. (2018). "Relationships between the planetary boundary layer height and surface pollutants derived from lidar observations over China: Regional pattern and influencing factors". In: *Atmospheric Chemistry and Physics* 18.21, pp. 15921–15935. DOI: 10.5194/acp-18-15921-2018.

Sun, W., Wang, D., Yao, L., Fu, H., Fu, Q., Wang, H., Li, Q., Wang, L., et al. (2019). "Chemistry-triggered events of PM2.5 explosive growth during late autumn and winter in Shanghai, China". In: *Environmental Pollution* 254, p. 112864. DOI: 10.1016/j.envpol.2019.07.032.

Sun, Y., Yin, H., Liu, C., Zhang, L., Cheng, Y., Palm, M., Notholt, J., Lu, X., et al. (2020). "Mapping the drivers of formaldehyde (HCHO) variability from 2015–2019 over eastern China: insights from FTIR observation and GEOS-Chem model simulation". In: *Atmospheric Chemistry and Physics*. DOI: 10.5194/acp-2020-544.

Tai, A. P., Mickley, L. J., and Jacob, D. J. (2010). "Correlations between fine particulate matter (PM2.5) and meteorological variables in the United States: Implications for the sensitivity of PM2.5 to climate change". In: *Atmospheric Environment* 44.32, pp. 3976–3984. DOI: 10.1016/j.atmosenv.2010.06.060.

The Guardian (2013). *Chinese struggle through 'airpocalypse' smog | China*. URL: https://www.theguardian.com/world/2013/feb/16/chinese-struggle-through-airpocalypse-smog (visited on 05/26/2021).

The World Bank (2021). *China Current GDP*. URL: https://data.worldbank.org/indicator/NY.GDP.MKTP.CD?locations=CN (visited on 05/13/2021).

The World Bank and State Enviromental Protection Administration (2007). *Cost of Pollution in China: Economic estimates of physical damages*. URL: https://siteresources.worldbank.org/INTEAPREGTOPENVIRONMENT/Resources/China%7B%5C_%7DCost%7B%5C_%7Dof%7B%5C_%7DPollution.pdf (visited on 05/12/2021).

Thurston, G. D., Burnett, R. T., Turner, M. C., Shi, Y., Krewski, D., Lall, R., Ito, K., Jerrett, M., et al. (2016). "Ischemic heart disease mortality and long-term exposure to source-related components of U.S. fine particle air pollution". In: *Environmental Health Perspectives* 124.6, pp. 785–794. DOI: 10.1289/ehp.1509777.

Triantafyllou, E., Diapouli, E., Tsilibari, E. M., Adamopoulos, A. D., Biskos, G., and Eleftheriadis, K. (2016). "Assessment of factors influencing PM mass concentration measured by gravimetric & beta attenuation techniques at a suburban site". In: *Atmospheric Environment* 131, pp. 409–417. DOI: 10.1016/j.atmosenv.2016.02.010.

Tröstl, J., Chuang, W. K., Gordon, H., Heinritzi, M., Yan, C., Molteni, U., Ahlm, L., Frege, C., et al. (2016). "The role of low-volatility organic compounds in initial particle growth in the atmosphere". In: *Nature* 533.7604, pp. 527–531. DOI: 10.1038/nature18271.

Tunnicliffe, W. S., Hilton, M. F., Harrison, R. M., and Ayres, J. G. (2001). "The effect of sulphur dioxide exposure on indices of heart rate variability in normal and asthmatic adults". In: *European Respiratory Journal* 17.4, pp. 604–608. DOI: 10.1183/09031936.01.17406040.

Turiel, J. S. and Kaufmann, R. K. (2021). "Evidence of air quality data misreporting in China: An impulse indicator saturation model comparison of local government-reported and U.S. embassy-reported PM2.5 concentrations (2015–2017)". In: *PLOS ONE* 16.4. Ed. by J. R. Lyons, e0249063. DOI: 10.1371/journal.pone.0249063.

Turner, M. C., Jerrett, M., Pope, C. A., Krewski, D., Gapstur, S. M., Diver, W. R., Beckerman, B. S., Marshall, J. D., et al. (2016). "Long-Term Ozone Exposure and Mortality in a Large Prospective Study". In: *American journal of respiratory and critical care medicine* 193.10, pp. 1134–1142. DOI: 10.1164/rccm.201508-1633OC.

Ulbrich, I. M., Canagaratna, M. R., Zhang, Q., Worsnop, D. R., and Jimenez, J. L. (2009). "Interpretation of organic components from Positive Matrix Factorization of aerosol mass spectrometric data". In: *Atmospheric Chemistry and Physics* 9.9, pp. 2891–2918. DOI: 10.5194/acp-9-2891-2009.

Uno, I., He, Y., Ohara, T., Yamaji, K., Kurokawa, J. I., Katayama, M., Wang, Z., Noguchi, K., et al. (2007). "Systematic analysis of interannual and seasonal variations of model-simulated tropospheric NO2 in Asia and comparison with GOME-satellite data". In: *Atmospheric Chemistry and Physics* 7.6, pp. 1671–1681. DOI: 10.5194/acp-7-1671-2007.

Van Dingenen, R., Dentener, F. J., Raes, F., Krol, M. C., Emberson, L., and Cofala, J. (2009). "The global impact of ozone on agricultural crop yields under current and future air quality legislation". In: *Atmospheric Environment* 43.3, pp. 604–618. DOI: 10.1016/j.atmosenv.2008.10.033.

Van Donkelaar, A., Martin, R. V., Brauer, M., Hsu, N. C., Kahn, R. A., Levy, R. C., Lyapustin, A., Sayer, A. M., and Winker, D. M. (2016). "Global Estimates of Fine Particulate Matter using a Combined Geophysical-Statistical Method with Information from Satellites, Models, and Monitors". In: *Environmental Science and Technology* 50.7, pp. 3762–3772. DOI: 10.1021/acs.est.5b05833.

Verstraeten, W. W., Neu, J. L., Williams, J. E., Bowman, K. W., Worden, J. R., and Boersma, K. F. (2015). "Rapid increases in tropospheric ozone production and export from China". In: *Nature Geoscience* 8.9, pp. 690–695. DOI: 10.1038/ngeo2493.

Wang, J., Zhang, M., Bai, X., Tan, H., Li, S., Liu, J., Zhang, R., Wolters, M. A., et al. (2017). "Large-scale transport of PM2.5 in the lower troposphere during winter cold surges in China". In: *Scientific Reports* 7.1, pp. 1–10. DOI: 10.1038/s41598-017-13217-2.

Wang, K., Tian, H., Hua, S., Zhu, C., Gao, J., Xue, Y., Hao, J., Wang, Y., and Zhou, J. (2016). "A comprehensive emission inventory of multiple air pollutants from iron and steel

industry in China: Temporal trends and spatial variation characteristics". In: *Science of the Total Environment* 559, pp. 7–14. DOI: 10.1016/j.scitotenv.2016.03.125.

Wang, S. W., Zhang, Q., Streets, D. G., He, K. B., Martin, R. V., Lamsal, L. N., Chen, D., Lei, Y., and Lu, Z. (2012). "Growth in NO x emissions from power plants in China: Bottom-up estimates and satellite observations". In: *Atmospheric Chemistry and Physics* 12.10, pp. 4429–4447. DOI: 10.5194/acp-12-4429-2012.

Wang, T., Wei, X. L., Ding, A. J., Poon, C. N., Lam, K. S., Li, Y. S., Chan, L. Y., and Anson, M. (2009). "Increasing surface ozone concentrations in the background atmosphere of Southern China, 1994-2007". In: *Atmospheric Chemistry and Physics* 9.16, pp. 6217–6227. DOI: 10.5194/acp-9-6217-2009.

Wang, W. and Wang, T. (1995). "On the origin and the trend of acid precipitation in China". In: *Water, Air, & Soil Pollution* 85.4, pp. 2295–2300. DOI: 10.1007/BF01186176.

Wang, Y., Chen, J., Wang, Q., Qin, Q., Ye, J., Han, Y., Li, L., Zhen, W., et al. (2019). "Increased secondary aerosol contribution and possible processing on polluted winter days in China". In: *Environment International* 127, pp. 78–84. DOI: 10.1016/j.envint.2019.03.021.

Watson, J. G., Tropp, R. J., Kohl, S. D., Wang, X., and Chow, J. C. (2017). "Filter Processing and Gravimetric Analysis for Suspended Particulate Matter Samples". In: *Aerosol Science and Engineering* 1.2, pp. 93–105. DOI: 10.1007/s41810-017-0010-4.

Wayne, R. P., Barnes, I., Biggs, P., Burrows, J. P., Canosa-Mas, C. E., Hjorth, J., Le Bras, G., Moortgat, G. K., et al. (1991). "The nitrate radical: Physics, chemistry, and the atmosphere". In: *Atmospheric Environment Part A, General Topics* 25.1, pp. 1–203. DOI: 10.1016/0960-1686(91)90192-A.

WHO (2006). *WHO Air quality guidelines for particulate matter, ozone, nitrogen dioxide and sulfur dioxide: global update 2005: summary of risk assessment*. Geneva: World Health Organization. DOI: 10.1016/0004-6981(88)90109-6.

Wiedinmyer, C., Akagi, S. K., Yokelson, R. J., Emmons, L. K., Al-Saadi, J. A., Orlando, J. J., and Soja, A. J. (2011). "The Fire INventory from NCAR (FINN): A high resolu-

tion global model to estimate the emissions from open burning". In: *Geoscientific Model Development* 4.3, pp. 625–641. DOI: 10.5194/gmd-4-625-2011.

Wikipedia Contributors (2021). *List of countries by electricity consumption*. URL: https://en.wikipedia.org/w/index.php?title=List%7B%5C_%7Dof%7B%5C_%7Dcountries%7B%5C_%7Dby%7B%5C_%7Delectricity%7B%5C_%7Dconsumption%7B%5C&%7Doldid=1009400219 (visited on 05/15/2021).

Wild, O. and Akimoto, H. (2001). "Intercontinental transport of ozone and its precursors in a three-dimensional global CTM". In: *Journal of Geophysical Research Atmospheres*. DOI: 10.1029/2000JD000123.

Wu, H., Tang, X., Wang, Z., Wu, L., Lu, M., Wei, L., and Zhu, J. (2018). "Probabilistic Automatic Outlier Detection for Surface Air Quality Measurements from the China National Environmental Monitoring Network". In: *Advances in Atmospheric Sciences* 35.12, pp. 1522–1532. DOI: 10.1007/s00376-018-8067-9.

Wu, J., Deng, Y., Huang, J., Morck, R., Yeung, B., and Kahn, M. E. (2014). *Comment on "incentives and Outcomes: China's Environmental Policy*. Tech. rep. 1. Cambridge, MA: National Bureau of Economic Research. DOI: 10.3386/w18754.

Wu, Z., Hu, M., Liu, S., Wehner, B., Bauer, S., Ma ßLing, A., Wiedensohler, A., Petäjä, T., et al. (2007). "New particle formation in Beijing, China: Statistical analysis of a 1-year data set". In: *Journal of Geophysical Research Atmospheres* 112.9, p. D09209. DOI: 10.1029/2006JD007406.

Xia, Y., Guan, D., Jiang, X., Peng, L., Schroeder, H., and Zhang, Q. (2016). "Assessment of socioeconomic costs to China's air pollution". In: *Atmospheric Environment* 139, pp. 147–156. DOI: 10.1016/j.atmosenv.2016.05.036.

Xiao, S., Wang, M. Y., Yao, L., Kulmala, M., Zhou, B., Yang, X., Chen, J. M., Wang, D. F., et al. (2015). "Strong atmospheric new particle formation in winter in urban Shanghai, China". In: *Atmospheric Chemistry and Physics* 15.4, pp. 1769–1781. DOI: 10.5194/acp-15-1769-2015.

Xu, W. Y., Zhao, C. S., Ran, L., Deng, Z. Z., Liu, P. F., Ma, N., Lin, W. L., Xu, X. B., et al. (2011). "Characteristics of pollutants and their correlation to meteorological conditions

at a suburban site in the North China Plain". In: *Atmospheric Chemistry and Physics* 11.9, pp. 4353–4369. DOI: 10.5194/acp-11-4353-2011.

Xue, T., Zheng, Y., Tong, D., Zheng, B., Li, X., Zhu, T., and Zhang, Q. (2019). "Spatiotemporal continuous estimates of PM2.5 concentrations in China, 2000–2016: A machine learning method with inputs from satellites, chemical transport model, and ground observations". In: *Environment International* 123, pp. 345–357. DOI: 10.1016/j.envint.2018.11.075.

Yamaji, K., Uno, I., and Irie, H. (2012). "Investigating the response of East Asian ozone to Chinese emission changes using a linear approach". In: *Atmospheric Environment*. DOI: 10.1016/j.atmosenv.2012.03.009.

Yao, L., Garmash, O., Bianchi, F., Zheng, J., Yan, C., Kontkanen, J., Junninen, H., Mazon, S. B., et al. (2018). "Atmospheric new particle formation from sulfuric acid and amines in a Chinese megacity". In: *Science* 361.6399, pp. 278–281. DOI: 10.1126/science.aao4839.

Yin, P., Brauer, M., Cohen, A., Burnett, R. T., Liu, J., Liu, Y., Liang, R., Wang, W., et al. (2017). "Long-term fine particulate matter exposure and nonaccidental and cause-specific mortality in a large national cohort of Chinese men". In: *Environmental Health Perspectives* 125.11, pp. 117002–1–117002–11. DOI: 10.1289/EHP1673.

Zhan, Y., Luo, Y., Deng, X., Zhang, K., Zhang, M., Grieneisen, M. L., and Di, B. (2018). "Satellite-Based Estimates of Daily NO2 Exposure in China Using Hybrid Random Forest and Spatiotemporal Kriging Model". In: *Environmental Science and Technology* 52.7, pp. 4180–4189. DOI: 10.1021/acs.est.7b05669.

Zhang, B., Cao, C., Gu, J., and Liu, T. (2016). "A new Environmental Protection Law, many old problems? Challenges to environmental governance in China". In: *Journal of Environmental Law* 28.2, pp. 325–335. DOI: 10.1093/jel/eqw014.

Zhang, F., Shi, Y., Fang, D., Ma, G., Nie, C., Krafft, T., He, L., and Wang, Y. (2020). "Monitoring history and change trends of ambient air quality in China during the past four decades". In: *Journal of Environmental Management* 260, p. 110031. DOI: 10.1016/j.jenvman.2019.110031.

Zhang, J. and Smith, K. R. (2007). "Household air pollution from coal and biomass fuels in China: Measurements, health impacts, and interventions". In: *Environmental Health Perspectives* 115.6, pp. 848–855. DOI: 10.1289/ehp.9479.

Zhang, L., Lee, C. S., Zhang, R., and Chen, L. (2017a). "Spatial and temporal evaluation of long term trend (2005–2014) of OMI retrieved NO2and SO2 concentrations in Henan Province, China". In: *Atmospheric Environment*. DOI: 10.1016/j.atmosenv.2016.11.067.

Zhang, L., Liao, H., and Li, J. (2010). "Impacts of Asian summer monsoon on seasonal and interannual variations of aerosols over eastern China". In: *Journal of Geophysical Research Atmospheres* 115.7, D00K05. DOI: 10.1029/2009JD012299.

Zhang, Q., Geng, G. N., Wang, S. W., Richter, A., and He, K. B. (2012a). "Satellite remote sensing of changes in NO x emissions over China during 1996-2010". In: *Chinese Science Bulletin* 57.22, pp. 2857–2864. DOI: 10.1007/s11434-012-5015-4.

Zhang, Q., Jiang, X., Tong, D., Davis, S. J., Zhao, H., Geng, G., Feng, T., Zheng, B., et al. (2017b). "Transboundary health impacts of transported global air pollution and international trade". In: *Nature* 543.7647, pp. 705–709. DOI: 10.1038/nature21712.

Zhang, Q., Quan, J., Tie, X., Li, X., Liu, Q., Gao, Y., and Zhao, D. (2015). "Effects of meteorology and secondary particle formation on visibility during heavy haze events in Beijing, China". In: *Science of the Total Environment* 502, pp. 578–584. DOI: 10.1016/j.scitotenv.2014.09.079.

Zhang, X. Y., Wang, Y. Q., Niu, T., Zhang, X. C., Gong, S. L., Zhang, Y. M., and Sun, J. Y. (2012b). "Atmospheric aerosol compositions in China: Spatial/temporal variability, chemical signature, regional haze distribution and comparisons with global aerosols". In: *Atmospheric Chemistry and Physics* 12.2, pp. 779–799. DOI: 10.5194/acp-12-779-2012.

Zhang, X., Wang, Z., Cheng, M., Wu, X., Zhan, N., and Xu, J. (2021). "Long-term ambient SO2 concentration and its exposure risk across China inferred from OMI observations from 2005 to 2018". In: *Atmospheric Research* 247, p. 105150. DOI: 10.1016/j.atmosres.2020.105150.

Zhang, Y.-L. and Cao, F. (2015). "Fine particulate matter (PM2.5) in China at a city level". In: *Scientific Reports* 5.2014, p. 14884. DOI: 10.1038/srep14884.

Zhao, B., Su, Y., He, S., Zhong, M., and Cui, G. (2016a). "Evolution and comparative assessment of ambient air quality standards in China". In: *Journal of Integrative Environmental Sciences* 13.2-4, pp. 85–102. DOI: 10.1080/1943815X.2016.1150301.

Zhao, C., Wang, Y., Yang, Q., Fu, R., Cunnold, D., and Choi, Y. (2010). "Impact of East Asian summer monsoon on the air quality over China: View from space". In: *Journal of Geophysical Research Atmospheres* 115.9, p. D09301. DOI: 10.1029/2009JD012745.

Zhao, D. and Sun, B. (1986). "Atmospheric Pollution from Coal Combustion in China". In: *Journal of the Air Pollution Control Association* 36.4, pp. 371–374. DOI: 10.1080/00022470.1986.10466074.

Zhao, D., Xiong, J., Xu, Y., and Chan, W. H. (1988). "Acid rain in southwestern China". In: *Atmospheric Environment (1967)* 22.2, pp. 349–358. DOI: 10.1016/0004-6981(88)90040-6.

Zhao, S., Yu, Y., Yin, D., He, J., Liu, N., Qu, J., and Xiao, J. (2016b). "Annual and diurnal variations of gaseous and particulate pollutants in 31 provincial capital cities based on in situ air quality monitoring data from China National Environmental Monitoring Center". In: *Environment International* 86, pp. 92–106. DOI: 10.1016/j.envint.2015.11.003.

Zhao, X. J., Zhao, P. S., Xu, J., Meng, W., Pu, W. W., Dong, F., He, D., and Shi, Q. F. (2013). "Analysis of a winter regional haze event and its formation mechanism in the North China Plain". In: *Atmospheric Chemistry and Physics* 13.11, pp. 5685–5696. DOI: 10.5194/acp-13-5685-2013.

Zheng, B., Tong, D., Li, M., Liu, F., Hong, C., Geng, G., Li, H., Li, X., et al. (2018a). "Trends in China's anthropogenic emissions since 2010 as the consequence of clean air actions". In: *Atmospheric Chemistry and Physics* 18.19, pp. 14095–14111. DOI: 10.5194/acp-18-14095-2018.

Zheng, C., Zhao, C., Li, Y., Wu, X., Zhang, K., Gao, J., Qiao, Q., Ren, Y., et al. (2018b). "Spatial and temporal distribution of NO2 and SO2 in Inner Mongolia urban agglomeration obtained from satellite remote sensing and ground observations". In: *Atmospheric Environment* 188, pp. 50–59. DOI: 10.1016/j.atmosenv.2018.06.029.

Zhu, J., Liao, H., and Li, J. (2012). "Increases in aerosol concentrations over eastern China due to the decadal-scale weakening of the East Asian summer monsoon". In: *Geophysical Research Letters* 39.9, p. 9809. DOI: 10.1029/2012GL051428.

Chapter 2

Substantial changes in air pollution across China during 2015–2017

Ben Silver[1], C .L. Reddington[1], S. R. Arnold[1] and D. V. Spracklen[1]

[1] School of Earth and Environment, University of Leeds, Leeds, United Kingdom

Published in *Environmental Research Letters* **13**(11), 13th November 2018

Available at: doi.org/10.1088/1748-9326/aae718

Abstract

China's rapid industrialisation and urbanisation has led to poor air quality. The Chinese government have responded by introducing policies to reduce emissions and setting ambitious targets for ambient $PM_{2.5}$, SO_2, NO_2 and O_3 concentrations. Previous satellite and modelling studies indicate that concentrations of these pollutants have begun to decline within the last decade. However, prior to 2012, air quality data from ground-based monitoring stations were difficult to obtain, limited to a few locations in major cities, and often unreliable. Since then, a comprehensive monitoring network, with over 1000 stations across China has been established by the Ministry of Ecology and Environment (MEE). We use a three-year (2015–2017) dataset consisting of hourly $PM_{2.5}$, O_3, NO_2 and SO_2 concentrations obtained from the MEE, combined with similar data from Taiwan and Hong Kong. We find that at 53% and 59% of stations, $PM_{2.5}$ and SO_2 concentrations have decreased significantly, with median rates across all stations of -3.4 and $-1.9\ \mu g\ m^{-3}\ yr^{-1}$ re-

spectively. At 50% of stations, O_3 maximum daily 8 h mean (MDA8) concentrations have increased significantly, with median rates across all stations of 4.6 $\mu g\,m^{-3}\,yr^{-1}$. It will be important to understand the relative contribution of changing anthropogenic emissions and meteorology to the changes in air pollution reported here.

Introduction

Rapid economic growth and large increase in emissions has led to serious air quality issues across China. Annual $PM_{2.5}$ (mass of particulate matter with a diameter less than 2.5 μm) exceeds 100 $\mu g\,m^{-3}$ in polluted regions of northeast China (Ma et al., 2014; Zhang and Cao, 2015). Exposure to ambient (outdoor) $PM_{2.5}$ is estimated to cause 0.87–1.36 million deaths each year across China (Apte et al., 2015; Lelieveld et al., 2015; Gu and Yim, 2016; Cohen et al., 2017). Health impacts from exposure to ambient $PM_{2.5}$ cause losses equal to 1.1% of gross domestic product at the national level (Xia et al., 2016) with losses of 1.3% in the Pearl River Delta (PRD) and 1.0% in Shanghai (Kan and Chen, 2004; Huang et al., 2012).

To address issues of poor air quality, the Chinese government has introduced policies to reduce pollutant emissions and has established ambient concentration targets for provincial and municipal authorities (Jin et al., 2016). Despite having developed a comprehensive environmental legal framework to control pollution during the 1980s and 1990s, most control methods were not widely enforced until the 2000s (Florig et al., 2002; Beyer, 2006; Feng and Liao, 2016). Desulfurization of coal-fired power plants, introduction of electrostatic precipitators (Liu et al., 2015), closure of polluting power plants and increased efficiency (Guan et al., 2014), have resulted in decreases in emissions of sulphur dioxide (SO_2) and $PM_{2.5}$ (Lu et al., 2010; Klimont et al., 2013; A et al., 2017). Shifts towards cleaner fuels and electricity for cooking and heating in rural areas has contributed to reduced residential $PM_{2.5}$ emissions (Tao et al., 2018). Regulation of nitrogen oxides (NO_x) has resulted in installation of NO_x filtering systems on power plants, phasing out heavily polluting factories and new emission standards for vehicles (Liu et al., 2017; Wu et al., 2017). NO_x emissions over 48 Chinese cities increased by 52% from 2005 to 2011 before decreasing by 21% between 2011–2015 (Liu et al., 2017). In response to the 2012–13 air pollution 'crisis,' where very poor air quality triggered a public outcry, the state council issued the 'Action Plan on Prevention and Control of Air Pollution' that prioritised $PM_{2.5}$

reduction in megacity regions (Sheehan et al., 2014; Wang et al., 2018). According to the estimates made in the Multi-resolution Emission Inventory for China, emissions of SO_2, NO_2, $PM_{2.5}$, PM_{10} (mass of particulate matter with a diameter less than 10 μm) and carbon monoxide (CO) have decreased during 2013–2017 (Zheng et al., 2018).

Understanding the impacts of changing emissions on pollutant concentrations is necessary to assess past management policies and identify future policy challenges. Longer term records of surface air pollutants are available across the PRD, showing that $PM_{2.5}$ concentrations increased between 2000–2005 before decreasing from 2005–2010 (Wang et al., 2016). Elsewhere across China a lack of widespread surface measurement data prior to 2012 means most previous analyses have relied on satellite data, visibility observations or emission estimates combined with modelling to establish air quality trends.

A number of studies have used satellite retrievals of aerosol optical depth to estimate trends in $PM_{2.5}$ concentrations. Peng et al. (2016) reported increased $PM_{2.5}$ concentrations across China between 1999–2011. Ma et al. (2016b) reported a positive trend in $PM_{2.5}$ across China between 2004–2007, followed by a negative trend between 2007–2013. Lin et al. (2018) found Chinese $PM_{2.5}$ concentrations increased between 2001–2005, before decreasing from 2006–2015. Fu et al. (2014) used visibility data across the North China Plain (NCP) to show a positive trend in low visibility days between 1980–1995, little trend between 1995–2003 followed by a reduction in low visibility days between 2003–2010, particularly in winter. Visibility data has also been used to estimate that annual mean $PM_{2.5}$ in Beijing increased between 1973–2013 by an average of 0.6 $\mu g\, m^{-3}\, yr^{-1}$ (Han et al., 2016). A modelling study suggests that population-weighted $PM_{2.5}$ concentrations across China increased by 53% between 1960–2010 and by 10%–35% between 1990–2010 (Butt et al., 2017). Li et al. (2017a) use satellite and *in situ* observations to downscale a global model and estimate that in East Asia, annual population-weighted mean $PM_{2.5}$ increased significantly by 0.86 $\mu g\, m^{-3}\, yr^{-1}$ during 1998–2013, with an insignificantly decreasing trend during 2006–2013.

Satellite observations show that SO_2 concentrations over the NCP region peaked in 2007, decreasing by 50% between 2005–2015 (Krotkov et al., 2016). Declines in SO_2 across China are also more widespread, with a 50% decline in SO_2 concentrations reported across the most polluted provinces in China between 2005–2015 (Ling et al., 2017; A et al., 2017). Li et al. (2017b) estimate that SO_2 loading over China decreased by a factor of five between

2007–2016, by which time 350 million fewer people were exposed to dangerous concentrations.

Satellite observations have shown that similarly to SO_2 and $PM_{2.5}$, nitrogen dioxide (NO_2) has begun to decrease across China (Zhang et al., 2012; Zhang et al., 2018; Irie et al., 2016; Krotkov et al., 2016). Across the NCP, NO_2 concentrations increased by 50% between 2005–2011, before returning to 2005 levels by 2015 (Krotkov et al., 2016). The same trend with a maximum in 2011 was observed when averaging across the whole of China (Irie et al., 2016). Gu et al. (2013) found that while the trend in NO_x emissions was positive across the whole of China during 2005–2010, the more economically developed regions such as the PRD and municipalities of Beijing and Shanghai had comparatively lower concentrations or negative trends.

Satellite observations suggest ozone (O_3) concentrations have been steadily increasing across China at a rate of 7% yr^{-1} between 2005–2010 (Verstraeten et al., 2015). Although there are no long term records of surface O_3 measurements in urban areas of China, there is evidence of positive trends at background sites. During 2003–2015, maximum daily average 8 h mean (MDA8) O_3 concentrations increased at a rate of 1.13 ppb yr^{-1} at a monitoring station 100 km northeast of Beijing (Ma et al., 2016a). An increase of 0.25 ppb yr^{-1} was recorded at a remote background site in western China between 1994–2013 (Xu et al., 2016), and in southern China, and at a background site in Hong Kong an increase of 0.58 ppb yr^{-1} between 1994–2007 was recorded (Wang et al., 2009).

Most of our understanding of recent trends in air pollution across China comes from satellite studies or from relatively few *in situ* observations. There have been very few attempts to use data from surface monitoring stations to assess recent trends. Here we use data from >1600 surface monitoring stations across China and Taiwan for the period 2015–2017 to explore recent trends in the concentrations of air pollutants.

Methods

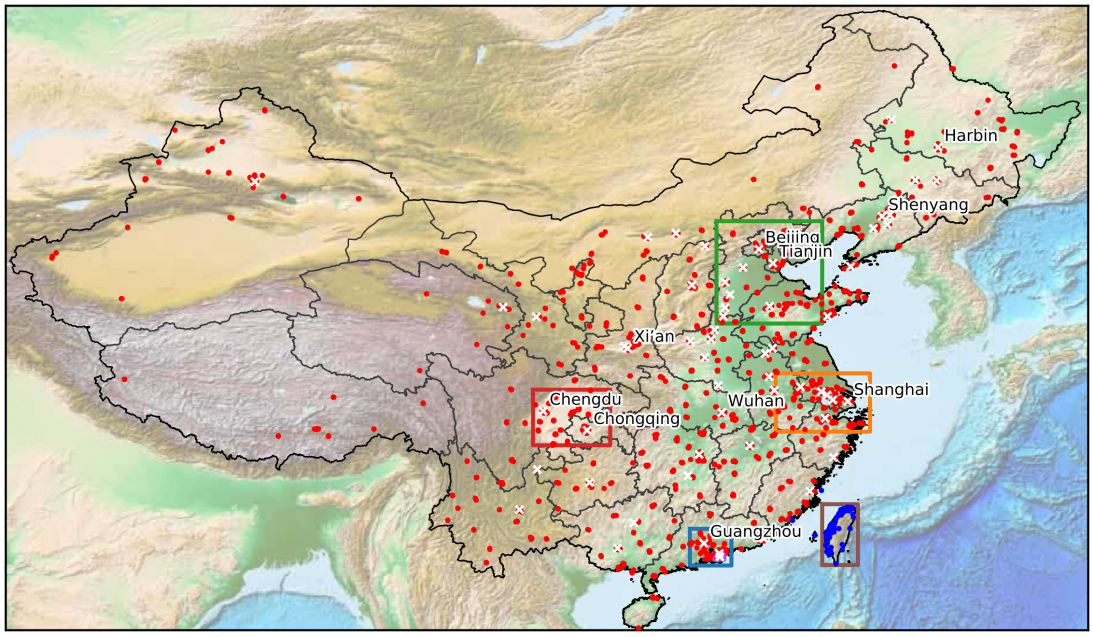

Figure 2.1: Location of air quality stations in Mainland China (red), Taiwan (blue) and Hong Kong (magenta) used in this analysis. The 60 largest cities by population are marked with white crosses, of which the 10 largest are labelled.

Three year time series (January 2015–December 2017) of hourly concentrations of $PM_{2.5}$, PM_{10}, CO, O_3, SO_2 and NO_2 were downloaded for stations operated by the environmental protection departments for Mainland China (MC), Hong Kong (HK) and Taiwan (TW). Data for MC was downloaded from `http://beijingair.sinaapp.com/` which had obtained the data from `http://pm25.in`, a mirror of data from the official Ministry of Ecology and Environment download platform (`http://106.37.208.233:20035/`). Similar data has been used in other studies (e.g. Rohde and Muller (2015), Liang et al. (2016), and Leung et al. (2018)). HK data was downloaded from the HK Environmental Protection department (`https://cd.epic.epd.gov.hk/EPICDI/air/station/`) and TW data was downloaded from the TW Environmental Protection Agency (`https://taqm.epa.gov.tw/taqm/en/YearlyDataDownload.aspx`). MC data has been described in detail by Zhang and Cao (2015). TW data (excluding aerosol measurements) was reported as a mole fraction, so these were converted into mass concentration to match MC and HK data by using meteorological data (73 stations), and assuming standard pressure and a temperature of 23 °C where this was unavailable (4 stations). Together these sources provided data from 1689 monitoring stations, with 13 from HK (the roadside stations are not used), 75 from TW and 1601 from MC. Locations of the stations are shown in Figure 2.1.

Table 2.1: The number of monitoring stations (# stations) available for each pollutant and the number of stations that were removed during data checking.

	Pollutant			
	NO_2	$PM_{2.5}$	O_3	SO_2
# stations	1689	1689	1687	1689
# stations with >5% consecutive repeats	148	100	1	N/A
# stations removed due to <90% of data being present	520	505	339	296
# stations removed due to 'day-to-day' repeats	10	37	11	25
# stations remaining in the analysis	1159	1147	1337	1368

Previously there have been doubts about the reliability of air quality monitoring data from China, due to manipulation of data by local environmental protection bureaus which resulted in discontinuities around air quality targets (Andrews, 2008; Ghanem and Zhang, 2014). However, by comparing Chinese data with data from United States Embassy and Consulate monitoring stations, it has been shown that data is more reliable since 2013 (Liang et al., 2016; Stoerk, 2016). Other quality issues with the MC data have been previously noted including a high proportion of repeating values at some sites (Rohde and Muller, 2015), and periods when reported $PM_{2.5}$ concentrations exceed PM_{10} concentrations (Liu et al., 2016b).

To address potential quality issues we applied the following procedure to all the data used in the study. First, we removed consecutive repeats from the data. Values were removed from NO_2 and $PM_{2.5}$ time series when there were >4 consecutive repeats, and for O_3 where there were >24 consecutive repeats. 148 and 100 stations contained >5% consecutive repeats for NO_2 and $PM_{2.5}$ respectively and 1 station contained >5% repeats for O_3. The data contain a small fraction (<0.04%) of zero values, which are unlikely to be accurate and could be caused by lower precision around the detection limit. We remove zero values from the time series. After consecutive repeats and zeroes have been removed, if <90% of hourly data is available for the whole time series, it is removed. Finally, to remove day-to-day repeats, data were flagged if the daily mean had a low coefficient of variation in a certain period (see Table A.1). If >60 days were flagged, the station is removed. The number of stations identified at each stage of data quality checking are shown in table 2.1. The thresholds used were chosen by applying the procedure with a range of thresholds, and manually examining the datasets to verify whether suspect data were removed. The thresholds applied for the different pollutants are given in supplementary table A.1. We test the sensitivity of our analysis to these thresholds and find the magnitude of the trends we calculate are not sensitive to the values of the thresholds we choose (supplementary

table A.1).

The hourly data is used to calculate monthly averages. We then deseasonalised the data (the results using non-deseasonalised data are shown in supplementary figure A.2). To analyse the three-year time series for monotonic, linear trends, the Mann-Kendall test was used to assess the significance of trends (using a threshold of $p < 0.05$), and the Theil–Sen estimator was used to calculate the magnitude of the trend. Both tests are resistant to outliers, and do not require any assumptions about the data used (Carslaw, 2015; Fleming et al., 2018). Absolute trends were converted to relative trends by dividing by the 2015 to 2017 mean. For O_3, the trend tests were also applied to the MDA8 metric, which is used in the World Health Organisation's (WHO) air quality guidelines (AQGs). The R package '*openair*,' which contains a set of tools developed specifically for analysing air quality data, was used to perform this stage of the analysis (Carslaw and Ropkins, 2012).

We specifically analyse trends for large urban clusters: Pearl River Delta (PRD), Yangtze River Delta (YRD), North China Plain (NCP), and Sichuan Basin (SCB). Additionally, we analyse trends for the Hong Kong Special Administrative Region (HK) (which is within the PRD domain) and Taiwan (TW).

Air pollution concentrations and trends

Annual mean concentrations of air pollutants during 2015–2017 are shown in Figure 2.2 and supplementary figures A.3 and A.4. Highest annual mean $PM_{2.5}$ concentrations are found in the provinces of Hebei, Henan and Shandong, which all have a median concentration of $>60\ \mu g\,m^{-3}$. Stations in Shanghai and Guangdong have lower $PM_{2.5}$ concentrations, while the lowest $PM_{2.5}$ concentrations (20–25 $\mu g\,m^{-3}$) are found in Hong Kong, Taiwan and Xizang. The highest concentrations of SO_2 are found in Shanxi, which has a median concentration of $>60\ \mu g\,m^{-3}$, and in Hebei which has a median concentration of 37 $\mu g\,m^{-3}$. High NO_2 concentrations are found across the Tianjin, Hebei and Beijing region, as well as Shanghai, Hong Kong and Chongqing. The provinces with the highest median O_3 concentrations are the high elevation provinces of Xizang and Qinghai. Hong Kong and Chongqing have some of the lowest O_3 concentrations.

Figure 2.2 also shows trends in air pollutants during 2015–2017. The median trend in annual mean $PM_{2.5}$ concentration across all stations is $-3.4\ \mu g\,m^{-3}\,yr^{-1}$ or $-7.2\%\ yr^{-1}$. This is comparable to Zheng et al. (2017), who find that the annual mean $PM_{2.5}$ across 74 Chinese

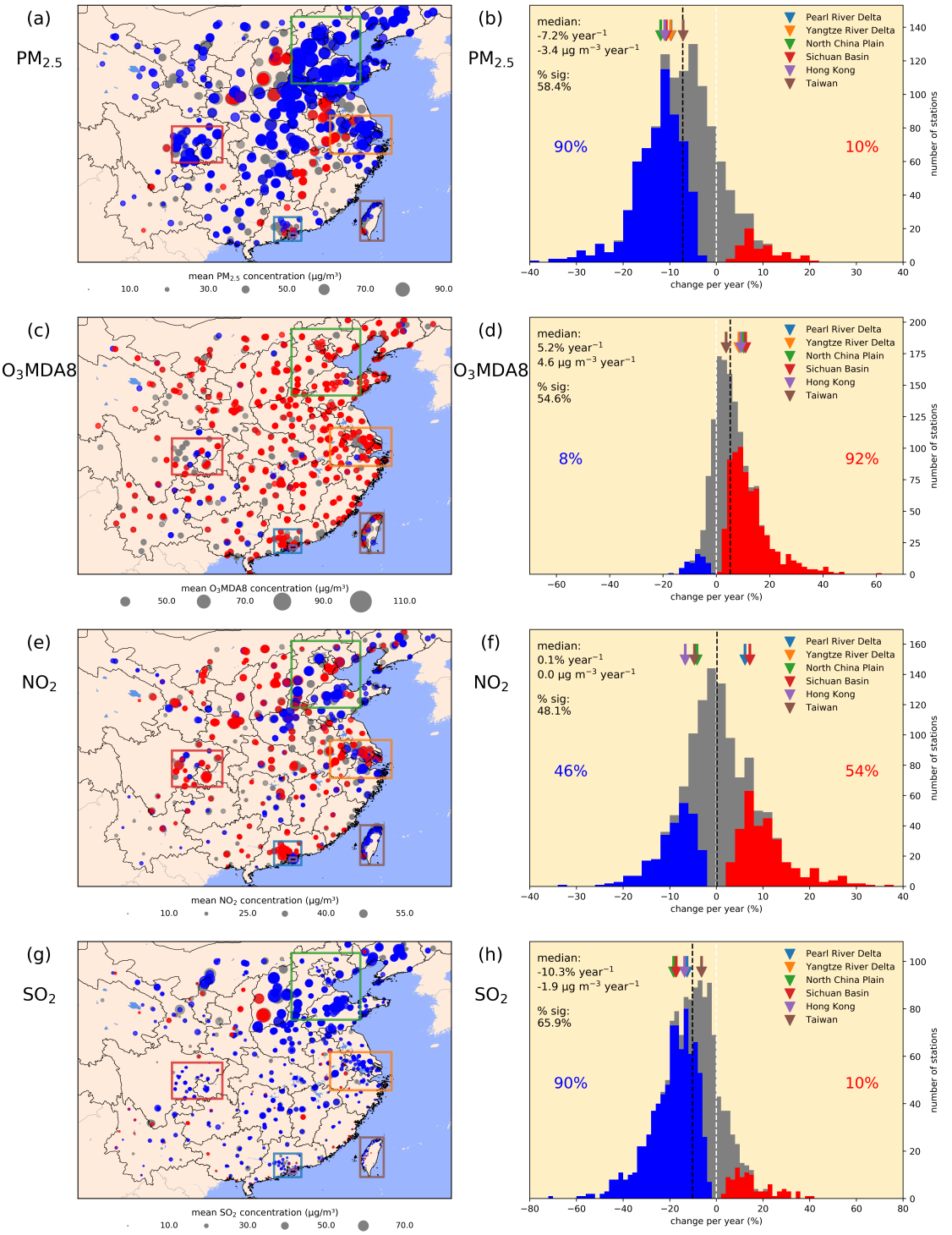

Figure 2.2: Trends in concentrations of (a), (b) $PM_{2.5}$, (c), (d) O_3 MDA8, (e), (f) NO_2, (g), (h) SO_2 across Mainland China, Hong Kong and Taiwan during 2015–2017. Left-hand panels (a), (c), (e), (g) show the sign of trend (blue: significant negative, red: significant positive, grey: insignificant) and mean concentration (size of circle). Right hand panels (b), (d), (f), (h) show the frequency of stations against the relative trends. The median relative and absolute trend as well as the percentage of stations with significant trends is shown on each panel. The percentage of significant trends that are negative (blue) or positive (red) are also shown. The black dotted line shows the median trend across all sites. Triangles show the median trend for the regional domains shown in the left-hand panels: Pearl River Delta (PRD), Yangtze River Delta (YRD), North China Plain (NCP), Sichuan Basin (SCB), Hong Kong Special Administrative Region (HK) and Taiwan (TW). The left panels are zoomed to show the trends over the more populous regions of China, while median trends and % of significant sites on the right panels refer to all Mainland China, Hong Kong and Taiwan.

cities decreased by 23.6% between 2013–2015 ($-7.9\%\ yr^{-1}$). Lin et al. (2018) used satellite data to suggest the Chinese $PM_{2.5}$ trend steepened from $-0.65\ \mu g\,m^{-3}\,yr^{-1}$ between 2006–2010 to $-2.3\ \mu g\,m^{-3}\,yr^{-1}$ between 2011–2015. Our work suggests that the rate of $PM_{2.5}$ decline has been sustained, or possibly even become faster, between 2015–2017. We find 58.4% of stations have significant $PM_{2.5}$ concentration trends, and of these, 90% are negative. PM_{10} concentrations exhibit similar trends (supplementary figure A.5). The fraction of stations meeting the WHO's first Interim Target for annual average $PM_{2.5}$ concentration of $35\ \mu g\,m^{-3}$ rose from 15% in 2015 to 20% in 2017.

Figure 2.3 shows the relative trends in air pollutants at the province level (supplementary figure A.6 shows absolute trends). Negative trends in $PM_{2.5}$ concentrations are widespread, with all provinces experiencing negative median trends except Shanxi and Jiangxi. Most provinces had trends of around $-10\%\ yr^{-1}$, with faster reductions in some areas including Beijing municipality ($-14.4\%\ yr^{-1}$). Widespread reductions in $PM_{2.5}$ concentrations are consistent with trends estimated from satellite data for the period 2011–2015 (Lin et al., 2018).

The median trend in annual mean SO_2 concentration across all stations is $-1.9\ \mu g\,m^{-3}\,yr^{-1}$ or $-10.3\%\ yr^{-1}$. 66% of stations have significant trends, and of these, 90% are negative. The mean exceedance rate of the WHO 24 h AQG fell from 10.8% in 2015 to 7.6% in 2017. Similarly to $PM_{2.5}$, negative trends in SO_2 concentrations are widespread across provinces (figure 2.3), with all having median negative trends apart from Hainan and Fujian, both of which have low absolute concentrations (supplementary figure A.3).

There is no median trend in annual mean NO_2 concentration ($0.0\ \mu g\,m^{-3}\,yr^{-1}$ or $0.1\%\ yr^{-1}$). 48% of stations have significant trends, and of these, 54% are positive. The percentage of the stations that comply with the WHO's annual mean AQG of $40\ \mu g\,m^{-3}$ has declined, from 71% in 2015 to 66% in 2017. There is more heterogeneity in the spatial distribution of trends, with median positive trends in the SCB, YRD and PRD domains, but median negative trends in HK, NCP and TW (figure 2.2). The greater spatial heterogeneity of NO_2 trends could be partly due to its comparatively shorter lifetime, so that neighbouring regions can have opposing trends (e.g. HK and the PRD). The NO_2 concentration trends we report for 2015–2017 are more variable that the consistent declines in NO_x emissions (Liu et al., 2016a; A et al., 2017) and NO_2 concentrations Krotkov et al. (2016) reported for the period 2011–2015.

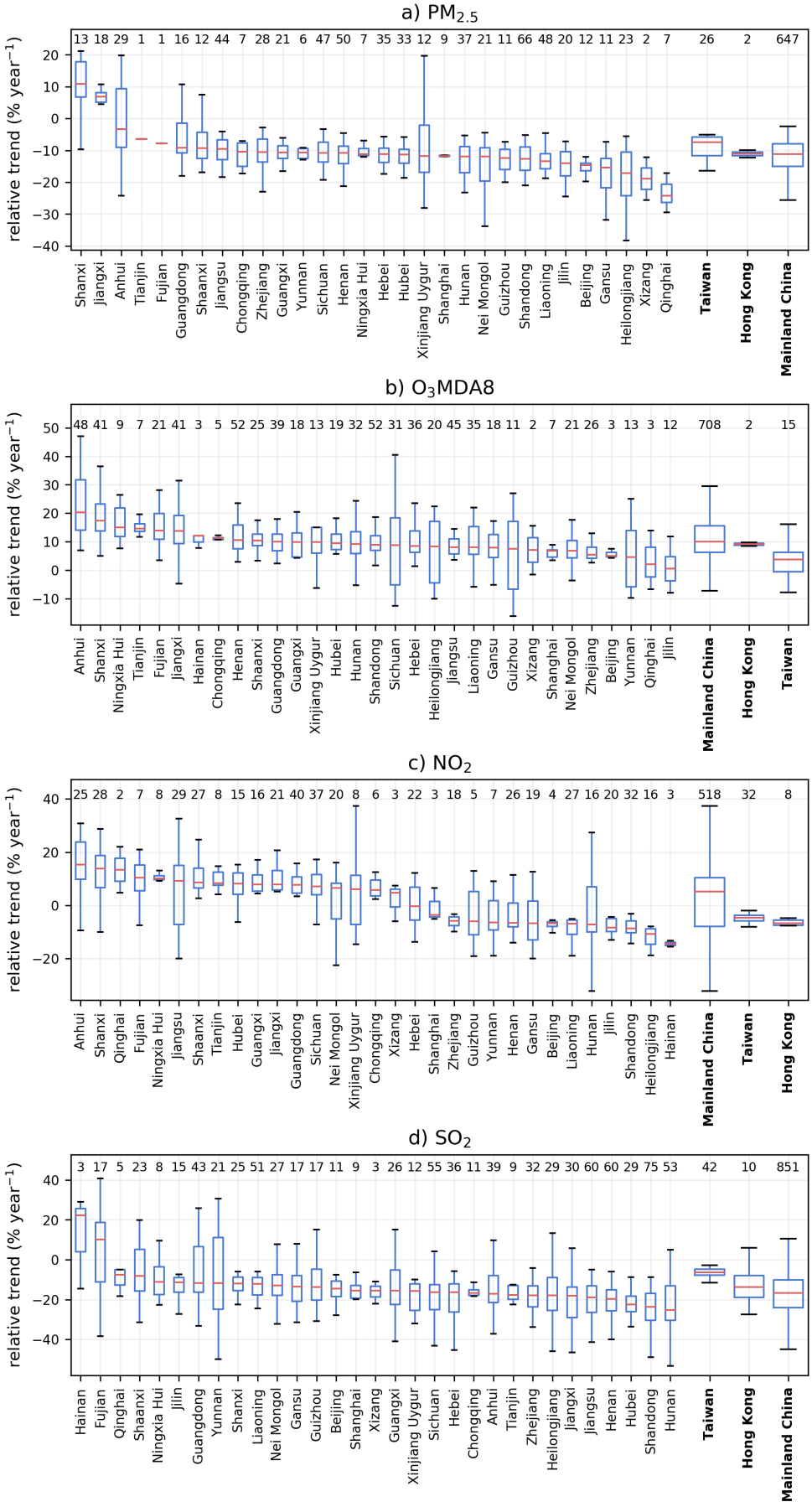

Figure 2.3: Relative trends in (a) $PM_{2.5}$, (b) O_3 MDA8, (c) NO_2 and (d) SO_2 by province or region (bolded). The median (red line), interquartile range (IQR) (box) and IQR $\pm$ IQR$*1.5$ (whiskers) of the trend across the stations in each province/region is shown. The number of stations in each province/region is indicated at the top of the plot.

In contrast to $PM_{2.5}$ and SO_2, annual mean O_3 MDA8 has a positive median trend of 4.6 $\mu g\,m^{-3}\,yr^{-1}$ or 5.2% yr^{-1}. 55% of stations have significant trends, and of these, 92% are positive. Averaging across all stations, the percentage of days where the WHO AQG (100 $\mu g\,m^{-3}$) was exceeded for MDA8 rose from 9.8% in 2015 to 12.4% in 2017. Annual mean O_3 concentrations show similar relative and absolute trends (supplementary figures A.7 and A.8). The Tropospheric Ozone Assessment Report, which did not aggregate trends specifically for China due to lack of stations with long records, also reports significant positive trends over East Asia (Chang et al., 2017; Fleming et al., 2018). All the megacity regions highlighted in figure 2.2 have medians greater than the overall median, and there are only 4 regions in figure 2.3 with median negative trends. During 2005–2013, Chinese megacity clusters shifted from a VOC-limited (NO_x saturated) O_3 production regime towards a mixed regime, due to reductions in NO_x emissions, which has lessened the NO_x titration effect resulting in increases in O_3 concentration (Jin and Holloway, 2015). Meanwhile, increasing NO_x emissions in less developed cities has led to a shift from NO_x limited regimes towards mixed regimes, which have high O_3 production efficiency (Jin and Holloway, 2015).

Discussion and conclusion

We find substantial changes in the concentrations of air pollutants across China during the period of 2015–2017. We report negative trends in annual mean $PM_{2.5}$ (3.4 $\mu g\,m^{-3}\,yr^{-1}$) and SO_2 ($-1.9\ \mu g\,m^{-3}\,yr^{-1}$) concentrations and positive trends in annual mean O_3 MDA8 (4.7 $\mu g\,m^{-3}\,yr^{-1}$) concentrations. The observed trends are widespread across China and occur consistently across most of the country. In contrast we find spatially variable changes in NO_2, with no overall trend across China. Trends in $PM_{2.5}$ and SO_2 concentrations are consistent with previous studies, that report negative trends in both $PM_{2.5}$ (Ma et al., 2016b; Lin et al., 2018) and SO_2 (Krotkov et al., 2016; A et al., 2017) between 2007 and 2015. Our study therefore suggests that declines in $PM_{2.5}$ and SO_2 concentrations that have been reported for 2007–2015 continued between 2015 and 2017.

The trends we report are calculated over a relatively short period and could be caused by a variety of different factors. Air pollution is strongly dependent on weather. Inter-annual variability in meteorology and synoptic weather conditions (Leung et al., 2018) may therefore play a role in the trends we observe here. Air pollution over China is in-

fluenced by variability in atmospheric circulation such as El Niño Southern Oscillation (ENSO) (Cao et al., 2015; Zhao et al., 2017) and the Asian monsoon (Li et al., 2016; Cai et al., 2017). El Niño years are associated with greater surface $PM_{2.5}$ in southern China and lesser $PM_{2.5}$ in northern China compared to La Niña years (Zhao et al., 2017). ENSO variability is therefore unlikely to cause the spatially extensive trends in air pollutants across all of China that we report. It is possible that ENSO may have retarded the reduction in surface $PM_{2.5}$ over northern China during 2015–2017. Changes in land cover and local meteorological conditions also alter the emissions of natural aerosol and trace gases (Fu et al., 2016), including dust and biogenic volatile organic compounds that can form secondary organic aerosol and alter concentrations of O_3. Leung et al. (2018) suggest that $PM_{2.5}$ across the NCP will decrease by 0.5 $\mu g\, m^{-3}$ by the 2050s due to climate change, substantially less than the changes we report over the past 3 years. Since the trends over the period 2015–2017 are consistent with trends over the period 2007–2015, occur consistently across the country and coincide with declining Chinese anthropogenic emissions (Zheng et al., 2018), we suggest that the trends are likely dominated by these emission changes. Future work needs to use air quality models to fully assess the contribution of different drivers of the trends reported here. It will be particularly important to establish what is causing the widespread increase in O_3 concentrations, so that emissions control policies can be most effectively targeted.

References

A, R. J. van der, Mijling, B., Ding, J., Elissavet Koukouli, M., Liu, F., Li, Q., Mao, H., and Theys, N. (2017). "Cleaning up the air: Effectiveness of air quality policy for SO2 and NOx emissions in China". In: *Atmospheric Chemistry and Physics* 17.3, pp. 1775–1789. DOI: 10.5194/acp-17-1775-2017.

Andrews, S. Q. (2008). "Inconsistencies in air quality metrics: 'Blue Sky' days and PM10 concentrations in Beijing". In: *Environmental Research Letters* 3.3, p. 034009. DOI: 10.1088/1748-9326/3/3/034009.

Apte, J. S., Marshall, J. D., Cohen, A. J., and Brauer, M. (2015). "Addressing Global Mortality from Ambient PM2.5". In: *Environmental Science and Technology* 49.13, pp. 8057–8066. DOI: 10.1021/acs.est.5b01236.

Beyer, S. (2006). "Environmental Law and Policy in the People's Republic of China". In: *Chinese Journal of International Law* 5.1, pp. 185–211. DOI: 10.1093/chinesejil/jmk002.

Butt, E. W., Turnock, S. T., Rigby, R., Reddington, C. L., Yoshioka, M., Johnson, J. S., Regayre, L. A., Pringle, K. J., et al. (2017). "Global and regional trends in particulate air pollution and attributable health burden over the past 50 years". In: *Environmental Research Letters*. DOI: 10.1088/1748-9326/aa87be.

Cai, W., Li, K., Liao, H., Wang, H., and Wu, L. (2017). "Weather conditions conducive to Beijing severe haze more frequent under climate change". In: *Nature Climate Change* 7.4, pp. 257–262. DOI: 10.1038/nclimate3249.

Cao, Z., Sheng, L., Liu, Q., Yao, X., and Wang, W. (2015). "Interannual increase of regional haze-fog in North China Plain in summer by intensified easterly winds and orographic forcing". In: *Atmospheric Environment* 122, pp. 154–162. DOI: 10.1016/j.atmosenv.2015.09.042.

Carslaw, D. (2015). "The openair manual open-source tools for analysing air pollution data". In: *King's College London* January, p. 287. URL: http://www.openair-project.org/PDF/OpenAir%7B%5C_%7DManual.pdf.

Carslaw, D. C. and Ropkins, K. (2012). "openair – Data Analysis Tools for the Air Quality Community". In: *R Journal* 4.1, pp. 20–29.

Chang, K.-L., Petropavlovskikh, I., Copper, O. R., Schultz, M. G., and Wang, T. (2017). "Regional trend analysis of surface ozone observations from monitoring networks in eastern North America, Europe and East Asia". In: *Elem Sci Anth* 5.0, p. 50. DOI: 10.1525/elementa.243.

Cohen, A. J., Brauer, M., Burnett, R., Anderson, H. R., Frostad, J., Estep, K., Balakrishnan, K., Brunekreef, B., et al. (2017). "Estimates and 25-year trends of the global burden of disease attributable to ambient air pollution: an analysis of data from the Global Burden of Diseases Study 2015". In: *The Lancet* 389.10082, pp. 1907–1918. DOI: 10.1016/S0140-6736(17)30505-6.

Feng, L. and Liao, W. (2016). "Legislation, plans, and policies for prevention and control of air pollution in China: Achievements, challenges, and improvements". In: *Journal of Cleaner Production* 112, pp. 1549–1558. DOI: 10.1016/j.jclepro.2015.08.013.

Fleming, Z. L., Doherty, R. M., Von Schneidemesser, E., Malley, C. S., Cooper, O. R., Pinto, J. P., Colette, A., Xu, X., et al. (2018). "Tropospheric ozone assessment report: Present-day ozone distribution and trends relevant to human health". In: *Elem Sci Anth* 6.1, p. 12. DOI: 10.1525/elementa.273.

Florig, H. K., Sun, G., and Song, G. (2002). "Evolution of particulate regulation in China - Prospects and challenges of exposure-based control". In: *Chemosphere* 49.9, pp. 1163–1174. DOI: 10.1016/S0045-6535(02)00246-1.

Fu, G. Q., Xu, W. Y., Yang, R. F., Li, J. B., and Zhao, C. S. (2014). "The distribution and trends of fog and haze in the North China Plain over the past 30 years". In: *Atmospheric Chemistry and Physics* 14.21, pp. 11949–11958. DOI: 10.5194/acp-14-11949-2014.

Fu, Y., Tai, A. P., and Liao, H. (2016). "Impacts of historical climate and land cover changes on fine particulate matter (PM2.5) air quality in East Asia between 1980 and 2010". In: *Atmospheric Chemistry and Physics* 16.16, pp. 10369–10383. DOI: 10.5194/acp-16-10369-2016.

Ghanem, D. and Zhang, J. (2014). "'Effortless Perfection:' Do Chinese cities manipulate air pollution data?" In: *Journal of Environmental Economics and Management* 68.2, pp. 203–225. DOI: 10.1016/j.jeem.2014.05.003.

Gu, D., Wang, Y., Smeltzer, C., and Liu, Z. (2013). "Reduction in NOxemission trends over China: Regional and seasonal variations". In: *Environmental Science and Technology* 47.22, pp. 12912–12919. DOI: 10.1021/es401727e.

Gu, Y. and Yim, S. H. (2016). "The air quality and health impacts of domestic trans-boundary pollution in various regions of China". In: *Environment International* 97, pp. 117–124. DOI: 10.1016/j.envint.2016.08.004.

Guan, D., Su, X., Zhang, Q., Peters, G. P., Liu, Z., Lei, Y., and He, K. (2014). "The socioeconomic drivers of China's primary PM2.5 emissions". In: *Environmental Research Letters* 9.2, p. 024010. DOI: 10.1088/1748-9326/9/2/024010.

Han, L., Zhou, W., and Li, W. (2016). "Fine particulate (PM2.5) dynamics during rapid urbanization in Beijing, 1973-2013". In: *Scientific Reports* 6.1, p. 23604. DOI: 10.1038/srep23604.

Huang, D., Xu, J., and Zhang, S. (2012). "Valuing the health risks of particulate air pollution in the Pearl River Delta, China". In: *Environmental Science and Policy* 15.1, pp. 38–47. DOI: 10.1016/j.envsci.2011.09.007.

Irie, H., Muto, T., Itahashi, S., Kurokawa, J.-i., and Uno, I. (2016). "Turnaround of Tropospheric Nitrogen Dioxide Pollution Trends in China, Japan, and South Korea". In: *Sola* 12.0, pp. 170–174. DOI: 10.2151/sola.2016-035.

Jin, X. and Holloway, T. (2015). "Spatial and temporal variability of ozone sensitivity over China observed from the Ozone Monitoring Instrument". In: *Journal of Geophysical Research* 120.14, pp. 7229–7246. DOI: 10.1002/2015JD023250.

Jin, Y., Andersson, H., and Zhang, S. (2016). "Air pollution control policies in China: A retrospective and prospects". In: *International Journal of Environmental Research and Public Health* 13.12. DOI: 10.3390/ijerph13121219.

Kan, H. and Chen, B. (2004). "Particulate air pollution in urban areas of Shanghai, China: Health-based economic assessment". In: *Science of the Total Environment* 322.1-3, pp. 71–79. DOI: 10.1016/j.scitotenv.2003.09.010.

Klimont, Z., Smith, S. J., and Cofala, J. (2013). "The last decade of global anthropogenic sulfur dioxide: 2000–2011 emissions". In: *Environmental Research Letters* 8.1, p. 014003. DOI: 10.1088/1748-9326/8/1/014003.

Krotkov, N. A., McLinden, C. A., Li, C., Lamsal, L. N., Celarier, E. A., Marchenko, S. V., Swartz, W. H., Bucsela, E. J., et al. (2016). "Aura OMI observations of regional SO2 and NO2 pollution changes from 2005 to 2015". In: *Atmospheric Chemistry and Physics* 16.7, pp. 4605–4629. DOI: 10.5194/acp-16-4605-2016.

Lelieveld, J., Evans, J. S., Fnais, M., Giannadaki, D., and Pozzer, A. (2015). "The contribution of outdoor air pollution sources to premature mortality on a global scale". In: *Nature* 525.7569, pp. 367–371. DOI: 10.1038/nature15371.

Leung, D. M., Tai, A. P., Mickley, L. J., Moch, J. M., Van Donkelaar, A., Shen, L., and Martin, R. V. (2018). "Synoptic meteorological modes of variability for fine particulate matter (PM2.5) air quality in major metropolitan regions of China". In: *Atmospheric Chemistry and Physics* 18.9, pp. 6733–6748. DOI: 10.5194/acp-18-6733-2018.

Li, C., McLinden, C., Fioletov, V., Krotkov, N., Carn, S., Joiner, J., Streets, D., He, H., et al. (2017a). "India Is Overtaking China as the World's Largest Emitter of Anthropogenic Sulfur Dioxide". In: *Scientific Reports* 7.1, p. 14304. DOI: 10.1038/s41598-017-14639-8.

Li, M., Liu, H., Geng, G., Hong, C., Liu, F., Song, Y., Tong, D., Zheng, B., et al. (2017b). "Anthropogenic emission inventories in China: A review". In: *National Science Review* 4.6, pp. 834–866. DOI: 10.1093/nsr/nwx150.

Li, Q., Zhang, R., and Wang, Y. (2016). "Interannual variation of the wintertime fog-haze days across central and eastern China and its relation with East Asian winter monsoon". In: *International Journal of Climatology* 36.1, pp. 346–354. DOI: 10.1002/joc.4350.

Liang, X., Li, S., Zhang, S., Huang, H., and Chen, S. X. (2016). "PM2.5 data reliability, consistency, and air quality assessment in five Chinese cities". In: *Journal of Geophysical Research* 121.17, pp. 10, 220–10, 236. DOI: 10.1002/2016JD024877.

Lin, C. Q., Liu, G., Lau, A. K., Li, Y., Li, C. C., Fung, J. C., and Lao, X. Q. (2018). "High-resolution satellite remote sensing of provincial PM2.5trends in China from 2001 to

2015". In: *Atmospheric Environment* 180, pp. 110–116. DOI: 10.1016/j.atmosenv.2018.02.045.

Ling, Z., Huang, T., Zhao, Y., Li, J., Zhang, X., Wang, J., Lian, L., Mao, X., et al. (2017). "OMI-measured increasing SO2 emissions due to energy industry expansion and relocation in northwestern China". In: *Atmospheric Chemistry and Physics* 17.14, pp. 9115–9131. DOI: 10.5194/acp-17-9115-2017.

Liu, F., Zhang, Q., Tong, D., Zheng, B., Li, M., Huo, H., and He, K. B. (2015). "High-resolution inventory of technologies, activities, and emissions of coal-fired power plants in China from 1990 to 2010". In: *Atmospheric Chemistry and Physics* 15.23, pp. 13299–13317. DOI: 10.5194/acp-15-13299-2015.

Liu, F., Zhang, Q., Van Der A, R. J., Zheng, B., Tong, D., Yan, L., Zheng, Y., and He, K. (2016a). "Recent reduction in NOx emissions over China: Synthesis of satellite observations and emission inventories". In: *Environmental Research Letters* 11.11, p. 114002. DOI: 10.1088/1748-9326/11/11/114002.

Liu, J., Li, W., and Li, J. (2016b). "Quality screening for air quality monitoring data in China". In: *Environmental Pollution* 216, pp. 720–723. DOI: 10.1016/j.envpol.2016.06.037.

Liu, Y. H., Liao, W. Y., Lin, X. F., Li, L., and Zeng, X. lan (2017). "Assessment of Co-benefits of vehicle emission reduction measures for 2015–2020 in the Pearl River Delta region, China". In: *Environmental Pollution* 223, pp. 62–72. DOI: 10.1016/j.envpol.2016.12.031.

Lu, Z., Streets, D. G., Zhang, Q., Wang, S., Carmichael, G. R., Cheng, Y. F., Wei, C., Chin, M., et al. (2010). "Sulfur dioxide emissions in China and sulfur trends in East Asia since 2000". In: *Atmospheric Chemistry and Physics* 10.13, pp. 6311–6331. DOI: 10.5194/acp-10-6311-2010.

Ma, Z., Xu, J., Quan, W., Zhang, Z., Lin, W., and Xu, X. (2016a). "Significant increase of surface ozone at a rural site, north of eastern China". In: *Atmospheric Chemistry and Physics* 16.6, pp. 3969–3977. DOI: 10.5194/acp-16-3969-2016.

Ma, Z., Hu, X., Huang, L., Bi, J., and Liu, Y. (2014). "Estimating ground-level PM2.5 in china using satellite remote sensing". In: *Environmental Science and Technology* 48.13, pp. 7436–7444. DOI: 10.1021/es5009399.

Ma, Z., Hu, X., Sayer, A. M., Levy, R., Zhang, Q., Xue, Y., Tong, S., Bi, J., et al. (2016b). "Satellite-based spatiotemporal trends in PM2.5concentrations: China, 2004-2013". In: *Environmental Health Perspectives* 124.2, pp. 184–192. DOI: 10.1289/ehp.1409481.

Peng, J., Chen, S., Lü, H., Liu, Y., and Wu, J. (2016). "Spatiotemporal patterns of remotely sensed PM2.5concentration in China from 1999 to 2011". In: *Remote Sensing of Environment* 174, pp. 109–121. DOI: 10.1016/j.rse.2015.12.008.

Rohde, R. A. and Muller, R. A. (2015). "Air pollution in China: Mapping of concentrations and sources". In: *PLoS ONE* 10.8. Ed. by A. Ding, e0135749. DOI: 10.1371/journal.pone.0135749.

Sheehan, P., Cheng, E., English, A., and Sun, F. (2014). "China's response to the air pollution shock". In: *Nature Climate Change* 4.5, pp. 306–309. DOI: 10.1038/nclimate2197.

Stoerk, T. (2016). "Statistical corruption in Beijing's air quality data has likely ended in 2012". In: *Atmospheric Environment* 127, pp. 365–371. DOI: 10.1016/j.atmosenv.2015.12.055.

Tao, S., Ru, M. Y., Du, W., Zhu, X., Zhong, Q. R., Li, B. G., Shen, G. F., Pan, X. L., et al. (2018). "Quantifying the rural residential energy transition in China from 1992 to 2012 through a representative national survey". In: *Nature Energy*, pp. 1–7. DOI: 10.1038/s41560-018-0158-4.

Verstraeten, W. W., Neu, J. L., Williams, J. E., Bowman, K. W., Worden, J. R., and Boersma, K. F. (2015). "Rapid increases in tropospheric ozone production and export from China". In: *Nature Geoscience* 8.9, pp. 690–695. DOI: 10.1038/ngeo2493.

Wang, L., Zhang, F., Pilot, E., Yu, J., Nie, C., Holdaway, J., Yang, L., Li, Y., et al. (2018). "Taking action on air pollution control in the Beijing-Tianjin-Hebei (BTH) region: Progress, challenges and opportunities". In: *International Journal of Environmental Research and Public Health* 15.2, p. 306. DOI: 10.3390/ijerph15020306.

Wang, T., Wei, X. L., Ding, A. J., Poon, C. N., Lam, K. S., Li, Y. S., Chan, L. Y., and Anson, M. (2009). "Increasing surface ozone concentrations in the background atmosphere of Southern China, 1994-2007". In: *Atmospheric Chemistry and Physics* 9.16, pp. 6217–6227. DOI: 10.5194/acp-9-6217-2009.

Wang, X., Chen, W., Chen, D., Wu, Z., and Fan, Q. (2016). "Long-term trends of fine particulate matter and chemical composition in the Pearl River Delta Economic Zone (PRDEZ), China". In: *Frontiers of Environmental Science and Engineering* 10.1, pp. 53–62. DOI: 10.1007/s11783-014-0728-z.

Wu, Y., Zhang, S., Hao, J., Liu, H., Wu, X., Hu, J., Walsh, M. P., Wallington, T. J., et al. (2017). "On-road vehicle emissions and their control in China: A review and outlook". In: *Science of the Total Environment* 574, pp. 332–349. DOI: 10.1016/j.scitotenv.2016.09.040.

Xia, Y., Guan, D., Jiang, X., Peng, L., Schroeder, H., and Zhang, Q. (2016). "Assessment of socioeconomic costs to China's air pollution". In: *Atmospheric Environment* 139, pp. 147–156. DOI: 10.1016/j.atmosenv.2016.05.036.

Xu, W., Lin, W., Xu, X., Tang, J., Huang, J., Wu, H., and Zhang, X. (2016). "Long-term trends of surface ozone and its influencing factors at the Mt Waliguan GAW station, China-Part 1: Overall trends and characteristics". In: *Atmospheric Chemistry and Physics* 16.10, pp. 6191–6205. DOI: 10.5194/acp-16-6191-2016.

Zhang, Q., Geng, G. N., Wang, S. W., Richter, A., and He, K. B. (2012). "Satellite remote sensing of changes in NO x emissions over China during 1996-2010". In: *Chinese Science Bulletin* 57.22, pp. 2857–2864. DOI: 10.1007/s11434-012-5015-4.

Zhang, X., Zhang, W., Lu, X., Liu, X., Chen, D., Liu, L., and Huang, X. (2018). "Long-term trends in NO2columns related to economic developments and air quality policies from 1997 to 2016 in China". In: *Science of the Total Environment* 639, pp. 146–155. DOI: 10.1016/j.scitotenv.2018.04.435.

Zhang, Y.-L. and Cao, F. (2015). "Fine particulate matter (PM2.5) in China at a city level". In: *Scientific Reports* 5.2014, p. 14884. DOI: 10.1038/srep14884.

Zhao, S., Zhang, H., and Xie, B. (2017). "The Effects of El Niño-South Oscillation on the Winter Haze Pollution of China". In: *Atmos. Chem. Phys* 185194.January 2013, pp. 1–24. DOI: 10.5194/acp-18-1863-2018.

Zheng, B., Tong, D., Li, M., Liu, F., Hong, C., Geng, G., Li, H., Li, X., et al. (2018). "Trends in China's anthropogenic emissions since 2010 as the consequence of clean air actions". In: *Atmospheric Chemistry and Physics* 18.19, pp. 14095–14111. DOI: 10.5194/acp-18-14095-2018.

Zheng, Y., Xue, T., Zhang, Q., Geng, G., Tong, D., Li, X., and He, K. (2017). "Air quality improvements and health benefits from China's clean air action since 2013". In: *Environmental Research Letters* 12.11. DOI: 10.1088/1748-9326/aa8a32.

Chapter 3

Pollutant emission reductions deliver decreased $PM_{2.5}$-caused mortality across China during 2015–2017

Ben Silver[1], L. Conibear[1] C .L. Reddington[1], C. Knote [2], S. R. Arnold[1] and D. V. Spracklen[1]

[1] School of Earth and Environment, University of Leeds, Leeds, United Kingdom

[2] Meteorological Institute, Ludwig Maximilian University of Munich, Theresienstr. 37, 80333 Munich, Germany

Published in *Atmospheric Chemistry and Physics* **20**, 15th November 2020

Available at: doi.org/10.5194/acp-20-11683-2020

Abstract

Air pollution is a serious environmental issue and leading contributor to disease burden in China. Rapid reductions in fine particulate matter concentrations and increased ozone concentrations occurred across China during 2015 to 2017. We used measurements of particulate matter with a diameter <2.5μm ($PM_{2.5}$) and ozone (O_3) from more than 1000 stations across China along with Weather Research and Forecasting model coupled with Chemistry (WRF-Chem) regional air quality simulations, to explore the drivers and impacts of observed trends. The measured nationwide median $PM_{2.5}$ trend of −3.4 $\mu g\,m^{-3}\,yr^{-1}$ was well simulated by the model (−3.5 $\mu g\,m^{-3}\,yr^{-1}$). With anthropogenic

emissions fixed at 2015 levels, the simulated trend was much weaker ($-0.6\ \mu g\ m^{-3}\ yr^{-1}$), demonstrating that interannual variability in meteorology played a minor role in the observed $PM_{2.5}$ trend. The model simulated increased ozone concentrations in line with the measurements but underestimated the magnitude of the observed absolute trend by a factor of 2. We combined simulated trends in $PM_{2.5}$ concentrations with an exposure–response function to estimate that reductions in $PM_{2.5}$ concentrations over this period have reduced $PM_{2.5}$ attributable premature mortality across China by 150 000 deaths yr^{-1}.

Introduction

Concentrations of particulate matter and ozone across China largely exceed international air quality standards (Reddington et al., 2019; Silver et al., 2018). This poor air quality is estimated to hasten the deaths of 870 000 - 2 470 000 people across China each year (Apte et al., 2015; Burnett et al., 2018; Cohen et al., 2017; Gu and Yim, 2016; Lelieveld et al., 2015). The Chinese government's efforts to improve air quality began in the 1990s, but emissions of pollutants continued to increase into the 21st century and air pollution worsened (Krotkov et al., 2016; Streets et al., 2008; Zhang et al., 2012). In 2013, China experienced episodes of severe particulate matter pollution (Zhang et al., 2016). In response, the Chinese government announced the Action Plan on the Prevention and Control of Air Pollution which focused on the reduction of fine particulate matter ($PM_{2.5}$) through stringent emission controls during 2012-2017 (Zheng et al., 2017).

Previous studies of trends in China's air quality

Satellite remote sensing studies have been used to show large changes in air pollution across China in recent decades, with positive trends in nitrogen dioxide (NO_2) (A et al., 2006), sulfur dioxide (SO_2) (Zhang et al., 2017) and $PM_{2.5}$ (Ma et al., 2016) during the 1990s and early 2000s. Trends in aerosol optical depth have been used to estimate changes in $PM_{2.5}$, which peaked around 2011 (Ma et al., 2016). NO_2 across China peaked around 2011 (De Foy et al., 2016; Irie et al., 2016), although concentrations in the Pearl River Delta (PRD) peaked earlier and western regions may have peaked later (Cui et al., 2015). Several remote sensing studies show that SO_2 concentrations in China peaked around 2006 (A et al., 2017; Krotkov et al., 2016; Zhang et al., 2017), matching the period of maximum emissions (Duan et al., 2016; Li et al., 2017a; Zheng et al., 2018). Analysis of measurements

from the Acid Deposition Monitoring Network in East Asia (EANET) shows a negative pH trend (i.e., becoming more acidic) from 1999 until a reversal occurs in 2006, matching peak SO_2 emissions and concentrations (Duan et al., 2016). Measurements of O_3 concentrations at background monitoring sites indicate positive trends in western China during 1994-2013 (Xu et al., 2016), and Taiwan during 1994-2003 (Chang and Lee, 2007), suggesting that O_3 has been increasing across China during the past two decades. More recently, measurements at urban sites, also show positive O_3 trends during 2005-2011 (Zhang et al., 2014).

The establishment of China's air pollution monitoring network, operated by the China National Environmental Monitoring Centre (CNEMC) (Wang et al., 2015), which includes measurements from over 1600 locations, has enabled more detailed analysis of recent air pollution changes (Silver et al., 2018; Zhai et al., 2019). Between 2015 and 2017, $PM_{2.5}$ concentrations across China decreased by 28% (Silver et al., 2018). Zhai et al. (2019) reported a 30-40% decrease in $PM_{2.5}$ concentrations during 2013-2017. In contrast O_3 concentrations have increased, with median concentration of O_3 across 74 key cities increasing from 141 $\mu g\,m^{-3}$ in 2013 to 164 $\mu g\,m^{-3}$ in 2017 (Huang et al., 2018). Silver et al. (2018) found that O_3 maximum 8 h mean concentrations (O_3MDA8) increased by 4.6% yr^{-1} over 2015-2017. Lu et al. (2020) reported positive trends in April-September O_3MDA8 at 90% of sites during 2013 to 2019. Positive regional O_3 trends remain even after meteorological variability has been removed (Li et al., 2019b). Trends in NO_2 are more variable, with a negative trend reported in eastern China and positive trends in western areas (Li and Bai, 2019). Silver et al. (2018) found that NO_2 had negative trends in Hong Kong and North China Plain regions, but positive trends in the Yangtze River Delta (YRD), Sichuan Basin (SCB) and PRD, and no overall trend at the national scale.

Identifying drivers of recent trends

Changes in the concentrations of air pollutants may be caused by changing emissions or by interannual variability of meteorology. Stringent emission controls have started to reduce emissions of various pollutants across China. Between 2013 and 2017, emissions of $PM_{2.5}$, SO_2 and NO_x (NO_2 + Nitrogen Oxide) declined whereas emissions of ammonia (NH_3) and non-methane volatile organic compounds (NMVOCs) remained fairly constant (Zheng et al., 2018). Zheng et al. (2018) also demonstrate that emission reductions were primarily driven by pollution controls, rather than decreasing activity rates. Meteo-

rological variability alters atmospheric mixing, deposition and transport, all of which can influence the concentration of pollutants. Separating the influence of meteorology and emissions on air pollutant concentrations is difficult, due to the interlinked nature of the chemistry-climate system (Jacob and Winner, 2009). However, to assess the efficacy of China's emissions reductions, it is necessary to separate these two factors.

There are two commonly used approaches to separate the influences of meteorology and emissions on variability in atmospheric pollutant abundances. The first approach uses statistical models, such as multi-linear regression, to control for the influence of meteorology and allowing the proportion of air pollutant concentration variability that can be explained by meteorological variables to be calculated (Tai et al., 2010). The second approach is to use an atmospheric chemistry transport model to simulate pollutant concentrations (Xing et al., 2011; Ansari et al., 2019).

There are a limited number of modelling studies that attempt to separate the influence of meteorology and emissions changes on recent air quality trends in China. Chen et al. (2019) use WRF-Chem with 2010 emissions to examine the drivers of trends in wintertime PM. Ding et al. (2019) use WRF-CMAQ to evaluate importance of emissions, meteorology and demographic changes on $PM_{2.5}$ related mortality during 2013-2017. Our paper adds to these previous studies by evaluating the ability of a online-coupled model (WRF-Chem) to capture trends in NO_2, O_3 and SO_2 as well as PM, using the most recent emissions and evaluated against a comprehensive measurement dataset. Through a comparison of multiple simulations, where either annual variability in emissions or meteorology are held constant, the relative influence of the two factors can be estimated. Here we analyse measurements and a regional air quality model to explore the role of changing anthropogenic emissions on air pollutant concentrations and human health across China during 2015 to 2017.

Materials and methods

Measurement dataset

We used hourly measurements from the CNEMC monitoring network (Wang et al., 2015) of $PM_{2.5}$, O_3, NO_2 and SO_2 for the period 2015–2017, which include data from over 1600 monitoring stations across mainland China and are available to download from `https://quotsoft.net/` (last access: 6 October 2020). These were combined with data from

Table 3.1: China's pollutant emissions (Tg yr^{-1}) during 2015 to 2017 from MEIC.

	SO_2	NO_x	NMVOC	NH_3	CO	TSP	PM_{10}	$PM_{2.5}$	BC	OC	CO_2
2015	16.9	23.7	28.6	10.5	153.6	21.9	12.3	9.1	1.4	2.5	10347.2
2016	13.4	22.5	28.4	10.2	142	17.9	10.8	8.1	1.3	2.3	10290.7
2017	10.5	21.9	28.6	10.2	136.2	16.7	10.2	7.6	1.2	2.1	10434.3

the Hong Kong Environmental Protection Department (`https://cd.epic.epd.gov.hk/EPICDI/air/station/`) (last access: 6 October 2020) and Taiwan's Environmental Protection Administration (`https://airtw.epa.gov.tw/CHT/Query/His_Data.aspx`) (last access: 6 October 2020). We conducted quality control on the measured data following the methods outlined in Silver et al. (2018), which include excluding data with a high proportion of repeated measurements and periods of low variability, which represent periods of missing or invalid data. The cleaned dataset included measurements from 1155 sites.

WRF-Chem model setup

We used the Weather Research and Forecasting model coupled with Chemistry (WRF-Chem) version 3.7.1 (Grell et al., 2005) to simulate trace gas and particulate pollution over China for 2015 to 2017. The model domain uses a Lambert conformal grid (11–48°N, 93–128°E) centred on eastern China with a horizontal resolution of 30 km. The model has 33 vertical layers, with the lowest layer ~29 m above the surface and the highest at 50 hPa (~19.6 km).

European Centre for Medium-Range Weather Forecasts (ECMWF) ERA-Interim fields were used to provide meteorological boundary and initial conditions, as well as to nudge the model temperature, winds and humidity above the boundary layer every 6 h. Restricting nudging to above the boundary layer allowed a more realistic representation of vertical mixing (Otte et al., 2012). Chemical boundary and initial conditions were provided by global fields from the Model for Ozone and Related Chemical Tracers version 4 (MOZART-4) chemical transport model (Emmons et al., 2010).

Anthropogenic emissions were from the Multi-resolution Emission Inventory for China (MEIC; `http://www.meicmodel.org`). (last access: 6 October 2020.) MEIC estimates emissions using a database of activity rates across residential, industrial, electricity generation, transportation and agricultural emission sectors combined with China-specific emission factors (Hong et al., 2017). We used the 2015 MEIC dataset, then used sector-

specific and species-specific scaling for 2016 and 2017 based on the emission totals estimated in Zheng et al. (2018). Table 3.1 shows emission totals for 2015, 2016 and 2017. Over the 2015 to 2017 period, Chinese emissions decreased by 38% for SO_2, 16% for $PM_{2.5}$ and 8% for NO_x. For regions outside the MEIC dataset, we used anthropogenic emissions from the EDGAR-HTAP_v2.2 emission inventory for 2010.

Biogenic emissions were generated online by the Model of Emissions of Gases and Aerosol from Nature (MEGAN) (Guenther et al., 2000). Biomass burning emissions were provided by the Fire Inventory from NCAR (FINN) version 1.5 (Wiedinmyer et al., 2011), which uses satellite fire observations of fires and land cover to estimate daily 1 km^2 emissions. Dust emissions were generated online using the Georgia Institute of Technology–Goddard Global Ozone Chemistry Aerosol Radiation and Transport (GOCART) model with Air Force Weather Agency (AFWA) modifications (LeGrand et al., 2019).

Gas-phase chemistry is simulated using the MOZART-4 scheme, and aerosol is treated by the Model for Simulating Aerosol Interactions and Chemistry (MOSAIC; Zaveri et al., 2008) scheme, including grid-scale aqueous chemistry and an extended treatment of organic aerosol (Hodzic and Jimenez, 2011; Hodzic and Knote, 2014). Four discrete size bins were used within MOSAIC (0.039–0.156, 0.156–0.625, 0.625–2.5, 2.5–10 μm) to represent the aerosol size distribution.

Model and measurement trend estimation

To separate the influence of changing anthropogenic emissions from interannual variability in meteorology, we conducted two 3-year simulations, both for 2015–2017. The first simulation (control) included interannual variability in both anthropogenic emissions and meteorology. The second simulation (fixed emissions) included interannual variability in meteorology but with anthropogenic emissions fixed at 2015 levels. Both simulations include interannual variability in biogenic and biomass burning emissions, allowing us to isolate the impacts of changing anthropogenic emissions.

Trends in the model data were calculated using the same method as the measurement data (Silver et al., 2018). The hourly data are averaged to monthly means, which are then deseasonalised using locally weighted scatterplot smoothing. The magnitude and direction of linear trends were calculated using the Theil–Sen estimator, a non-parametric method that is resistant to outliers (Carslaw, 2015). The Mann–Kendall test was used to

assess the significance of trends, using a threshold of $p<0.05$. This stage of the analysis was performed using the R package *openair* (Carslaw and Ropkins, 2012).

Health impact estimation

Health impacts are estimated for ambient $PM_{2.5}$ using the Global Exposure Mortality Model (GEMM; (Burnett et al., 2018)), which uses cohort studies to estimate health risks integrated over a range of$PM_{2.5}$ concentrations. GEMM applies a supralinear association between exposure and risk at lower concentrations and then a near-linear association at higher concentrations. We used the GEMM for non-accidental mortality (non-communicable disease, NCD, plus lower respiratory infection, LRI), using parameters including the China cohort (Burnett et al., 2018). For ambient O_3, we used the methodology of the Global Burden of Disease (GBD) study for 2017 (GBD 2017 Risk Factor Collaborators, 2018) to estimate the mortality caused by chronic obstructive pulmonary disease, which is based on exposure and risk information from five epidemiological cohorts. It estimates a near-linear relationship between exposure and risk at lower concentrations of O_3 and a sub-linear association at higher concentrations. The United Nations-adjusted population count dataset for 2015 at $0.05° \times 0.05°$resolution was obtained from the Gridded Population of the World, Version 4, along with population age distribution from GBD2017. Health impacts depend on population count, population age and baseline mortality rates, which have changed over the period studied (Butt et al., 2017). To isolate the impacts of changing air pollution, other variables were kept constant for 2015–2017.

Measured and modelled trend comparison

Model evaluation

For comparison with the measurements, we sampled the model at the station locations using linear interpolation. Over 2015–2017, the model simulated $PM_{2.5}$ (normalised mean bias (NMB) =0.49), O_3 (NMB=−0.13) and SO_2 (NMB=0.07) well, while it overestimated NO_2 concentrations by a factor of around 2 (NMB=1.17). Model biases were similar to previous model studies in China (Supplement Table B.1). We also evaluated the model against speciated aerosol measurements from the Surface PARTiculate mAtter Network (SPARTAN; (Snider et al., 2015; Snider et al., 2016)) site in Beijing (`https://www.spartan-network.org/beijing-china`, last access: 2 July 2020) (Fig. B.4), as well as from Zhou et al. (2019)

Table 3.2: Model evaluation shown as a normalised mean bias (NMB). Evaluation is shown separately for the control and fixed emission simulations. The NMB for 2015-2017 is compared to individual years.

	$PM_{2.5}$	O_3	NO_2	SO_2
Control				
2015-2017	0.49	-0.15	1.20	0.09
2015	0.50	-0.12	1.32	0.17
2016	0.47	-0.14	1.20	0.05
2017	0.50	-0.21	1.10	0.04
Fixed emissions				
2015-2017	0.57	-0.18	1.26	0.35
2015	0.50	-0.12	1.32	0.17
2016	0.56	-0.16	1.28	0.31
2017	0.66	-0.24	1.20	0.65

(Fig. B.5) and from across China (Li et al., 2017b) (Fig. SB.6). Measurements reported by Li et al. (2017b) were made from various years spanning 2006 to 2013 and do not match the years simulated by the model. Comparison against these data shows that the model underestimates the sulfate fraction in $PM_{2.5}$, while it overestimates the nitrate fraction. Underestimation of sulfate in comparison to Li et al. (2017b) will partly be caused by the large decline in SO_2 emissions that has occurred in the last decade (Zheng et al., 2018). Underestimate of sulfate, particularly in winter, and overestimation of nitrate are consistent with previous modelling studies (Shao et al., 2019), including those using WRF-Chem (Zhou et al., 2019). Newly proposed mechanisms to explain the rapid sulfate formation in China's winter haze (Gen et al., 2019; Shao et al., 2019; Xue et al., 2014; Zhang et al., 2019) need to be included and evaluated in models.

Varying emissions scenario

Figures 3.1 and 3.2 compare measured and simulated air quality trends over China during 2015 to 2017. The measurements show widespread decline in $PM_{2.5}$ and SO_2 concentrations, widespread increase in O_3MDA8 and spatially variable trends in NO_2 concentrations, as reported previously (Silver et al., 2018). The model (control simulation) simulates the widespread decline in $PM_{2.5}$ concentrations, with the median measured trend across China ($-3.4\ \mu g\,m^{-3}\,yr^{-1}$) well simulated by the model ($-3.5\ \mu g\,m^{-3}\,yr^{-1}$). However, as the above comparisons with speciated aerosol measurements show, the underlying trends in individual aerosol species may contain inaccuracies that affect the overall $PM_{2.5}$ trend. In the measurements, 90% of significant trends are negative, and 10% of significant trends are positive, with positive trends mostly being in the Fenwei Plain region,

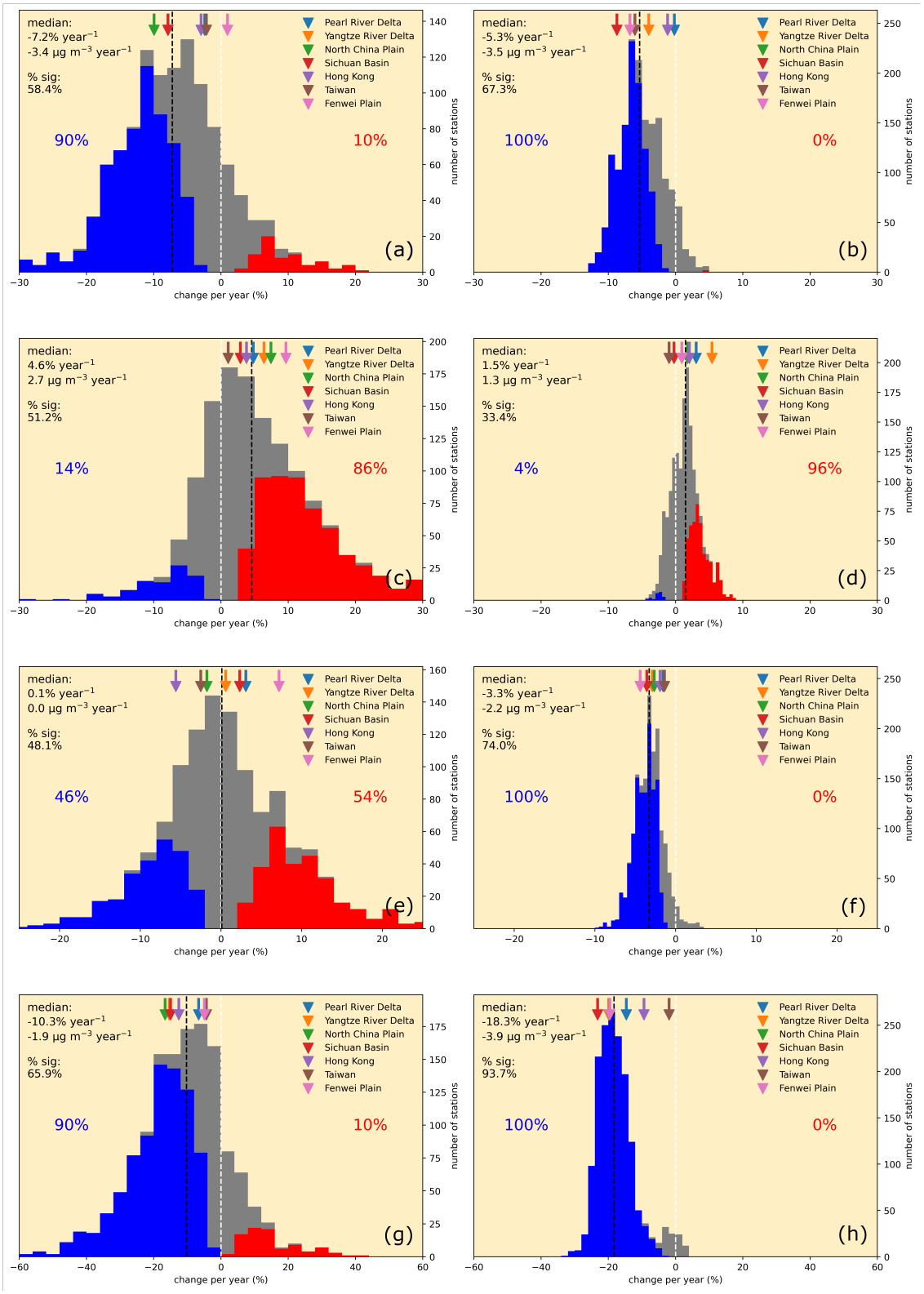

Figure 3.1: Histograms showing the frequency distribution of trends in concentrations of (a, b) $PM_{2.5}$, (c, d) O_3MDA8, (e, f) NO_2 and (g, h) SO_2 across China and Taiwan during 2015–2017. Measured trends (left-hand panels) are compared to simulated trends (right-hand panels). The median relative and absolute trend as well as the percentage of stations with significant trends are shown in each panel. The percentage of significant trends that are negative (blue) or positive (red) are also shown. The dotted black line shows the median trend across all sites, while the dotted white line shows zero. Arrows show the median trend for the regional domains: Pearl River Delta (PRD), Yangtze River Delta (YRD), North China Plain (NCP), Sichuan Basin (SCB), Hong Kong (HK), Taiwan (TW) and the Fenwei Plain (FWP).

Jiangxi and Anhui. No significant positive trends are simulated by the model, possibly due to the coarse resolution of the model and the simplified scaling we apply to emissions for 2016 and 2017.

WRF-Chem captures the widespread increase in O_3MDA8 but underestimates the magnitude of the trend by a factor of 2 (2.7 $\mu g\,m^{-3}\,yr^{-1}$) in the measurements, versus 1.3 $\mu g\,m^{-3}\,yr^{-1}$ simulated by WRF-Chem. WRF-Chem simulates negative O_3MDA8 trends in the Sichuan Basin and Taiwan, whereas in the measured data, all regions have positive median trends.

The measurements show zero overall median trend in NO_2 concentrations, with 46% of sites with significant trends being negative and 54% positive. In contrast, WRF-Chem simulates widespread reductions in NO_2 concentrations, with 100% of significant sites exhibiting negative trends and a negative nationwide median trend of $-2.2\ \mu g\,m^{-3}\,yr^{-1}$. The 7.0% nationwide median decline in simulated NO_2 concentrations over 2015–2017 matches the 7.6% decline in Chinese NOx emissions in the MEIC. The measurements show a widespread decline in SO_2 concentrations, with a median nationwide trend of $-1.9\ \mu g\,m^{-3}\,yr^{-1}$. WRF-Chem captures the direction of the trend, but the magnitude of the trend is overestimated by a factor of 2. The 32.5% decline in simulated nationwide median SO_2 concentrations over 2015–2017 matches the 37.8% decline in SO_2 emissions in the MEIC.

Fixed emissions scenario

The model simulation where anthropogenic emissions in China were fixed at 2015 levels has a weak negative$PM_{2.5}$ trend ($-0.6\ \mu g\,m^{-3}\,yr^{-1}$), a factor of 6 smaller than either the control simulation or the measurements (Fig. 3.3). This suggests that the measured negative$PM_{2.5}$ trend has largely been driven by decreased anthropogenic emissions, with limited impact from interannual variability in meteorology. Chen et al. (2019) also concluded that emission reductions were the primary cause of reduced wintertime$PM_{2.5}$ across China during 2015–2017. Cheng et al. (2019) found that local and regional reductions in anthropogenic emissions were the dominant cause of reduced $PM_{2.5}$ concentrations in Beijing between 2013 and 2017. The median O_3MDA8 trend in the fixed emission simulation is 0.0 $\mu g\,m^{-3}\,yr^{-1}$. This suggests that interannual meteorological variation had little influence on O_3 trends at the China-wide scale during 2015–2017, which were largely driven by changing emissions. However, meteorological variability did drive regional

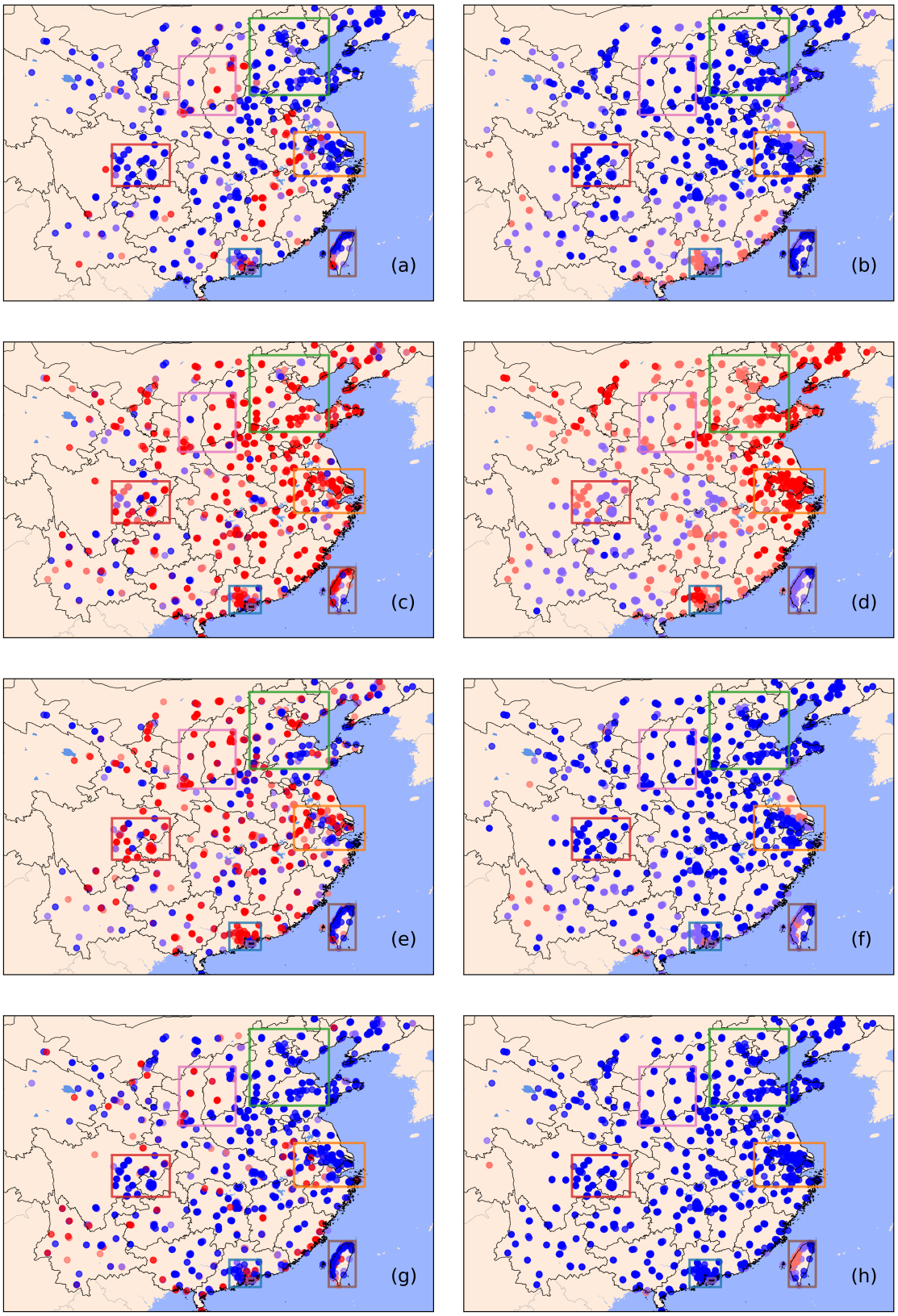

Figure 3.2: Map showing the spatial distribution of trends in concentrations of (a, b) $PM_{2.5}$, (c, d) O_3MDA8, (e, f) NO_2 and (g, h) SO_2 across China and Taiwan during 2015–2017. Measured trends (left-hand panels) are compared to simulated trends (right-hand panels). Red indicates a significant positive trend, whereas blue indicates a significant negative trend. Light coloured circles indicated a statistically insignificant trend. Coloured boxes show the regional domains: Pearl River Delta (blue), Yangtze River Delta (orange), North China Plain (green), Sichuan Basin (red), Hong Kong (purple), Taiwan (brown) and the Fenwei Plain (pink).

changes in O_3. For example, in Guizhou province, a trend of $-2.5\ \mu g\,m^{-3}\,yr^{-1}$ was calculated in the fixed emissions simulation. Li et al. (2019a) also report that the positive ozone trend over 2013 to 2017 is due to changes in anthropogenic emissions, and the magnitude of their estimated trend of 1-3 ppbv yr^{-1} (approximately 2-6 $\mu g\,m^{-3}\,yr^{-1}$) is comparable to the 2.6 $\mu g\,m^{-3}\,yr^{-1}$ trend found in this study. Lu et al. (2019) analysed changes in O_3 between 2016 and 2017 and concluded that hotter and drier conditions in 2017 contributed to higher O_3 concentrations in that year. Liu and Wang (2020a) reported a complex O_3 response during 2013 to 2017, with changing anthropogenic emission increasing O_3MDA8 in urban areas and decreasing it in rural areas, whereas meteorological changes drove regionally contrasting changes in O_3MDA8 through changes in cloud cover, wind and temperature and through driving changes in biogenic emissions.

The fixed emission simulation also has a smaller NO_2 trend ($-0.5\ \mu g\,m^{-3}\,yr^{-1}$) compared to the control simulation ($-2.2\ \mu g\,m^{-3}\,yr^{-1}$), demonstrating that emission reductions that are estimated in the MEIC are also the main reason for the negative simulated NO_2 trend. However, unlike $PM_{2.5}$ and O_3, the NO_2 trend calculated from the fixed emission simulation more closely matches the measured trend. This may suggest that the MEIC has overestimated the NO_2 emission reductions during 2015–2017. This suggestion is supported by recent satellite studies which found a slowing down or even reversal of NO_2 reductions during 2016–2019 (Li et al., 2019c), no significant trend in NO_2 during 2013–2017 (Huang et al., 2018) and increases in NO_2 concentration in the YRD, PRD and Fenwei Plain (FWP) regions during 2015–2017 (Feng et al., 2019). If NO_x emissions decline too strongly in the MEIC, this may contribute to the simulated underestimate of the positive observed O_3MDA8 trend in areas of China with NO_x-limited or mixed ozone regimes that cover the majority of China (Jin and Holloway, 2015). Other work has suggested that increased O_3 concentrations are possibly linked to the rapid decline in aerosol (Li et al., 2019b). Liu and Wang (2020b) found that the reasons for increased O_3 concentrations during 2013–2017 were regionally dependent and that anthropogenic volatile organic compound (VOC) emission reductions of 16%–24% would have been needed to avoid increased concentrations. Table 3.2 compares the $PM_{2.5}$, O_3, SO_2 and NO_2 measurements for the control and fixed emission simulations in 2015, 2016 and 2017. In the control simulation, model biases remain similar during 2015–2017. In the fixed emission simulation, model biases for $PM_{2.5}$, O_3 and SO_2 increase between 2015 and 2017. This further suggests that changing anthropogenic emissions during 2015–2017 have been the dominant cause of changing

concentrations.

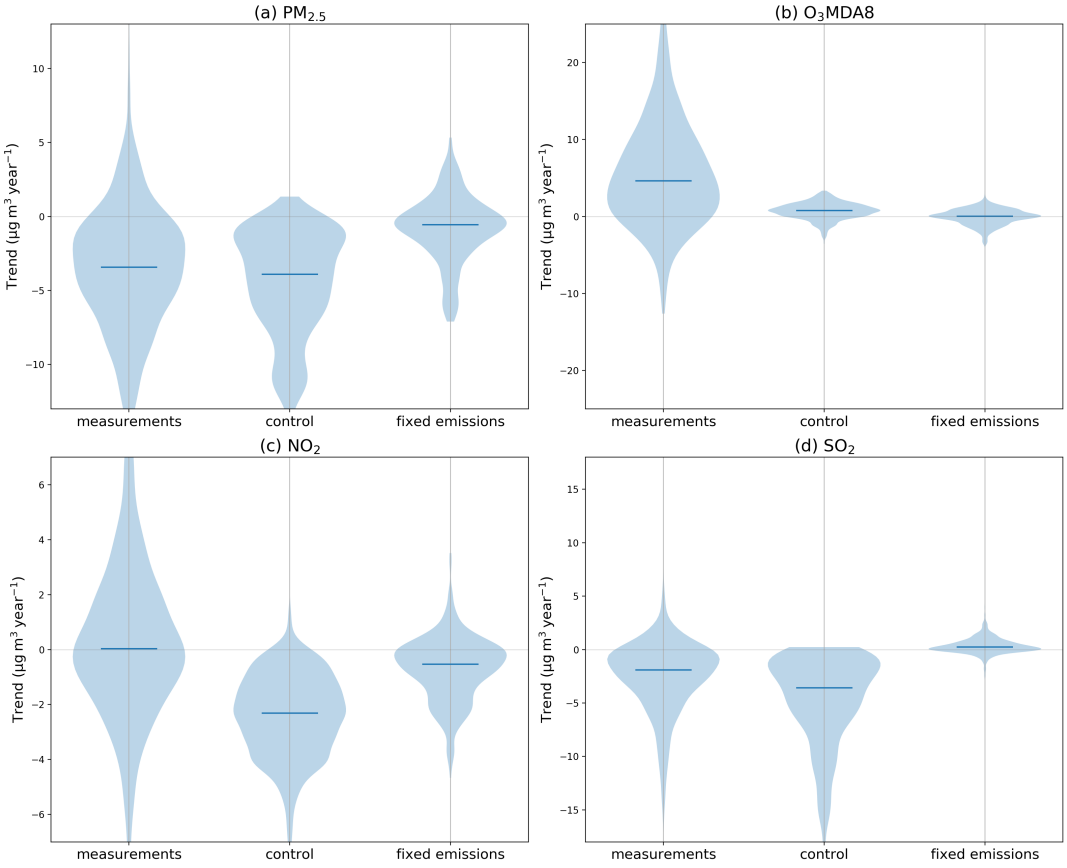

Figure 3.3: Comparison of measured and simulated concentration trends during 2015 to 2017. The left violin plot shows the measured trend, the centre shows the simulated trend with varying emissions and meteorology (control) and the right shows the simulated trends for the fixed emissions simulation. (a) $PM_{2.5}$, (b) O_3MDA8, (c) NO_2 and (d) SO_2. The solid line shows the median absolute trend, and the shaded area shows a smoothed relative frequency distribution.

An important future step is to understand how changing anthropogenic emissions, in terms of emission species or emission sectors, have contributed to observed trends in pollutant concentrations. Residential and industrial emissions are dominant causes of $PM_{2.5}$ concentrations across much of China (Reddington et al., 2019), but it is not clear which emission sectors have contributed most to observed $PM_{2.5}$ trends. Cheng et al. (2019) suggest that emission controls in the residential and industrial sectors were the dominant causes for reduced $PM_{2.5}$ in Beijing between 2014 and 2017. Measurements of aerosol composition (Li et al., 2017b; Weagle et al., 2018) add confidence to model simulations and can inform our understanding of how aerosol chemistry responds to emission changes. However, except for Beijing, there are insufficient measurement data of how aerosol composition has changed across China in recent years. Li et al. (2019a) found large declines in wintertime organics and sulfate and smaller declines in nitrate and ammonium in Beijing

between 2014 and 2017. Zhou et al. (2019) also analysed aerosol composition data from Beijing and found large declines in all aerosol components except nitrate between the periods 2011–2012 and 2017–2018. Continuous measurements of aerosol composition across China are required to determine how different aerosol components are contributing to the observed $PM_{2.5}$ trend and to evaluate simulated responses to emission changes.

Health impacts of changes to $PM_{2.5}$ and O_3 concentrations

$PM_{2.5}$ health impacts

The control run simulated nationwide population-weighted mean $PM_{2.5}$ concentration decreased by 12.8% (10.1 $\mu g\,m^{-3}$), from 79.2 $\mu g\,m^{-3}$ in 2015 to 69.1 $\mu g\,m^{-3}$ in 2017. Greater decreases were simulated in more polluted and highly populated regions such as Beijing (-15.3 $\mu g\,m^{-3}$), Tianjin (-19.4 $\mu g\,m^{-3}$), Chongqing (province) (-14.2 $\mu g\,m^{-3}$) and Henan (-22.3 $\mu g\,m^{-3}$). Using the methodology of Burnett et al. (2018), we estimate that mortality due to exposure to$PM_{2.5}$ decreased from 2 800 000 (confidence interval, CI: 2 299 000-3 302 000) premature mortalities in 2015 to 2 650 000 premature mortalities in 2017. The simulated reduction in $PM_{2.5}$ concentrations therefore reduced the number of premature mortalities attributable to $PM_{2.5}$ exposure by 150 000 (CI: 129 000-170 000) annual premature mortalities across China. The 12.8% reduction in$PM_{2.5}$ exposure only led to a 5% reduction in attributable mortality due to the non-linearity of the exposure–response function, which is less sensitive at higher exposure ranges (Conibear et al., 2018). The largest absolute reductions in premature mortality occur in Henan (15 000 deaths yr^{-1}), Sichuan, Hebei and Tianjin (11 000 deaths yr^{-1}) (Fig. 3.4). The decline in $PM_{2.5}$ exposure also led to reduced morbidity, with the rate of disability-adjusted life years (DALYs) per 100 000 population reduced from 5517 to 5227, with the largest changes occurring in central provinces such as Hubei (Supplement Fig. B.3). Our results are comparable to Zheng et al. (2017), who found that population-weighted annual mean $PM_{2.5}$ concentrations decreased 21.5% during 2013–2015, resulting in a premature mortality decrease of 120 000 deaths yr^{-1}. Ding et al. (2019) estimated that during 2013–2017, a nationwide$PM_{2.5}$ decrease of 9 $\mu g\,m^{-3}\,yr^{-1}$ caused premature mortalities per year to decrease by 287 000, using the methodology from the GBD 2015 study, which estimates health impacts as having a weaker and less linear relationship to $PM_{2.5}$ concentrations. Yue et al. (2020) estimated that the annual number of mortalities in China attributable to$PM_{2.5}$ decreased by

64 000 (7%) from 2013 to 2017. Zhang et al. (2019) reported a 32% decline in population-weighted$PM_{2.5}$ concentration during 2013 to 2017, largely due to strengthened industrial emission standards and cleaner residential fuels.

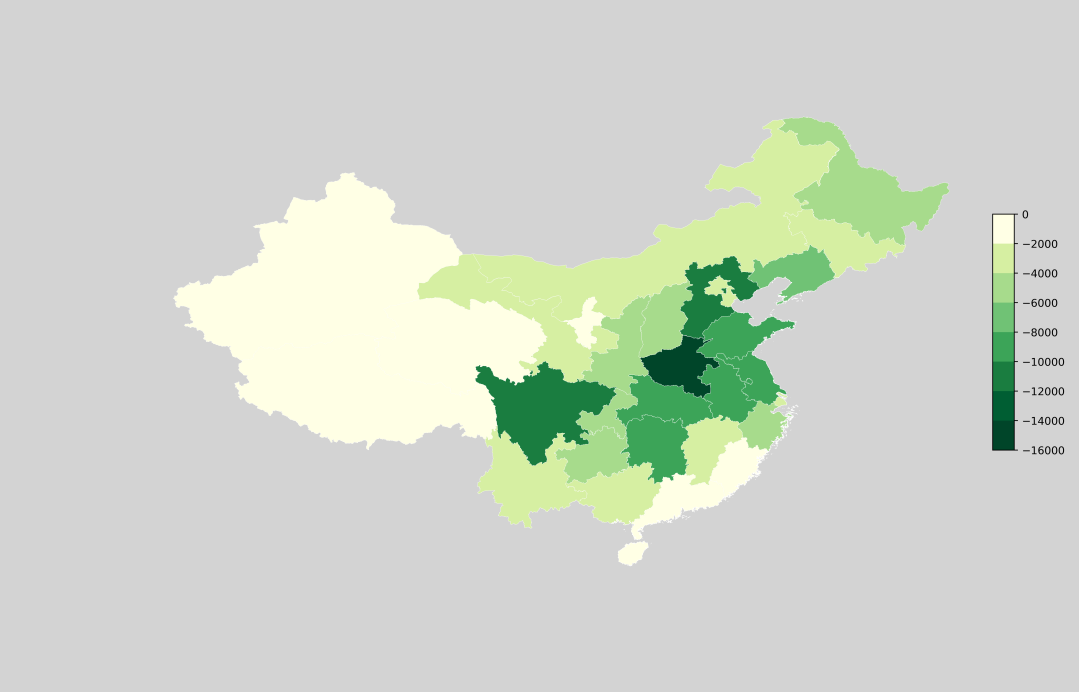

Figure 3.4: Simulated change during 2015–2017 in annual premature mortality per year due to changes in exposure to ambient $PM_{2.5}$. Results are shown at the province scale.

O_3 health impacts

Increasing O_3 concentrations will result in an increase in health impacts that will act to offset some of the health benefits from declining $PM_{2.5}$ concentrations. WRF-Chem simulated O_3 concentrations across China during 2015-2017 to within 15% (NM = −0.13), which is consistent with previous studies, but underestimated the magnitude of the observed O_3 trend. To provide an estimate of the health impacts due to exposure to O_3 we used simulated concentrations to estimate average exposure to O_3 over the 2015–2017 period. We estimate that exposure to O_3 caused an average of 143 000 (CI: 106 000-193 000) premature mortalities each year over 2015-2017. Applying the simulated change in O_3 concentrations would underestimate the change in exposure that has occurred. Instead, we estimated the impacts of increased O_3 by multiplying the average health impacts over 2015-2017 by the measured relative change in O_3MDA8. Assuming linear behaviour, the 15% measured increase in O_3MDA8 would result in an increase of 21 000 premature mortalities per year. The exposure-outcome function is in reality sub-linear, so this is likely to be an overestimate. Regardless, this is substantially smaller than the 150 000 reduction in

annual premature mortality due to reduced $PM_{2.5}$. We therefore suggest that changes in Chinese air pollution over 2015-2017 have likely had an overall beneficial impact on human health. The dominance of the $PM_{2.5}$ reduction over the O_3 increase on health impacts is also found in Dang and Liao (2019), who reported that a 21% reduction in $PM_{2.5}$ and a 12% increase in O_3 concentration between 2012 and 2017 resulted in 268 000 fewer annual mortalities overall.

Conclusions

We used the WRF-Chem model to explore the drivers and impacts of changing air pollution across China during 2015–2017. A simulation with annually updated emissions was able to reproduce the measured negative trends in $PM_{2.5}$ concentrations over China during 2015–2017 while overestimating the negative trend in SO_2 and NO_2 and underestimating the positive trend in O_3. By comparing this with a simulation where emissions are held constant at 2015 levels, but meteorological forcing was updated, we show that interannual meteorological variation was not the main driver of the substantial trends in air pollutants that were observed across China during 2015–2017. Our work shows that reduced anthropogenic emissions are the main cause of reduced $PM_{2.5}$ concentrations across China, suggesting that the Chinese government's "Air Pollution Prevention and Control Action Plan" has been effective at starting to control particulate pollution. We estimate that the 12.8% reduction in population-weighted $PM_{2.5}$ concentrations that occurred during 2015–2017 has reduced premature mortality due to exposure to $PM_{2.5}$ by 5.3%, preventing 150 000 premature mortalities across China annually. Despite these substantial reductions, $PM_{2.5}$ concentrations still exceed air quality guidelines and cause negative impacts on human health. We estimate that exposure to O_3 during 2015–2017 causes on average 143 000 premature mortalities across China each year. Increases in O_3 concentration over 2015–2017 may have increased this annual mortality by about 20 000 premature mortalities per year, substantially less than the reduction in premature mortality due to declining particulate pollution. Changes in air pollution across China during 2015–2017 are therefore likely to have led to overall positive benefits to human health, amounting to a ~5% reduction of the ambient air pollution disease burden. However, to achieve larger reductions in disease burden, further reductions in $PM_{2.5}$ concentrations are required, and pollution controls need to be designed that simultaneously reduce $PM_{2.5}$ and O_3 concentrations.

References

A, R. J. van der, Peters, D. H., Eskes, H., Boersma, K. F., Van Roozendael, M., De Smedt, I., and Kelder, H. M. (2006). "Detection of the trend and seasonal variation in tropospheric NO2 over China". In: *Journal of Geophysical Research Atmospheres* 111.12. DOI: 10.1029/2005JD006594.

A, R. J. van der, Mijling, B., Ding, J., Elissavet Koukouli, M., Liu, F., Li, Q., Mao, H., and Theys, N. (2017). "Cleaning up the air: Effectiveness of air quality policy for SO2 and NOx emissions in China". In: *Atmospheric Chemistry and Physics* 17.3, pp. 1775–1789. DOI: 10.5194/acp-17-1775-2017.

Ansari, T. U., Wild, O., Li, J., Yang, T., Xu, W., Sun, Y., and Wang, Z. (2019). "Effectiveness of short term air quality emission controls: A high-resolution model study of Beijing during the APEC period". In: *Atmospheric Chemistry and Physics Discussions*. DOI: 10.5194/acp-2018-1173.

Apte, J. S., Marshall, J. D., Cohen, A. J., and Brauer, M. (2015). "Addressing Global Mortality from Ambient PM2.5". In: *Environmental Science and Technology* 49.13, pp. 8057–8066. DOI: 10.1021/acs.est.5b01236.

Burnett, R., Chen, H., Szyszkowicz, M., Fann, N., Hubbell, B., Pope, C. A., Apte, J. S., Brauer, M., et al. (2018). "Global estimates of mortality associated with longterm exposure to outdoor fine particulate matter". In: *Proceedings of the National Academy of Sciences of the United States of America* 115.38, pp. 9592–9597. DOI: 10.1073/pnas.1803222115.

Butt, E. W., Turnock, S. T., Rigby, R., Reddington, C. L., Yoshioka, M., Johnson, J. S., Regayre, L. A., Pringle, K. J., et al. (2017). "Global and regional trends in particulate air pollution and attributable health burden over the past 50 years". In: *Environmental Research Letters*. DOI: 10.1088/1748-9326/aa87be.

Carslaw, D. (2015). "The openair manual open-source tools for analysing air pollution data". In: *King's College London* January, p. 287. URL: http://www.openair-project.org/PDF/OpenAir%7B%5C_%7DManual.pdf.

Carslaw, D. C. and Ropkins, K. (2012). "openair – Data Analysis Tools for the Air Quality Community". In: *R Journal* 4.1, pp. 20–29.

Chang, S. C. and Lee, C. T. (2007). "Evaluation of the trend of air quality in Taipei, Taiwan from 1994 to 2003". In: *Environmental Monitoring and Assessment*. DOI: 10.1007/s10661-006-9262-1.

Chen, D., Liu, Z., Ban, J., Zhao, P., and Chen, M. (2019). "Retrospective analysis of 2015-2017 wintertime PM2.5 in China: Response to emission regulations and the role of meteorology". In: *Atmospheric Chemistry and Physics*. DOI: 10.5194/acp-19-7409-2019.

Cheng, J., Su, J., Cui, T., Li, X., Dong, X., Sun, F., Yang, Y., Tong, D., et al. (2019). "Dominant role of emission reduction in PM2.5 air quality improvement in Beijing during 2013-2017: A model-based decomposition analysis". In: *Atmospheric Chemistry and Physics* 19.9, pp. 6125–6146. DOI: 10.5194/acp-19-6125-2019.

Cohen, A. J., Brauer, M., Burnett, R., Anderson, H. R., Frostad, J., Estep, K., Balakrishnan, K., Brunekreef, B., et al. (2017). "Estimates and 25-year trends of the global burden of disease attributable to ambient air pollution: an analysis of data from the Global Burden of Diseases Study 2015". In: *The Lancet* 389.10082, pp. 1907–1918. DOI: 10.1016/S0140-6736(17)30505-6.

Conibear, L., Butt, E. W., Knote, C., Arnold, S. R., and Spracklen, D. V. (2018). "Residential energy use emissions dominate health impacts from exposure to ambient particulate matter in India". In: *Nature Communications*. DOI: 10.1038/s41467-018-02986-7.

Cui, H., Chen, W., Dai, W., Liu, H., Wang, X., and He, K. (2015). "Source apportionment of PM2.5in Guangzhou combining observation data analysis and chemical transport model simulation". In: *Atmospheric Environment* 116, pp. 262–271. DOI: 10.1016/j.atmosenv.2015.06.054.

Dang, R. and Liao, H. (2019). "Radiative Forcing and Health Impact of Aerosols and Ozone in China as the Consequence of Clean Air Actions over 2012–2017". In: *Geophysical Research Letters* 46.21, pp. 12511–12519. DOI: 10.1029/2019GL084605.

De Foy, B., Lu, Z., and Streets, D. G. (2016). "Satellite NO2 retrievals suggest China has exceeded its NOx reduction goals from the twelfth Five-Year Plan". In: *Scientific Reports* 6. DOI: 10.1038/srep35912.

Ding, D., Xing, J., Wang, S., Liu, K., and Hao, J. (2019). "Estimated Contributions of Emissions Controls, Meteorological Factors, Population Growth, and Changes in Baseline Mortality to Reductions in Ambient PM2.5 and PM2.5-Related Mortality in China, 2013-2017". In: *Environmental health perspectives*. DOI: 10.1289/EHP4157.

Duan, L., Yu, Q., Zhang, Q., Wang, Z., Pan, Y., Larssen, T., Tang, J., and Mulder, J. (2016). "Acid deposition in Asia: Emissions, deposition, and ecosystem effects". In: *Atmospheric Environment*. DOI: 10.1016/j.atmosenv.2016.07.018.

Emmons, L. K., Walters, S., Hess, P. G., Lamarque, J. F., Pfister, G. G., Fillmore, D., Granier, C., Guenther, A., et al. (2010). *Description and evaluation of the Model for Ozone and Related chemical Tracers, version 4 (MOZART-4)*. Tech. rep. 1, pp. 43–67. DOI: 10.5194/gmd-3-43-2010.

Feng, Y., Ning, M., Lei, Y., Sun, Y., Liu, W., and Wang, J. (2019). "Defending blue sky in China: Effectiveness of the "Air Pollution Prevention and Control Action Plan" on air quality improvements from 2013 to 2017". In: *Journal of Environmental Management* 252, p. 109603. DOI: 10.1016/j.jenvman.2019.109603.

GBD 2017 Risk Factor Collaborators (2018). "Global, regional, and national comparative risk assessment of 84 behavioural, environmental and occupational, and metabolic risks or clusters of risks for 195 countries and territories, 1990-2017: A systematic analysis for the Global Burden of Disease Stu". In: *The Lancet*. DOI: 10.1016/S0140-6736(18)32225-6.

Gen, M., Zhang, R., Huang, D. D., Li, Y., and Chan, C. K. (2019). "Heterogeneous Oxidation of SO2 in Sulfate Production during Nitrate Photolysis at 300 nm: Effect of pH, Relative Humidity, Irradiation Intensity, and the Presence of Organic Compounds". In: *Environmental Science and Technology* 53.15, pp. 8757–8766. DOI: 10.1021/acs.est.9b01623.

Grell, G. A., Peckham, S. E., Schmitz, R., McKeen, S. A., Frost, G., Skamarock, W. C., and Eder, B. (2005). "Fully coupled "online" chemistry within the WRF model". In: *Atmospheric Environment*. DOI: 10.1016/j.atmosenv.2005.04.027.

Gu, Y. and Yim, S. H. (2016). "The air quality and health impacts of domestic trans-boundary pollution in various regions of China". In: *Environment International* 97, pp. 117–124. DOI: 10.1016/j.envint.2016.08.004.

Guenther, A., Geron, C., Pierce, T., Lamb, B., Harley, P., and Fall, R. (2000). "Natural emissions of non-methane volatile organic compounds, carbon monoxide, and oxides of nitrogen from North America". In: *Atmospheric Environment* 34.12, pp. 2205–2230. DOI: 10.1016/S1352-2310(99)00465-3.

Hodzic, A. and Jimenez, J. L. (2011). "Modeling anthropogenically controlled secondary organic aerosols in a megacity: A simplified framework for global and climate models". In: *Geoscientific Model Development* 4.4, pp. 901–917. DOI: 10.5194/gmd-4-901-2011.

Hodzic, A. and Knote, C. (2014). "MOZART gas-phase chemistry with MOSAIC aerosols". In: *Atmospheric Chemistry Division (ACD), National Center for Atmospheric Research (NCAR)*, p. 7.

Hong, C., Zhang, Q., He, K., Guan, D., Li, M., Liu, F., and Zheng, B. (2017). "Variations of China's emission estimates: Response to uncertainties in energy statistics". In: *Atmospheric Chemistry and Physics* 17.2, pp. 1227–1239. DOI: 10.5194/acp-17-1227-2017.

Huang, J., Pan, X., Guo, X., and Li, G. (2018). "Health impact of China's Air Pollution Prevention and Control Action Plan: an analysis of national air quality monitoring and mortality data". In: *The Lancet Planetary Health*. DOI: 10.1016/S2542-5196(18)30141-4.

Irie, H., Muto, T., Itahashi, S., Kurokawa, J.-i., and Uno, I. (2016). "Turnaround of Tropospheric Nitrogen Dioxide Pollution Trends in China, Japan, and South Korea". In: *Sola* 12.0, pp. 170–174. DOI: 10.2151/sola.2016-035.

Jacob, D. J. and Winner, D. A. (2009). "Effect of climate change on air quality". In: *Atmospheric Environment* 43.1, pp. 51–63. DOI: 10.1016/j.atmosenv.2008.09.051.

Jin, X. and Holloway, T. (2015). "Spatial and temporal variability of ozone sensitivity over China observed from the Ozone Monitoring Instrument". In: *Journal of Geophysical Research* 120.14, pp. 7229–7246. DOI: 10.1002/2015JD023250.

Krotkov, N. A., McLinden, C. A., Li, C., Lamsal, L. N., Celarier, E. A., Marchenko, S. V., Swartz, W. H., Bucsela, E. J., et al. (2016). "Aura OMI observations of regional SO2 and NO2 pollution changes from 2005 to 2015". In: *Atmospheric Chemistry and Physics* 16.7, pp. 4605–4629. DOI: 10.5194/acp-16-4605-2016.

LeGrand, S. L., Polashenski, C., Letcher, T. W., Creighton, G. A., Peckham, S. E., and Cetola, J. D. (2019). "The AFWA dust emission scheme for the GOCART aerosol model in WRF-Chem v3.8.1". In: *Geoscientific Model Development* 12.1, pp. 131–166. DOI: 10.5194/gmd-12-131-2019.

Lelieveld, J., Evans, J. S., Fnais, M., Giannadaki, D., and Pozzer, A. (2015). "The contribution of outdoor air pollution sources to premature mortality on a global scale". In: *Nature* 525.7569, pp. 367–371. DOI: 10.1038/nature15371.

Li, H., Cheng, J., Zhang, Q., Zheng, B., Zhang, Y., Zheng, G., and He, K. (2019a). "Rapid transition in winter aerosol composition in Beijing from 2014 to 2017: Response to clean air actions". In: *Atmospheric Chemistry and Physics* 19.17, pp. 11485–11499. DOI: 10.5194/acp-19-11485-2019.

Li, K. and Bai, K. (2019). "Spatiotemporal associations between PM2.5 and SO2 as well as NO2 in China from 2015 to 2018". In: *International Journal of Environmental Research and Public Health* 16.13, p. 2352. DOI: 10.3390/ijerph16132352.

Li, K., Jacob, D. J., Liao, H., Shen, L., Zhang, Q., and Bates, K. H. (2019b). "Anthropogenic drivers of 2013–2017 trends in summer surface ozone in China". In: *Proceedings of the National Academy of Sciences of the United States of America*. DOI: 10.1073/pnas.1812168116.

Li, M., Liu, H., Geng, G., Hong, C., Liu, F., Song, Y., Tong, D., Zheng, B., et al. (2017a). "Anthropogenic emission inventories in China: A review". In: *National Science Review* 4.6, pp. 834–866. DOI: 10.1093/nsr/nwx150.

Li, R., Bo, H., and Wang, Y. (2019c). "Slowing-down reduction and possible reversal trend of tropospheric NO2 over China during 2016 to 2019". In: *arXiv*. URL: http://arxiv.org/abs/1907.06525.

Li, Y. J., Sun, Y., Zhang, Q., Li, X., Li, M., Zhou, Z., and Chan, C. K. (2017b). "Real-time chemical characterization of atmospheric particulate matter in China: A review". In: *Atmospheric Environment* 158, pp. 270–304. DOI: 10.1016/j.atmosenv.2017.02.027.

Liu, Y. and Wang, T. (2020a). "Worsening urban ozone pollution in China from 2013 to 2017 - Part 1: The complex and varying roles of meteorology". In: *Atmospheric Chemistry and Physics* 20.11, pp. 6305–6321. DOI: 10.5194/acp-20-6305-2020.

– (2020b). "Worsening urban ozone pollution in China from 2013 to 2017 - Part 2: The effects of emission changes and implications for multi-pollutant control". In: *Atmospheric Chemistry and Physics* 20.11, pp. 6323–6337. DOI: 10.5194/acp-20-6323-2020.

Lu, X., Zhang, L., Chen, Y., Zhou, M., Zheng, B., Li, K., Liu, Y., Lin, J., et al. (2019). "Exploring 2016-2017 surface ozone pollution over China: Source contributions and meteorological influences". In: *Atmospheric Chemistry and Physics* 19.12, pp. 8339–8361. DOI: 10.5194/acp-19-8339-2019.

Lu, X., Zhang, L., Wang, X., Gao, M., Li, K., Zhang, Y., Yue, X., and Zhang, Y. (2020). "Rapid Increases in Warm-Season Surface Ozone and Resulting Health Impact in China since 2013". In: *Environmental Science and Technology Letters*. DOI: 10.1021/acs.estlett.0c00171.

Ma, Z., Hu, X., Sayer, A. M., Levy, R., Zhang, Q., Xue, Y., Tong, S., Bi, J., et al. (2016). "Satellite-based spatiotemporal trends in PM2.5concentrations: China, 2004-2013". In: *Environmental Health Perspectives* 124.2, pp. 184–192. DOI: 10.1289/ehp.1409481.

Otte, T. L., Nolte, C. G., Otte, M. J., and Bowden, J. H. (2012). "Does nudging squelch the extremes in regional climate modeling?" In: *Journal of Climate* 25.20, pp. 7046–7066. DOI: 10.1175/JCLI-D-12-00048.1.

Reddington, C. L., Conibear, L., Knote, C., Silver, B. J., Li, Y. J., Chan, C. K., Arnold, S. R., and Spracklen, D. V. (2019). "Exploring the impacts of anthropogenic emission sectors on PM2.5 and human health in South and East Asia". In: *Atmospheric Chemistry and Physics*. DOI: 10.5194/acp-19-11887-2019.

Shao, J., Chen, Q., Wang, Y., Lu, X., He, P., Sun, Y., Shah, V., Martin, R., et al. (2019). "Heterogeneous sulfate aerosol formation mechanisms during wintertime Chinese haze events: Air quality model assessment using observations of sulfate oxygen isotopes in Beijing". In: *Atmospheric Chemistry and Physics* 19.9, pp. 6107–6123. DOI: 10.5194/acp-19-6107-2019.

Silver, B., Reddington, C. L., Arnold, S. R., and Spracklen, D. V. (2018). "Substantial changes in air pollution across China during 2015-2017". In: *Environmental Research Letters* 13.11. DOI: 10.1088/1748-9326/aae718.

Snider, G., Weagle, C. L., Martin, R. V., Van Donkelaar, A., Conrad, K., Cunningham, D., Gordon, C., Zwicker, M., et al. (2015). "SPARTAN: A global network to evaluate and enhance satellite-based estimates of ground-level particulate matter for global health applications". In: *Atmospheric Measurement Techniques* 8.1, pp. 505–521. DOI: 10.5194/amt-8-505-2015.

Snider, G., Weagle, C. L., Murdymootoo, K. K., Ring, A., Ritchie, Y., Stone, E., Walsh, A., Akoshile, C., et al. (2016). "Variation in global chemical composition of PM2.5: emerging results from SPARTAN". In: *Atmospheric Chemistry and Physics* 16.15, pp. 9629–9653. DOI: 10.5194/acp-16-9629-2016.

Streets, D. G., Yu, C., Wu, Y., Chin, M., Zhao, Z., Hayasaka, T., and Shi, G. (2008). "Aerosol trends over China, 1980-2000". In: *Atmospheric Research* 88.2, pp. 174–182. DOI: 10.1016/j.atmosres.2007.10.016.

Tai, A. P., Mickley, L. J., and Jacob, D. J. (2010). "Correlations between fine particulate matter (PM2.5) and meteorological variables in the United States: Implications for the sensitivity of PM2.5 to climate change". In: *Atmospheric Environment* 44.32, pp. 3976–3984. DOI: 10.1016/j.atmosenv.2010.06.060.

Wang, S., Li, G., Gong, Z., Du, L., Zhou, Q., Meng, X., Xie, S., and Zhou, L. (2015). "Spatial distribution, seasonal variation and regionalization of PM2.5 concentrations in China". In: *Science China Chemistry*. DOI: 10.1007/s11426-015-5468-9.

Weagle, C. L., Snider, G., Li, C., Van Donkelaar, A., Philip, S., Bissonnette, P., Burke, J., Jackson, J., et al. (2018). "Global Sources of Fine Particulate Matter: Interpretation of PM2.5 Chemical Composition Observed by SPARTAN using a Global Chemical Transport Model". In: *Environmental Science and Technology* 52.20, pp. 11670–11681. DOI: 10.1021/acs.est.8b01658.

Wiedinmyer, C., Akagi, S. K., Yokelson, R. J., Emmons, L. K., Al-Saadi, J. A., Orlando, J. J., and Soja, A. J. (2011). "The Fire INventory from NCAR (FINN): A high resolution global model to estimate the emissions from open burning". In: *Geoscientific Model Development* 4.3, pp. 625–641. DOI: 10.5194/gmd-4-625-2011.

Xing, J., Zhang, Y., Wang, S., Liu, X., Cheng, S., Zhang, Q., Chen, Y., Streets, D. G., et al. (2011). "Modeling study on the air quality impacts from emission reductions and

atypical meteorological conditions during the 2008 Beijing Olympics". In: *Atmospheric Environment*. DOI: 10.1016/j.atmosenv.2011.01.025.

Xu, W., Lin, W., Xu, X., Tang, J., Huang, J., Wu, H., and Zhang, X. (2016). "Long-term trends of surface ozone and its influencing factors at the Mt Waliguan GAW station, China-Part 1: Overall trends and characteristics". In: *Atmospheric Chemistry and Physics* 16.10, pp. 6191–6205. DOI: 10.5194/acp-16-6191-2016.

Xue, L., Wang, T., Louie, P. K., Luk, C. W., Blake, D. R., and Xu, Z. (2014). "Increasing external effects negate local efforts to control ozone air pollution: A case study of Hong Kong and implications for other chinese cities". In: *Environmental Science and Technology* 48.18, pp. 10769–10775. DOI: 10.1021/es503278g.

Yue, H., He, C., Huang, Q., Yin, D., and Bryan, B. A. (2020). "Stronger policy required to substantially reduce deaths from PM2.5 pollution in China". In: *Nature Communications* 11.1, pp. 1–10. DOI: 10.1038/s41467-020-15319-4.

Zaveri, R. A., Easter, R. C., Fast, J. D., and Peters, L. K. (2008). "Model for Simulating Aerosol Interactions and Chemistry (MOSAIC)". In: *Journal of Geophysical Research Atmospheres*. DOI: 10.1029/2007JD008782.

Zhai, S., Jacob, D. J., Wang, X., Shen, L., Li, K., Zhang, Y., Gui, K., Zhao, T., and Liao, H. (2019). "Fine particulate matter (PM_{2.5}) trends in China, 2013–2018: separating contributions from anthropogenic emissions and meteorology". In: *Atmospheric Chemistry and Physics*. DOI: 10.5194/acp-19-11031-2019.

Zhang, L., Lee, C. S., Zhang, R., and Chen, L. (2017). "Spatial and temporal evaluation of long term trend (2005–2014) of OMI retrieved NO2and SO2 concentrations in Henan Province, China". In: *Atmospheric Environment*. DOI: 10.1016/j.atmosenv.2016.11.067.

Zhang, Q., Yuan, B., Shao, M., Wang, X., Lu, S., Lu, K., Wang, M., Chen, L., et al. (2014). "Variations of ground-level O3 and its precursors in Beijing in summertime between 2005 and 2011". In: *Atmospheric Chemistry and Physics*. DOI: 10.5194/acp-14-6089-2014.

Zhang, Q., Geng, G. N., Wang, S. W., Richter, A., and He, K. B. (2012). "Satellite remote sensing of changes in NO x emissions over China during 1996-2010". In: *Chinese Science Bulletin* 57.22, pp. 2857–2864. DOI: 10.1007/s11434-012-5015-4.

Zhang, Q., Zheng, Y., Tong, D., Shao, M., Wang, S., Zhang, Y., Xu, X., Wang, J., et al. (2019). "Drivers of improved PM2.5 air quality in China from 2013 to 2017". In: *Proceedings of the National Academy of Sciences of the United States of America* 116.49, pp. 24463–24469. DOI: 10.1073/pnas.1907956116.

Zhang, Y., Zhang, X., Wang, L., Zhang, Q., Duan, F., and He, K. (2016). "Application of WRF/Chem over East Asia: Part I. Model evaluation and intercomparison with MM5/CMAQ". In: *Atmospheric Environment* 124, pp. 285–300. DOI: 10.1016/j.atmosenv.2015.07.022.

Zheng, B., Tong, D., Li, M., Liu, F., Hong, C., Geng, G., Li, H., Li, X., et al. (2018). "Trends in China's anthropogenic emissions since 2010 as the consequence of clean air actions". In: *Atmospheric Chemistry and Physics* 18.19, pp. 14095–14111. DOI: 10.5194/acp-18-14095-2018.

Zheng, Y., Xue, T., Zhang, Q., Geng, G., Tong, D., Li, X., and He, K. (2017). "Air quality improvements and health benefits from China's clean air action since 2013". In: *Environmental Research Letters* 12.11. DOI: 10.1088/1748-9326/aa8a32.

Zhou, W., Gao, M., He, Y., Wang, Q., Xie, C., Xu, W., Zhao, J., Du, W., et al. (2019). "Response of aerosol chemistry to clean air action in Beijing, China: Insights from two-year ACSM measurements and model simulations". In: *Environmental Pollution* 255, p. 113345. DOI: 10.1016/j.envpol.2019.113345.

Chapter 4

The impact of COVID-19 control measures on air quality in China

Ben Silver[1], X. He[1,2], S. R. Arnold[1] and D. V. Spracklen[1]

[1] School of Earth and Environment, University of Leeds, Leeds, United Kingdom
[2] School of Environmental Science and Engineering, Southern University of Science and Technology, Shenzhen, People's Republic of China

Published in *Environmental Research Letters* **15**(8), 28th July 2020
Available at: doi.org/10.1088/1748-9326/aba3a2

Abstract

The outbreak of Coronavirus Disease 2019 (COVID-19) in China in January 2020 prompted substantial control measures including social distancing measures, suspension of public transport and industry, and widespread cordon sanitaires ('lockdowns'), that have led to a decrease in industrial activity and air pollution emissions over a prolonged period. We use a 5-year dataset from China's air quality monitoring network to assess the impact of control measures on air pollution. Pollutant concentration time series are decomposed to account for the inter-annual trend, seasonal cycles and the effect of Lunar New Year, which coincided with the COVID-19 outbreak. Over 2015–2019, there were significant negative trends in particulate matter ($PM_{2.5}$, -6% yr^{-1}) and sulphur dioxide (SO_2, -12% yr^{-1}) and nitrogen dioxide (NO_2, -2.2% yr^{-1}) whereas there were positive trends in ozone (O_3, +

2.8% yr^{-1}). We quantify the change in air quality during the LNY holiday week, during which pollutant concentrations increase on LNY's day, followed by reduced concentrations in the rest of the week. After accounting for interannual trends and LNY we find NO_2 and PM concentrations were significantly lower during the lockdown period than would be expected, but there were no significant impacts on O_3. Largest reductions occurred in NO_2, with concentrations 27.0% lower on average across China, during the lockdown. Average concentrations of $PM_{2.5}$ and PM_{10} across China were, respectively, 10.5% and 21.4% lower during the lockdown period. The largest reductions were in Hubei province, where NO_2 concentrations were 50.5% lower than expected during the lockdown. Concentrations of affected pollutants returned to expected levels during April, after control measures were relaxed.

Introduction

The outbreak of Coronavirus Disease 2019 (COVID-19) began in the megacity of Wuhan (population 11 million) in central China, with cases first being reported on December 27, 2019. Media reports of an unknown pneumonia outbreak began to appear on December 31, with the outbreak officially being reported to the World Health Organisation (WHO) on the same day (World Health Organization (WHO), 2020). The cause of the disease was confirmed as a novel coronavirus on January 7 2020 (Wu and McGoogan, 2020). The Chinese government quickly implemented control measures, such as isolation, quarantine and social distancing. Dramatic actions to control the disease were taken, as entire cities were quarantined across China. This began with Wuhan being 'locked-down' on January 23, followed by another 14 cities in Hubei province the next day (Kraemer et al., 2020). Cases of the disease were soon reported in China's other provinces, with every other province reporting their first case between January 18 to 25 (Liu et al., 2020). Public transport networks, schools and entertainment venues were suspended (Tian et al., 2020), and the Lunar New Year (LNY) national holiday was extended, to delay the return of hundreds of millions to their cities of work, and citizens were encouraged to work from home.

The control measures are likely to have resulted in a substantial decrease in air pollutant emissions across China. In the industrial sector, widespread suspensions of production resulted in the largest ever decrease in the Purchasing Managers Index, which tracks in-

dustrial output in China (National Bureau of Statistics of China, 2020c; Prescott, 2020). The monthly growth rate in industrial production, which in 2019 had averaged + 0.5%, fell to −2.78% in January 2020 and −26.63% in February 2020 (National Bureau of Statistics of China, 2020b). In the power generation sector, electricity generation in January and February dropped by 8.2%, compared with 2019. As restrictions began to be eased during March, the economy started to recover, with March power generation lower by 4.6% compared with the previous year (National Bureau of Statistics of China, 2020a). CO_2 emissions may have decreased by 25% during the first few weeks of lockdowns (CarbonBrief, 2020).

The control measures and resultant emission reductions are likely to have influenced China's air quality, and impacts have been widely reported in the media. According to measurements made by NASA's TROPOMI satellite, there was a 20% larger than previous year's drop in Nitrogen Dioxide (NO_2), between the period before LNY to the period after (Liu et al., 2020). However, understanding the impacts of control measures on air quality is complicated by several compounding factors. The control measures coincided with the LNY, the largest holiday in China. The LNY is typically a week long and results in well-documented impacts on air pollution (Tan et al., 2009; Gong et al., 2014; Lai and Brimblecombe, 2017). China's air quality has been changing rapidly in recent years, with large reductions in SO_2 and PM concentrations and increased O_3 (A et al., 2017; Lu et al., 2018; Silver et al., 2018). These trends in pollutants are due to declining emissions (Zheng et al., 2017; Ding et al., 2019; Silver et al., 2020), and need to be accounted for when analysing any impact of the lockdown on pollutant concentrations.

Although China's air quality has improved in recent years, it continues to suffer a severe health burden caused by indoor and outdoor air pollution, with 12% of deaths in China in 2017 attributable to this risk factor (James et al., 2018). Understanding trends in air quality is essential to assess the effectiveness of recent air quality measures and help inform future air pollution mitigation (Zhao et al., 2017). The application of control measures during the COVID-19 outbreak provides an opportunity to analyse the potential air quality improvements resulting from a reduction in emissions, as well as a 'natural experiment' from which theories of chemistry-climate interactions can be tested.

To understand the impact of the control measures instigated during the COVID-19 outbreak, it is necessary to compare pollutant concentrations in 2020 with expected concen-

trations had the COVID-19 outbreak not occurred. Here, we use time series of China-wide measurements of key pollutant concentrations between January 2015 an April 2020 to isolate changes that occurred during the COVID-19 lockdown period compared with concentrations that would otherwise be expected based on recent trends, seasonality, and the effects of LNY. We do not assess the relative contribution of emissions and meteorology to observed changes during the lockdown.

Methodology

Data

We obtained data from China's national network of air quality monitoring stations, which is operated by the China National Environmental Monitoring Center (CNEMC). The network consists of 1640 automatic measurement stations located throughout mainland China, which report measurements of particulate matter ($PM_{2.5}$ and PM_{10}), nitrogen dioxide (NO_2), ozone (O_3), sulphur dioxide (SO_2) and carbon monoxide (CO). The data was downloaded from https://quotsoft.net/ (formerly http://beijingair.sinaapp.com/), which aggregates the real-time data reported on the official website of the CNEMC. The dataset covers the period from January 2015 to April 2020. For this study, stations with a time-series of >58 months and >90% data availability were used. We used the same data quality methods as in Silver et al. (2018), excluding data with high proportion of repeat measurements and periods of very low variability. The number of excluded stations is provided in the supplementary table 1 (available online at `stacks.iop.org/ERL/15/084021/mmedia`).

Time series decomposition

When comparing the air quality in China during the lockdown in 2020, to the same period of previous years, it is necessary to account for several interacting factors, including interannual trends, seasonal cycle and the effects of Chinese LNY. LNY is based on the lunar calendar, so in the Gregorian calendar, the holiday falls on a different date between late January and late February each year.

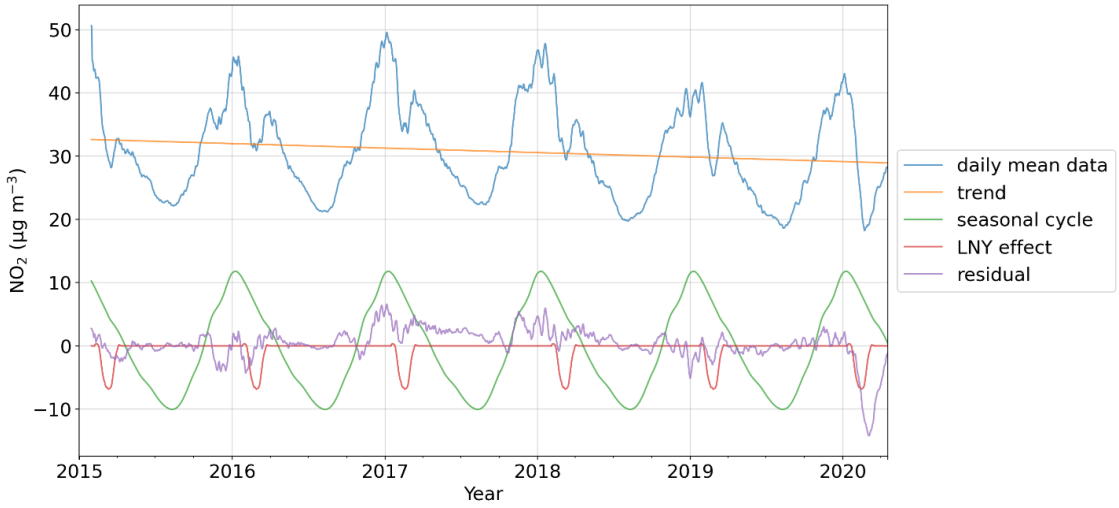

Figure 4.1: Average of the NO_2 ($\mu g\, m^{-3}$) time series (blue), decomposed into its the trend (yellow), seasonal cycle (green), Lunar New Year (LNY) effect (red) and residual (purple) components. The time series show the average concentration across all stations included in the study from the China National Environmental Monitoring Centre network. A 30-day rolling mean has been applied to smooth the data.

The time series are decomposed separately for each pollutant at each station, using daily data. The 2015–2019 time series are used to calculate the trend, seasonal cycle and effect of LNY, for each pollutant at each station, and these patterns are applied to 2020. The 2020 residuals are then analysed to assess the extent to which pollutant concentrations were affected during the lockdown period.

Figure 4.1 shows this method for NO_2, and the remaining pollutants are shown in Supplementary Figure C.1. The data is analysed and visualised using the Python libraries *pandas* and *matplotlib* (Hunter, 2007; McKinney, 2010). The trend is calculated using the method in Silver et al. (2018), using the Theil–Sen estimator to calculate the monotonic, linear trends (Sen, 1968; Carslaw and Ropkins, 2012). The trend is subtracted from the daily mean data, and the resulting detrended data is smoothed using locally weighted scatterplot smoothing (LOWESS) using the statsmodels Python library (Cleveland, 1979; Seabold and Perktold, 2010). A 30-day window for the LOWESS filter is used to approximate the background seasonal concentration. The period between 14 d prior and 21 d after LNY is removed and replaced with interpolated data. Both the seasonal smoothing and LNY data are averaged across years, to give separate seasonal cycle and LNY effect timeseries. These time series are subtracted from the detrended data, to give the residual time series, which represents departures from the expected concentration based on the trend, seasonal cycle, and LNY effect.

The residual concentrations are used to assess how much the concentration of pollutants deviated from their expected concentration, based on long-term trends, seasonality and LNY impacts. At each station, we apply a 7-day centered rolling mean to the residual time series, giving a time series of 7 d mean residuals (7DMR). We express this in relative terms (%) by dividing the residual timeseries by the sum of the trend, seasonal and LNY components. Taking the median during the lockdown period (defined below) allows for comparison between different pollutants and regions. The 7DMR represents a longer-term deviation from the expected concentration, averaging out day-to-day variability. Supplementary Figure C.3 the effects of using different averaging periods.

To analyze the influence of the COVID-19 control measures, we define the 'lockdown period' as January 23 to March 31, 2020. The lockdown was officially lifted in Wuhan on April 8th, though restrictions were eased in other parts of China earlier than this, and some social distancing measures have remained in place. Generally, restrictions were lifted gradually, so it is likely that emissions will gradually return to normal. We analyse data at the national level and for the following regions: the Mid-Yangtze Basin (MYB) in central China (which includes Hubei province); the North China Plain (NCP) which includes the capital Beijing, as well as Tianjin municipality and Hebei province; the Yangtze River Delta (YRD) which includes Shanghai; the Sichuan Basin (SCB) which includes Chengdu and Chongqing; the Fenwei Plain (FWP) which includes Xi'an; and the Pearl River Delta (PRD), which includes Guangzhou and Shenzhen.

Results

Inter-annual trends

There are significant inter-annual trends in air pollutant concentrations. Our previous work, Silver et al. (2018) found that during 2015–2017 across much of China, there were significant negative trends in $PM_{2.5}$ and SO_2, whereas for O_3, there were widespread significant positive trends. Here we show that significant trends have continued across much of China.

Figure 4.2 shows the 2015–2019 trends in air pollutants across China. SO_2 has the strongest negative trend, with 89% of stations reporting significant reductions and a median trend of $-12.0\%\ \mathrm{yr}^{-1}$ or $-2.6\ \mu\mathrm{g\,m^{-3}\,yr^{-1}}$. For $PM_{2.5}$, 81% of stations report a significant reduction, with a median trend of $-6.0\%\ \mathrm{yr}^{-1}$ or $-3.0\ \mu\mathrm{g\,m^{-3}\,yr^{-1}}$. For NO_2, 44% of stations

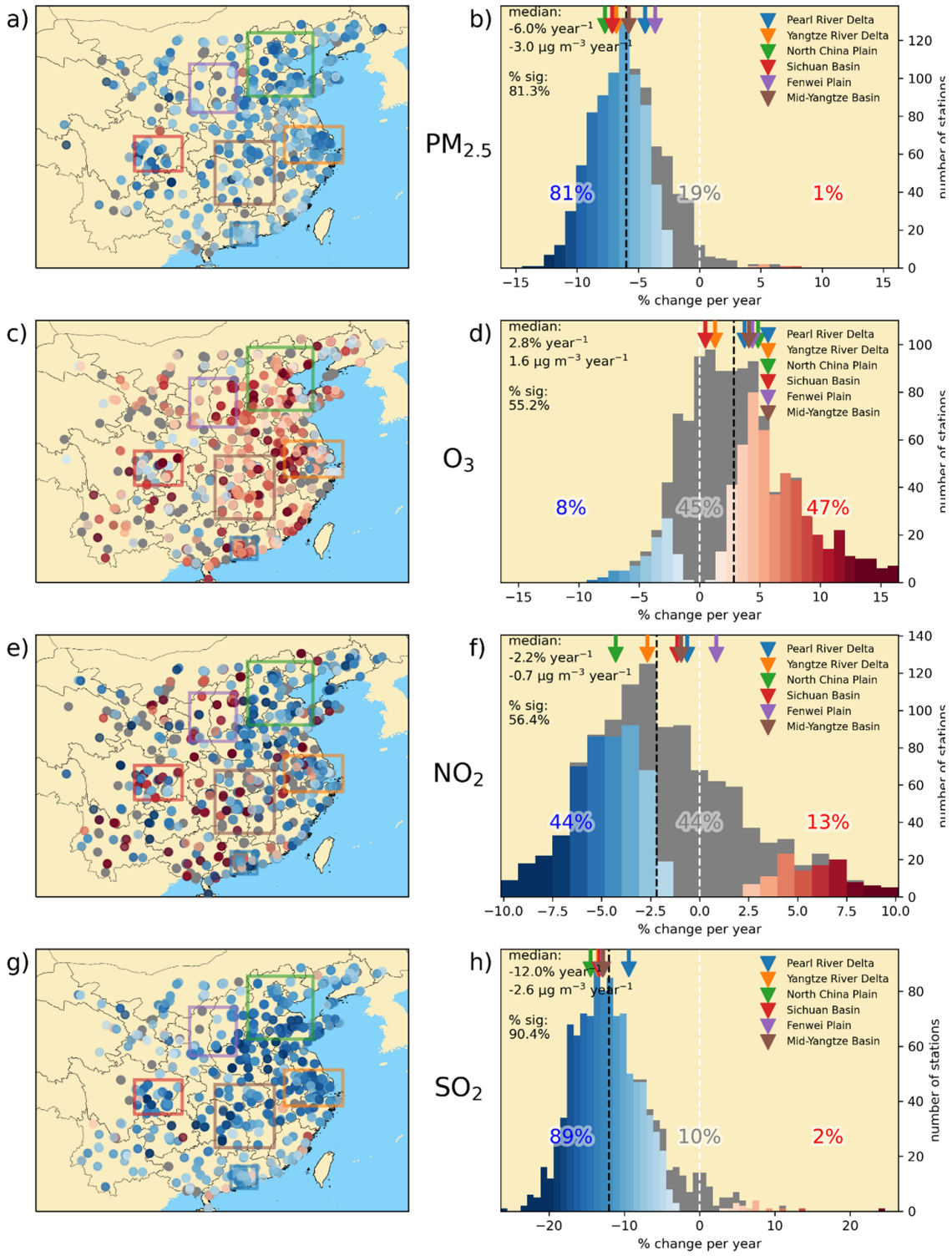

Figure 4.2: Trends in concentrations of (a), (b) $PM_{2.5}$, (c), (d) O_3, (e), (f) NO_2, (g), (h) SO_2 across China during 2015–2019. Left-hand panels (a), (c), (e), (g) show the spatial distribution of the trend and mean concentration (size of circle). Right hand panels (b), (d), (f), (h) show the frequency of stations against the relative trends. The points on the map are coloured by the same scale as the histogram. The median relative and absolute trend as well as the percentage of stations with significant trends is shown beside the histograms. The percentage of trends that are negative (blue) or positive (red) are also shown. The black dotted line shows the median trend across all sites. Triangles show the median trend for the regional domains shown in the left-hand panels: Pearl River Delta (PRD), Yangtze River Delta (YRD), North China Plain (NCP), Sichuan Basin (SCB), and Fenwei Plain (FWP).

report a significant reduction, with a median trend of -2.2% yr^{-1} or -0.7 $\mu g\,m^{-3}\,yr^{-1}$. Unlike the other pollutants, O_3 concentrations have increased, with 47% of stations reporting a significant positive trend, and a median trend of 2.8% yr^{-1} or 1.6 $\mu g\,m^{-3}\,yr^{-1}$. Changes in air pollutant concentrations are pervasive, with all analysed regions showing increased O_3 and decreased $PM_{2.5}$ and SO_2.

The variability of the magnitude and direction of trends highlights the importance of accounting for the inter-annual trend at each station individually, as we do here. For example, at a station with a positive trend, we might expect a decrease in concentration during the outbreak to be moderated, while at one with a negative trend, we account for the fact that the concentration likely would have been reduced under normal circumstances.

Seasonal cycle

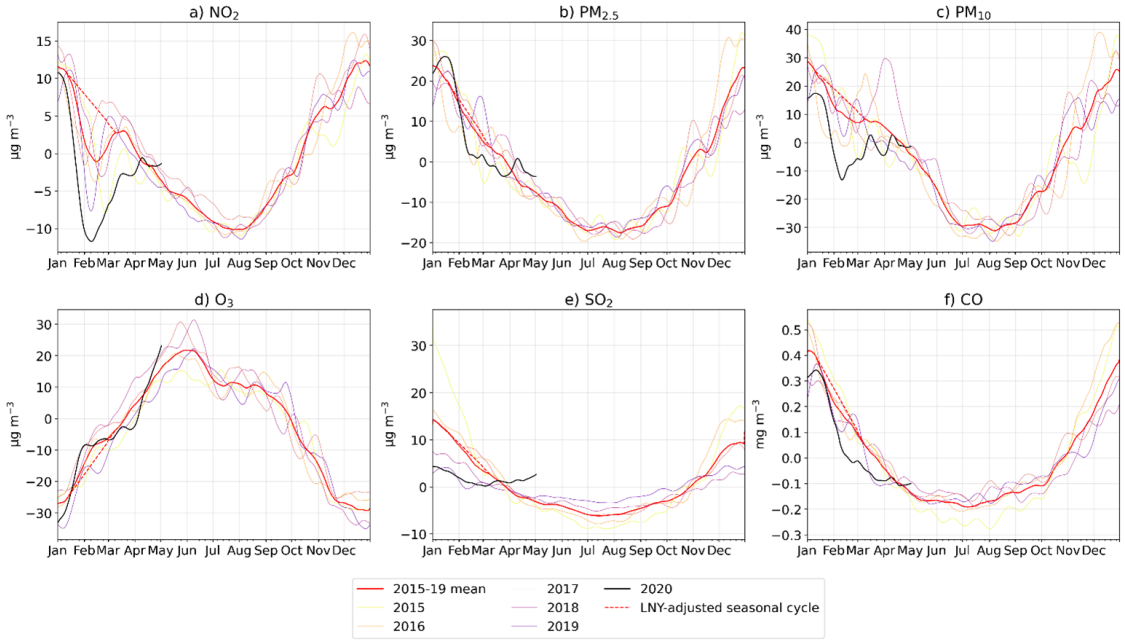

Figure 4.3: Comparison of the detrended concentrations for (a) NO_2, (b) $PM_{2.5}$, (c) PM_{10}, (d) O_3, (e) SO_2 and (f) CO. The data is smoothed using a LOWESS filter. The 2015–2019 average is shown as a solid red line, the dotted line shows data after the Lunar New Year effect has been removed and replaced with interpolated data. Individual years are shown as shades of red and 2020 is shown as a black line.

Figure 4.3 shows the mean seasonal cycle of pollutant concentrations during 2015 to 2019. In general, the pollutants concentrations peak in the winter, except for O_3, which peaks in early summer. The effect of LNY is visible for some pollutants, especially NO_2. However, since this is not caused by seasonal changes and does not occur on the same date each year, we extract this signal from the seasonal cycle (shown as the red dotted line) and

analyse separately.

Lunar New Year

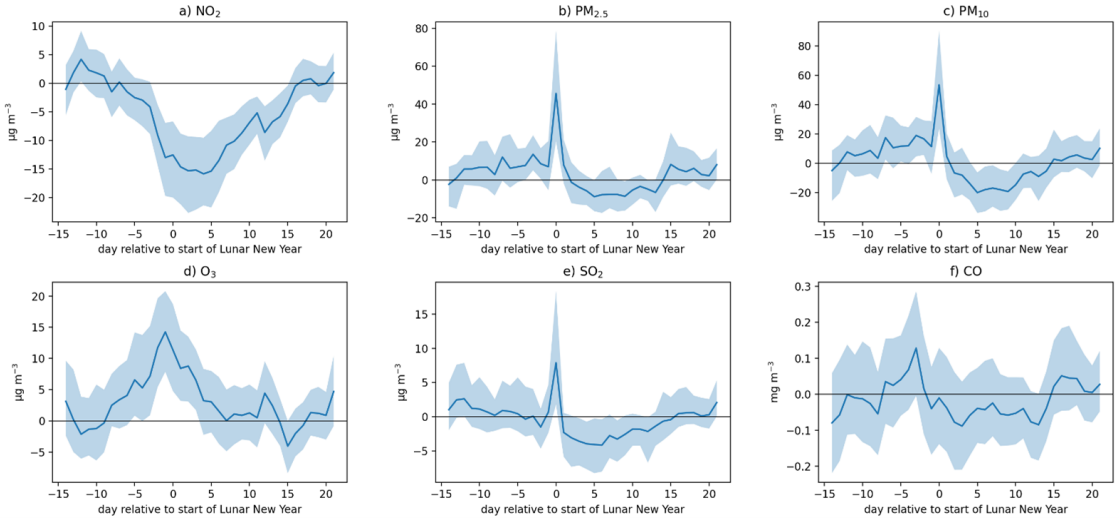

Figure 4.4: Average 2015–2019 detrended concentrations of (a) NO_2, (b) $PM_{2.5}$, (c) PM_{10}, (d) O_3, (e) SO_2 and (f) CO during Lunar New Year (LNY). Concentrations are presented relative to the start date of LNY, from 14 d before the first day of LNY till 21 d after. Average detrended concentrations (blue line) and 25th and 75th percentiles (blue shading) are shown.

Figure 4.4 shows the impact of LNY on pollutant concentrations. PM, CO, and SO_2 concentrations all increase on the first day of LNY, likely caused by emissions from fireworks (Jiang et al., 2015; Feng et al., 2016; Lai and Brimblecombe, 2017). On this day, $PM_{2.5}$ and PM_{10} concentrations are on average 46 and 53 $\mu g\,m^{-3}\,yr^{-1}$ higher, respectively. During the remainder of LNY, concentrations of all pollutants except O_3 are lower than usual. $PM_{2.5}$ and PM_{10} concentrations are 6.7 and 15.2 $\mu g\,m^{-3}\,yr^{-1}$ lower respectively. NO_2 is on average 14.5 $\mu g\,m^{-3}\,yr^{-1}$ lower during the LNY holiday. O_3 concentrations are higher during LNY, and are negatively correlated with NO_2. This likely demonstrates a reduction in the NO_x (NO_2 + NO) titration effect, where O_3 is removed in the presence of high concentrations of NO.

The effects of LNY mean that simply comparing monthly averages between different years during this period could be misleading. In some years LNY occurs in January whereas in other years it occurs in February. Controlling for the LNY effect is important, as it allows comparison across years.

Table 4.1: The proportion of stations that record their minimum and maximum 7 day mean residual during the lockdown period.

	minimum (% of stations)	maximum (% of stations)
NO_2	46.0	0.4
$PM_{2.5}$	26.8	1.2
PM_{10}	40.2	0.1
SO_2	18.5	0.2
O_3	1.5	1.5
CO	14.8	1.4

Residual analysis

Figure 4.5 shows the anomaly in pollutant concentrations after the inter-annual trend, seasonal cycle and LNY effect have been removed. Results before, during and after the lockdown period, are displayed as the 7DMR concentration. Full results for each province and city are attached as csv files in the supplement.

NO_2

For NO_2, 46.0% stations across China record their lowest 7DMR during the lockdown period (table 4.1). During the lockdown period, the median 7DMR concentration was -27.0% ($-8.0\ \mu g\,m^{-3}\,yr^{-1}$) (table 4.2), with a maximum difference of -56.2% occurring on February 16. The median z-score of the 7DMR during lockdown is -2.3, and falls below -5 (Figure 4.7). The minimum z-score during the lockdown was lower than for any previous time over the period analysed (Supplementary Figure C.2), indicating that the lockdown resulted in an unusually extreme negative anomaly. A decrease in NO_2 during lockdown was observed across China, ranging from -25.9% in the YRD to -30.5% in the SCB. The most negative residuals occurred in Hubei (-50.5%, Figure 4.6). Here, the end of LNY was changed to March 10, extending it for 5 weeks (Chen et al., 2020), whereas in the rest of China it was extended for 1 week.

Particulate matter

A median negative residual in PM concentration across China occurred during the lockdown, although it is not as extreme as that for NO_2. For $PM_{2.5}$, 26.8% of stations recorded their minimum 7DMR concentration. During the lockdown period, the median 7DMR concentration was -10.5% ($-3.7\ \mu g\,m^{-3}\,yr^{-1}$) (table 4.2)), with a maximum difference of -39.4% occurring on February 18. Across different regions, the decrease in $PM_{2.5}$ dur-

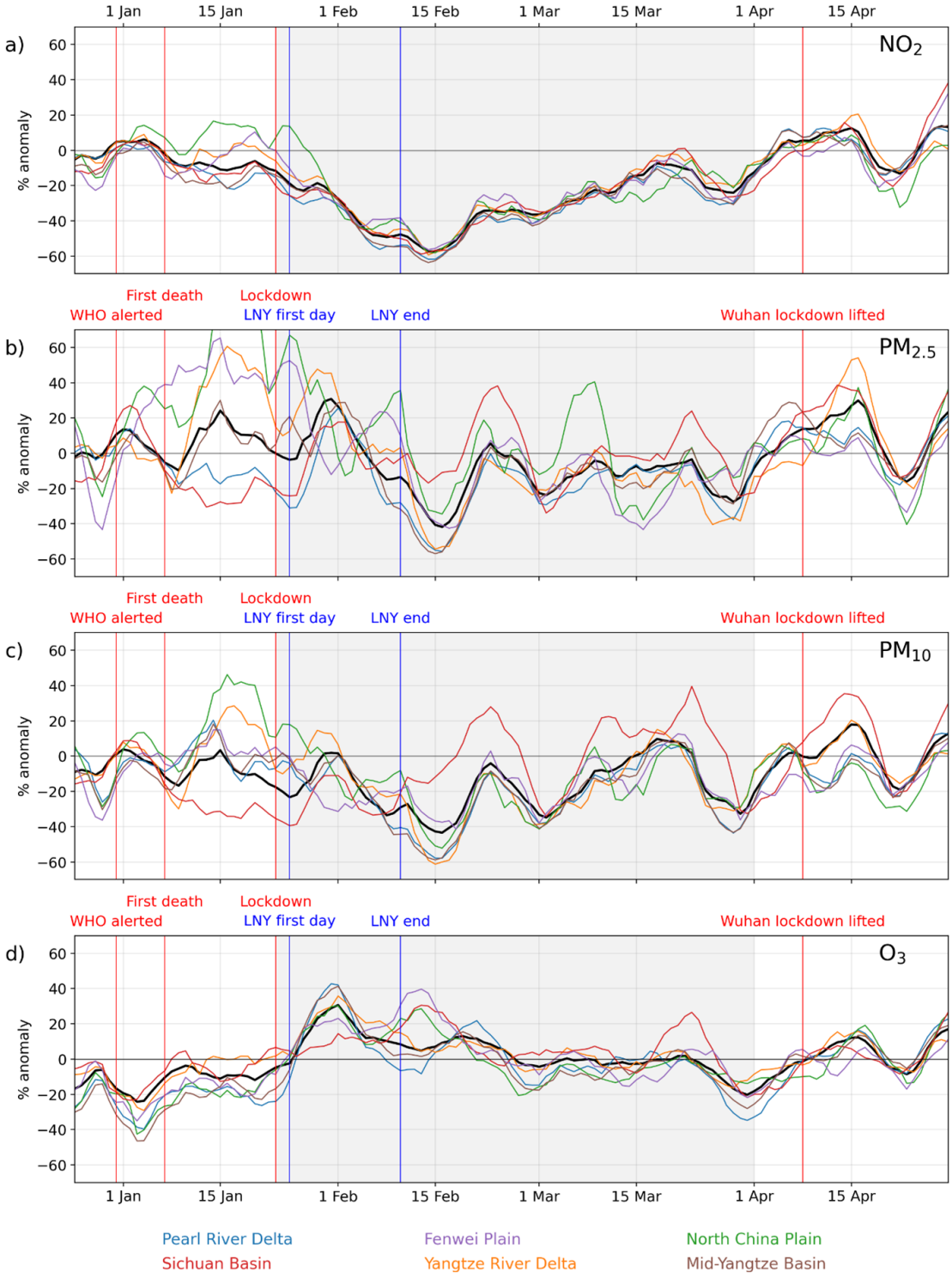

Figure 4.5: Time series of the relative anomaly (%) during 2020 in the 7 d residual mean concentration of (a) NO_2, (b) $PM_{2.5}$, (c) PM_{10} and (d) O_3. This is calculated by dividing the 7 d mean of the residual component of by the sum of the seasonal, trend and Lunar New Year components. The black line shows the median across all stations, with the coloured lines showing the medians across regions. The 'lockdown period,' defined as 23 January to 31 March, is shaded.

Table 4.2: Median 7 day mean residual (7DMR) concentrations during the lockdown period. For each pollutant, the residual is expressed in absolute ($\mu g\,m^{-3}$ 3) and relative (%) terms, and a z-score. Results shown for all China and individual regions.

		China	Pearl river delta	Yangtze river delta	North China plain	Sichuan ba
	residual ($\mu g\,m^{-3}$)	-8.0	-10.1	-9.4	-11.3	-8.6
NO_2	relative residual (%)	-27.0	-30.1	-25.9	-28.5	-30.5
	z-score	-2.3	-2.0	-2.0	-1.9	-2.0
	residual ($\mu g\,m^{-3}$)	-3.7	-7.5	-4.4	-0.8	-1.4
$PM_{2.5}$	relative residual (%)	-10.5	-17.2	-12.1	-2.0	-3.9
	z-score	-0.7	-0.9	-0.7	-0.3	-0.2
	residual ($\mu g\,m^{-3}$)	-14.7	-16.8	-15.0	-18.0	-8.4
PM_{10}	relative residual (%)	-21.4	-20.8	-20.3	-17.5	-9.9
	z-score	-1.3	-1.0	-1.1	-0.8	-0.5
	residual ($\mu g\,m^{-3}$)	0.1	-1.3	2.1	-1.6	2.8
O_3	relative residual (%)	0.2	-2.4	3.3	-2.8	5.1
	z-score	-0.1	-0.2	0.2	-0.3	0.4
	residual ($mg\,m^{-3}$)	-0.1	-0.1	-0.1	-0.1	-0.1
CO	relative residual (%)	-12.1	-13.5	-11.2	-7.8	-12.8
	z-score	-1.3	-1.2	-1.0	-0.4	-1.2

ing the lockdown is quite variable, ranging from −17.2% in the PRD, to −2.0% in the NCP.

The median z-score of the 7DMR during lockdown is −0.7 (table 4.2), with a minimum of −2.7. This indicates that during most of the lockdown period, $PM_{2.5}$ concentrations were low, but not to the same extent as NO_2. However, when comparing the lockdown period to other periods of the same length (69 d), the lockdown period experienced the most negative average residual recorded in the last 5 years (Supplementary Figure C.2). The PM_{10} residual timeseries shows a similar temporal pattern to that of $PM_{2.5}$, but its relative residual concentration is around twice as extreme as $PM_{2.5}$.

PM concentrations recover to normal levels earlier than NO_2 (Figure 4.5), though the initial reduction in concentrations is of similar magnitude to NO_2 in some regions, with the PM in the YRD, PRD and MYB being ˜60% lower in mid-February.

Prior to lockdown, during in mid-January, $PM_{2.5}$ residual concentrations are unusually high in some regions of China, with the FWP, YRD and NCP all reaching a z-score of over + 2 during January, and concentrations ˜50%–100% above the trend-adjusted seasonal mean. Figure 4.6 shows that some stations, mostly in north-Eastern China, experienced high positive anomalies during lockdown of >40%.

O_3

For O_3, 1.5% of stations recorded their minimum 7DMR concentration during the lockdown period, while 1.5% recorded their maximum. These proportions are much lower than for NO_2 or PM, indicating that that O_3 residual concentrations were less extreme. Across China the median O_3 7DMR during the lockdown was + 0.2%, with a range of −2.4 to 5.1% between the six regions.

It should be noted that unlike the other pollutants, winter is the seasonal minimum for O_3 concentrations across much of China (Figure 4.3) (Gao et al., 2020). During winter, O_3 production across much of China may be primarily volatile organic compound (VOC)-limited, while during spring and summer, more regions become NO_x limited (Jin and Holloway, 2015). Formation regimes of O_3 also vary across the country based on both emissions of precursors and climate (Wang et al., 2020). The spatial and temporal heterogeneity of O_3 production regimes, and the array of precursors involved in O_3 formation, results in a complex response of O_3 to the change in emissions during lockdown.

CO

A median negative residual in CO is also recorded during the lockdown period, although it is not as extreme as that for NO_2. For CO, 14.8% of stations recorded their minimum 7DMR concentration. During the lockdown period, the median 7DMR concentration was −12.1% (table 4.2), with a maximum difference of −28.5% occurring on February 20. Across different regions, the decrease in CO during the lockdown is quite variable, ranging from −16.5% in the FWP to −7.8% in the NCP. The CO time series are shown in supplementary figures C.5 and C.6.

SO_2

Rapid reductions in SO_2 during 2015–2019 (Figure 4.2, −12% yr^{-1}) result in reduced amplitude of seasonal cycle (Figure 4.3). This rapid change in seasonal cycle means that extracting the average 2015–2019 seasonal cycle impacts the residuals calculated in 2020. Therefore, although the residual concentration remains negative throughout the lockdown period, it cannot be shown that this was an unusual departure from the expected concentration based the interannual-trend and seasonal cycle. The SO_2 time series are shown in Supplementary Figures C.5 and C.6.

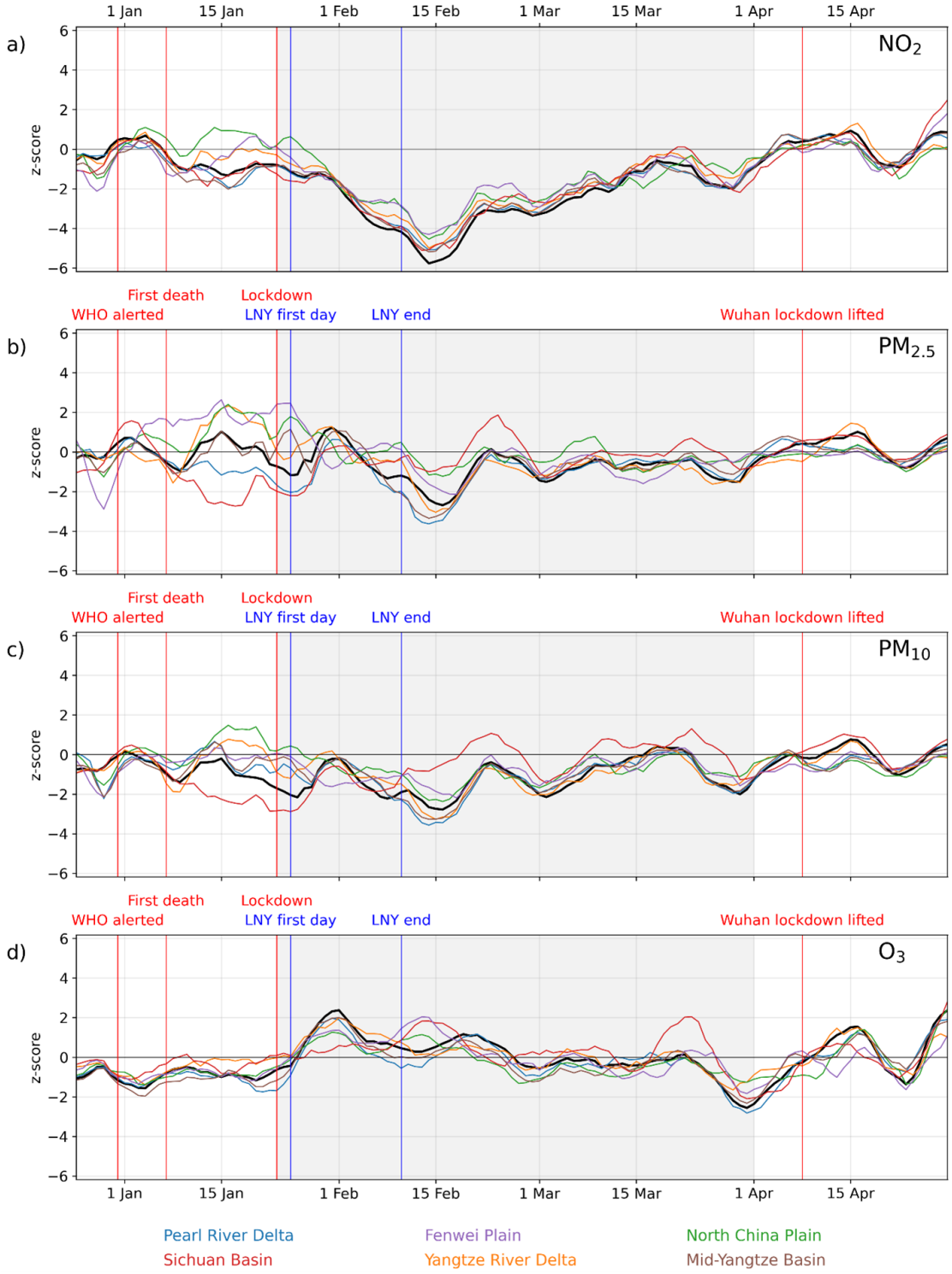

Figure 4.7: Time series of z-score during 2020 for (a) NO_2, (b) $PM_{2.5}$, (c) PM_{10} and (d) O_3. The black line shows the median across all stations, with the coloured lines showing the medians across regions. The 'lockdown period,' which is defined as 23 January to 31 March, is shaded.

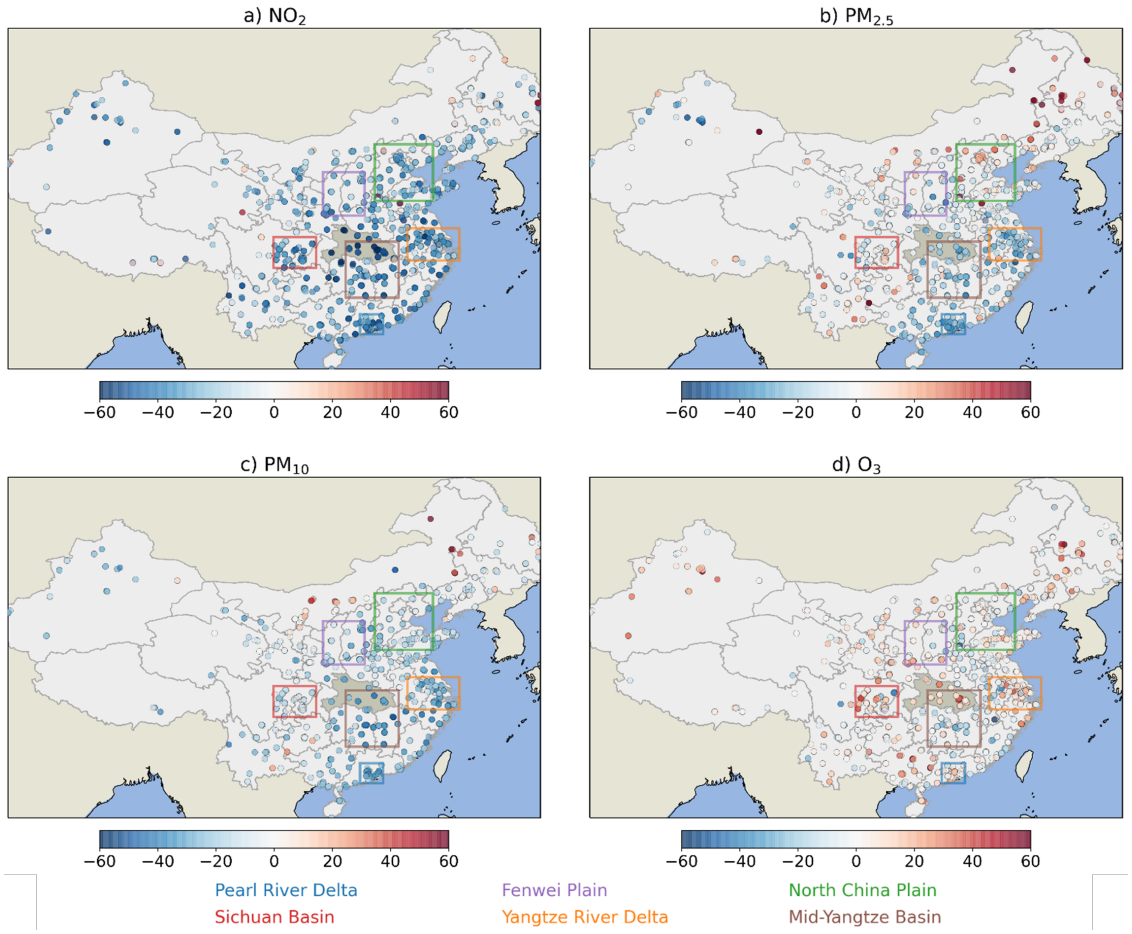

Figure 4.6: Spatial distribution of the median residual anomaly (%) during the lockdown period (23 January 2020–31 March 2020) in (a) NO_2 (b) $PM_{2.5}$, (c) PM_{10} and (d) O_3. Hubei province is shaded.

Discussion and conclusions

We analysed air pollutant concentrations from China's air quality network to examine the impact of the COVID-19 control measures on air quality. We show that quantifying the impact of the lockdown requires careful consideration of interacting factors, including interannual trends, seasonal cycle and the LNY.

Large changes in air pollutant concentrations have occurred in China in recent years. We show strong reductions in $PM_{2.5}$, PM_{10}, SO_2 and NO_2 and increased in O_3 concentrations during 2015–2019. These long-term changes in air pollutants continue previously identified trends during 2015–2017 (Silver et al., 2018). These long-term changes in pollutant concentrations are largely driven by changes in emissions (Zheng et al., 2017; Ding et al., 2019; Silver et al., 2020).

We show that LNY holiday results in consistent changes in pollutant concentrations across

China during 2015–2019, with all pollutant concentrations except O_3 are lower than normal. Similar effects have been reported for Nanjing (Kong et al., 2015) and Taiwan (Tan et al., 2009). Gong et al. (2014) reported a 9% reduction in PM_{10} concentrations during LNY across 323 stations in eastern China. Reductions in PM, SO_2 and NO_2 concentrations are attributed to lower emissions from traffic and coal combustion, and increased O_3 due to NO_x titration. The coincidence of LNY and COVID-19 control measures means it is important to account for LNY impacts when assessing the impacts of control measures.

We estimated that COVID-19 control measures resulted in reductions in NO_2, PM and CO concentrations during the lockdown period, defined here as January 23 to March 31, 2020. After accounting for the long-term trend, seasonal cycle and LNY, we estimated that China-wide concentrations in major air pollutants were reduced, with NO_2 reduced by 27.0%, $PM_{2.5}$ by 10.5%, PM_{10} by 21.4% and CO by 12.1%. We found little change in O_3 concentrations.

By comparing the residual concentrations during the lockdown period in 2020 to those during the previous five years, we show that unusual air pollution concentrations occurred during the lockdown. It is likely that these unusual concentrations, most notably for NO_2, were caused by emissions changes rather than unusual meteorological events, due to the extended duration (NO_2 stays below -2 z-score for a month), the consistency of the result across most of China, reports of substantially decreased activity in emissions sectors, and the co-occurrence of unusual concentrations with the enforcement and lifting of the lockdown. A full assessment of the role of meteorology is now needed to clarify the relative contributions of emissions and meteorology to observed concentrations during the lockdown.

Chinese NO_x emissions are dominated by transport (35%), industry (35%), and power generation (19%) (Zheng et al., 2018), all of which are likely to have been affected by the lockdown. Reduction in emission from these dominant sectors and short lifetime together explain the larger reduction in NO_2 compared to other pollutants. $PM_{2.5}$ concentrations in China are heavily influenced by residential emissions (Reddington et al., 2019), which are likely to have been less influenced by the control measures. The larger relative reductions in PM_{10} and CO compared to $PM_{2.5}$, may be due to a greater reduction in primary emission sources and the greater contribution of secondary aerosol to $PM_{2.5}$. Reductions in emissions of VOC and NO_x combined with changes in PM concentrations result in little

overall change in O_3 concentrations.

Despite decreases in pollutant concentrations during the last 10 years, China continues to suffer from poor air quality and a large disease burden resulting from air pollution (Zhao et al., 2018). The control measures and associated emissions reductions during the COVID-19 outbreak provide a useful natural experiment. Analysing the change in pollutant concentrations during this period can help us understand the impacts of emission reductions on air quality. Future work quantifying emission reductions and simulating atmospheric chemistry during this period, will help elucidate how emissions reductions change PM composition and radical chemistry, as well examining the influence of meteorology.

Acknowledgements

We acknowledge AIA Group and Natural Environment Research Council (NE/N006895/1) for funding. We thank Xiaolei Wang for collecting and distributing the air quality data.

References

A, R. J. van der, Mijling, B., Ding, J., Elissavet Koukouli, M., Liu, F., Li, Q., Mao, H., and Theys, N. (2017). "Cleaning up the air: Effectiveness of air quality policy for SO2 and NOx emissions in China". In: *Atmospheric Chemistry and Physics* 17.3, pp. 1775–1789. DOI: 10.5194/acp-17-1775-2017.

CarbonBrief (2020). *Analysis: coronavirus temporarily reduced China's CO2 emissions by a quarter*. URL: www.carbonbrief.org/analysis-coronavirus-has-temporarily-reduced-chinas-co2-emissions-by-a-quarter (visited on 04/23/2020).

Carslaw, D. C. and Ropkins, K. (2012). "openair – Data Analysis Tools for the Air Quality Community". In: *R Journal* 4.1, pp. 20–29.

Chen, S., Yang, J., Yang, W., Wang, C., and Bärnighausen, T. (2020). *COVID-19 control in China during mass population movements at New Year*. DOI: 10.1016/S0140-6736(20)30421-9.

Cleveland, W. S. (1979). "Robust locally weighted regression and smoothing scatterplots". In: *Journal of the American Statistical Association*. DOI: 10.1080/01621459.1979.10481038.

Ding, D., Xing, J., Wang, S., Liu, K., and Hao, J. (2019). "Estimated Contributions of Emissions Controls, Meteorological Factors, Population Growth, and Changes in Baseline Mortality to Reductions in Ambient PM2.5 and PM2.5-Related Mortality in China, 2013-2017". In: *Environmental health perspectives*. DOI: 10.1289/EHP4157.

Feng, J., Yu, H., Su, X., Liu, S., Li, Y., Pan, Y., and Sun, J. H. (2016). "Chemical composition and source apportionment of PM2.5 during Chinese Spring Festival at Xinxiang, a heavily polluted city in North China: Fireworks and health risks". In: *Atmospheric Research* 182, pp. 176–188. DOI: 10.1016/j.atmosres.2016.07.028.

Gao, M., Gao, J., Zhu, B., Kumar, R., Lu, X., Song, S., Zhang, Y., Jia, B., et al. (2020). "Ozone pollution over china and india: Seasonality and sources". In: *Atmospheric Chemistry and Physics* 20.7, pp. 4399–4414. DOI: 10.5194/acp-20-4399-2020.

Gong, D. Y., Wang, W., Qian, Y., Bai, W., Guo, Y., and Mao, R. (2014). "Observed holiday aerosol reduction and temperature cooling over East Asia". In: *Journal of Geophysical Research* 119.11, pp. 6306–6324. DOI: 10.1002/2014JD021464.

Hunter, J. D. (2007). "Matplotlib: A 2D graphics environment". In: *Computing in Science and Engineering*. DOI: 10.1109/MCSE.2007.55.

James, S. L., Abate, D., Abate, K. H., Abay, S. M., Abbafati, C., Abbasi, N., Abbastabar, H., Abd-Allah, F., et al. (2018). "Global, regional, and national incidence, prevalence, and years lived with disability for 354 Diseases and Injuries for 195 countries and territories, 1990-2017: A systematic analysis for the Global Burden of Disease Study 2017". In: *The Lancet* 392.10159, pp. 1789–1858. DOI: 10.1016/S0140-6736(18)32279-7.

Jiang, Q., Sun, Y. L., Wang, Z., and Yin, Y. (2015). "Aerosol composition and sources during the Chinese Spring Festival: Fireworks, secondary aerosol, and holiday effects". In: *Atmospheric Chemistry and Physics* 15.11, pp. 6023–6034. DOI: 10.5194/acp-15-6023-2015.

Jin, X. and Holloway, T. (2015). "Spatial and temporal variability of ozone sensitivity over China observed from the Ozone Monitoring Instrument". In: *Journal of Geophysical Research* 120.14, pp. 7229–7246. DOI: 10.1002/2015JD023250.

Kong, S., Li, X., Li, L., Yin, Y., Chen, K., Yuan, L., Zhang, Y., Shan, Y., and Ji, Y. (2015). "Variation of polycyclic aromatic hydrocarbons in atmospheric PM2.5 during winter haze period around 2014 Chinese Spring Festival at Nanjing: Insights of source changes, air mass direction and firework particle injection". In: *Science of the Total Environment* 520, pp. 59–72. DOI: 10.1016/j.scitotenv.2015.03.001.

Kraemer, M. U., Yang, C. H., Gutierrez, B., Wu, C. H., Klein, B., Pigott, D. M., Plessis, L. du, Faria, N. R., et al. (2020). "The effect of human mobility and control measures on the COVID-19 epidemic in China". In: *Science* 368.6490, pp. 493–497. DOI: 10.1126/science.abb4218.

Lai, Y. and Brimblecombe, P. (2017). "Regulatory effects on particulate pollution in the early hours of Chinese New Year, 2015". In: *Environmental Monitoring and Assessment* 189.9. DOI: 10.1007/s10661-017-6167-0.

Liu, F., Page, A., Strode, S. A., Yoshida, Y., Choi, S., Zheng, B., Lamsal, L. N., Li, C., et al. (2020). "Abrupt declines in tropospheric nitrogen dioxide over China after the outbreak of COVID-19". In: *arXiv*. URL: http://arxiv.org/abs/2004.06542.

Lu, X., Hong, J., Zhang, L., Cooper, O. R., Schultz, M. G., Xu, X., Wang, T., Gao, M., et al. (2018). "Severe Surface Ozone Pollution in China: A Global Perspective". In: *Environmental Science and Technology Letters*. DOI: 10.1021/acs.estlett.8b00366.

McKinney, W. (2010). "Data Structures for Statistical Computing in Python". In: *Proceedings of the 9th Python in Science Conference*.

National Bureau of Statistics of China (2020a). *Energy production in May of 2020*. URL: http://www.stats.gov.cn/english/PressRelease/202006/t20200616%7B%5C_%7D1760489.html (visited on 04/25/2020).

– (2020b). *Energy production in the First Two Months of 2020*. URL: http://www.stats.gov.cn/english/PressRelease/202003/t20200317%7B%5C_%7D1732703.html (visited on 04/23/2020).

– (2020c). *Purchasing Managers Index for February 2020*. URL: http://www.stats.gov.cn/english/PressRelease/202003/t20200302%7B%5C_%7D1729254.html (visited on 04/23/2020).

Prescott, K. (2020). *Chinese manufacturing hits record low amid coronavirus outbreak*. URL: https://www.bbc.com/news/business-51689178.

Reddington, C. L., Conibear, L., Knote, C., Silver, B. J., Li, Y. J., Chan, C. K., Arnold, S. R., and Spracklen, D. V. (2019). "Exploring the impacts of anthropogenic emission sectors on PM2.5 and human health in South and East Asia". In: *Atmospheric Chemistry and Physics*. DOI: 10.5194/acp-19-11887-2019.

Seabold, S. and Perktold, J. (2010). "Statsmodels: Econometric and Statistical Modeling with Python". In: *PROC. OF THE 9th PYTHON IN SCIENCE CONF*.

Sen, P. K. (1968). "Estimates of the Regression Coefficient Based on Kendall's Tau". In: *Journal of the American Statistical Association* 63.324, pp. 1379–1389. DOI: 10.1080/01621459.1968.10480934.

Silver, B., Reddington, C. L., Arnold, S. R., and Spracklen, D. V. (2018). "Substantial changes in air pollution across China during 2015-2017". In: *Environmental Research Letters* 13.11. DOI: 10.1088/1748-9326/aae718.

Silver, B., Conibear, L., Reddington, C. L., Knote, C., Arnold, S. R., and Spracklen, D. V. (2020). "Pollutant emission reductions deliver decreased PM2.5-caused mortality across China during 2015-2017". In: *Atmospheric Chemistry and Physics* 20.20, pp. 11683–11695. DOI: 10.5194/acp-20-11683-2020.

Tan, P. H., Chou, C., Liang, J. Y., Chou, C. C., and Shiu, C. J. (2009). "Air pollution "holiday effect" resulting from the Chinese New Year". In: *Atmospheric Environment* 43.13, pp. 2114–2124. DOI: 10.1016/j.atmosenv.2009.01.037.

Tian, H., Liu, Y., Li, Y., Wu, C. H., Chen, B., Kraemer, M. U., Li, B., Cai, J., et al. (2020). "An investigation of transmission control measures during the first 50 days of the COVID-19 epidemic in China". In: *Science* 368.6491, pp. 638–642. DOI: 10.1126/science.abb6105.

Wang, X., Shen, Z., Tang, Z., Li, G., Lei, Y., Zhang, Q., Zeng, Y., Xu, H., et al. (2020). "Characteristics of Surface Ozone in Five Provincial Capital Cities of China during 2014–2015". In: *Atmosphere*. DOI: 10.3390/atmos11010107.

World Health Organization (WHO) (2020). *Novel Coronavirus*. Tech. rep. 6, pp. 1–19. URL: https://apps.who.int/iris/bitstream/handle/10665/330762/nCoVsitrep23Jan2020-eng.pdf.

Wu, Z. and McGoogan, J. M. (2020). "Characteristics of and Important Lessons from the Coronavirus Disease 2019 (COVID-19) Outbreak in China: Summary of a Report of 72314 Cases from the Chinese Center for Disease Control and Prevention". In: *JAMA - Journal of the American Medical Association* 323.13, pp. 1239–1242. DOI: 10.1001/jama.2020.2648.

Zhao, B., Zheng, H., Wang, S., Smith, K. R., Lu, X., Aunan, K., Gu, Y., Wang, Y., et al. (2018). "Change in household fuels dominates the decrease in PM2.5 exposure and premature mortality in China in 2005–2015". In: *Proceedings of the National Academy of Sciences of the United States of America*. DOI: 10.1073/pnas.1812955115.

Zhao, H., Ma, W., Dong, H., and Jiang, P. (2017). "Analysis of co-effects on air pollutants and CO2emissions generated by end-of-pipe measures of pollution control in China's coal-fired power plants". In: *Sustainability (Switzerland)* 9.4, p. 499. DOI: 10.3390/su9040499.

Zheng, B., Tong, D., Li, M., Liu, F., Hong, C., Geng, G., Li, H., Li, X., et al. (2018). "Trends in China's anthropogenic emissions since 2010 as the consequence of clean air actions". In: *Atmospheric Chemistry and Physics* 18.19, pp. 14095–14111. DOI: 10.5194/acp-18-14095-2018.

Zheng, Y., Xue, T., Zhang, Q., Geng, G., Tong, D., Li, X., and He, K. (2017). "Air quality improvements and health benefits from China's clean air action since 2013". In: *Environmental Research Letters* 12.11. DOI: 10.1088/1748-9326/aa8a32.

Chapter 5

Conclusions

5.1 Synthesis of results

The overall aim for this thesis was to understand the drivers of recent trends in China's air quality, and identify pathways for pollution mitigation. The first publication included (Chapter 2), was, at the time of publication, the first study to quantify the trends in air quality across China measured by the newly-released CNEMC network. This research indicated that concentrations of the pollutant which is most harmful to human health, $PM_{2.5}$, were falling rapidly across China during 2015-2017. This informed the research direction of the second included piece of published research (Chapter 3), which used the WRF-Chem model to separate the contribution of interannnual variability in meteorology with the estimated decrease in emissions to the trends observed in Chapter 2. This also included an estimate of the likely effects on excess mortality and morbidity that would result from the modelled changes in air quality, and evaluated the ability of the WRF-Chem model and MEIC emission estimated to capture observed trends. The third piece of included published work (Chapter 4) quantified the changes in air quality that occurred during the implementation of COVID-19 control measures in China. This COVID-19 lockdown provided an opportunity for a natural experiment of a similar nature to the modelled experiments conducted in Reddington et al. (2019) and Chapter 3, as emissions from particular sectors in China, were greatly reduced. It also extended the trends calculated in Chapter 2 to the period of 2015-2019, and quantified the typical effects of the Lunar New Year holiday on air pollution in China.

5.1.1 Key findings

$PM_{2.5}$ exposure is decreasing rapidly across China

My analysis of the CNEMC data shows that $PM_{2.5}$ has been decreasing rapidly in China during 2015-2019, at a rate of on average 6.0% yr^{-1} (see Figure 4.2). The trend is also widespread, with a significant negative trend was found at over two thirds of measurement stations, with each of the China's megacity regions having a median negative trend. Less than 1% of stations had a significant increasing trend over this time. The widespread decrease in $PM_{2.5}$ has been confirmed by recent satellite observations (Wei et al., 2021) and inferred from modelling studies that use the latest emission inventory estimates (Zhang et al., 2019).

The GBD estimated that air pollution as the third greatest risk factor causing death and disability in China in 2009, but by 2019 its relative burden had reduced but 3.4%, falling to the fourth greatest risk (Abbafati et al., 2020). In Chapter 3, my analysis showed that the expected premature mortality attributed to $PM_{2.5}$ fell by 150 000 deaths yr^{-1} during 2015-2017, decreasing by around 5.4%. However, we did not consider the effect of changing population size and age distributions. Although $PM_{2.5}$ is decreasing rapidly, future population changes (i.e. larger and older populations) could counteract a decrease in the absolute number of avoided premature mortalities (Wang et al., 2019b).

O_3 exposure is increasing

My analysis of the CNEMC data shows that O_3 levels have been steadily rising across much of China during 2015-2019, at an average rate of 2.8% yr^{-1} (see Figure 4.2). A statistically significant positive trend is found at a quarter of stations, while a significant negative trend is found at less than 5%. Few long-term observational records of O_3 concentrations exist in China, but measurements at background sites and satellite studies indicate that positive trends in O_3 have in China occurred since at least 2000 (Verstraeten et al., 2015).

Premature mortality that can be attributed to O_3 in 2015 was found to be 143 000, and we estimated that it could be rising by rates of up to 21 000 yr^{-1}. The CNEMC trends reported in Chapter 4 indicate O_3 has continued to rise, at a rate of 2.8% yr^{-1} during 2015-2019. Madaniyazi et al. (2016) found that O_3 concentrations would continue to increase in China up to 2030 under current legislation, and mortalities could continue to increase even under maximum feasible abatement depending on population growth. However,

even under their most pessimistic scenario, when ozone-attributed premature mortalities increase by 450 000 during 2005-2030, this remains within the same order of magnitude as $PM_{2.5}$ mortalities, indicating that controlling both pollutants should be prioritised.

Observed trends are emissions driven rather than meteorologically driven

Although the trends identified in Chapter 2 were statistically robust and widespread in China, due to lack of long data records, their relatively short length (three years) meant that the contribution of interannual meteorological variability to these trends was highly uncertain. Furthermore, in 2015 there was a strong El Niño event, that may have increased $PM_{2.5}$ concentrations across, particularly in the North China Plain region (Chang et al., 2016).

Therefore, in Chapter 3 I used two WRF-Chem simulations to compare the the air quality using MEIC emissions estimates for 2015-2017, with a counterfactual scenario had emissions remained at 2015 levels, but driven by real 2016 and 2017 meteorology. The model was able to reproduce the negative trends in $PM_{2.5}$ at a similar magnitude to the observed trends. When emissions were held at 2015 levels, the overall $PM_{2.5}$ trend was close to zero, indicating that meteorological variability could not explain the large negative trends in $PM_{2.5}$. This indicates that the El Niño in 2015 did not sufficiently perturb $PM_{2.5}$ concentrations to induce the observed trends (see Figure B.2a).

However, the model underestimated the magnitude of the observed O_3 trend by a factor of 2 (2.7 $\mu g\, m^{-3}\, yr^{-1}$ was observed, 1.3 $\mu g\, m^{-3}\, yr^{-1}$ was simulated). This could be because the resolution of the model was too low to capture the high NO_x environments present in urban centres, and therefore underestimated the effect of NO_x titration of O_3. Additionally, due to unavailability of updated emission inventories, the emissions changes reported by Zheng et al. (2018) were applied uniformly across the domain, while observed NO_2 trends were more spatially heterogenous during 2015-2017 (see Chapter 2). A more accurate representation of NO_2 emissions trends and well as other species may have improved the models ability to capture the O_3 trend.

The implications of the modest improvements in air quality during COVID-19 lockdown

In the early days of the coronavirus outbreak in China during 2020, headlines claimed a large improvement in air quality had resulted (e.g. Weizhen Tan (2020)). However, I

conducted a more careful analysis of the CNEMC data that accounted for 2015-2019 trends and the effect of the Lunar New Year holiday, and quantified its typical impact. I found that NO_2 decreases had been substantial, dropping to less than half of their expected weekly mean concentrations by mid-February, and an average of 27.0% lower during the entire lockdown period. However there was an increase in weekly mean O_3 levels, which were 10-40% higher than expected across different regions of China three weeks after the initial lockdown. After this, they returned to expected levels for the remainder of lockdown.

The effect on $PM_{2.5}$ concentrations was overall modest, on average 10.5% lower during the lockdown period. However in northern China, $PM_{2.5}$ levels were unexpectedly high in the weeks preceding the lockdown. This could have been due to the meteorological situation prevailing at that time in northern China, which my analysis did not account for. Leung et al. (2020) find that the reduction in NO_2 emissions during the lockdown may have increased the atmospheric oxidising capacity, leading to greater secondary PM formation.

Positive health impacts of the COVID-19 lockdown due to improvement in air quality were likely modest, due to the $PM_{2.5}$ concentrations being on average 90% of their usual levels. Furthermore, air quality changes were relatively short-term, with pollutant concentrations returning to expected levels less that 3 months after the initial lockdown (Figure 4.3). For this reason, the avoided mortality attributed to the improvement in air quality during lockdown measures is relatively small, with Chen et al. (2020) estimating that across China 8911 NO_2-related and 3214 $PM_{2.5}$-related deaths were avoided.

A subsequent analysis by Zheng et al. (2020) used satellite data and bottom up emissions analyses to confirm that emissions from transport and industry sectors were most reduced by the COVID-19 lockdown, while residential and power sector were much less impacted. This result aligns with $PM_{2.5}$ source attribution work such as Reddington et al. (2019) and Liu et al. (2016) who find that, especially in winter, the residential sector is a large contributor to $PM_{2.5}$ concentrations. Therefore, only minor reductions in $PM_{2.5}$ would be expected as a result of substantially reducing transport emissions.

Table 5.1: Comparison of the three-year trends estimated in Chapter 2 and five-year trends estimated in Chapter 4

	Median trend ($\mu g\,m^{-3}\,yr^{-1}$)	
	Chapter 2 (2015-2017)	Chapter 4 (2015-2019)
$PM_{2.5}$	−3.4	−3.0
O_3MDA8	4.6	1.6
NO_2	0.0	−0.7
SO_2	−1.9	−2.6

5.2 Discussion of uncertainties

5.2.1 Uncertainties in trend estimates

The three-year trends first estimated in Chapter 2 are calculated using only three years of monitoring data. This is due to monitoring data prior to 2015 being unavailable from (`http://beijingair.sinaapp.com/`), despite the CNEMC network being established in 2012. Measured air pollutant trends can never completely reflect the underlying trends in emissions due to the meteorological dependencies of air pollutant concentrations in the atmosphere, meaning that measured trends are sensitive to inter-annual variability in meteorological conditions. For this reason, measurement trends are typically reported for longer periods (a decade or more), so that inter-annual variability can be 'averaged out.'

In Chapter 4, the trends are re-calculated using an additional two years of data. A comparison of the trend estimates are shown in Table 5.1. Except for NO_2, which had no median trend in Chapter 2, the direction of the trends estimated between the two periods is consistent. However, the large difference between the trends (e.g. O_3 changes from 4.6 to 1.6 $\mu g\,m^{-3}\,yr^{-1}$) highlights how changing the sample period can affect the trend. The NO_2 trend becomes overall negative up to 2019, with the proportion of stations recording a significant positive trend decreasing from 54 to 13%. This could indicate that while the widespread decrease in NO_x that has been observed since 2012 slowed during 2015-2017, as shown in (Hou et al., 2019), and that the decrease has continued in subsequent years.

5.2.2 Model uncertainties and limitations

While the WRF-Chem simulations performed in Chapter 3 were an attempt to resolve some of the questions raised by Chapter 2, the modelling came with its own set of uncertainties. One key source of uncertainty in chemical transport models is the anthropogenic emission inventory. Uncertainties in China's emissions, expressed as 95% confidence in-

tervals are estimated to range from as low as $\pm 12\%$ for SO_2 to $\pm 271\%$ for organic carbon (Li et al., 2017). These large uncertainty ranges are due to high uncertainties in the underlying emission factor and activity rate data.

As well as the inherent uncertainty in MEIC, additional uncertainty is added by the uniform scaling factors that were applied for each pollutant and each sector across the domain. This was due to lack of access to updated versions of MEIC. Therefore, any spatial heterogeneity in emission change estimates have been lost. This will contribute to the model's inability to accurately capture the spatial pattern in trends, particularly the O_3 trend. For example, the O_3 production regime varies across China from NO_x-limited to VOC limited. The NO_2 trend results from Chapter 2 suggest that trends in NO_x vary across China during 2015-2017. However, due to the uniform scaling applied to the inventory, all regions were simulated with a modest decrease in NO_x emissions. Therefore, any increase in O_3 that is driven by a reduction in NO_x in a VOC-limited regime could be underestimated.

Furthermore, necessary simplifications within the WRF-Chem model such as lumped VOC chemistry and physical parametrisations induce further uncertainty. An example of this is boundary layer schemes, which are parametrisations of turbulent processes such as vertical heat and moisture that occur within the planetary boundary layer (PBL) (Nielsen-Gammon et al., 2010). There are several different PBL parametrisations available in WRF-Chem, and they have each been shown to have varying accuracy under various conditions (e.g. topography, wind speeds), with a recent evaluation finding wind speed and direction biases of up to 50-300% (Zhang et al., 2021). However, due to limitations of time and computing resources, a thorough evaluation of the effect PBL-scheme choice on the accuracy of the physical simulation was not possible. Therefore, we used a previous model setup which had been shown to simulate important chemical species such as $PM_{2.5}$ well in previous work (Conibear et al., 2018; Reddington et al., 2019), which was nudged above the boundary layer to prevent drift. Given more resources, it would be useful to evaluate the different PBL-schemes against a network of ground-level meteorological data.

5.3 Future research directions

Figure 3.4 indicates that although trends are primarily emissions driven, inter-annual variability in meteorology can still have large regional impact on year-to-year air quality vari-

ability. 5-years of model simulations by Wang et al. (2020b) with fixed emissions during 2013-2017 found anomalies of up to 20% in provincial mean yearly $PM_{2.5}$ concentrations. This suggests that air quality in China is likely to be substantially affected by changing climate patterns, which should be further investigated. The modelled effects of meteorology on secondary $PM_{2.5}$ formation remain highly uncertain and relatively less well understood (Tai et al., 2010; Wang et al., 2019a). Additionally, the large decrease in aerosol loading over China will change the magnitude and nature of aerosol-climate interactions (Liu et al., 2019). Recent studies suggest that reducing $PM_{2.5}$ concentrations could be reponsible for increased O_3 concentrations. However, the cause of any such effect could have various mechanisms, including a decrease in mixing layer depth suppression by aerosol, decrease in heterogeneous uptake of HO_2, or increase in photolysis.

Modelling the meteorological dependencies of air pollution using CNEMC data

Accounting for the effects of meteorology on air pollutant trends using a model such as WRF-Chem (i.e. Chapter 3) proved a computationally complex and uncertain process. Recent studies, e.g. Grange et al. (2018) have shown the use of machine learning models for assessing the impact of air pollution control interventions while accounting for meteorological conditions. Using this technique with CNEMC data, along with meteorological reanalysis data could be a useful alternative method for assessing the impact of meteorology on air pollutant trends in China. Additionally, this could be useful for extracting statistical relationships between air pollutant concentrations and parameters such as wind speed, and temperature, which could prove useful for forecasting how China's changing climate will impact air quality.

Understanding the drivers of the O_3 trend

Multiple recent studies, including Wang et al. (2020a), Zhao et al. (2020), and Zhao et al. (2021) as well as my work has highlighted the contrasting trends of $PM_{2.5}$ and O_3. However, it remains unclear as to what extent decreases in aerosol loading might be contributing to the rise in O_3 formation, through either chemical or physical effects, versus the effect of changing emissions. As discussed in Chapter 1.2.4, atmospheric aerosols can increase boundary layer stability, humidity and light extinction. Therefore, a reduction in aerosol loading could create more favourable conditions for O_3 formation, the rate of which increases under higher radiation and lower humidity conditions (Kavassalis and Murphy,

2017). However, the contrasting trends could also be explained by changes in emissions on the concentrations of O_3. For example, a decrease in NO_x emissions might lead to a decrease in $PM_{2.5}$ concentrations as less nitrate precursors are available for secondary PM formation. However, the same NO_x emissions decrease could cause O_3 concentrations to increase in NO_x-saturated urban areas, through a reduction of O_3 titration by NO_x.

Aerosols also interact with the photochemical reactions involved in O_3 formation via heterogeneous chemical reactions. Aerosols can irreversibly absorb NO_3, NO_2 and HO_2, and hydrolyse N_2O_5 (Liao and Seinfeld, 2005). Lou et al. (2014) show that these interactions have mixed effects on O_3 formation rates, but their simulation showed that overall in China, they led to a decrease in O_3. Li et al. (2019) used the GEOS-Chem model to apportion the rising O_3 trend during 2013-2017 between changes in emissions, photolysis and heterogeneous reactions, and found that the reduction in HO_2 uptake due to reduced aerosol concentration was the main driver of the positive O_3 trend. Liu and Wang (2020) using WRF-CMAQ paint a more complex picture, showing that decreases in NO_x emissions increase O_3 in urban areas but decrease it in rural, decrease in SO_2 emissions enhance O_3 formation via increase in photolysis and decrease in heterogeneous uptake. However they find that the importance of these effects vary between different regions in China. They conclude that large reductions in VOC emissions, 16-24% would be necessary to avoid the O_3 increase that results from other emissions changes.

However, both studies will be sensitive to the assumptions made in the gaseous and aerosol chemical schemes used in their models. For example, GEOS-Chem assumes a constant HO_2 uptake rate for all aerosol types, that is based on a limited number of laboratory studies. The results of these studies should be repeated using fully-coupled models that have more detailed aerosol heterogeneous chemistry so that the sensitivity of their conclusions to assumptions made about aerosol uptake rates can be more comprehensively evaluated.

References

Abbafati, C., Abbas, K. M., Abbasi-Kangevari, M., Abd-Allah, F., Abdelalim, A., Abdollahi, M., Abdollahpour, I., Abegaz, K. H., et al. (2020). "Global burden of 87 risk factors in 204 countries and territories, 1990–2019: a systematic analysis for the Global Burden of Disease Study 2019". In: *The Lancet* 396.10258, pp. 1223–1249. DOI: 10.1016/S0140-6736(20)30752-2.

Chang, L., Xu, J., Tie, X., and Wu, J. (2016). "Impact of the 2015 El Nino event on winter air quality in China". In: *Scientific Reports* 6.1, pp. 1–6. DOI: 10.1038/srep34275.

Chen, K., Wang, M., Huang, C., Kinney, P. L., and Anastas, P. T. (2020). "Air pollution reduction and mortality benefit during the COVID-19 outbreak in China". In: *The Lancet Planetary Health* 4.6, e210–e212. DOI: 10.1016/S2542-5196(20)30107-8.

Conibear, L., Butt, E. W., Knote, C., Arnold, S. R., and Spracklen, D. V. (2018). "Residential energy use emissions dominate health impacts from exposure to ambient particulate matter in India". In: *Nature Communications*. DOI: 10.1038/s41467-018-02986-7.

Grange, S. K., Carslaw, D. C., Lewis, A. C., Boleti, E., and Hueglin, C. (2018). "Random forest meteorological normalisation models for Swiss PM10 trend analysis". In: *Atmospheric Chemistry and Physics* 18.9, pp. 6223–6239. DOI: 10.5194/acp-18-6223-2018.

Hou, Y., Wang, L., Zhou, Y., Wang, S., Liu, W., and Zhu, J. (2019). "Analysis of the tropospheric column nitrogen dioxide over China based on satellite observations during 2008–2017". In: *Atmospheric Pollution Research* 10.2, pp. 651–655. DOI: 10.1016/j.apr.2018.11.003.

Kavassalis, S. C. and Murphy, J. G. (2017). "Understanding ozone-meteorology correlations: A role for dry deposition". In: *Geophysical Research Letters*. DOI: 10.1002/2016GL071791.

Leung, D. M., Shi, H., Zhao, B., Wang, J., Ding, E. M., Gu, Y., Zheng, H., Chen, G., et al. (2020). "Wintertime Particulate Matter Decrease Buffered by Unfavorable Chemical Processes Despite Emissions Reductions in China". In: *Geophysical Research Letters* 47.14, e2020GL087721. DOI: 10.1029/2020GL087721.

Li, K., Jacob, D. J., Liao, H., Shen, L., Zhang, Q., and Bates, K. H. (2019). "Anthropogenic drivers of 2013–2017 trends in summer surface ozone in China". In: *Proceedings of the National Academy of Sciences of the United States of America*. DOI: 10.1073/pnas.1812168116.

Li, M., Liu, H., Geng, G., Hong, C., Liu, F., Song, Y., Tong, D., Zheng, B., et al. (2017). "Anthropogenic emission inventories in China: A review". In: *National Science Review* 4.6, pp. 834–866. DOI: 10.1093/nsr/nwx150.

Liao, H. and Seinfeld, J. H. (2005). "Global impacts of gas-phase chemistry-aerosol interactions on direct radiative forcing by anthropogenic aerosols and ozone". In: *Journal of Geophysical Research D: Atmospheres* 110.18, pp. 1–22. DOI: 10.1029/2005JD005907.

Liu, J., Mauzerall, D. L., Chen, Q., Zhang, Q., Song, Y., Peng, W., Klimont, Z., Qiu, X., et al. (2016). "Air pollutant emissions from Chinese households: A major and underappreciated ambient pollution source". In: *Proceedings of the National Academy of Sciences* 113.28, pp. 7756–7761. DOI: 10.1073/pnas.1604537113.

Liu, S., Xing, J., Zhao, B., Wang, J., Wang, S., Zhang, X., and Ding, A. (2019). "Understanding of Aerosol–Climate Interactions in China: Aerosol Impacts on Solar Radiation, Temperature, Cloud, and Precipitation and Its Changes Under Future Climate and Emission Scenarios". In: *Current Pollution Reports* 5.2, pp. 36–51. DOI: 10.1007/s40726-019-00107-6.

Liu, Y. and Wang, T. (2020). "Worsening urban ozone pollution in China from 2013 to 2017 - Part 2: The effects of emission changes and implications for multi-pollutant control". In: *Atmospheric Chemistry and Physics* 20.11, pp. 6323–6337. DOI: 10.5194/acp-20-6323-2020.

Lou, S., Liao, H., and Zhu, B. (2014). "Impacts of aerosols on surface-layer ozone concentrations in China through heterogeneous reactions and changes in photolysis rates". In: *Atmospheric Environment* 85, pp. 123–138. DOI: 10.1016/j.atmosenv.2013.12.004.

Madaniyazi, L., Nagashima, T., Guo, Y., Pan, X., and Tong, S. (2016). "Projecting ozone-related mortality in East China". In: *Environment International* 92-93, pp. 165–172. DOI: 10.1016/j.envint.2016.03.040.

Nielsen-Gammon, J. W., Hu, X. M., Zhang, F., and Pleim, J. E. (2010). "Evaluation of planetary boundary layer scheme sensitivities for the purpose of parameter estimation". In: *Monthly Weather Review* 138.9, pp. 3400–3417. DOI: 10.1175/2010MWR3292.1.

Reddington, C. L., Conibear, L., Knote, C., Silver, B. J., Li, Y. J., Chan, C. K., Arnold, S. R., and Spracklen, D. V. (2019). "Exploring the impacts of anthropogenic emission sectors on PM2.5 and human health in South and East Asia". In: *Atmospheric Chemistry and Physics*. DOI: 10.5194/acp-19-11887-2019.

Tai, A. P., Mickley, L. J., and Jacob, D. J. (2010). "Correlations between fine particulate matter (PM2.5) and meteorological variables in the United States: Implications for the sensitivity of PM2.5 to climate change". In: *Atmospheric Environment* 44.32, pp. 3976–3984. DOI: 10.1016/j.atmosenv.2010.06.060.

Verstraeten, W. W., Neu, J. L., Williams, J. E., Bowman, K. W., Worden, J. R., and Boersma, K. F. (2015). "Rapid increases in tropospheric ozone production and export from China". In: *Nature Geoscience* 8.9, pp. 690–695. DOI: 10.1038/ngeo2493.

Wang, P., Guo, H., Hu, J., Kota, S. H., Ying, Q., and Zhang, H. (2019a). "Responses of PM 2.5 and O 3 concentrations to changes of meteorology and emissions in China". In: *Science of the Total Environment* 662, pp. 297–306. DOI: 10.1016/j.scitotenv.2019.01.227.

Wang, Q., Wang, J., Zhou, J., Ban, J., and Li, T. (2019b). "Estimation of PM 2·5 -associated disease burden in China in 2020 and 2030 using population and air quality scenarios: a modelling study". In: *The Lancet Planetary Health* 3.2, e71–e80. DOI: 10.1016/S2542-5196(18)30277-8.

Wang, Y., Gao, W., Wang, S., Song, T., Gong, Z., Ji, D., Wang, L., Liu, Z., et al. (2020a). "Contrasting trends of PM2.5 and surface-ozone concentrations in China from 2013 to 2017". In: *National Science Review* 7.8, pp. 1331–1339. DOI: 10.1093/nsr/nwaa032.

Wang, Y., Wild, O., Chen, H., Gao, M., Wu, Q., Qi, Y., Chen, X., and Wang, Z. (2020b). "Acute and chronic health impacts of PM2.5 in China and the influence of interannual meteorological variability". In: *Atmospheric Environment*. DOI: 10.1016/j.atmosenv.2020.117397.

Wei, J., Li, Z., Sun, L., Xue, W., Ma, Z., Liu, L., Fan, T., and Cribb, M. (2021). "Extending the EOS Long-Term PM2.5 Data Records Since 2013 in China: Application to the VIIRS Deep Blue Aerosol Products". In: *IEEE Transactions on Geoscience and Remote Sensing*. DOI: 10.1109/TGRS.2021.3050999.

Weizhen Tan (2020). *Coronavirus: China's air pollution levels, smog show hit to the economy*. URL: https://www.cnbc.com/2020/02/24/coronavirus-chinas-air-pollution-levels-smog-show-hit-to-the-economy.html (visited on 05/26/2021).

Zhang, L., Xin, J., Yin, Y., Chang, W., Xue, M., Jia, D., and Ma, Y. (2021). "Understanding the major impact of planetary boundary layer schemes on simulation of vertical wind structure". In: *Atmosphere* 12.6, p. 777. DOI: 10.3390/atmos12060777.

Zhang, Q., Zheng, Y., Tong, D., Shao, M., Wang, S., Zhang, Y., Xu, X., Wang, J., et al. (2019). "Drivers of improved PM2.5 air quality in China from 2013 to 2017". In: *Proceedings of the National Academy of Sciences of the United States of America* 116.49, pp. 24463–24469. DOI: 10.1073/pnas.1907956116.

Zhao, H., Chen, K., Liu, Z., Zhang, Y., Shao, T., and Zhang, H. (2021). "Coordinated control of PM2.5 and O3 is urgently needed in China after implementation of the "Air pollution prevention and control action plan"". In: *Chemosphere* 270, p. 129441. DOI: 10.1016/j.chemosphere.2020.129441.

Zhao, S., Yin, D., Yu, Y., Kang, S., Qin, D., and Dong, L. (2020). "PM2.5 and O3 pollution during 2015–2019 over 367 Chinese cities: Spatiotemporal variations, meteorological and topographical impacts". In: *Environmental Pollution* 264, p. 114694. DOI: 10.1016/j.envpol.2020.114694.

Zheng, B., Geng, G., Ciais, P., Davis, S. J., Martin, R. V., Meng, J., Wu, N., Chevallier, F., et al. (2020). "Satellite-based estimates of decline and rebound in China's CO2 emissions during COVID-19 pandemic". In: *Science Advances* 6.49, eabd4998. DOI: 10.1126/sciadv.abd4998.

Zheng, B., Tong, D., Li, M., Liu, F., Hong, C., Geng, G., Li, H., Li, X., et al. (2018). "Trends in China's anthropogenic emissions since 2010 as the consequence of clean air actions". In: *Atmospheric Chemistry and Physics* 18.19, pp. 14095–14111. DOI: 10.5194/acp-18-14095-2018.

Appendix A

Supplementary material for Chapter 2

Table A.1: Coefficient of variation threshold and rolling window span for each pollutant. Flagging anomalous data used a simple method that looked for low variation in daily means within a rolling window. First, data was resampled to give daily means. Then, within each window, the coefficient of variation (standard deviation/mean) is calculated. If the coefficient of variation is less than a threshold value, the period is flagged. The threshold and rolling window span were adjusted for each pollutant by manually checking the data verify that the correct periods were flagged.

Pollutant	Coefficient of variation threshold	Rolling window span (days)
NO_2	0.04	10
SO_2	0.04	14
O_3	0.05	12
$PM_{2.5}$	0.03	4

Table A.2: Sensitivity of calculated mean trends to the threshold value used for removal of flagged plots. Absolute trends are shown for different thresholds of flagged days.

Flagged days removal threshold	60 (as used in paper)	1000 (no sites removed)	30 (stricter)	10 (very strict)
Total stations removed (sum of all species)	74	0	308	926
$PM_{2.5}$ absolute trend ($\mu g\,m^{-3}\,yr^{-1}$)	−3.4	−3.4	−3.5	−4.1
O_3 MD8A absolute trend ($\mu g\,m^{-3}\,yr^{-1}$)	4.6	4.6	4.5	4.5
NO_2 absolute trend ($\mu g\,m^{-3}\,yr^{-1}$)	0	0	0	0
SO_2 absolute trend ($\mu g\,m^{-3}\,yr^{-1}$)	−1.9	−1.9	−1.9	−2.0

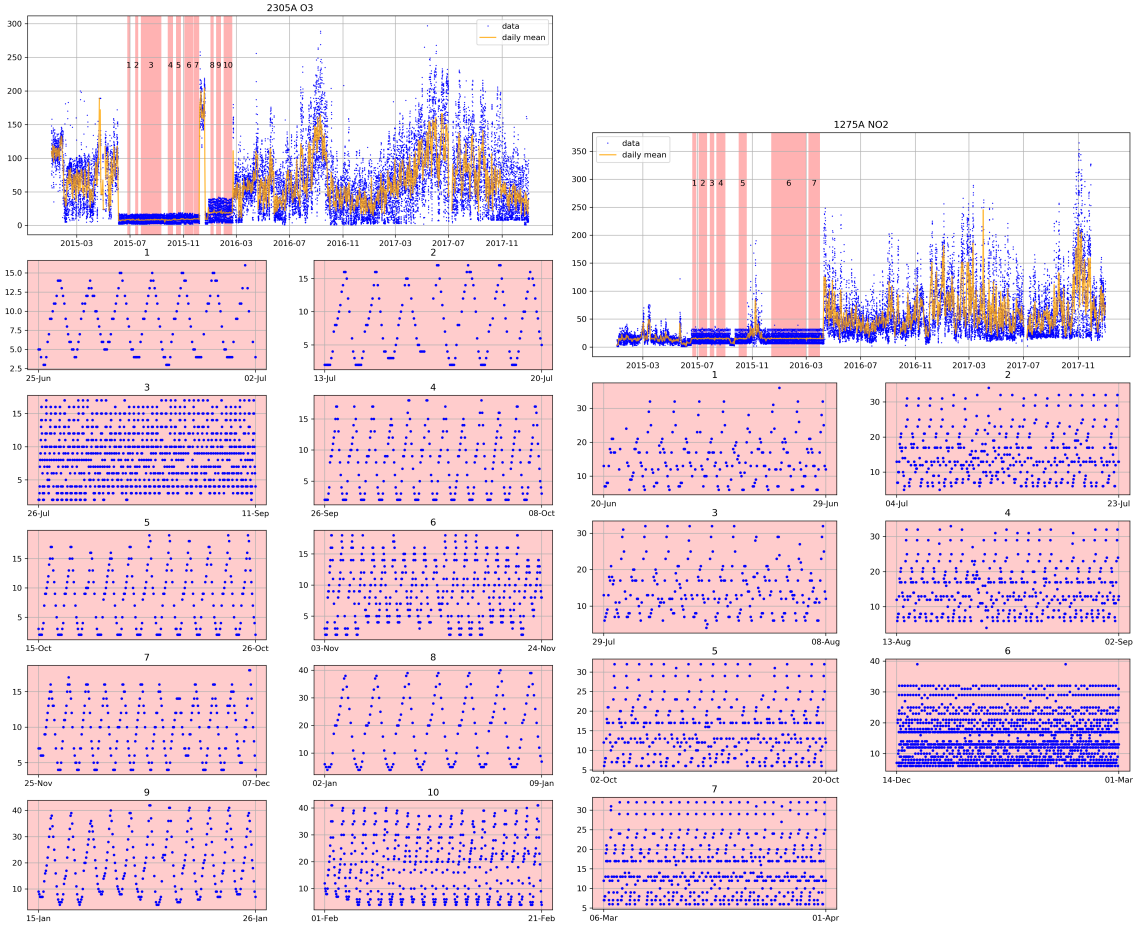

Figure A.1: Example of the anomalies found when cleaning data, and output of algorithm used to identify anomalies. The algorithm identifies anomalous periods of data where there is low variation in the coefficient of variation across a period of days (details in Supplementary Table 1). The periods with anomalous data are highlighted in red, and labelled with a number, which corresponds to the zoomed-in view of that period below. The left hand group of plots (a) shows an example for O_3, and the right hand plots (b) show an example for NO_2 data. The y axes of all plots show the concentration in $\mu g\,m^{-3}$, and the x axes show the date.

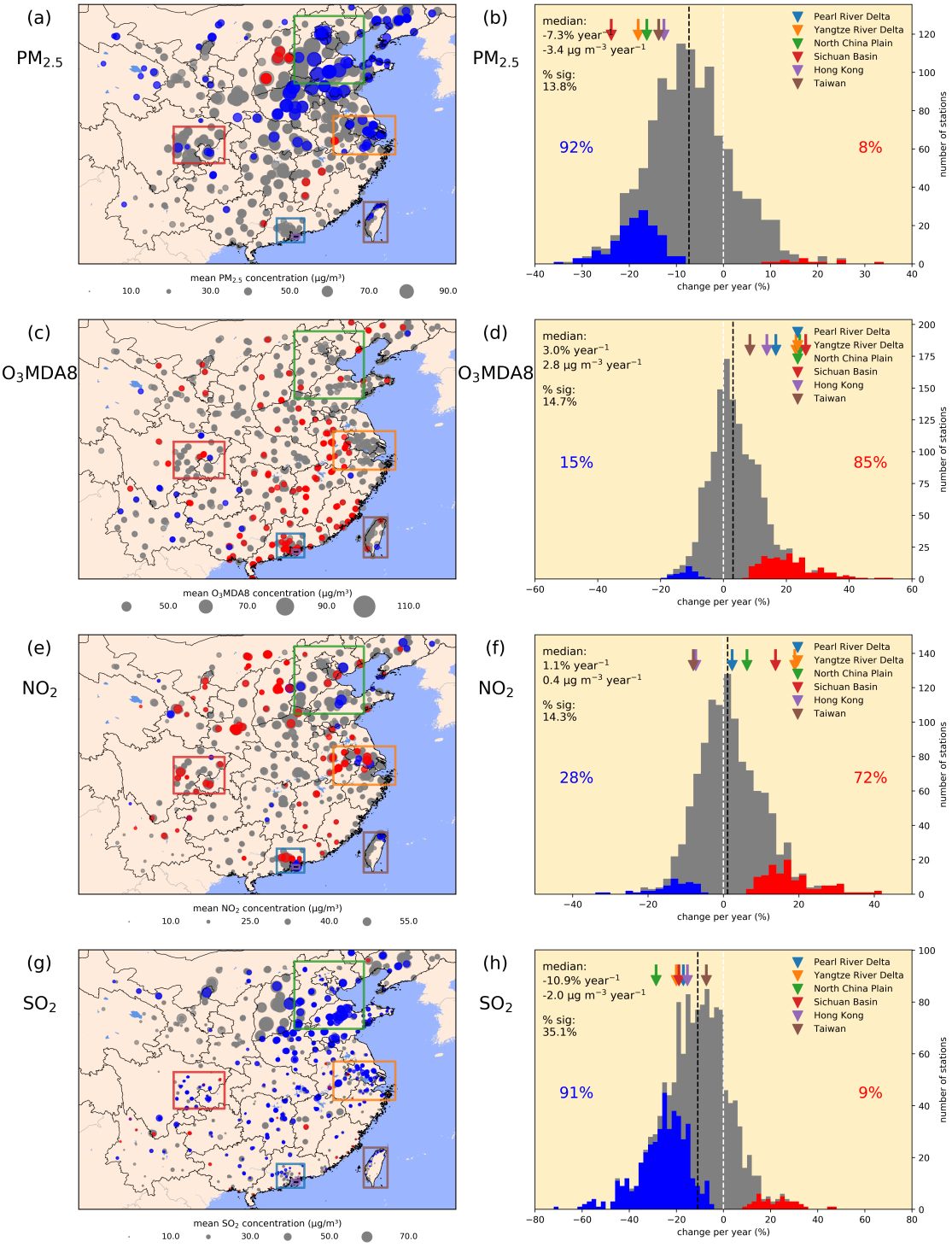

Figure A.2: The same as Figure 2.2 but trends are calculate using data that has not been deseasonalised

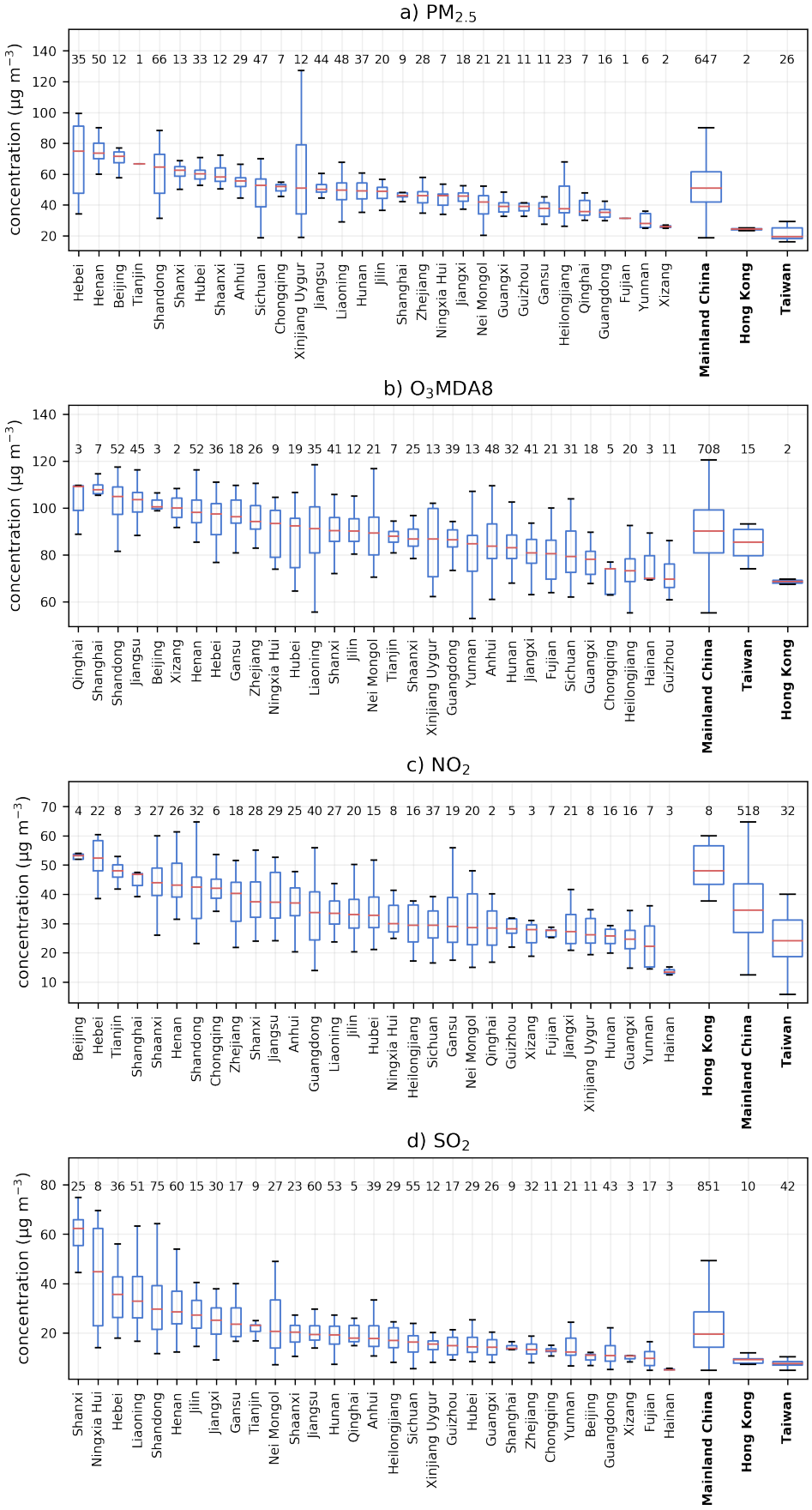

Figure A.3: Three year (2015-2017) mean concentrations of (a) $PM_{2.5}$, (b) O_3 MDA8, (c) NO_2 and (d) SO_2 by province or region. The median (red line), interquartile range (IQR) (box) and IQR $\pm$IQR*1.5 (whiskers) of the trend across the stations in each province/region are shown. The number of stations in each province/region are indicated at the top of the plot.

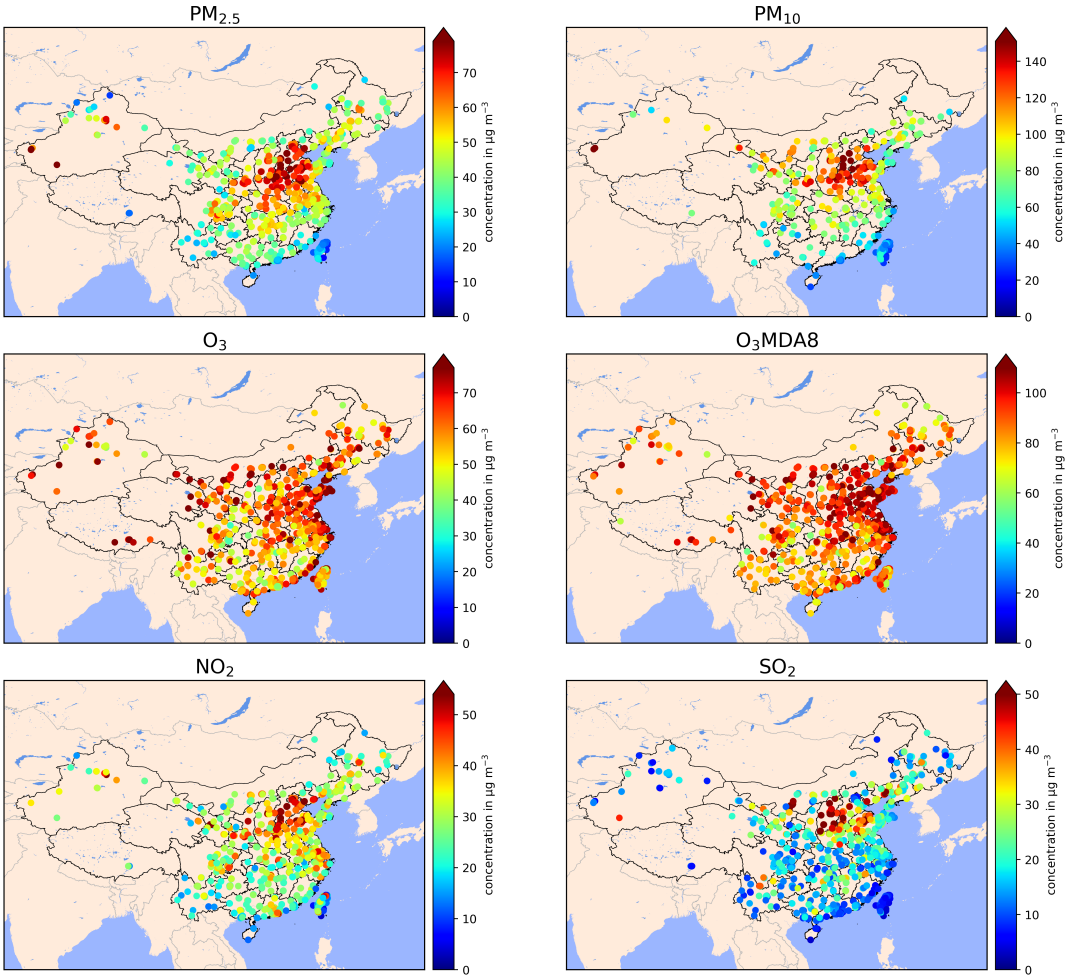

Figure A.4: Mean concentration of $PM_{2.5}$, PM_{10}, O_3, O_3 MDA8, NO_2 and SO_2 over the period 2015 to 2017.

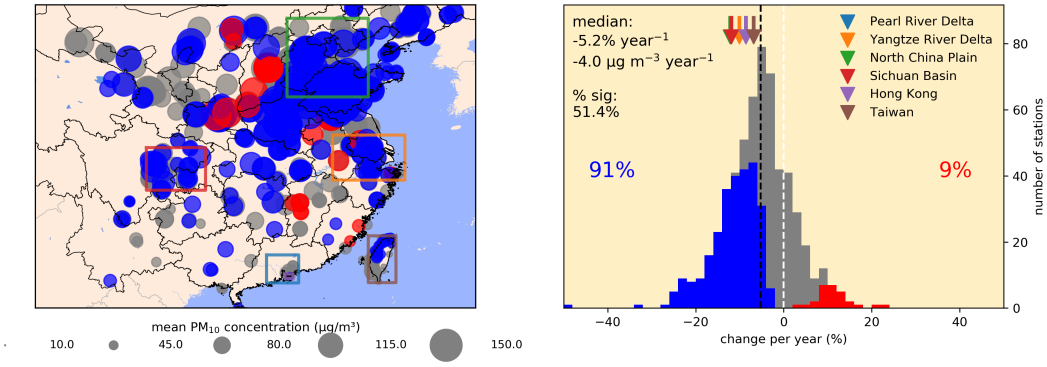

Figure A.5: The same as Figure 2.2 but showing trends in PM_{10}

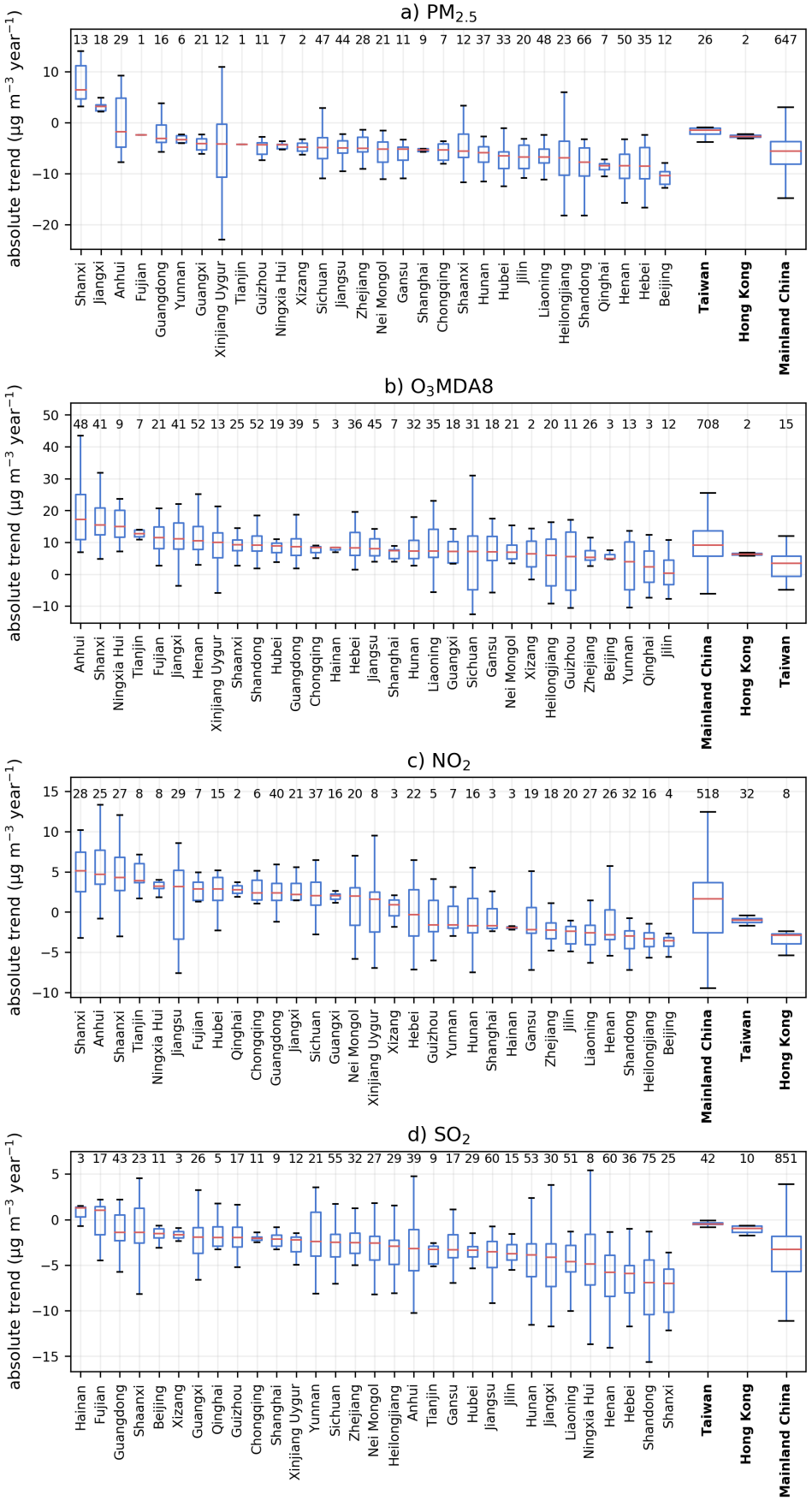

Figure A.6: The same as Figure 2.3 but showing absolute trends in $\mu g\,m^{-3}$

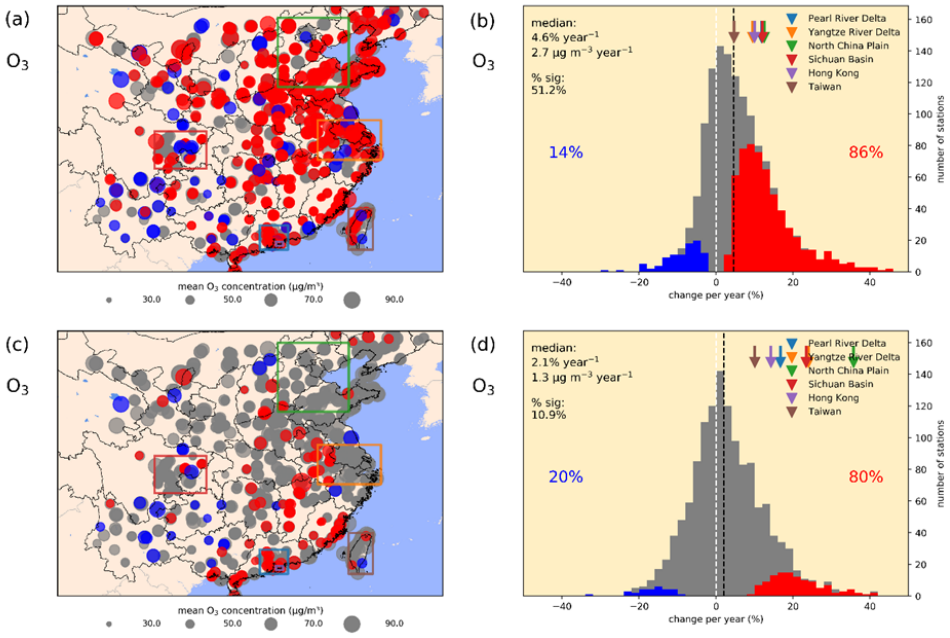

Figure A.7: Trends in (a,b) deseasonalised and (c,d) non-deseasonalised O_3 concentrations across Mainland China, Hong Kong and Taiwan during 2015 to 2017. Left hand panel shows the sign of trend (blue: significant negative, red: significant positive, grey: insignificant) and mean concentration during 2015 to 2017 (size of circle). Right hand panel shows the frequency of stations against the relative trends per year. The median relative and absolute trend as well as the percentage of stations with significant trends is shown on each panel. The percentage of significant trends that are negative (blue) or positive (red) are also shown. The black dotted line shows the median trend across all sites. Triangles show the median trend for the regional domains shown in the left-hand panels: Pearl River Delta (PRD), Yangtze River Delta (YRD), North China Plain (NCP), Sichuan Basin (SCB), Hong Kong Special Administrative Region (HK) and Taiwan (TW). The left panel is zoomed to show the trends over the more populous regions of China, while median trends and % of significant sites on the right panel refers to Mainland China, Hong Kong and Taiwan.

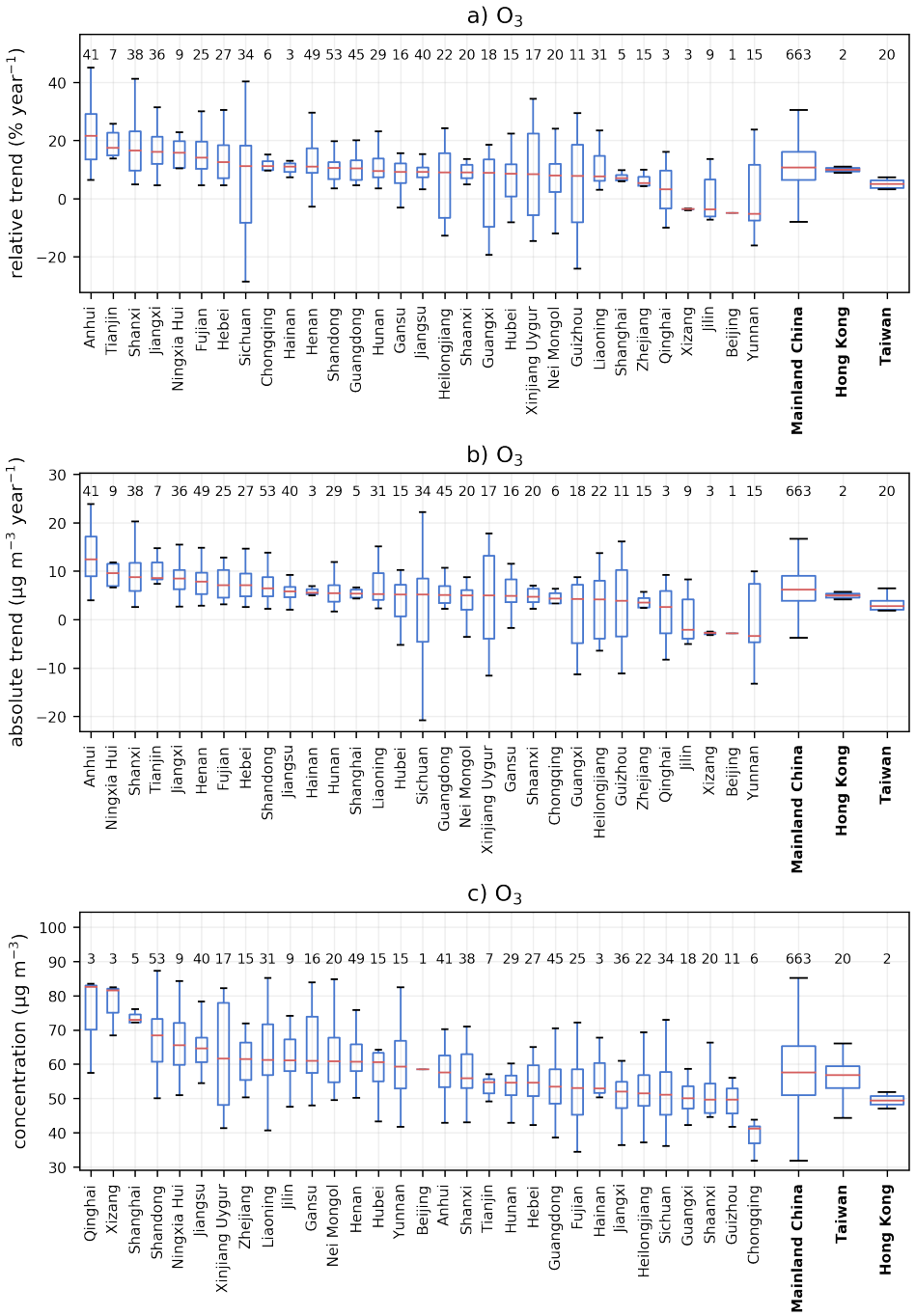

Figure A.8: Annual mean O_3 by province or region. (a) Relative trends (b) absolute trends (c) three year (2015-2017) mean concentrations. The median (red line), interquartile range (IQR) (box) and IQR $\pm$ IQR*1.5 (whiskers) of the trend across the stations in each province/region is shown. The number of stations in each province/region is indicated at the top of the panels

Appendix B

Supplementary material for Chapter 3

Table B.1: Comparison of normalised mean bias (NMB) evaluation statistics from studies simulating the air quality in China using the WRF-Chem model (excludes studies that assimilate chemical data).

Source	$PM_{2.5}$	PM_{10}	O_3	NO_2	SO_2	CO
Zhang et al. (2016) (Hong Kong)		-0.47 to -0.07	0.88 to 1.6	-0.88 to -0.83	-0.84 to -0.59	-0.72 to -0.55
Zhang et al. (2016) (China)		-0.38 to -0.03			-0.8 to -0.72	
(Wang et al., 2016) (N China, January)	0.28 to 0.47	0.00 to 0.08		0.09 to 0.27	0.33 to 0.91	0.01 to 0.12
Zhou et al. (2017) (forecast)		-0.36		-0.05	-0.18	-0.4
This paper	0.49	-0.09	-0.15	1.2	0.09	-0.35

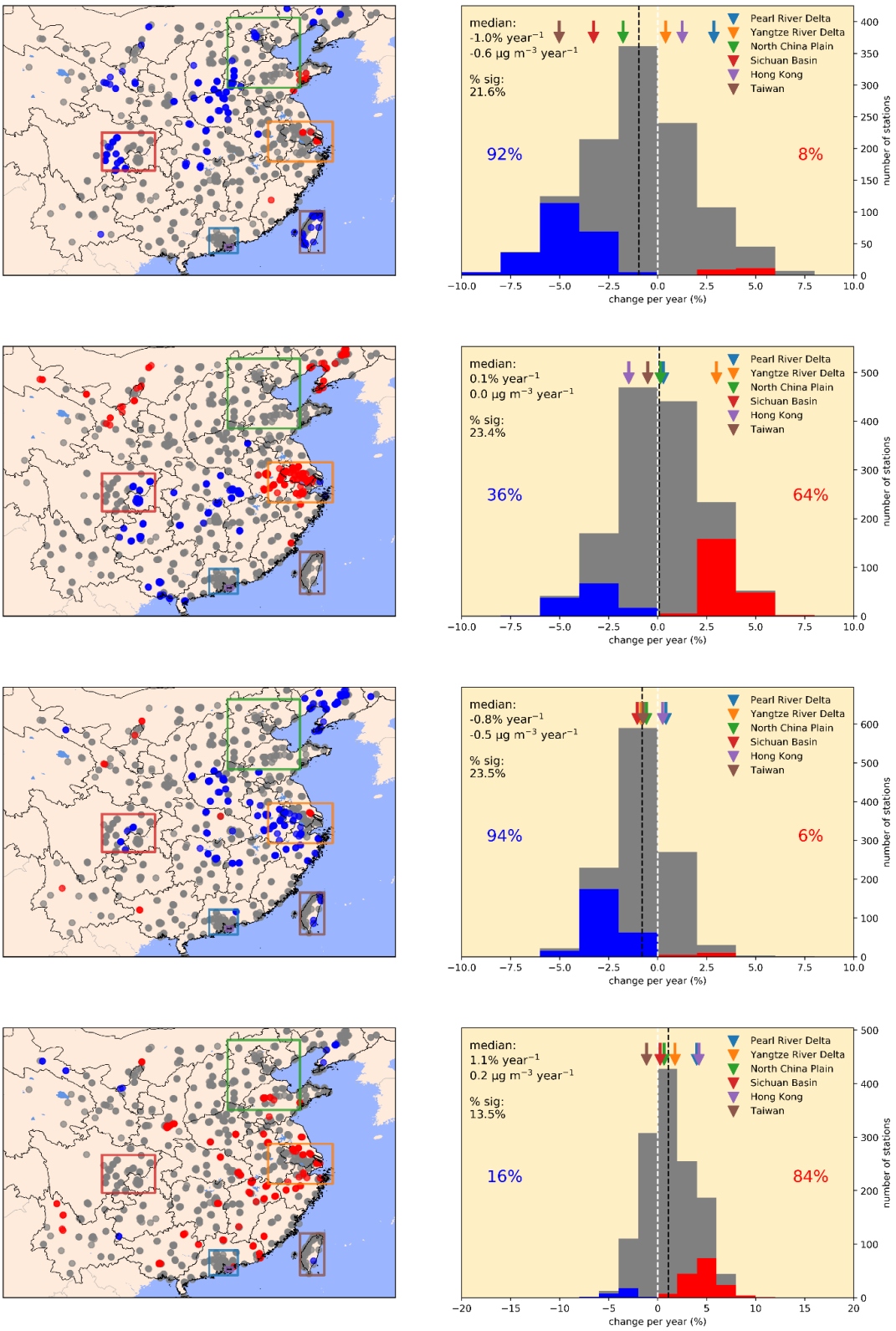

Figure B.1: Maps and histograms showing the frequency distribution of trends in concentrations of (a,b) $PM_{2.5}$, (c,d) O_3 MDA8, (e,f) NO_2, (g,h) SO_2 across China and Taiwan during 2015–2017 using the model data from the fixed emissions run, sampled at the locations of stations in the measurement dataset. The median relative and absolute trend as well as the percentage of stations with significant trends is shown on each panel. The percentage of significant trends that are negative (blue) or positive (red) are also shown. The black dotted line shows the median trend across all sites, while the white dotted line shows zero. Arrows show the median trend for the regional domain: Pearl River Delta (PRD), Yangtze River Delta (YRD), North China Plain (NCP), Sichuan Basin (SCB), Hong Kong (HK), Taiwan (TW) and the Fenwei Plain (FWP)

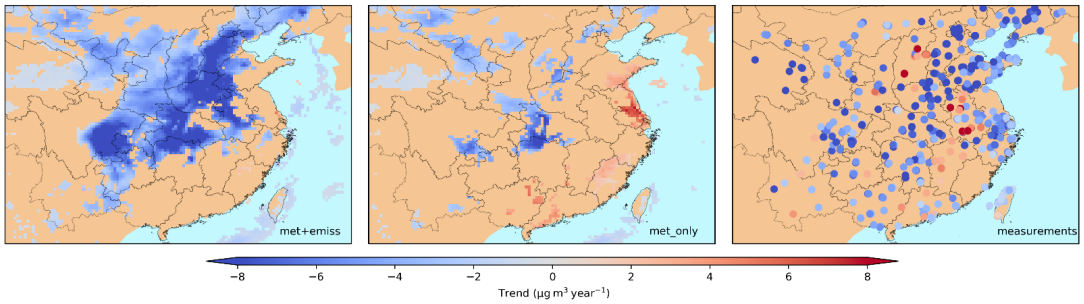

(a) $PM_{2.5}$

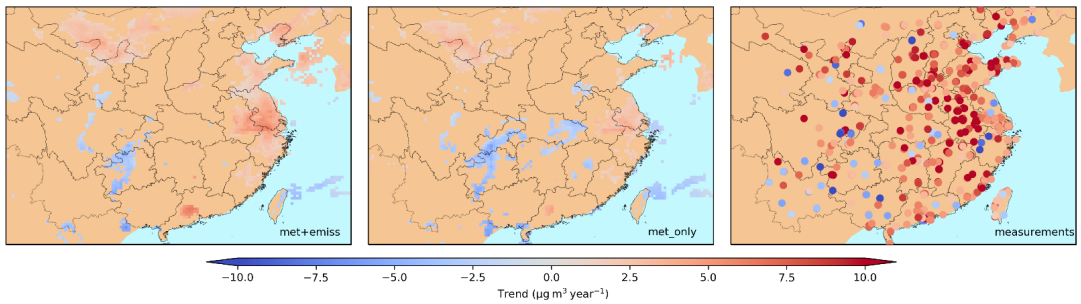

(b) O_3

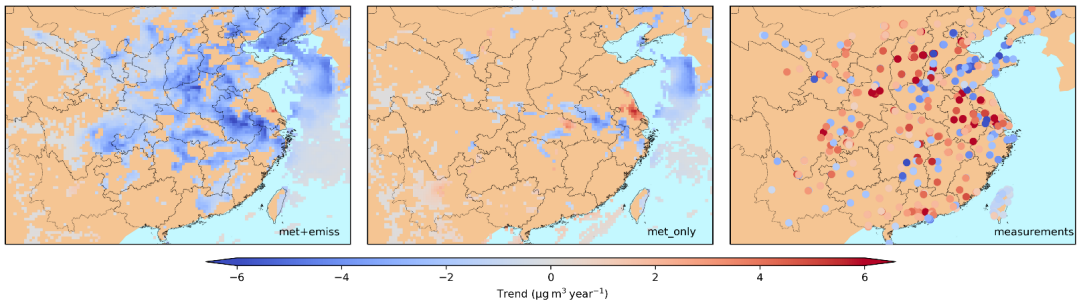

(c) NO_2

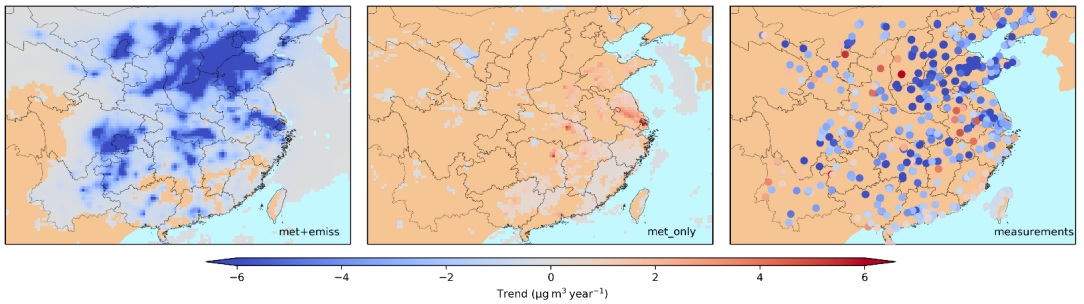

(d) SO_2

Figure B.2: Maps comparing the calculated trends in the control model run (left) the fixed emissions model run (centre), and the measurement data (right) for (a) $PM_{2.5}$, (b) O_3, (c) NO_2, (d) SO_2 across China and Taiwan during 2015–2017 . The trend was calculated at each grid cell in the model runs, and at each station in the measurements dataset. Only statistically significant trends are shown.

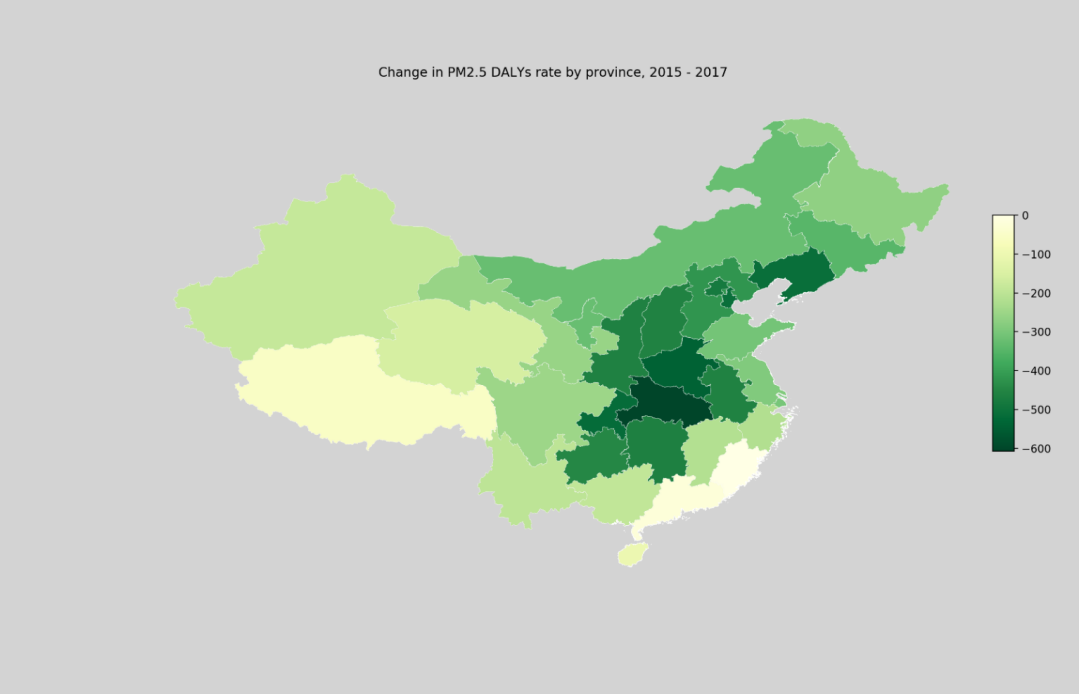

Figure B.3: Simulated change during 2015-2017 in disability adjusted life years rate (per 100000 population, per year) due to changes in exposure to ambient $PM_{2.5}$. Results are shown at the province scale.

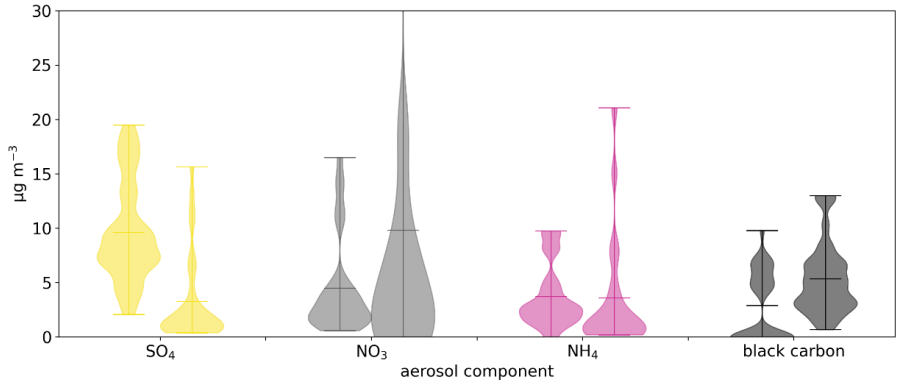

Figure B.4: Comparison between measured (left violin) and simulated (right violin) aerosol species concentrations during 2015-2017. Measurements are from the SPARTAN site in Beijing (available at `https://www.spartan-network.org/beijing-china`)

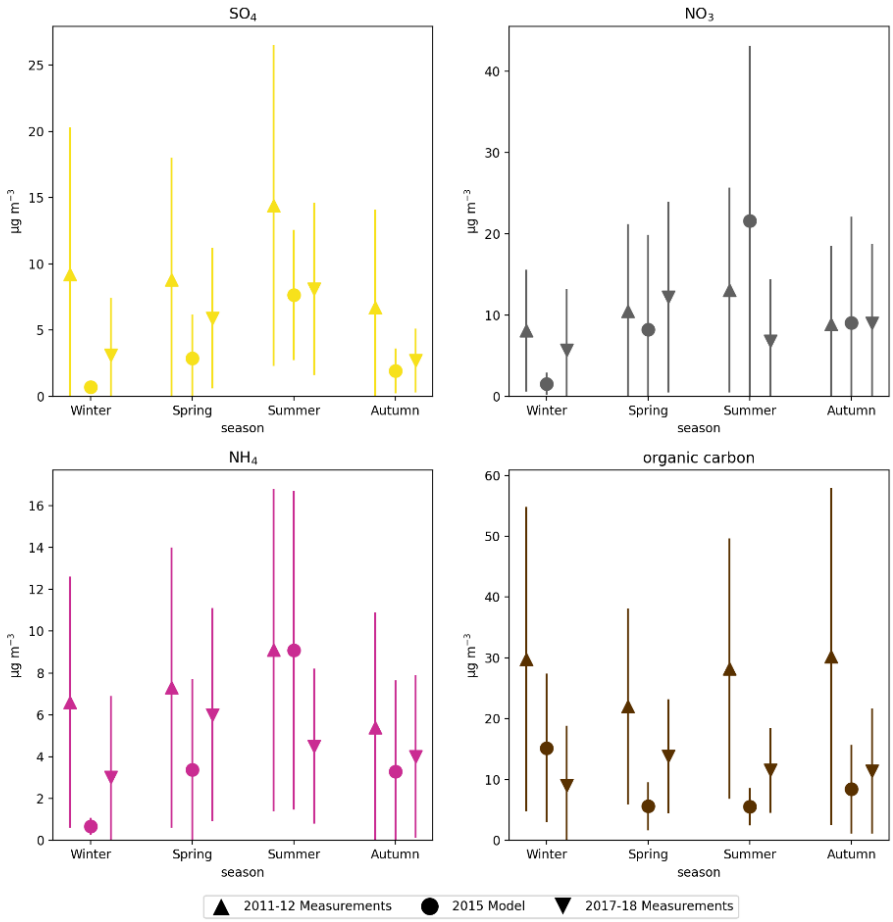

Figure B.5: Comparisons between measured (triangles) and modelled (circles) aerosol species concentrations. The bars show the standard deviation of the seasonal means. Measurements are taken using an Aerodyne Aerosol Chemical Speciation Monitor and are taken from Zhou et al. (2019). The measurements had a time resolution of around 15 minutes and averaged by season

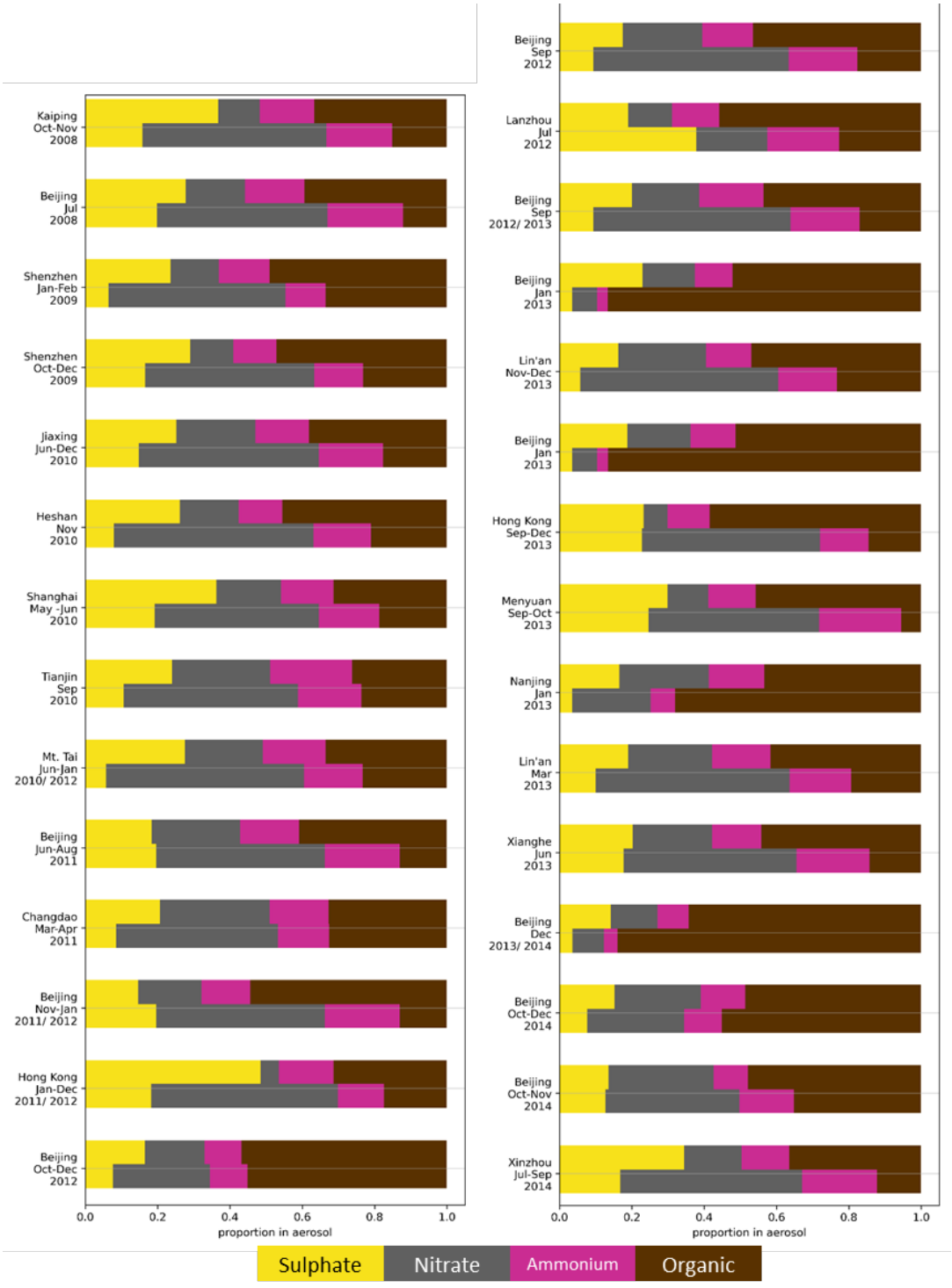

Figure B.6: Comparison between measured (upper bars) and simulated (lower bars) aerosol species concentrations reported as a fraction. Measurements are from Li et al. (2017) and span 2006 to 2013. Simulated concentrations are from 2015

Appendix C

Supplementary material for Chapter 4

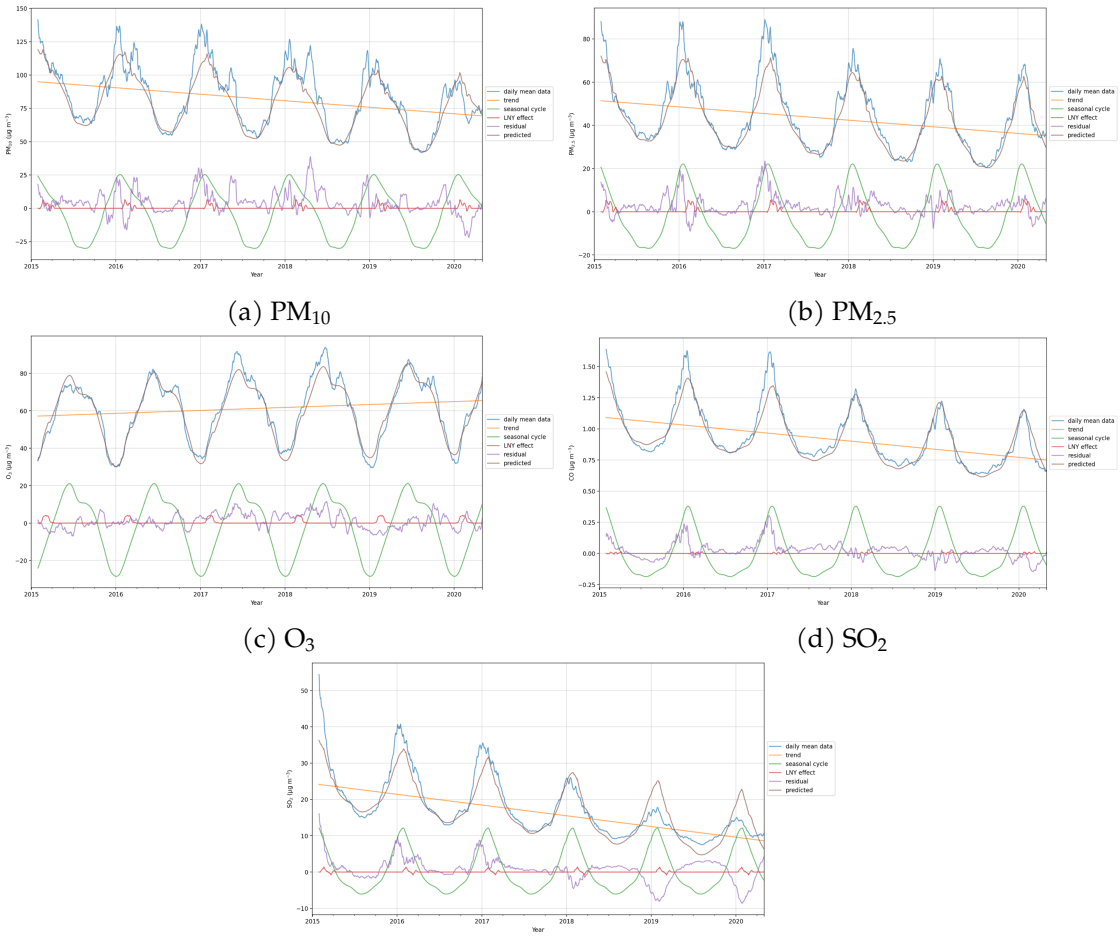

(a) PM_{10}

(b) $PM_{2.5}$

(c) O_3

(d) SO_2

(e) CO

Figure C.1: Figure 4.1 reproduced but using the other five pollutants

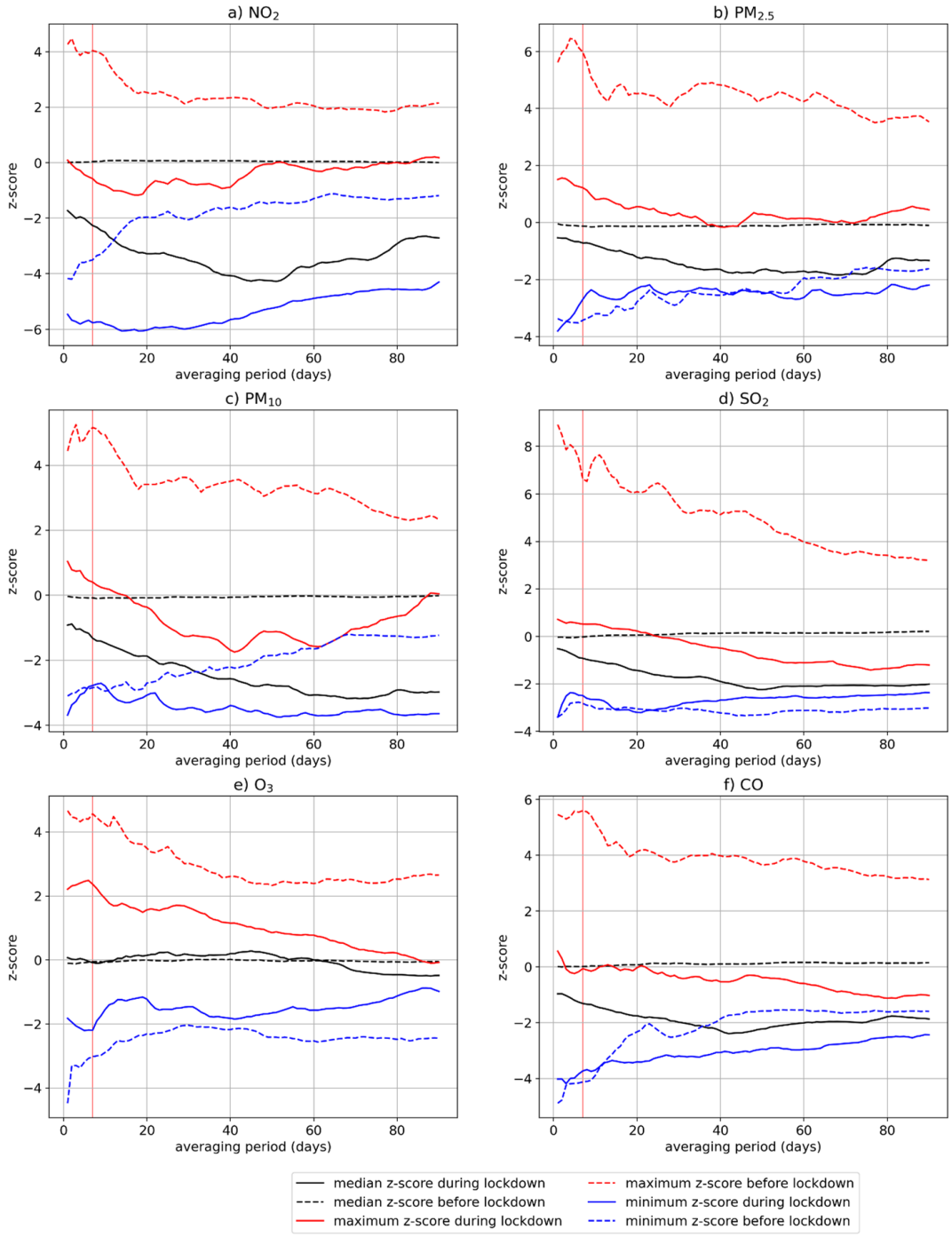

Figure C.2: Minimum (blue), median (black) and maximum (red) z-scores of the residual concentration in a)NO_2, b) $PM_{2.5}$, c) PM_{10}, d) SO_2, e) O_3 and f) CO, with the median in the portion of the time series before the start of lockdown (January 23rd, dotting line) and after (solid line).

Table C.1: Table detailing the frequency of stations removed in each stage of the data cleaning process.

	NO_2	CO	$PM_{2.5}$	PM_{10}	SO_2	O_3
Number of stations	1633	1633	1633	1633	1633	1633
<90% data available	330	332	340	739	330	331
Flagged as anomalous	23	2	259	2	64	25
Remaining stations	1280	1299	1034	892	1239	1277

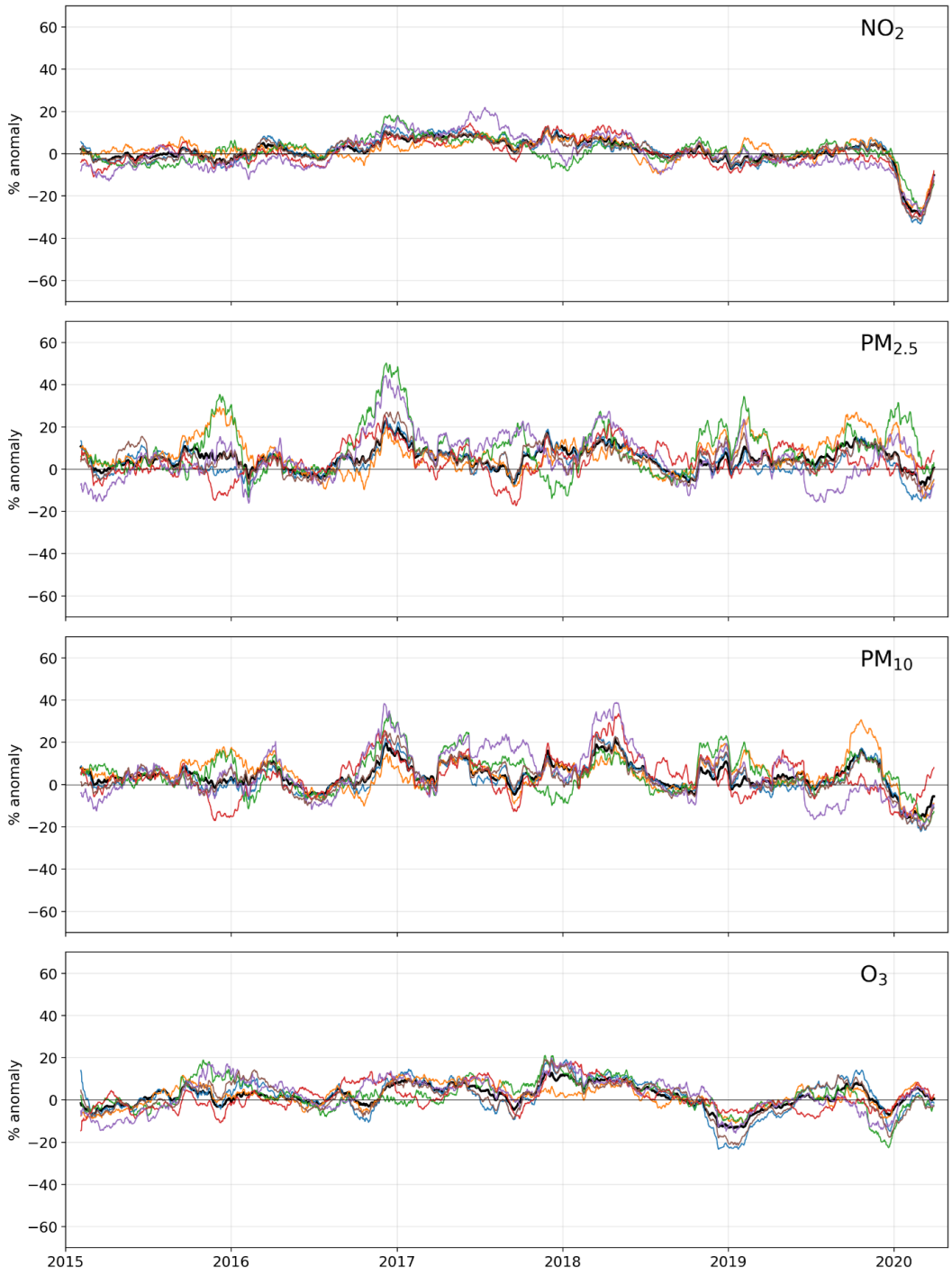

Figure C.3: Time series since 2015 of the relative anomaly (%) in the 7-day residual mean concentration of a) NO_2, b) $PM_{2.5}$, c) PM_{10} and d) O_3. This is calculated by dividing the 7-day mean of the residual component of the time series by the sum of the 7 day rolling means of the seasonal, trend and Lunar New Year effect components.

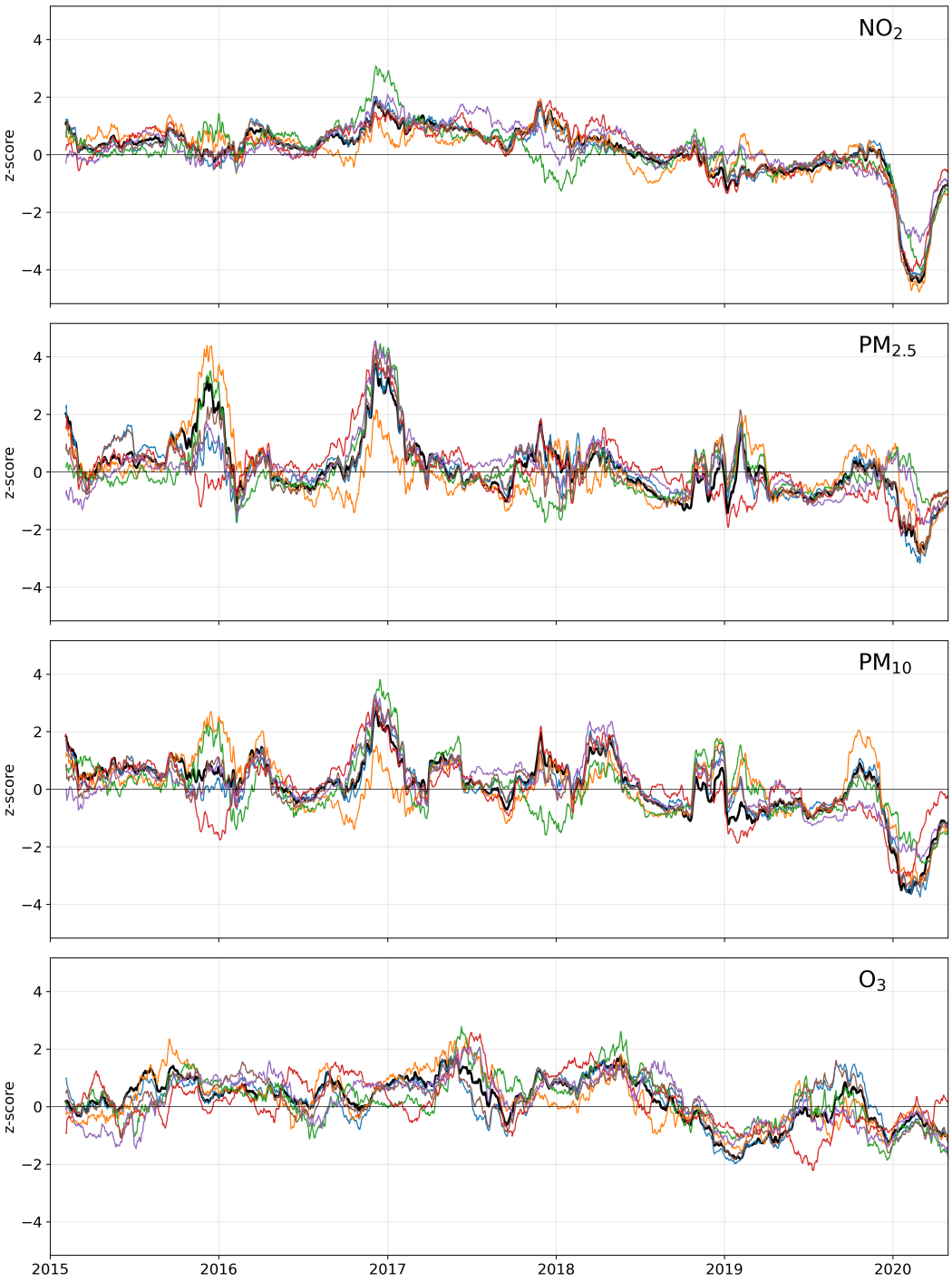

Figure C.4: Time series of z-score since 2015 for a) NO_2, b) $PM_{2.5}$, c) PM_{10} and d) O_3. The black line shows the median across all stations, with the coloured lines showing the medians across regions.

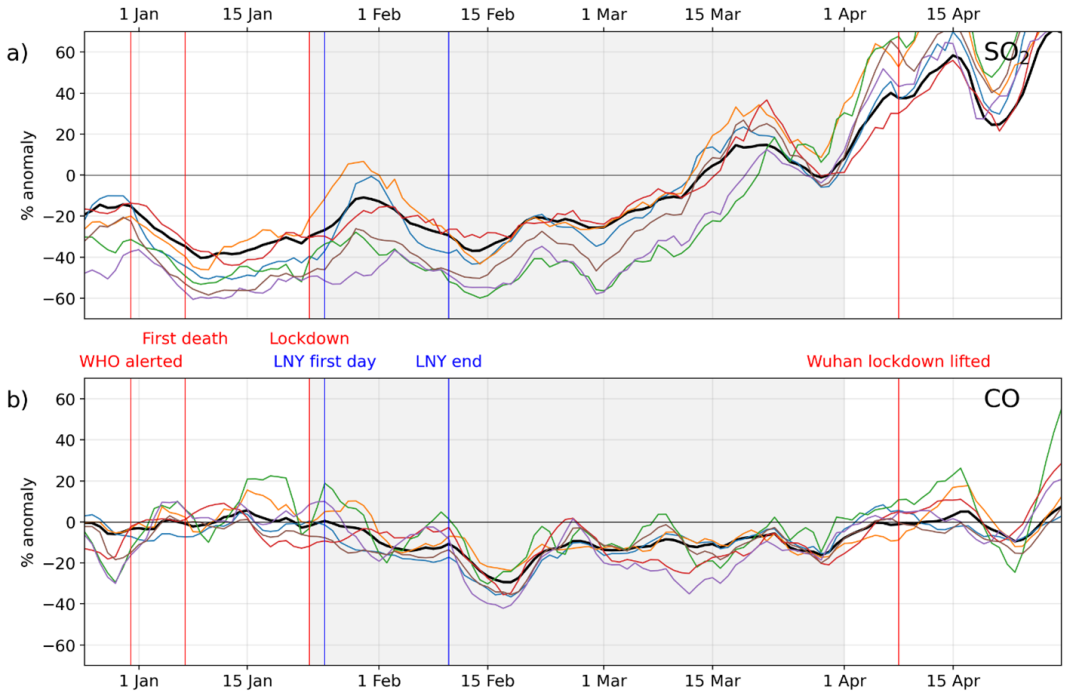

Figure C.5: Time series of the relative anomaly (%) during 2020 in the 7-day residual mean concentration of a) SO_2 and b) CO. This is calculated by dividing the 7-day mean of the residual component of the time series by the sum of the 7 day rolling means of the seasonal, trend and Lunar New Year effect components. The black line shows the median across all stations, with the coloured lines showing the medians across regions. The 'lockdown period,' which is defined as 23rd January to 31st March, is shaded.

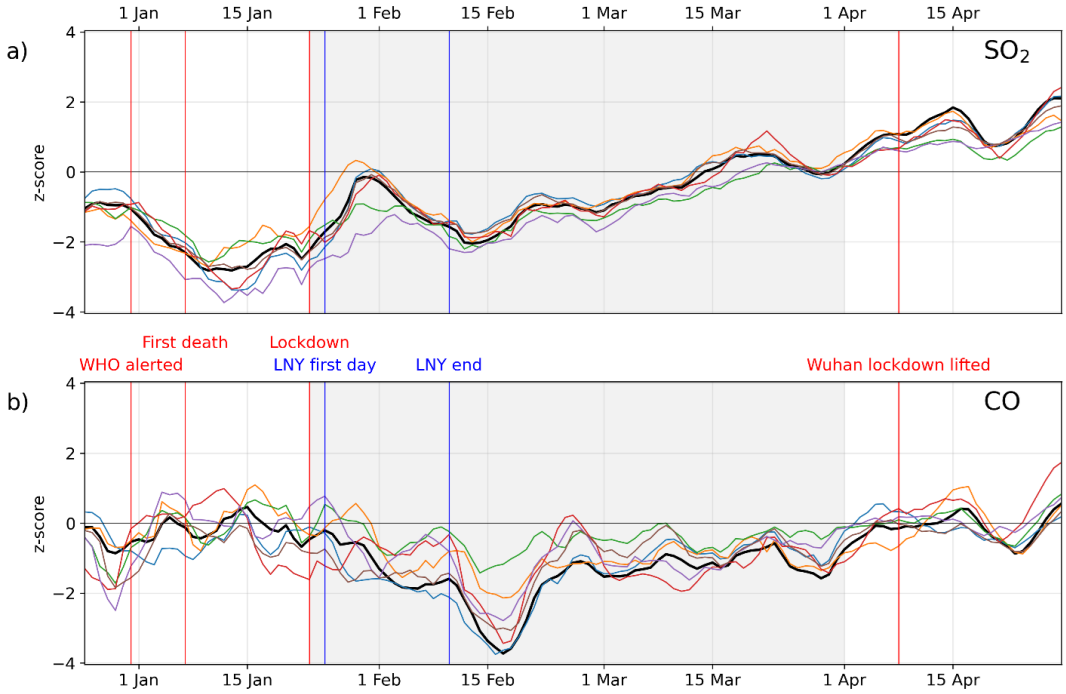

Figure C.6: Time series of z-score during 2020 for a) SO_2 and b) CO. The black line shows the median across all stations, with the coloured lines showing the medians across regions. The 'lockdown period,' which is defined as 23rd January to 31st March, is shaded.